Insert into Running Workflow

GRAYSCALE NAME:

19890019921 GS

HARDCOPY NAME:

Contract NAS9-17511
MCR-86-654

Final
Report

March 1987

Study of Sampling Systems for Comets and Mars

Prepared for:
National Aeronautics and
Space Administration
Johnson Space Center
Houston, Texas 77058

MARTIN MARIETTA

MCR-86-654
NAS9-17511

Final
Report

April 1987

COMET/MARS SAMPLING SYSTEM

Prepared by:

R.J. Amundsen
B.C. Clark

MARTIN MARIETTA
DENVER AEROSPACE
P.O. Box 179
Denver, Colorado 80201

FOREWORD

This is the Final Report under Contract NAS9-17511. The purpose of this Study was to determine concepts and approaches to drilling and several other sampling techniques, for both a Comet Nucleus Sample Return mission and a Mars Sample Return mission.

This program was performed under the direction of Dr. B. C. Clark. The deputy director was R. J. Amundsen. The authors are indebted to contributions by several others, including S. K. Anderson, B. J. Cook, F. M. Kustas, M. S. Misra, P. S. Thompson, and M. G. Thornton. Special acknowledgement is given to R. S. Murray for outstanding efficiency and skill in generating illustrations which demonstrate the various technical concepts presented in this report.

COMET/MARS SAMPLING SYSTEM
FINAL REPORT OUTLINE

1.0 Introduction

2.0 Background

3.0 Mars Sampling

- 3.1 Science Strategy
- 3.2 Vehicle/Mobility Issues
- 3.3 Contingency sampling
- 3.4 Sampling Methods
  - 3.4.1 Regolith/Conglomerate
  - 3.4.2 Rock Sampling
  - 3.4.3 Total Returned Samples
- 3.5 Drilling
  - 3.5.1 Drill Design
  - 3.5.2 Thermal Impact of Drilling
  - 3.5.3 Drill Materials
- 3.6 Sample Storage
  - 3.6.1 Canister Design
  - 3.6.2 Thermal Buffering

4.0 Comet Sampling

- 4.1 Science
- 4.2 Sampling Methology
- 4.3 Nucleus Sampling
- 4.4 Mantle sampling
- 4.5 Sample Storage

5.0 Summary and Recommendations

6.0 Bibliography

Appendix A Drill Thermal Analysis

Appendix B Drilling Test Facilities

1.0 INTRODUCTION

Scientific exploration of the solar system has made outstanding discoveries through remote sensing of the surfaces of dozens of the planets and satellites of the solar system. In a few cases in situ analyses have been possible--including instrumental measurements of surface material on the moon, Mars, Venus, and matter in the coma of P/Comet Halley. Instruments are now being readied for analyzing the surface of Phobos; plans are being developed for comet nucleus penetrator and coma dust and gas analyzers.

In spite of this progress, it is now widely realized that remotely operated instruments have their practical limits. For example, a measurement of the isotopic abundances of natural decay chain radioisotopes has never been accomplished remotely, even though such "age dating" instruments have been often considered. Relative to the techniques now employed on a more or less routine basis in several leading-edge laboratories around the world, most automated instruments would be either of very narrow capability, or else of broad range but limited accuracy. Likewise, the exhaustive petrographic examination of rocks and soil mineral grains requires extensive sample preparation, rapid scanning by a trained observer, and delicate micromanipulation. Many sophisticated laboratory techniques often defy successful automation.

Advanced laboratory techniques often involve large, massive equipment. Examples include inductively-coupled plasma (ICP) trace element analyzers, nuclear magnetic resonance (NMR) instruments, ultrahigh resolution mass spectrometers, and combined ion microprobe/Auger analyzers. The total number of laboratory techniques that can be brought to bear on problems of petrogenesis and weathering history of geologic specimens is today impressively large and diverse, as attested to by the multiple approaches that have been successfully applied to the study of lunar samples, Antarctic meteorites, and other unique specimens. Miniaturization and ruggedization of each and every technique, even if it were technically possible, is also ruled out by budget and spacecraft mass restrictions.

For these several reasons, returning samples from high-priority geological targets provides the greatest potential for detailed data and scientific insight into the origin and processes that have shaped these bodies. The two targets most often mentioned by scientists and identified by formal study committees are the nucleus of a comet and the surface of Mars--the former because it is expected to provide a sampling of primitive material preserved by low temperature storage since the origins of the solar system; the second, because Mars appears to be the most geologically interesting and Earth-like of the terrestrial planets.

2.0 BACKGROUND

The only sample return missions that have been carried out by the United States were the Apollo missions to the lunar surface. This sample return was not autonomous; it was accomplished by the actions of the astronauts. The U.S. has never attempted an automated sample return mission, although this has been achieved by the Soviets on their Luna missions. Many studies of automated sample returns have been performed, mainly with regard to Mars missions.

The Apollo 15, 16, and 17 missions brought back a total of 3.5 kg of drill core material that is still being analyzed in Earth laboratories. This material has been shared between many laboratories in the U.S. and abroad, and has been of the highest importance in the growth of our understanding of our satellite, the moon. The sampling device used on each of the lunar missions was the Apollo Lunar Surface Drill (ALSD), Figures 2-1 and 2-2, developed at Martin Marietta. This drill system underwent eight years of development, and achieved between 85 and 98% core recovery on the three missions. The ALSD was capable of both coring and solid bit drilling. In coring configuration, the system consisted of a sealed rotary percussive power head, coring stem sections, and coring bits. The stem sections and coring bits were attached to the drill head by the astronaut via threaded fittings. No drilling flush was used; the outer surfaces of the stems were fluted for mechanical removal of drill cuttings. The cutting action was performed by individual tungsten carbide cutters brazed into the bit.

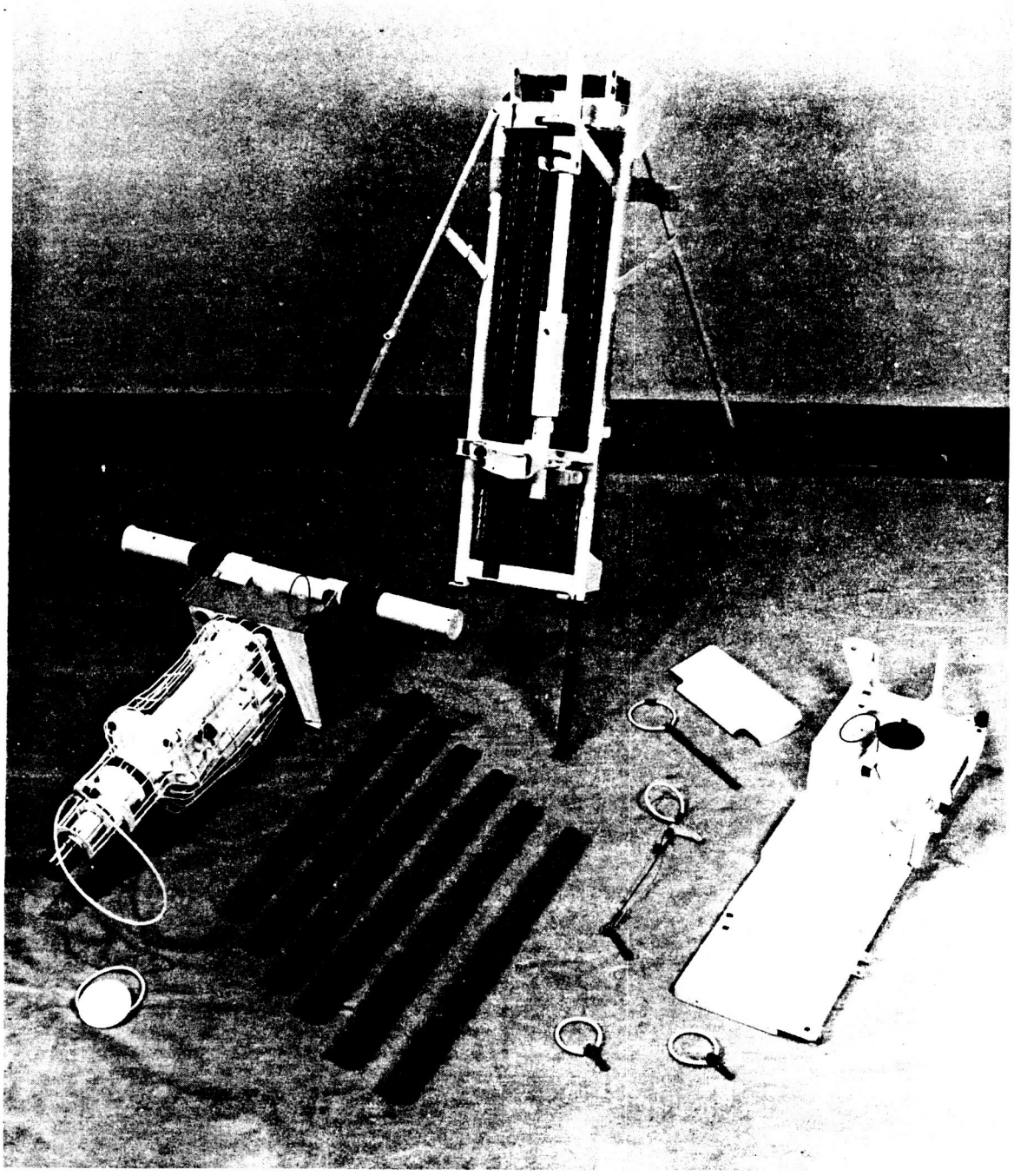

Figure 2-1 Apollo Lunar Surface Drill and Parts

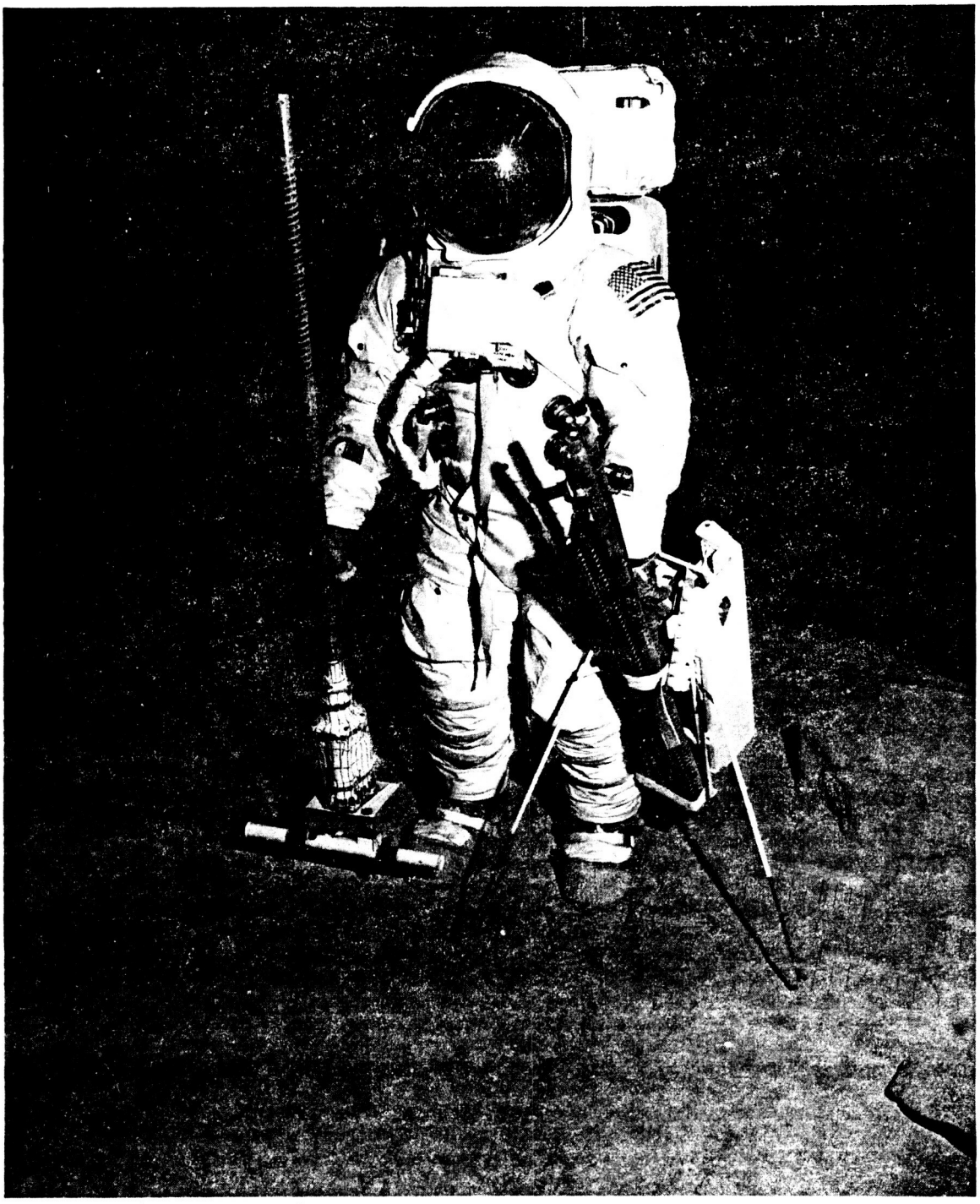

Figure 2-2 Apollo Lunar Surface Drill

The drill was designed to core a hole 1.032-in. in diameter and three meters in depth. On each of the three missions the full depth of drilling was achieved, approximately 100 inches. The titanium alloy Ti-6Al-4V was used for the core stems.

The current study evaluates top-level options for sample return missions to both Mars and a comet. For a Mars mission, this includes the configuration of the sampling vehicle, the sampling strategy, methods of sampling the variety of martian materials, and approaches for sealing and storing the acquired samples. For a cometary mission, this includes the spacecraft configuration, sampling strategies for cometary materials, and storing samples for an undisturbed return to Earth. Drilling is a sampling method common to both missions, and is examined in detail. Included are design of a drilling system, analysis of materials, and analysis of the thermal effect of drilling on the cored material.

3.0 MARS SAMPLING

3.1 SCIENCE STRATEGY

The strategy for sampling on a planet whose surface exhibits diverse atmospheric and geologic processes is necessarily more complex than that for sampling a cometary nucleus. Mars is an excellent example of such a planetary surface, with its wind blown dust, vesicular rocks, sand deposits, bedrock, and two or three kinds of ices. Igneous and eolian sediments seem obvious from photogeological interpretations. The presence of chemical sediments and metamorphosed units are less certain, but not unlikely. Stratigraphic mapping demonstrates a complex history, and resurfacing and stripping processes may have removed much of the evidence from the view of the orbital perspective.

Understanding the root magmatic processes that formed the lithosphere may be mainly a matter of obtaining a relatively few representative igneous rock samples, although the episodic nature of past events could complicate this issue. Gaining insight into weathering processes and the long-range climatic trends and cycles that have operated will require even more extensive sampling. Soils, airborne dust, partially weathered rocks, and deep sediments are all candidate materials that will be sought. The presence and forms of water (and CO_2) in minerals or as surface and subsurface ice deposits will provide information needed to trace the history of volatiles on Mars. Microenvironments conducive to biological activity, such as endolithic niches or fumarolic vents, are also of great interest.

From the standpoint of maximizing the science value of sample return, it would seem most prudent to make every effort to diversify the sample suite as much as possible. This can be accomplished by sampling each of the many types of geologic materials that will be available, by screening the samples to the extent practical to weed out repeats, and by sacrificing quantity of any one type to quality/diversity of many types via the technique of subsampling (i.e., creating splits and bringing back only one or a few of the portions). Microanalytical techniques today accomplish extremely sophisticated results on micro- and even nanogram quantities of material, obviating the need for substantial amounts of samples for most purposes.

A strawman example of sample types and approaches are given in Table 3.1-1.

3.2 VEHICLE/MOBILITY ISSUES

A rover on Mars will be necessary if sampling from a range of geologic units is to be accomplished. A rover is assumed to mean a vehicle with wheels, tracks, walker legs, or other locomotion over heterogeneous terrain. The rover must have one or more sample handling devices, a camera, and some type of sample storage system. Rovers have been proposed that employ an umbilical tether back to the lander for power and communication. This eliminates the need for power, navigation, communication and data systems on the rover, but severely limits the range of the rover. This design also adds technical

Table 3.1-1 Mars Sample Types Sampling Methods

Rock	
Small Rocks	Rake Sieve
Large Rocks	Chipper Crusher Slabbing Saw Rock Holding Device
Boulders	Coring Drill Chipper Slabbing Saw
Soil	
Wind-blown	Wind Sock, Cup Arrays
Surface Material	Scoop, Contact samples Magnet
Deep Soil	Coring Drill Drive Tube Trencher
Ice-Laden Permafrost	Coring Drill Drive Tube

difficulties in stowage, deployment, and maintenance of the tether. The power supply on an untethered rover is usually assumed to be an RTG, because solar panels would not be operable at night or during a major dust storm. Other vehicles that have been proposed for Mars transport include a "Mars Ball", which is an enclosed rolling sampler, balloons, and a powered glider.

To achieve the greatest reliability and flexibility in sampling from the rover, use of two robot arms can be considered. One could be a high-resolution arm capable of delicate motion and precision, which would perform any operations requiring high accuracy. The other arm could be used mainly for operations requiring strength, and would be more rugged but with less positioning accuracy. For redundancy, the arms would each have the capability to perform many of the actions of the other, but would be optimized for reliability and long-life within their own sphere of duties. Figure 3.2-1 portrays a possible rover design that illustrates these points.

Another concept for increasing the flexibility of the rover is a mini-rover. This would be a very small vehicle capable of leaving the rover for short periods of time. The mini-rover could move on the surface within sight of the rover's cameras and select rocks or test the soil, using battery power and minimum instrumentation. The other function of the mini-rover would be exploring and sampling regions that are too rough or dangerous to be reliably traversed by the rover itself.

3.3 MARS CONTINGENCY SAMPLING

A contingency sample will be gathered from the lander in a manner that is completely independent of all sampling and rover systems. Figure 3.3-1 portrays one concept that consists of an automated arm deploying a small sample canister to take a scoop sample of regolith fines and lithic fragments and sealed by an attached lid. This lander arm can also be used to emplace the standard sample canister onboard the ascent vehicle, e.g., to act as a back-up to the arm on the rover that performs this function. The contingency sample can be placed in the base of the sample canister enclosure, or a separate storage compartment could be provided. Placement of the contingency sample in

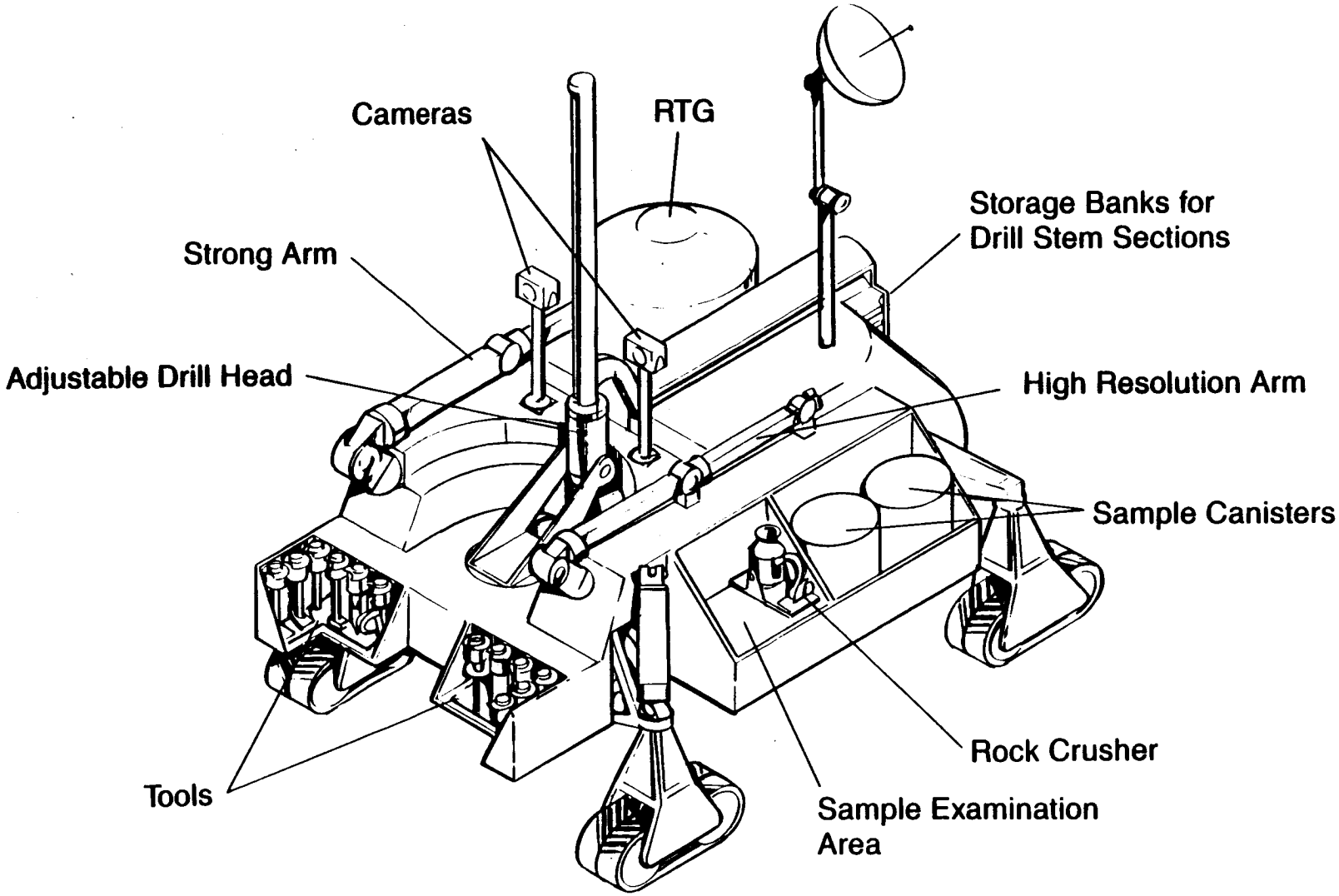

Figure 3.2-1 Mars Sample Return Rover

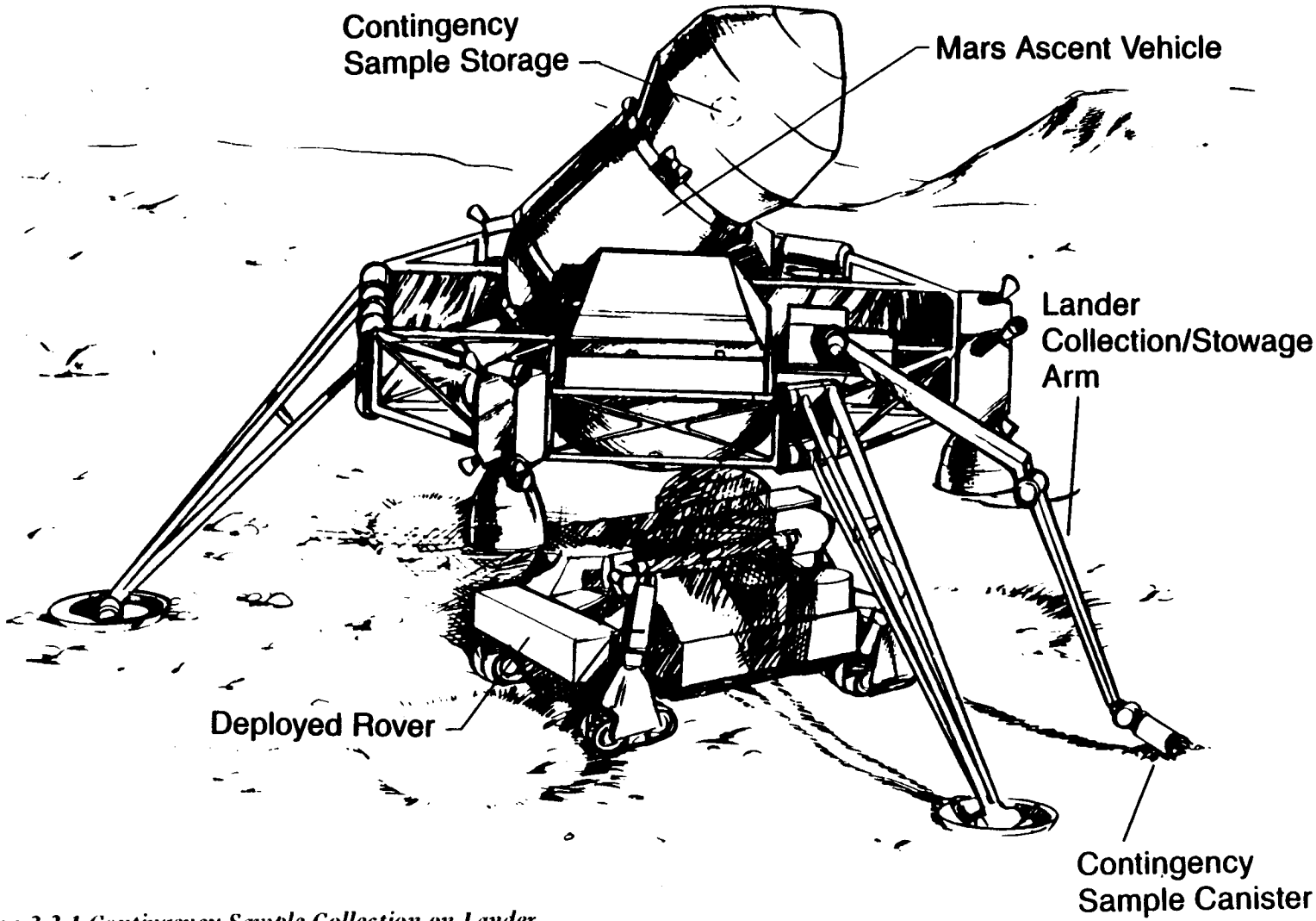

Figure 3.3-1 Contingency Sample Collection on Lander

a position below the standard sample canister assumes that the sample canister will not already be in its final position in the return vehicle at landing. Once the standard sample canister is loaded and stowed, however, the contingency sample could be difficult or impossible to access. The drawback of a separate door for the contingency sample is that it entails different motions for the two stowing operations.

The contingency sample canister would be a small cylinder (approximately 4 in. dia by 3 in. high). The lid could employ a soft metal ring that is deformed to make an acceptable seal even if the surfaces were contaminated during the sampling operation. A more complex option is to use a metal seal ring with a protective cover that is removed before final sealing.

Another level of contingency planning would be to send the rover on an initial foray that involves little risk and is within range of the lander cameras or sensing equipment. This expedition would be devoted to collection of as many sample types as are in the nearby landing area, with minimum risk to rover systems. A standard sample canister would be brought back to the lander and placed in the ascent vehicle ready for launch. The rover could then embark on a more ambitious mission, to collect samples from more distant regions and/or more complex terrains on the planet. If for some reason the rover is unable to return with these additional samples, the return vehicle can launch with the local samples. With a sufficiently adaptable sample canister assembly, this process could be carried out several times, with higher priority samples replacing the ones collected earlier. The initial contingency sample might also be replaced later with a higher priority sample.

3.4 SAMPLING METHODS

3.4.1 Regolith/Conglomerate Sampling

The scientific requirements for the sampling of regolith on Mars include surface material, deep and potentially ice-laden regolith, unconsolidated fines, and wind-blown or settled dust. Samples of each should be taken, with flexibility as to the order of acquisition, and reliable methods of preventing cross-contamination. A collection of sampling methods is presented in Table 3.4.1-1.

Table 3.4.1-1 Candidate Sampling Techniques for Mars

Rock:

Chipper--impact pick, vibrating pencil

Crusher--sledge hammer, sliding-sided box, claw & hammers

Saw--sections or wedges of rocks

Rake, Sieve Box--collect and separate rocks from soil

Solid Drill--collect cuttings

Coring Drill--core samples from large rocks

Soil:

Coring Drill--sample cores of regolith, including permafrost areas

Sand Drill--"sampling window" drill for small samples of non-cohesive soils

Drive Tubes--produces mini-cores with minimum mechanical & thermal disturbance

Trencher--buckets to take samples or expose deeper soil in a trench

Scoop-- samples of surface soil

Contact Sampler--maze trapping of topmost soil grains

Wind Sock--strain windblown particles from atmosphere, can be set up as long-term

General:

Universal Arm and Tool Kit--with drill head, chipper, manipulator,etc.

Mini-rover--explores dangerous or rough areas

Anchors--auger into soil for stability during sampling or equipment deployment

The most satisfactory way to obtain samples of deep regolith is core drilling. A core sample requires only one hole the size of the sample, and produces a length of relatively undisturbed material that represents the stratigraphy of the original material. Core drilling involves minimum physical or thermal disturbance of the sample, and produces samples already encased in a protective stem. The samples cannot be analyzed without removing them from this casing, which creates a problem if the sampling requirements involve immediate testing of the soil. Core drilling is the best method for retrieving very deep material as there is no restriction on depth of drilling, as long as sections can be added to the stem.

One problem with standard core drills is retaining loose or noncohesive material. Even with a specially designed core retainer at the end of the stem section, often more than half of the sample core is lost during withdrawal of the drill from the hole. A type of drill that has been used for procuring samples of unconsolidated material is the "sand drill", pictured in Figure 3.4.1-1. This is a solid-bit drill that has an internal movable structure of pistons. While the drill is progressing to the required depth, the pistons block holes or windows in the drill stem. When the desired depth has been attained the pistons are depressed, aligning cups in the internal structure with windows in the stem. The drill is rotated or operated and loose soil enters through the windows until the cups are filled with material. The piston structure is then returned to its initial position and the drill is withdrawn from the hole. Caps can be added as part of the piston structure so that when the drill is removed from the hole the sample cups are already individually sealed.

Trenching can be used to form a deep hole that is wider and offers the viewing of soil horizons. A sample trencher is shown in Figure 3.4.1-2. The digging elements can be "sample buckets" as shown, or they can be pockets on a rotary belt for shallower sampling. The trenching operation can be carried out continuously, and samples viewed immediately. Thus it is a good candidate for a sampler that would be used to test the surface soil whenever the rover is halted.

A device to perform continous analysis of the surface over which the rover is moving is very desirable for finding unusual regions that should be sampled. A trencher is a better sampler than a drill for

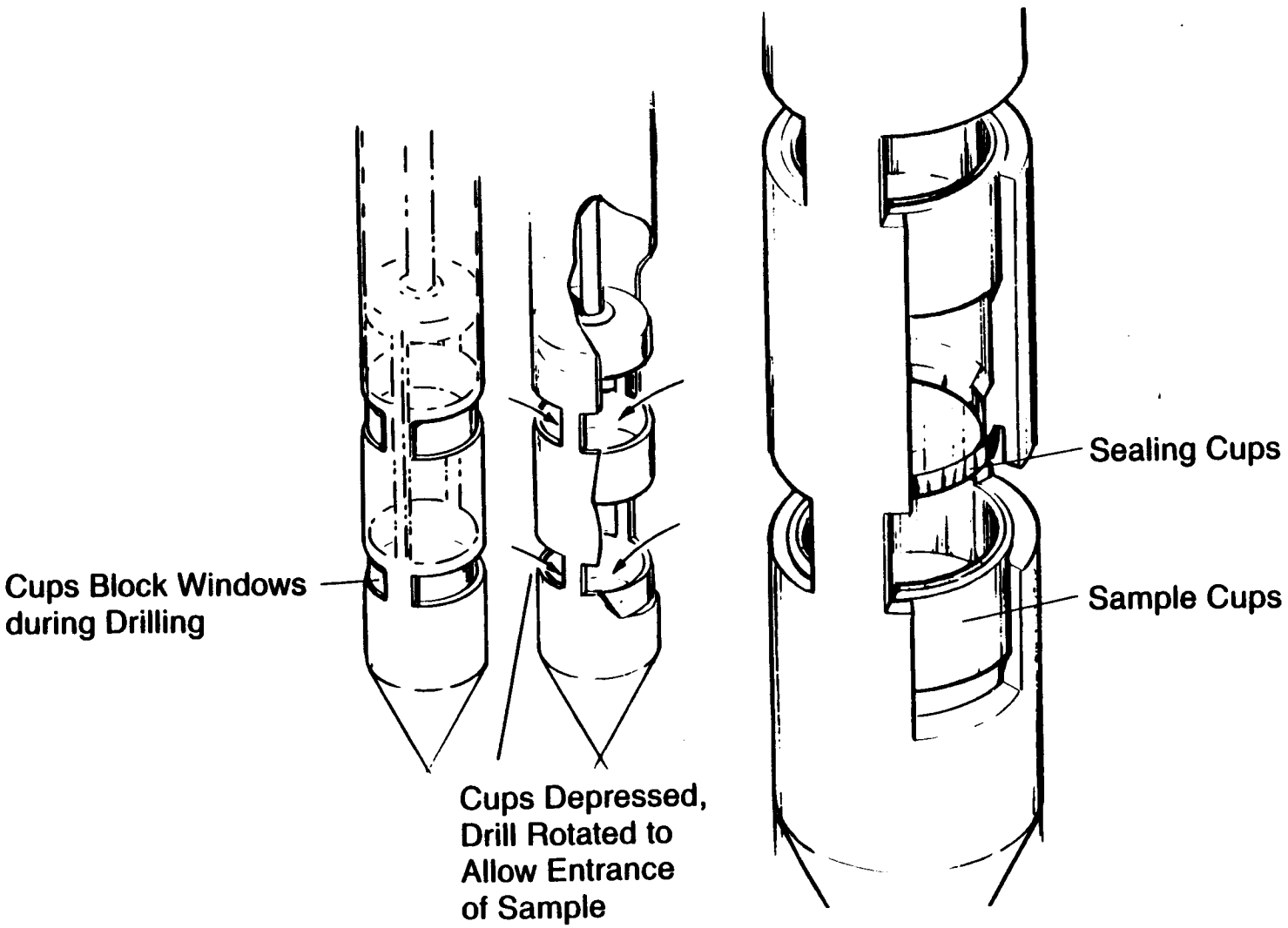

Figure 3.4.1-1 Sand Drill for Sampling of Noncohesive Soils

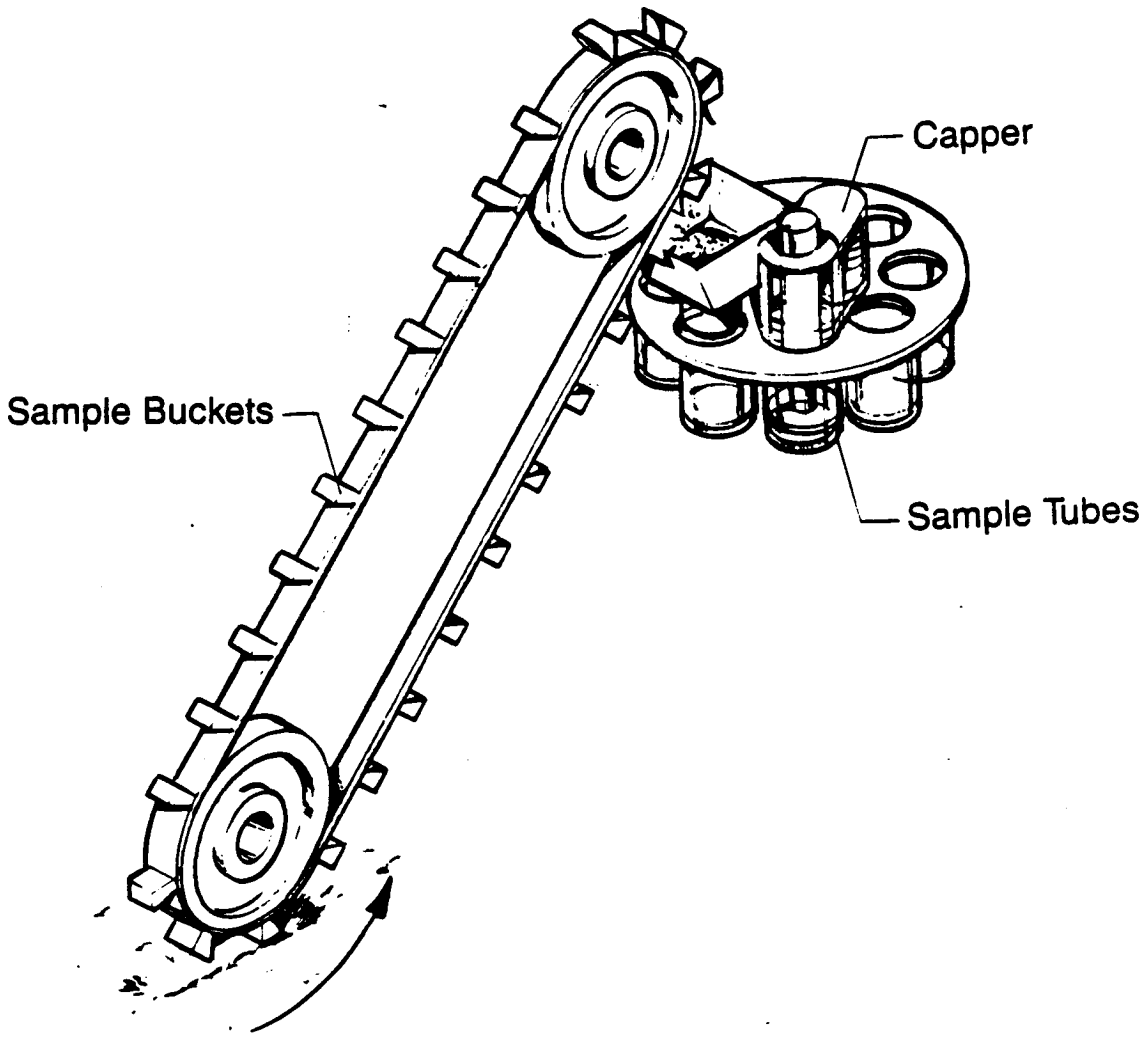

Figure 3.4.1-2 Regolith Sampling with Trencher

this purpose, as it can be carried out from a moving rover with little or no preparation required, and the samples can be analyzed immediately. However, in trenching, a significant fraction of the energy is used to form the hole, so the sampling operation is less energy-efficient than coring. The cross contamination of material between different depths is considerable, unless the sampling buckets have a sealed top that is forced open by pressure against the hole bottom. For these reasons, trenching could be a viable alternative for continuous surface sampling or infrequent deep trenching to view stratigraphy, but is not as satisfactory a candidate as a coring drill for standard deep samples.

Drive tube samplers have often been used as a low-power method to gather shallow undisturbed cores of sample. These drive tubes can take a more represenative core of material than core drilling, but are restricted in the depths attainable. A single drive tube of the desired diameter range (0.3 to 1.0 cm) should not exceed about 25 cm in length to prevent excessive structural problems and loss of sample. To sample more deeply, several drive samples must be taken progressively. The hole must be cased for this operation to avoid hole collapse, which adds equipment and complexity to the operation. Even if the hole were cased, sequential samples will show some cross contamination between depths. Drive tubes are best used as a shallow sampler, and they have the same advantage as drill core samples in producing a cased sample that can be sealed and stored without further processing.

Two types of drive tubes are shown in Figure 3.4.1-3. The "soda-straw" sampler will penetrate best for samples of soft regolith. The small diameter of this sampler provides stratigraphic information at many different locations for minimum returned mass. A core retainer should be unnecessary, as a large fraction of the sample is held by surface friction against the tube walls. The second drive tube type is the same diameter as the drill, and would be used to obtain a sample undisturbed by drilling in materials too dense for use of the "soda-straw". The optimum dimensions for a drive tube for best core recovery and ease of penetration have been determined in many studies. Figure 3.4.1-4 illustrates a typical drive tube that would be useful for shallow core samples. For the best core recovery, this sampler

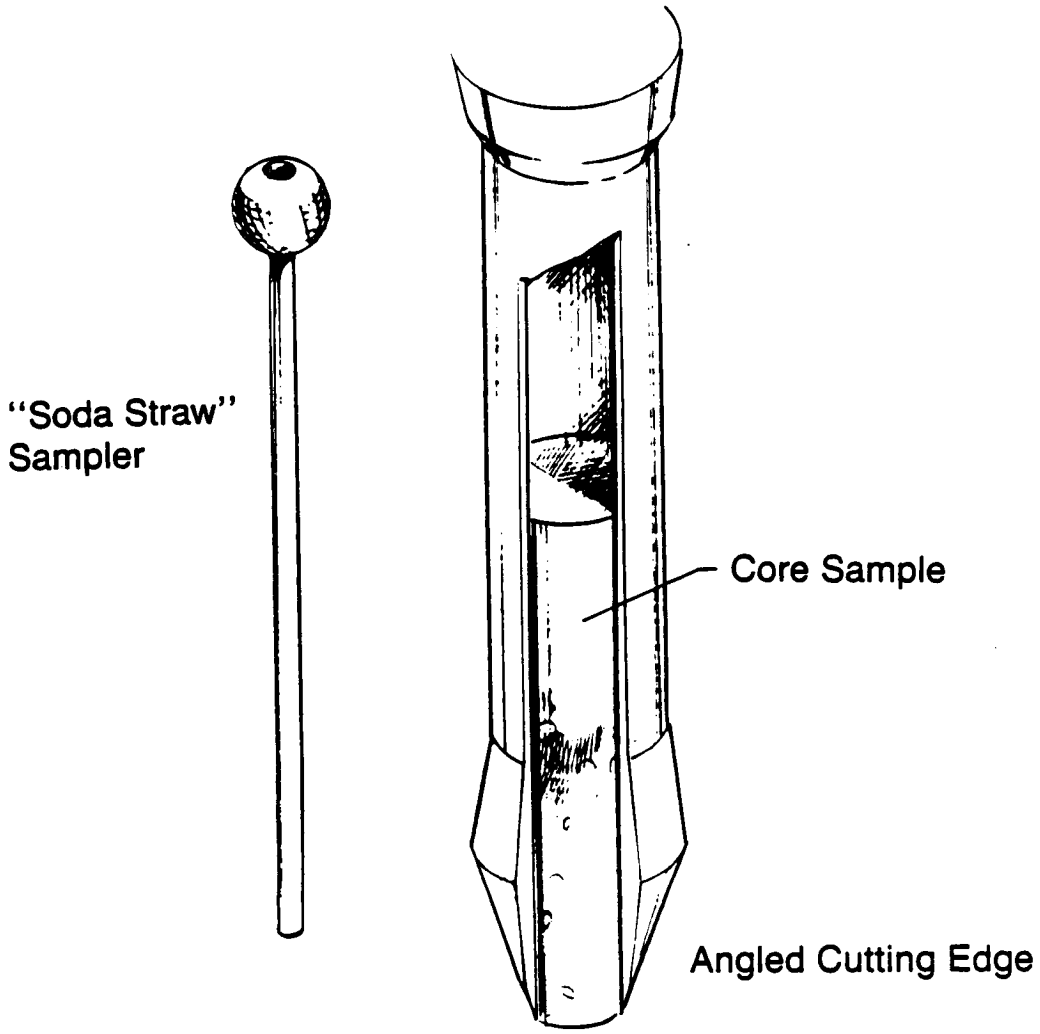

Figure 3.4.1-3 Drive Tube Samplers

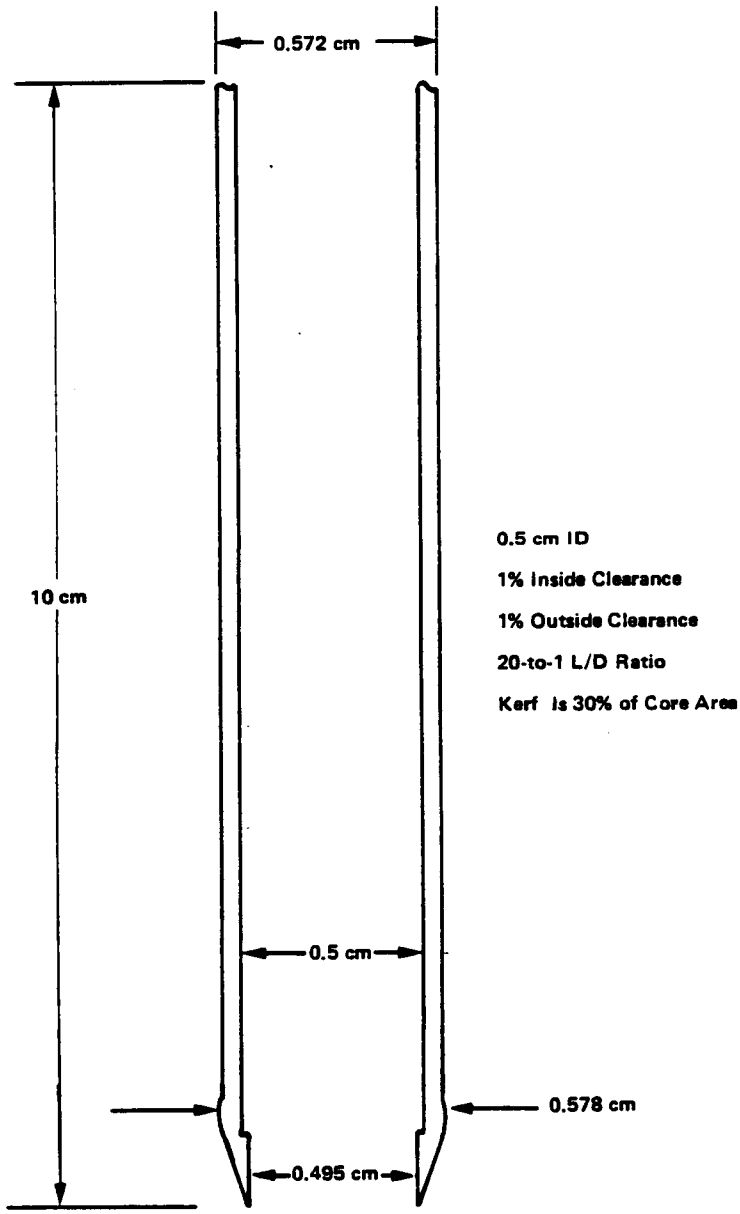

Figure 3.4.1-4 Drive Tube Design

should be pushed into the soil with a steady force, rather than percussive motion. The axial drill force is suggested to supply this motion; this is particularly simple to implement if the drill stems, sampling arm(s), and drive tube all have identical connections, allowing drive tube samples to be taken via both the drill and sampling arm.

Because there are many different materials to be sampled on Mars, some with relatively unknown parameters, flexibility in the sampling methodology is an important criterion. One feature that makes the sampling operation much more adaptable is to include a wide selection of sampling tools and devices on the rover. A universal arm that has at its disposal a complete kit of sampling tools should be considered. This concept is illustated in Figure 3.4.1-5; a selection of sampling tools are shown later in Section 3.4.2. The arm has sufficient mobility and electrical connections to satisfy the requirements of each tool. It attaches to each with an identical bayonet lock connection, requiring only a push and turn motion to hold the tool rigidly in all directions. With two degrees of freedom motion at the "shoulder" where the arm attaches to the rover, one degree of freedom at the elbow, and only rotation at the "wrist" where it attaches to the tool, the arm will have sufficiently flexible mobility. The tools could include sampling devices and testing devices such as a camera with variable lens systems, an elemental analysis device, and a penetrometer.

Saltating/Settled Particle Collection--The topmost layer of fines is of scientific importance because it can represent eolian materials transported from remote areas of Mars. To sample only the surface layer, a sticky or rough-surfaced tape can be used, or selective sampling can be done with a magnetic contact sampler. The "tape-wheel" sampler, described below in Section 4.4, would be capable of taking a large number of these.

Other samples that are of special scientific interest are the saltating grains produced by the Martian winds. The method for collecting these particles must be capable of long-term use, must collect most or all of the impinging particles, and should allow storage of the samples in a volume- and mass-efficient manner. Three methods of accomplishing this are shown in Figures 3.4.1.6 thru 3.4.1-8. First is an analogue to the Earth wind sock, using

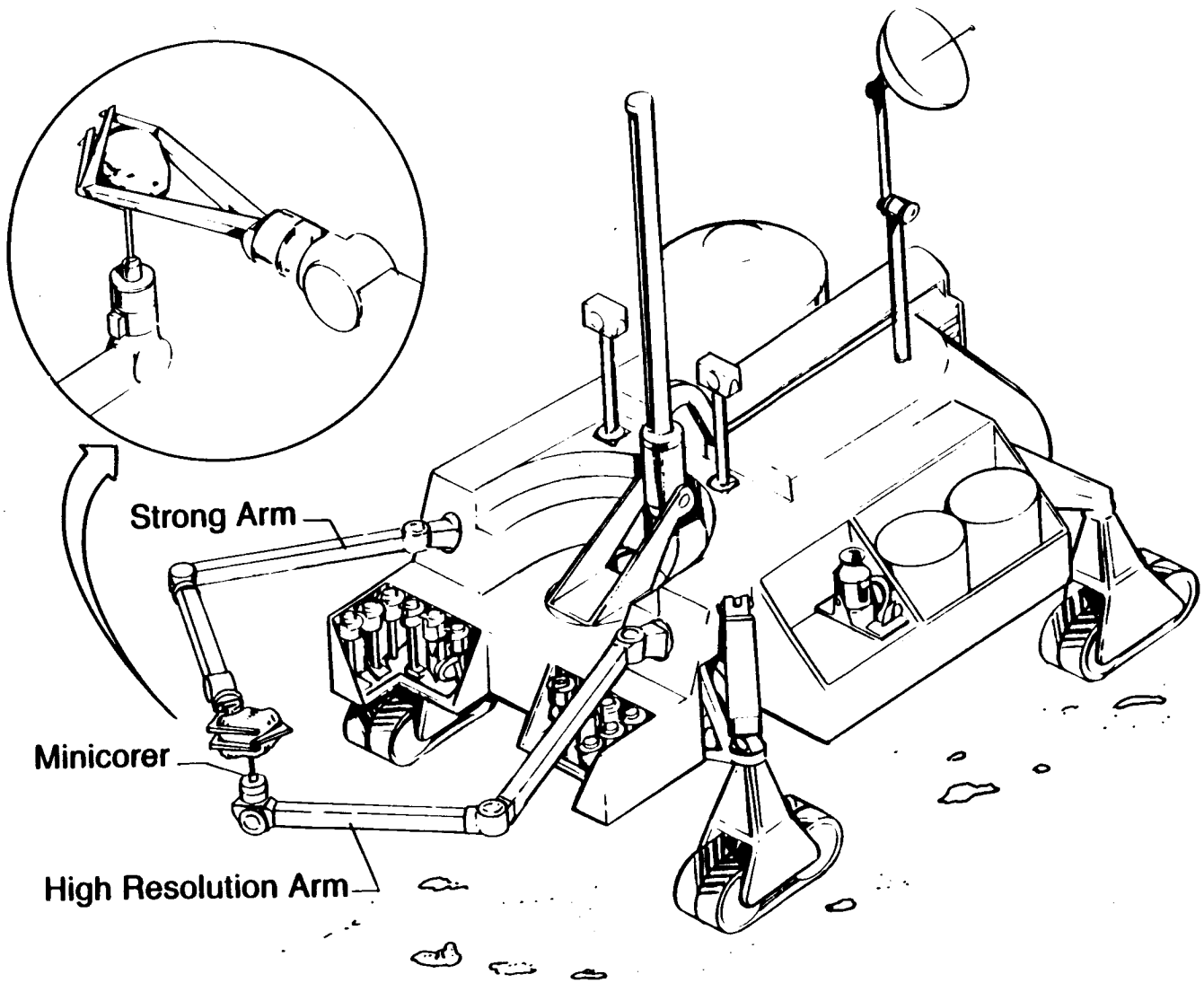

Figure 3.4.1-5 Operation of Universal Arms

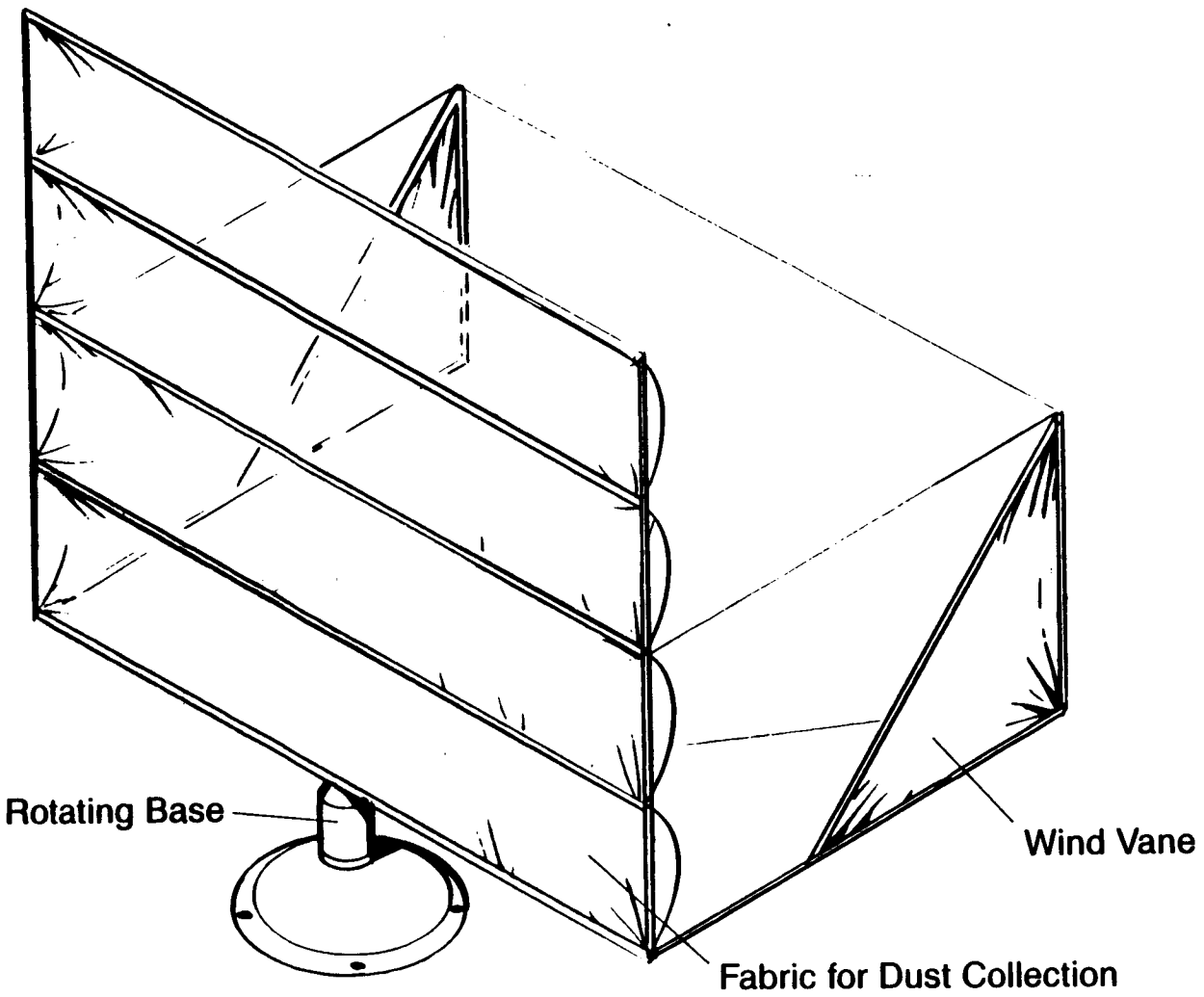

Figure 3.4.1-6 Collection of Wind-Blown Dust by Wind Sock

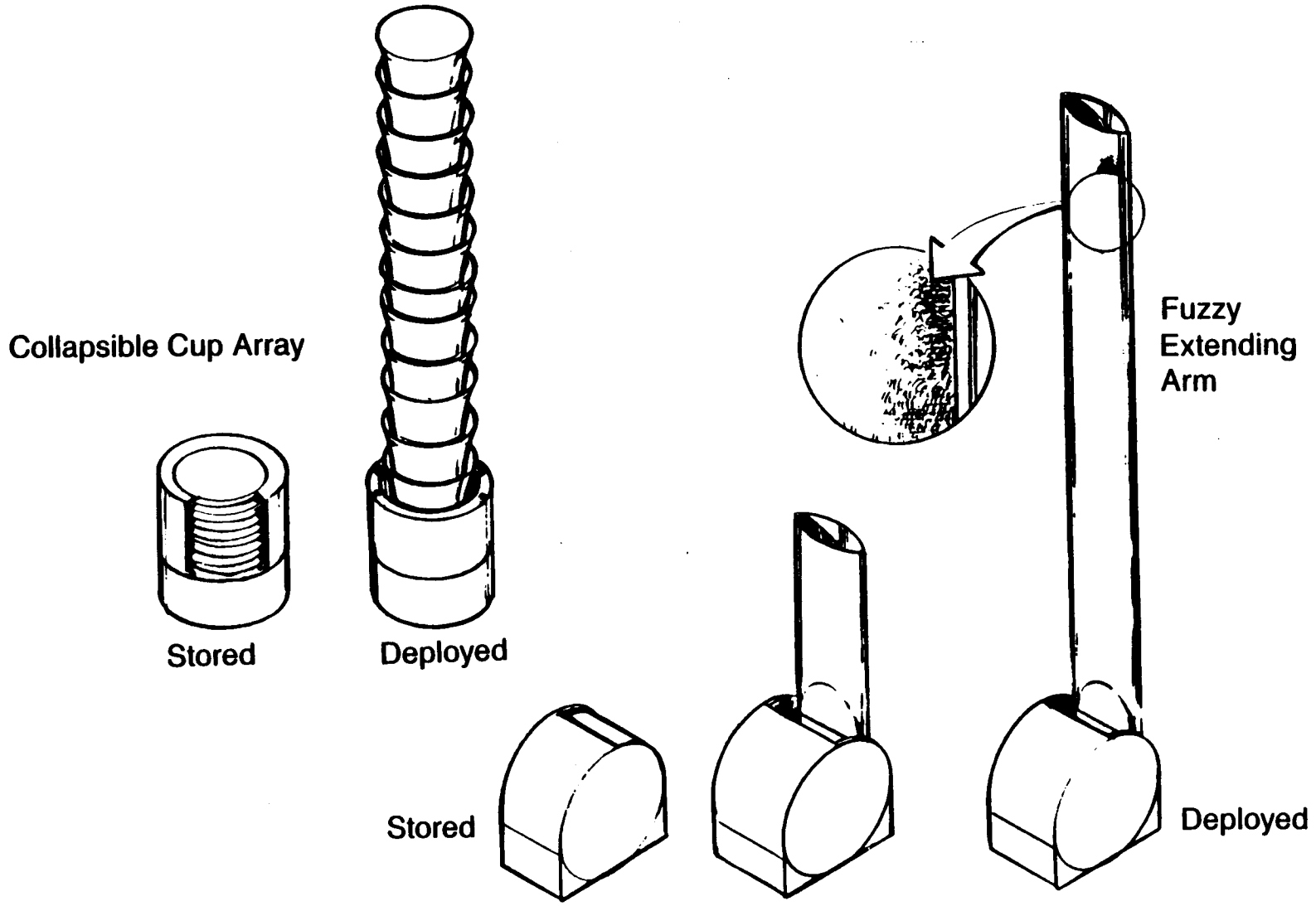

Figure 3.4.1-7 Collection of Wind-Blown Dust

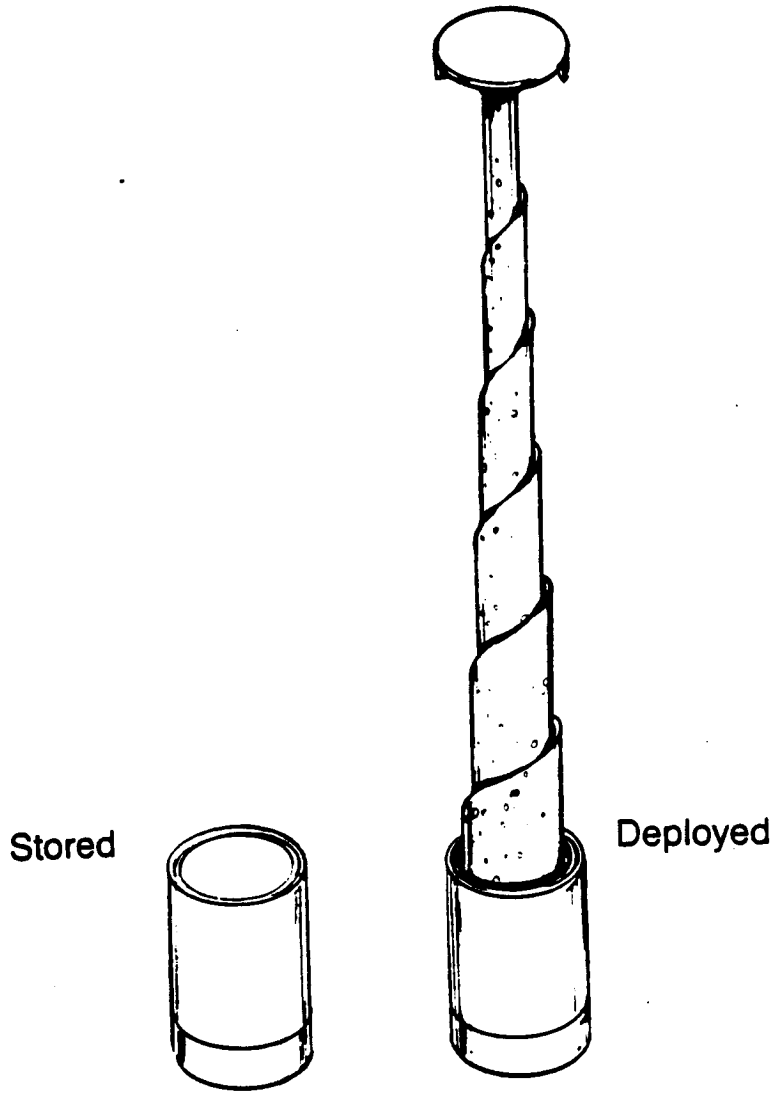

Figure 3.4.1-8 Collection of Wind-Blown Particles by "Flypaper" Spiral

half cylinders of fabric to collect the dust, and wind vanes to keep the rotatable assembly pointed into the wind. The fabric cylinders are stretched on a lightweight structure of wires that collapse easily for storage. After sample collection, the wires may be withdrawn from the length of the cylinders and the mesh rolled for insertion in a return tube. The collapsible cup assembly also uses a fabric windsock arrangement, and the collected dust is funneled into the bottom of each fabric partition. The cups are then collapsed into a compact package for return, with a seal on the lid to eliminate intersample contamination and also to acquire an atmospheric sample. Another compact collection method for airborne particles is an expanding arm with a sticky or fuzzy surface. Two methods of storing this arm are shown as a "fly-paper" spiral and in a compressed roll. The spiral has a clearance between the tape surfaces in the stored configuration, so that particles are not scraped off as it recoils. This can be deployed upward by a telescoping tube, or downward, using a weighted cord. The weighted cord is dropped to expand the spiral, and reeled in after collection with a rotary motor. The compressed roll keeps the particles separated although it may crush them somewhat in storage. The rolled arm method has the advantage that the arm can be deployed by its own spring force, as was done with the Viking lander sampler arms.

Particles that settle naturally out of the atmosphere can be gathered by flat plates or cups. These collectors can be attached to the rover, or deployed for long-term collection and retrieved just prior to launch. All these methods for dust collection are automatic and can be deployed near the lander for long-term collection. This avoids contamination from rover activities, and allows the rover to operate independent of the dust collection experiments.

3.4.2 Rock Sampling

The simplest way to obtain a possibly diverse suite of rocks is to scoop up quantities of regolith and sieve out the lithic fragments. Alternatively, a rake may be used to sift the rock fragments from the soil and bring them to the rover. Sieve/scoop and rake tools for use on a rover arm are shown in Figure 3.4.2-1. This method can be extended by using various sized sieves to select specific size ranges of rocks.

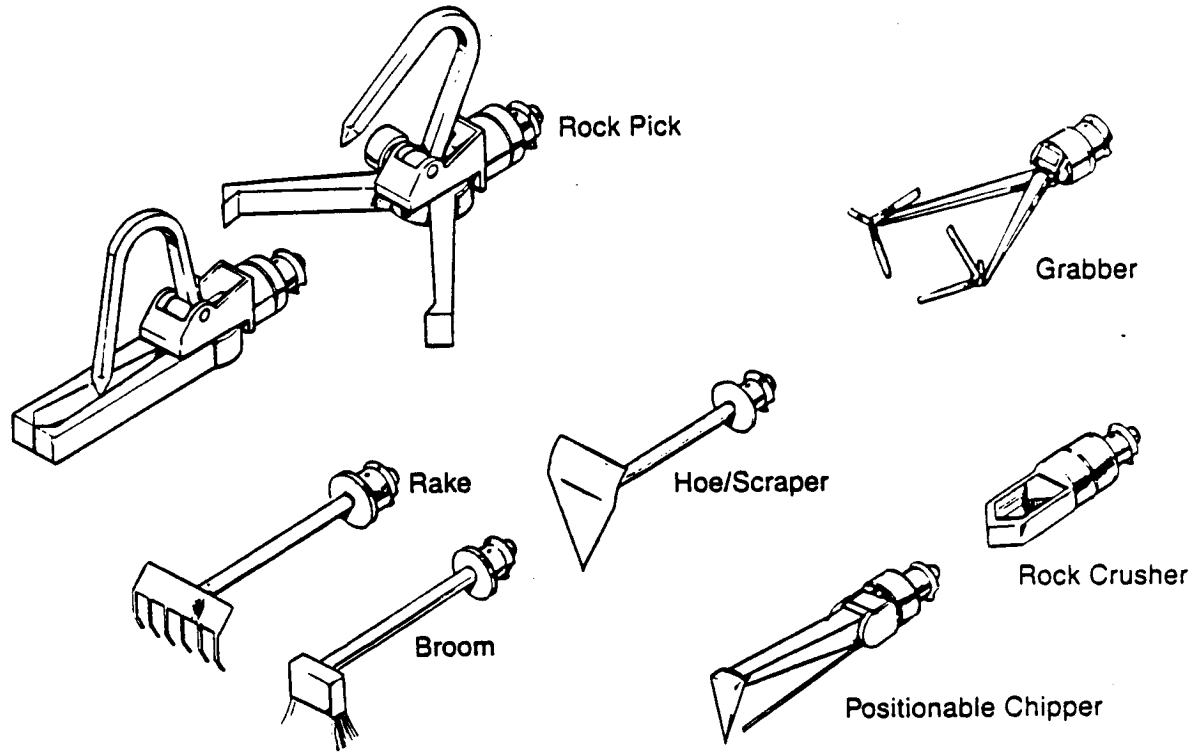

(a) Tools for Rover Strong Arm

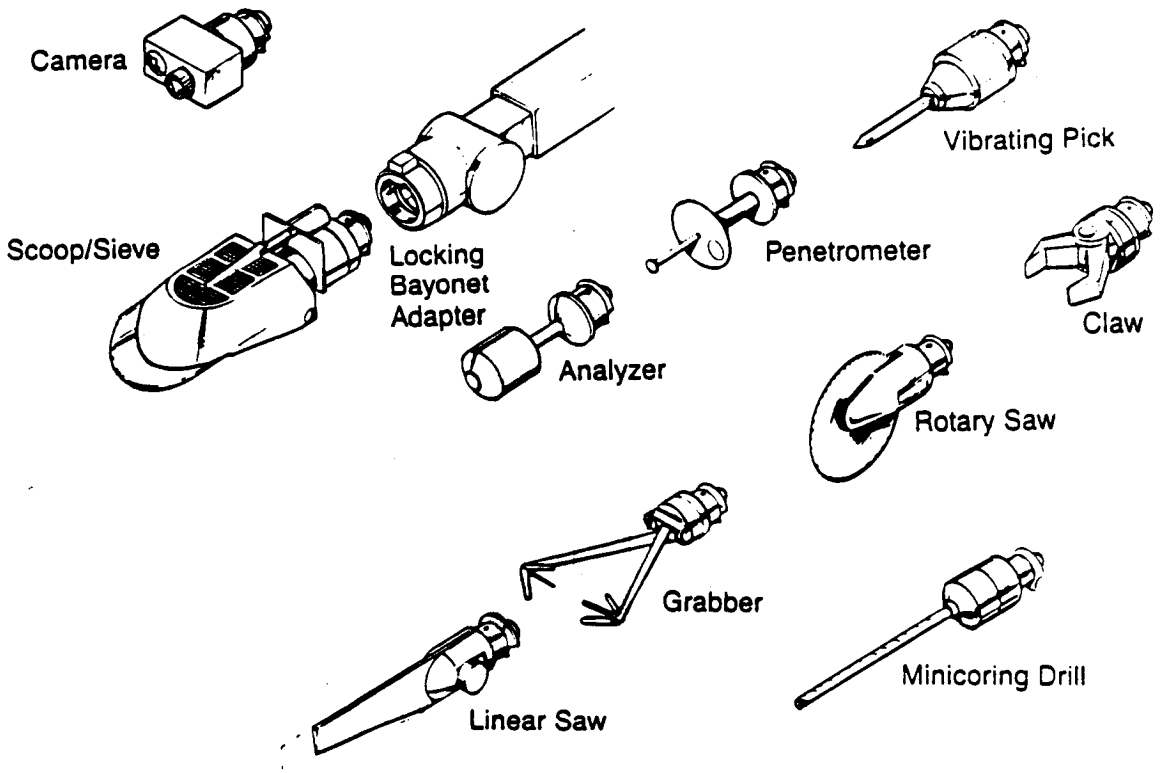

(b) Tools for Rover High-Resolution Arm

Figure 3.4.2-1

Considerable scientific interest centers on bedrock and the weathered rinds of larger rocks, so a method for sampling these is also highly desirable. Samples of larger rocks can be produced by chipping or crushing to obtain representative fragments. Alternatively, samples can be obtained by coring, or by sawing a wedge from the rock. Chipping tools can act either on loose, movable rocks or on implanted rock, such as a large boulder or bedrock slab. Loose rocks must be held stationary by a rover arm or other device before they can be processed. Rock-holding mechanisms for each arm are pictured in Figure 3.4.2-1a. These tools use two hinged levers, each with three stiff splayed fingers to capture a rock from opposite sides. The fingers interleave, so that the tool is extremely flexible in terms of the size of rock it can hold. An impact chipping or sawing method would then be used on the rock by a second, independent tool. For soft or frangible rocks, crushing can be used to reduce the rock sample size without excessive forces. A mechanism to hold and crush a rock is pictured in Figure 3.4.2-1b. This can hold a moderate range of rock sizes, or can be closed on a protuberance of a larger rock. A slow drive, such as a rotary screw drive, closes the jaws and crushes the rock or clod. This method is not appropriate for hard rocks because extremely high forces are required to break most hard rocks by slow crushing.

There are several methods for obtaining fragments from a stabilized rock. Shown in Figure 3.4.2-1 are a vibrating pick which operates by weakening sections of the rock with steady vibration, and spring-loaded chippers that break off small chips or flakes by the impact of a sharp edge. There are two versions of the chipper: (1) a spring-loaded sharp pointed pick with attached gripping hands, and (2) a pick with an attached positioning sensor. The gripping pick can be used on loose rocks or boulders with an irregular surface. The positionable pick allows selection of a promising spot on a boulder for chipping, and can be maneuvered to chip a sample from the exact selected area.

Another approach is to use explosive charges to break the rock apart. A shaped explosive charge on the end of the rugged manipulator arm would impact the rock and detonate, shattering the rock. A wire cage around the rock would contain flying chips, and a pan underneath the cage would collect suitably sized rock samples that fall through. This method is probably unsuitable because of hazard and contamination concerns.

A large sledgehammer can be attached to the rover and used to break chips from medium-sized rocks, boulders, or bedrock. The head of the hammer would constitute a large mass penalty and so should be designed as a lightweight hollow head filled by Martian fines after landing. This device could also be used in the acquisition of seismic data. A small recorder unit placed on the ground some distance away could measure the seismic waves produced by the sledgehammer striking either bedrock or an impact plate on the soil surface. The seismic information, essential to the measurement of bedrock depth, could be taken while the rover breaks rock at several different locations. Data on the receiving units could be stored in a reusable solid-state memory, and transferred to the rover as each unit is retrieved.

A compact device has been developed specifically for the purpose of crushing rocks in a Martian setting. This rock crusher, pictured in Figures 3.4.2-2 and 3.4.2-3, uses a spring-loaded head and an anvil to repeatedly impact a contained rock. This tool would be used on rocks that are acquired by the manipulator arms or sieve mechanism. The arms and other systems on the rover could work independently of the rock crusher, simply selecting appropriately sized chips for permanent storage when the operation was completed.

Coring and sawing are methods that obtain more representative samples of the entire depth of a weathered rock rind or stratified rock. Either the linear or rotary saw can be used to cut thin wedges or slices of a gripped rock or large boulder. Core drilling can also be used on either small rocks or large boulders, but a special technique may be required to remove the rock sample core from a boulder. When a single hole is drilled, the base of the core may not break off and permit its removal. Thus, if the first core is not recovered, a second hole is drilled at an angle to the first, Figure 3.4.2-4. The base of the second core will break off at the point where it intersects the first hole, allowing facile removal.

The rock cores could be taken by the regolith drill, but this results in large rock cores and stringent requirements for ruggedness of the regolith drill. A preferable concept may be to take rock cores about 0.5 cm in diameter, which are more readily acquired by a rugged mini-drill.

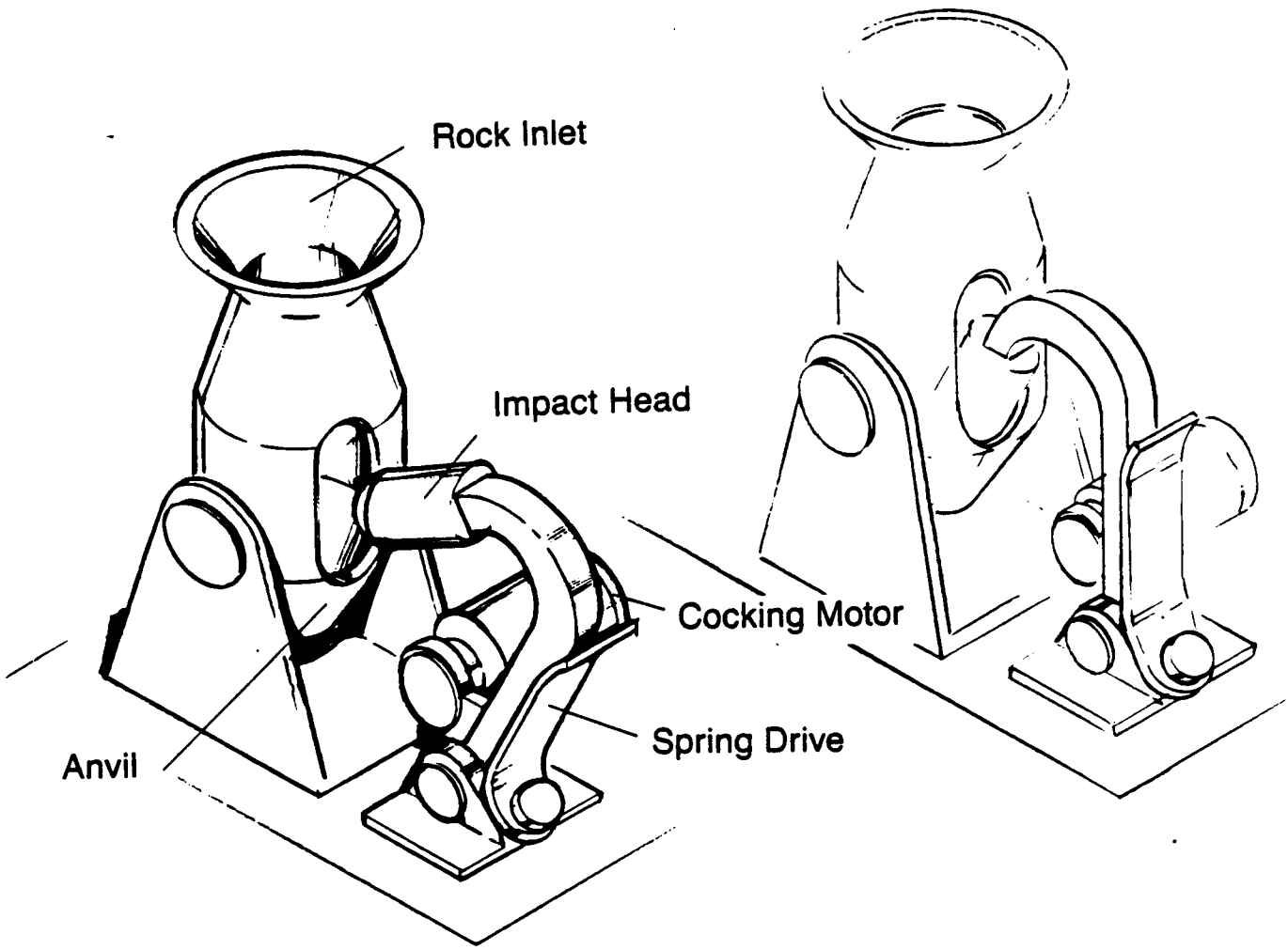

Figure 3.4.2-2 Rock Crusher

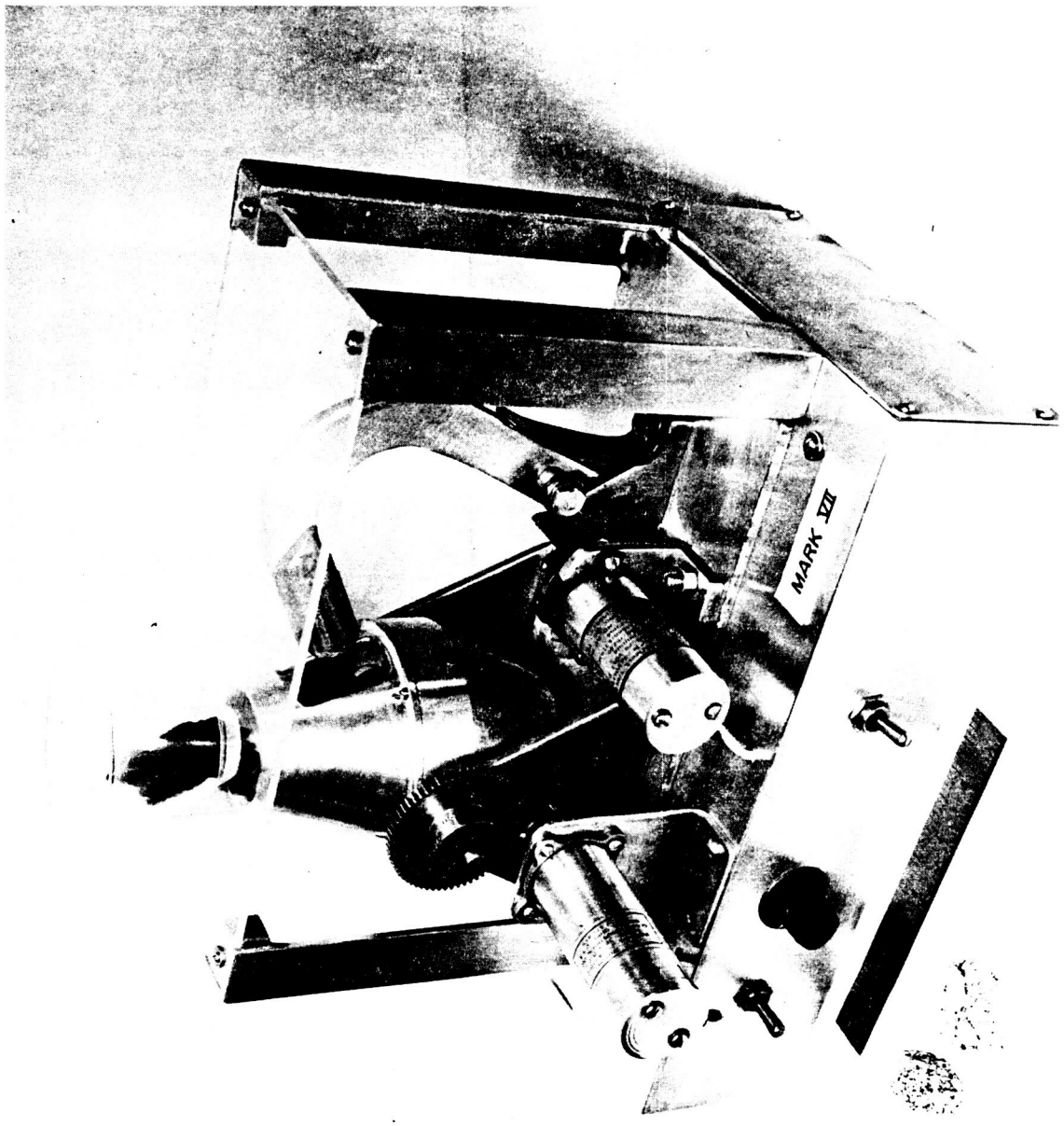

Figure 3.4.2-3 Rock Crusher

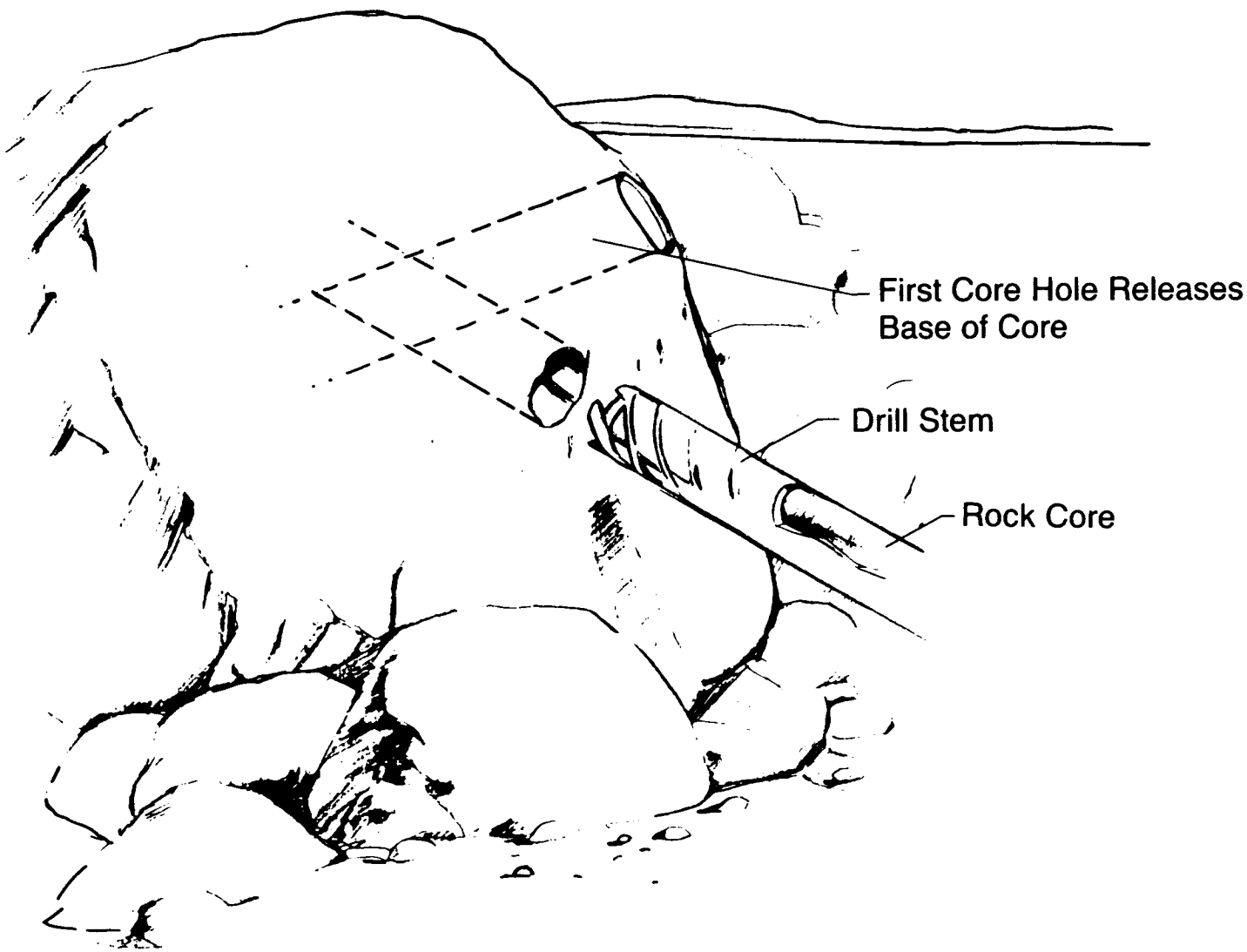

Figure 3.4.2-4 Acquisition of Rock Core by Angled Drilling

3.4.3 Total Returned Samples

A selection of methods for sampling will allow not only redundancy, but flexibility in the types of samples collected and ease of operation as each tool can be optimized for each material. Taking a wide variety of samples has the potential for highly leveraged scientific payoff. Some desired sample types are described in Table 3.4.3-1. With sufficiently small samples, hundreds can be returned in an appropriately adaptable sample return canister. Table 3.4.3-2 demonstrates possible return loads for three different returned sample masses. The large number of samples allows sampling not only of many sites, but more thorough sampling of selected sites and a greater variety of sample types.

3.5 DRILLING

3.5.1 Drill Design

Design of a drilling system involves consideration of the power system, the stem design, the bit design, the method for withdrawing a core or sample, and the materials used. The primary requirement on the drill system is that it have the capability to acquire a core. This eliminates the use of solid drill bits, or other novel methods of drilling: i.e., laser, erosion, spark, explosive, etc., as in Table 3.5.1-1. A solid drill bit can be used if only a rough sample of the material is required, and the ejected cuttings constitute sufficiently representative material. The next requirement is that the core be relatively undisturbed during the sampling process, especially with regard to its thermal state. This eliminates many of the methods that have been used successfully in the Antarctic, such as thermal, erosion, and electrolytic drills. These drills can produce a well-consolidated core in icy materials, but the outer surface of the core has been melted and refrozen. Because a sample return mission will probably be using a much smaller diameter coring drill than these Earth-based rigs, an unacceptably high fraction of the core would be disturbed. The only approach that would allow use of these drilling methods would be to take a large diameter core (at least 8 cm) and then subsample the core to keep the returned sample mass low and the sample relatively undisturbed. A larger drilling rig will require proportionately more mass of equipment shipped to Mars. These methods are also not

Table 3.4.3-1 Criteria for Scientific Sampling (Mars)

Type	Mass (g)	Volume (cm^3)
A. Small rocks (density 2.5 to 3.5 g/cm^3)		
1. Size		
Major dimension: 0.5 to 2 cm	.05 to 22	.02 to 6.3*
	*Assumes 2 cm dia. x 2 cm high	
2. Quantity		
Required: 10		
Desired: 1000		
B. Regolith fines (density 0.8 to 2.5 g/cm^3)		
1. Scoop sample		
Half-cylinder, 1 cm I.D., 5 cm long	1.6-4.9	2.0
2. Drive tubes		
.2-.4 cm I.D.,10-25 cm long	.24-8.0	.785-3.1
3. Drill cores		
a. Drill core diameter		
For scientific analysis: 0.5 cm	10-31.4 g/m	19.6 cm^3/m
Minimize thermal processing of sample:	TBD cm	
b. Drill depth		
To exceed Viking depth: 0.23 m		
To reach permafrost zone, 45° latitude:	7 m	
To reach permafrost zone, 60° latitude:	0.3 to 2.3 m	
To reach permafrost zone, 80° latitude:	0.2 to 1.8 m	
(note: basalt to montmorillonite)		
c. Secondary sampling		
0.4 cm dia., at 1 cm intervals (40%)	5 to 13	5 (100 samples)
C. Duricrust		
1. Peds and clods	same as A.1	
see small rocks		
2. Stratigraphically preserved		
see regolith drill cores (covered in item B.3 above)		
D. Large rocks and bedrock		
1. Lithic fragments (chips)		
a. Size		
0.5 to 2 cm	same as A.1	
b. Number		
Required: 1		
Desired: 100		
2. Core drill samples from large rocks and bedrock		
(note: Shallow cores of specific locations on large rocks are of greater interest than random chips to the exobiologists and weathering scientists)		
a. Size		
0.5 to 1.0 cm diameter		
0.5 to 4 cm long	0.25 to 11	0.1 to 3.1
b. Number		
Required: 1		
Desired: 100		

Table 3.4.3-1 (concluded)

E. Atmospheric dust		
1. Settling dust		
Cup collector: 10 cm dia. x 0.2 cm tall	12 to 38	15
2. Saltating particles		
Multiple windsocks, ground level to cup collector	5 to 20	TBD
F. Atmospheric gas		
1. Total sample		
will be obtained when containers sealed		N/A
2. Concentrated sample		
cold molecular sieve		
G. Engineering materials		
Purpose is to test degradation effects (erosion, corrosion, thermal stressing) on key materials		N/A
100 ea. of 1 cm-dia samples, in cap, bottom or insert		

Table 3.4.3-2 Returned Samples from Mars

Sample Type	Number in : 1 kg	2 kg	5 kg
Rocks, chips, duricrust clods (0.02-6.3 cm^3 ea)	47	92	263
Regolith scoops (half-cyl, 1 cm dia by 5 cm)	5	10	25
Regolith drive tubes (0.5 cm dia by 20 cm)	15	30	50
Regolith cores (1 cm dia by 1m, subsampled)	5 m	10 m	20 m
Rock cores (1 cm dia by 4 cm long)	12	25	50
Settling dust (cups @ 10 g ea)	1	2	3
Saltating particles (10 g ea)	2	3	5
Total samples	87	172	416

Table 3.5.1-1 Mars Drilling Approaches

- Rotary
- Rotary-Percussive
- Independently Programmable Rotary Percussive (IPRP)
- Exotic
  - Thermal
  - Explosive
  - Spark
  - Calyx (pellet drill)
  - Erosion
  - Ultrasonic
  - Plasma
  - Electron Beam
  - Laser
  - Chemical

extremely flexible in terms of the type of material that they will operate in, which is a critical factor for Mars with its potentially wide range of materials.

The approach that fits these multiple requirements best is a rotary-percussive drill. This device is ideal for coring, and can be made as small as necessary. The smallest standard size is about 3 cm (1.3 in.) in diameter but there are no inherent reasons that the drill could not be made smaller with appropriate choices of materials and drive system. It is commonly used for exploratory drilling because the rotary-percussive action operates well in many material types. Rotary drills have been found to be optimum for soft soils and some soft rock for hard rocks, excessive axial bit pressure is necessary for cutting in rotary mode. The percussive mode is often used for these harder rocks. When the two are combined, they can drill a large range of geologic materials.

With new advances in automation and Artificial Intelligence (AI), it is possible to improve the system over the normally fixed percussive and rotation rates. The most effective method of drilling will be different for different materials, varying from rotation alone to pure indexed percussion. For example, for certain materials a harder percussive blow, faster rotation, or higher axial force will produce more efficient, minimum disturbance drilling. A drill that can respond to the situation and modify its operating parameters to fit the conditions would have major advantages over conventional drilling techniques, especially when the subterrain is to a large extent unknown and could contain heterogeneities. This is the advantage of the independently programmable rotary and percussive (IPRP) system suggested herein. A microprocessor oversees the drilling operation and not only responds instantly to the type of material being drilled, but monitors the effectiveness of the cutting and acts accordingly. The microprocessor would have a feedback capability; the memory would begin operation with a certain set of parameters for assumed material properties, vary the drilling operation as necessary, and store the information about all parameters as drilling progressed.

The depth requirement for both a comet and the Martian surface is that the drill be able to sample one meter or more in depth. Because one-meter-long core samples cannot be returned within proposed spacecraft configurations, some type of sample folding or subsectioning is required. Subsectioning can be done by physically cutting the stem, using either sectioning or mini-coring; by having presectioned, separable sections of the drill stem or core liner; by using a full-length drill stem that is flexible and thus does not require a meter-long space; or by pushing the core sample out of the drill stem into shorter containers. A flexible drill stem has been used successfully by the Soviets on their Luna 24 mission, and it is attractive in that it requires a minimum of extra equipment for sectioning and capping. However, all sample material collected in a single coring operation must be returned, which will limit the variety of returned samples severely. Also it has inherent reliabilty problems in terms of strength of a flexible drill stem, and the problem of trying to coil the flexible stem if there is a rock or dense soil section in the core. The inner liner, rather than the stem, could be made flexible for storage, but strength and folding around a rock are still factors of concern. The concept of forcing the sample out of the drill stem, Figure 3.5.1-1, involves high probabilities of cross contamination, redisturbance, and intramixing of the core sample, and possibly loss of sample. It does allow selection of returned samples to some extent, lowering the required return mass; because of the ease but inexactitude of this method, it could be used in conjunction with another subsectioning method. A presectioned stem or short liners offer the advantage of no additional subsectioning, along with some capability for selection of desired samples, especially if there is some onboard analysis system. However, a presectioned stem has problems with regard to reliability and sealing of sections after they are separated. Short liners, if they can be developed into a practical method, offer many advantages, but share the problems of any liner system, as discussed below. This type of internal liner was developed for the Apollo mission; careful analysis of its performance should be made to more fully understand the features of this idea.

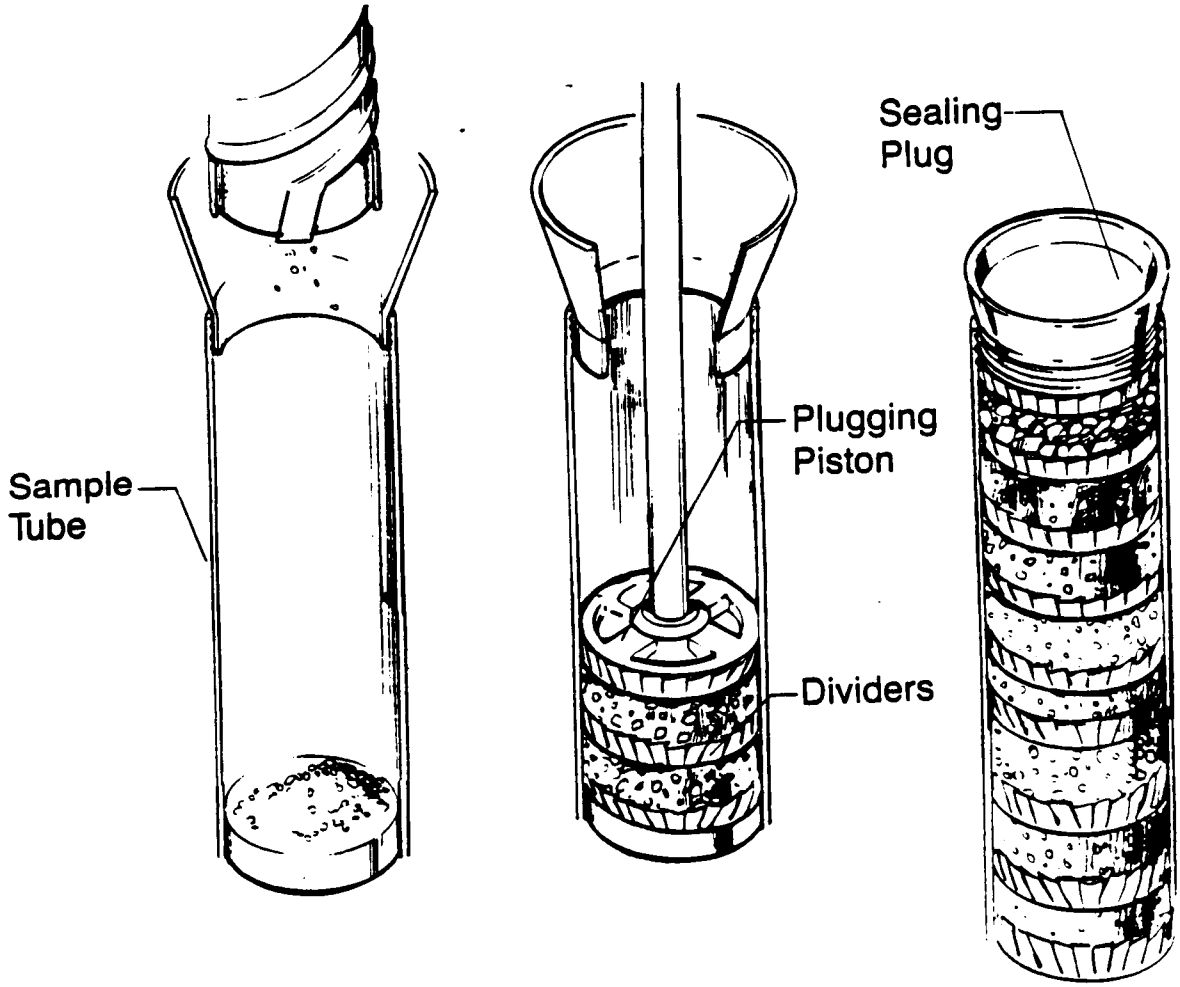

Figure 3.5.1-1 Storage of Regolith and Lithic Samples

Physical cutting of the drill stem to separate the core has the disadvantage of secondary heating of the sample, but allows selection of returned samples. Use of a saw to linearly section the stem disturbs only the material near the cut, but involves problems with storage because the full sections may be difficult to seal. If the saw distorts the stem shape, the section will not seal well with end caps and also will be difficult to fit into its assigned storage space. However, a saw would have other uses such as subsectioning of rock, as shown in Figure 3.5.1-2.

Subsampling of the drill stem, portrayed in Figure 3.5.1-3, allows return of a much smaller but representative fraction of the sample, with provision for selection of the portions to be subcored. A mini-drill could be part of the sampling equipment for other purposes, such as mini-core sampling of rocks. This mini-drill would need to be powerful in order to cut through the drill stem material of the regolith drill, depending on the type of material used and whether it could be pre-holed to some degree. The cross-drilling could produce thermal transients that would have to be controlled. The mini-drill would be operated vertically, and drill upward through the stem, so that no sample would be lost to gravity wasting and no core retainer would be necessary. The sections of drilled-out stem material would act as plugs to separate the subsamples from each other. When the minicorer was filled, it would be sealed at the top and detached from the drill head or rover arm. This mini-corer could be the same diameter as the "soda-straw" drive tubes (0.5 cm) to aid in storage efficiency.

Sealing of the subsamples is also a factor in selecting the method of separation. Some samples should be hermetically sealed when acquired to prevent loss of volatile components. Plugs can be inserted into the tube sections, or the ends can be capped. Either method could use a metal foil crushed between the two surfaces to provide the hermetic seal. Plugs do not have the inherent problem of extending beyond the edge of the tube and wasting storage space; they fit within the envelope of the tube and allow storage in a space just large enough for the tube itself. Both plugs and caps would have serrations matching the surface of each core section, and a metal foil that is crushed along the serrations to provide the seal. The plugs may be

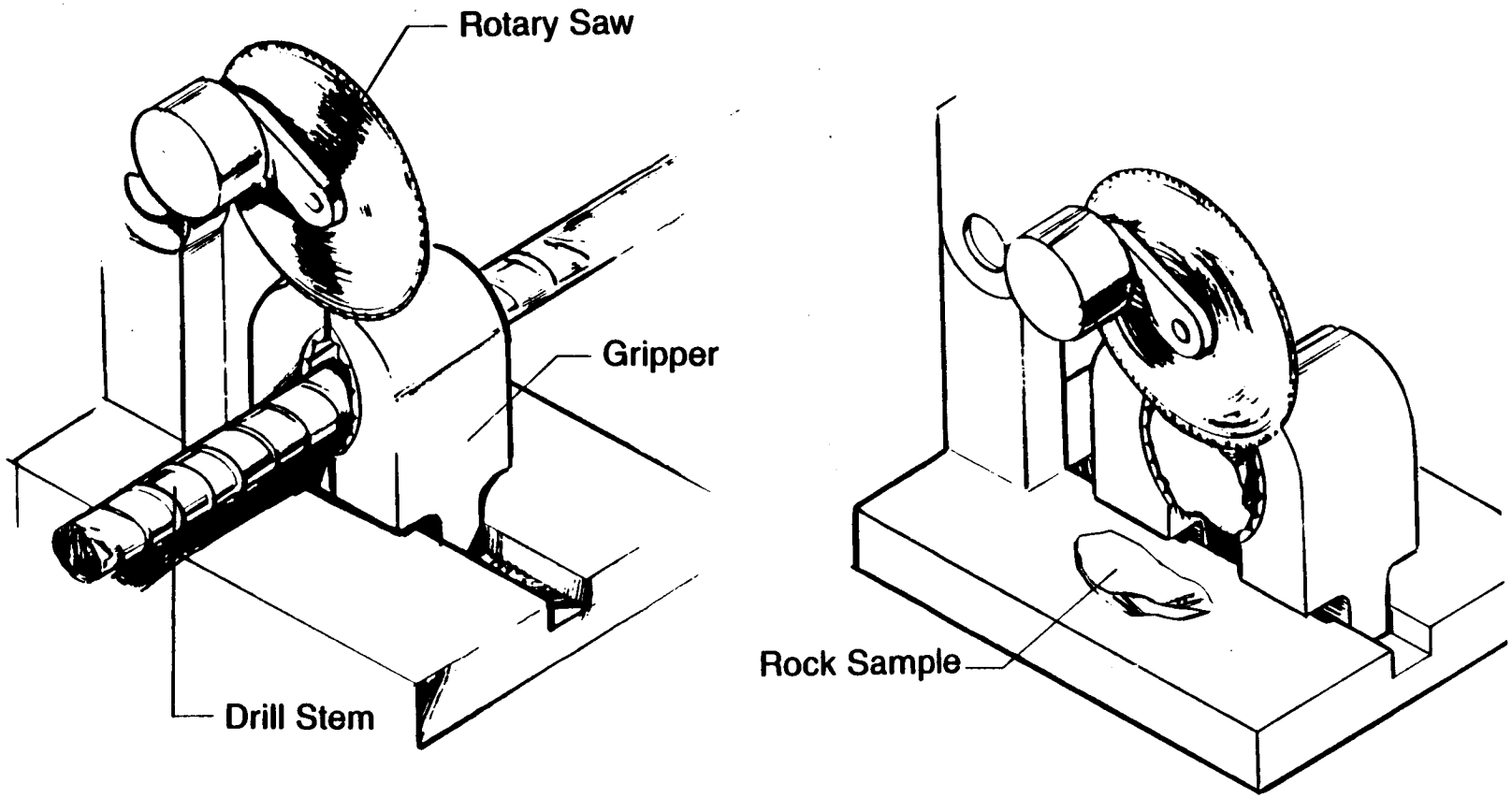

Figure 3.5.1-2 Subsectioning of Drill Stem and Rock Using Rotary Saw

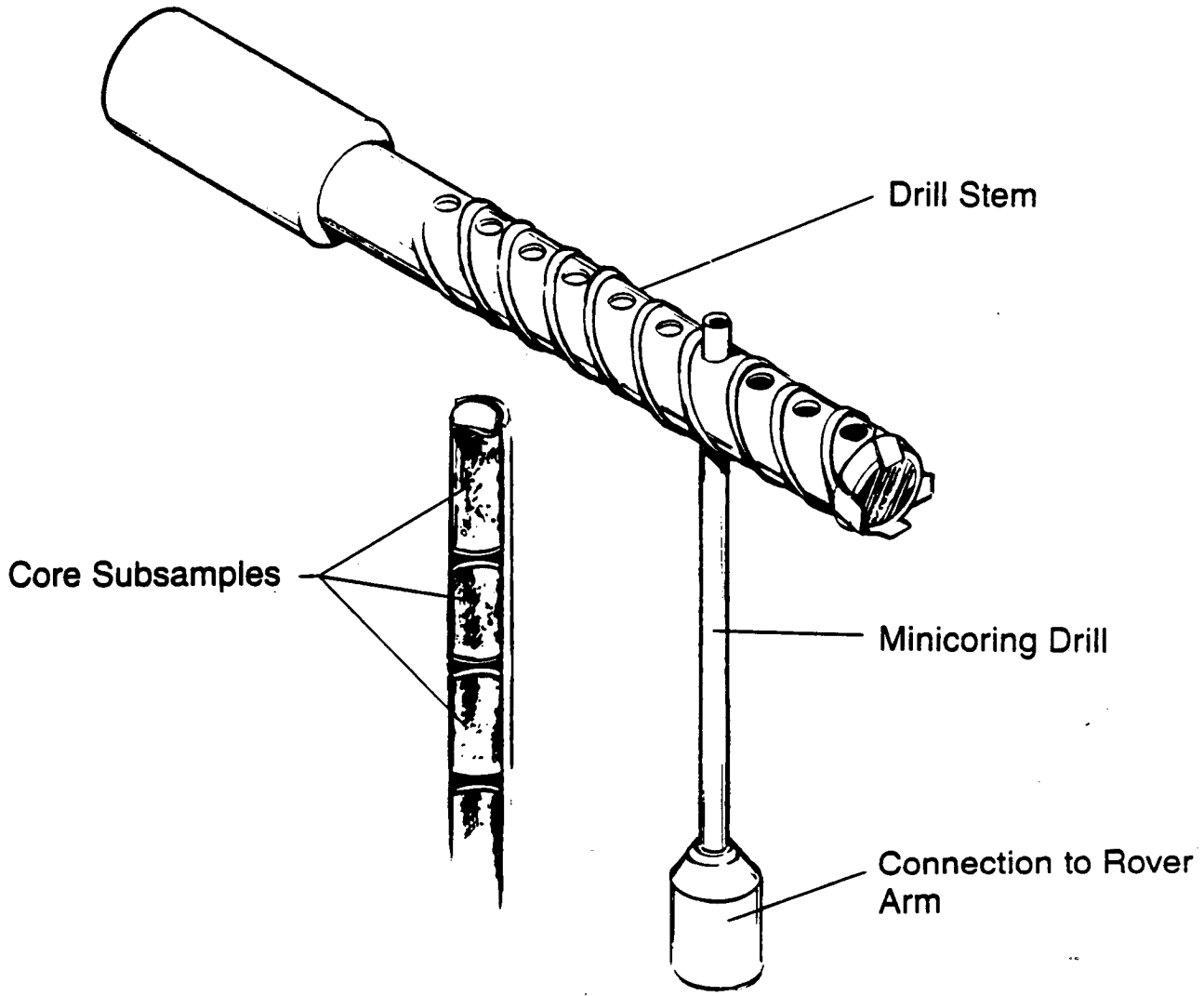

Figure 3.5.1-3 Core Subsampling by Minidrill on Rover Arm

inserted into a tube where some sample has been lost and take up the extra space, thus allowing less sample movement and disturbance, especially during the accelerations of launch and re-entry. However, they are difficult to insert into a full tube section, whereas caps can be placed over a section that is completely full.

To sum up, the method of subsectioning will have a great effect on the design of the drilling system, and detailed study should be performed on several of these methods. Segmented stem and liner designs should be developed in more depth to resolve the engineering concerns, and the mini-drill should be examined for practicality, thermal disturbance, and material selection. Choice of the subsampling method will also depend on the mission emphasis: e.g., low return mass, minimum volumes, redundancy, sample environmental control, etc.

The design of the drill stem and bit is made more challenging by the desired small diameter of the drill. Many drilling concerns and techniques have never been evaluated for a 1-cm diameter drill, and results from larger drills may not be applicable. Thus, though many approaches can be preliminarily evaluated, there is not sufficient empirical data in the literature to make absolute decisions based on past experience. Some decisions may be made through analysis alone, while others will require testing and experimentation.

The single-barrel design of the drill stem uses a single hollow-core barrel with a hollow bit secured to one end. The liner approach uses a double-core barrel, the inner one holding the sample and the outer transmitting the drilling forces. The double-core barrel allows better core recovery under some conditions, because the inner core barrel offers some protection, but it involves a more complex drill design and forces the cutting edge (kerf) of the drill to be wider. A wider kerf will require more drilling energy and cause more sample disturbance. The only compelling reason to go to a double-barrel system would be use of an internal liner that can be removed when filled, with a new one inserted while the drill remains in situ. This would allow several samples to be taken from the same hole, each already a proper length for storage without the need for segmenting. The drill stems themselves could potentially be reused, which could be a mass savings. Concerns with this approach include fitting subsequent liners into the stem that may have become dust-covered, development of a

method for withdrawal of the liners, and transmission of the drive forces to the liner if necessary. There are two options for an inner core barrel: it could rotate with the drill, or remain stationary with respect to the sample. The stationary liner obviously provides more protection for the core sample, but it must be attached to the drill system via a swivel bearing. This bearing is difficult to maintain in a clean condition during drilling, especially when the drilling operation is to be autonomous, with no human maintenance. A rotating liner would cause more sample disturbance, but is simpler to implement. Unfortunately, because the proposed drill size is smaller than standard, information on the amount of increase in sample disturbance is not available from present data.

An additional option that could be implemented with a liner-stem system is a retractable bit. Coring bits capable of withdrawal through the entire drill stem have been developed and used. For very deep drilling this could be an advantage, because the bit can be drawn up for examination or replacement without removing the stem and thus losing the drill hole to collapse. This can only be used with an inner-liner drill design, as the bit must be withdrawn through an empty coring stem. This option adds complexity to the drilling system, but could potentially be of use on more ambitious missions.

The bit for a coring rotary-percussive drill will be a simple core bit face with protruding cutters. Detailed design of the bit involves a number of parameters. For ease of removal, the bit could be threaded onto the drill stem, or this connection can be accomplished with a bayonet lock similar to the arm-tool connection. This would be useful, as stem segments would then fit to one another, the arm, and/or the power head with an identical bayonet connection. It has been found in other coring studies that better core recovery is achieved when the cutters present a smoothly curving surface to the core. Other factors in the design of the cutting edge include cutter spacing, rake angle, relief angle and clearances. General statements about the selection of these parameters can be made by drawing on previous studies, but the final method of selecting most of these parameters must be by testing. Even after testing and optimization experiments, it may be desirable to provide a selection of bits to allow optimum cutting in differing materials, as well as universal bits for less-efficient cutting in all materials.

A core retainer is potentially one of the most important components of a drill, as in certain sample types (e.g., unconsolidated fines) it is possible to lose a high percentage of the sample as the drill is withdrawn. There are two basic types of core catchers, with many variations. The first is spring fingers, or leaves, in a radial arrangement of curved spring metal flaps, as shown in Figure 3.5.1-4a. The fingers are pushed back as material enters the stem, and are biased to spring back into position across the bottom of the stem when forward progression of the drill stops. The fingers can be of varying stiffness and geometry to accommodate the type of material to be drilled. Loose materials require soft fingers that will not impede the entrance of the soil, but closely spaced to prevent loss of soil. Stiffer fingers are used for the more dense soils that would not allow closure of the soft fingers, and are usually more widely spaced because there is less danger of core seepage through the fingers. Soft fingers cannot be used for an extremely dense soil, as they do not have sufficient spring force to penetrate and grip the core. A variation of this is the polymeric sleeve, which is used for very soft soils, and completely closes off the opening of the drill when drilling ceases. A concern with many of the finger type core catchers is that the fingers protrude into the stem opening and impede sample acquisition during drilling. One way to avoid this is to conceal the fingers behind the end of the liner or a secondary flap so that the fingers are only allowed to spring out when the drill is withdrawn. This is complex mechanically, increases the stem wall size, and thus adds to the drill kerf width, and usually entails the loss of the first portion of core during the lag before the springs are released. The fingers can be held back and released electrically, but this adds to the complexity and cutting area of the drill. The fingers could also be oriented horizontally and held back behind the end of the bit or liner, or a machined-in shelf. Thus there would be very little lag; as soon as the stem began to raise the fingers would spring out and close off the opening. Again, this causes the drilling kerf to be wider, but this method does not introduce any impediment to entrance of the core. This is not a standard form for a core-retainer, and would have to be developed and tested.

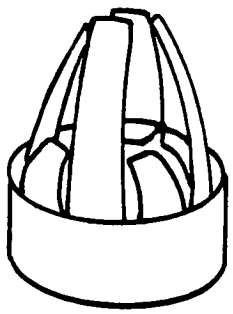

Ⓐ Spring Type

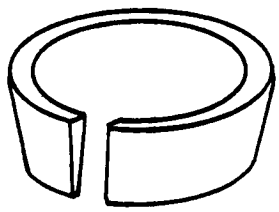

Ⓑ Split Ring Type

Figure 3.5.1-4 Core Retainers

A split-ring is the second type of commonly used core catcher. This is a beveled ring that fits into the bit, as shown in Figure 3.5.1-4b. The ring is split so that when pressure is applied on the outside the diameter compresses substantially. When the drill stem is raised, the ring is forced higher into the bit where it compresses and grips the core material more tightly. This has been used with great success in retaining cores of well-consolidated material. A combination method, the modified split-ring, consists of a split-ring with spring fingers at intervals. This is most often used now because it works acceptably in most types of materials.

Other methods of retaining a core that have been used include "burn-in", which is a way of consolidating the section of the core within the bit by running the drill with no forward motion and no flush until the cuttings and heated core clog the bit sufficiently to allow withdrawal without core loss. This is obviously not an optimum method for either undisturbed cores or long lifetimes of the cutting tools. A wire core-cutter has been used in well-consolidated material to aid in breaking off the base of the core. This method uses wires strung along the drill stem to the bit that are pulled taut at the conclusion of drilling. The wires in the bit are drawn away from the walls until they tighten across the center of the core. This effectively cuts the core from the base material, but does not aid in holding the core while the stem is withdrawn. A method developed in Switzerland involves the use of thin metal ribbons that deploy along the inside of the stem as the core enters. These are of great use in drawing up a whole core, but again they require a wider drill kerf and could be difficult to implement in a small stem. Auxiliary core barrels are a method for preserving a high percentage of the core without using a wide drilling kerf. The sample is drilled with a single-barrel core drill, and then an auxiliary core barrel, larger in diameter, is drilled or pressed down around the original drill stem. Either a core retainer or activated flaps on the second barrel then serve to hold the core in as both the auxiliary and original stems are raised together. An auxiliary barrel of this type could be taken on the mission, and used only if an extremely noncohesive soil is encountered.

A core catcher is necessary only if the unsupported core is likely to be lost from the stem during withdrawal. Most commercial drilling operations use 3 to 5-inch diameter drills that generally need some type of core-catching device. However, the smaller drills are less likely to lose core as there is a larger ratio of support area to core mass. Very little operation has been done with a drill as small as the one proposed for a Mars sample return mission, 1 cm in diameter. For this reason, it is difficult to know if a core catcher will even be required. Experimentation would have to be performed before a final recommendation could be made. The general core catcher to use could be a modified split-ring, and the bits could be designed so that the drill can be run either with or without the core catcher. A selection of soft-finger spring core catchers could also be part of the equipment, as loose, unconsolidated material is most likely to require the use of a core catcher.

Another drilling tradeoff is the question of whether to use a drilling flush to aid in removal of cuttings. Choosing to do so has a great effect on the amount of equipment required for drilling. A flushing system requires a compressor, lines for routing gas through the drill stem, and bottom flush holes in the bit. A liquid is eliminated as an option for the flushing fluid because of the probability of extensive contamination of the core. The Martian atmosphere could be compresssed to provide flush gas, which minimizes contamination of the sample, but allows condensation onto the stem gas lines, within the core or on the outer surface of the drill. The advantages of a flush are that it is the best way of removing cuttings from the hole bottom, it carries heat away from the bit and sample core, and once installed it would have several other uses. Gas jets can clean off work surfaces, moving parts, camera lenses, and rock surfaces. Compressed gas can be used as the impulse for low force drives. The proper implementation of a compressed gas system would also allow its use for a pneumatic impact drive: the simplest way to achieve the percussive action of the drill.

3.5.2 Thermal Impact of Drilling

Rigorous scientific analysis of samples returned from another planet or comet requires that the samples be preserved in a condition as close as possible to their original *in situ* state. The sample condition includes chemical, physical, phase, and thermal states and

environments. Both Martian and cometary material will contain important scientific information in the form of physical structure, composition, phases and proportion of ices, and elemental composition/mineralogy of the grains. This information could be lost by heating of the sample, which would change the phase of the components and allow migration or escape of the volatiles. A thermal analysis of the drilling operation is important because drilling will be the first contact with the sample where thermal alteration is possible. Drill cores of deep regolith are the material most likely to contain permafrost and thus are vulnerable to thermal transients. After the drilling operation, selected core samples will be sealed as quickly as possible. All other thermal transients such as solar and planetary heating, launch, Earth orbit insertion, and transit to testing facilities could heat the sample to cause phase change and, under extreme conditions, could cause actual loss of vapors from the sealed but safety-vented container. The thermal transient during drilling is one of the most important to control because it can cause alteration of the sample before it comes under the control of the rover or spacecraft equipment.

A second, but more pragmatic reason for this analysis is to determine the difficulties that may be encountered in drilling: inordinate heating of the drill stem and bit, melting of the drilled material at the bit, and refreezing of the cuttings as they progress up the drill stem. This problem was observed in an earlier study in which the Apollo Lunar Drill was tested in a simulated Martian permafrost. The drill did not cut through the ice/soil conglomerate without material melting at the drill bit and refreezing in the spiral flutes, and stuck fast in each test after relatively little progression, its flutes so packed with frozen cuttings that it could no longer penetrate. However, many aspects of this test did not fully simulate the true space drilling environment because it was performed in air, with the drill initially at room temperature and a small, relatively warm sample bed (stabilized at -50°C as compared to -140°C for a comet or -50 to -90°C for Mars). Also, the ice/soil bed was constructed to give the hardest possible drilling conditions; it was said to approximate the drilling hardness of basalt. This is not a

normal characteristic of natural permafrost deposits, although it may constitute the "worst case" drilling environment for engineering design purposes.. It is recommended that the thermal predictions described below be verified by testing under conditions that more closely approximate the true environment of the mission than did these earlier tests.

The thermal analysis was performed to gain understanding of the drilling conditions that would exist in a colder body, under low pressure, with a drilling system at the ambient temperature. Two Martian environments were selected: a temperature of 185 K for the polar cap regions where material would be mostly ice, and 215 K for the nominal Martian subsurface, nonpolar regions that could contain soil, ice, lithic fragments, and bedrock. Many variables could not be evaluated in the thermal model: the loss of vapors as the ices sublimate upon exposure to vacuum, the actual microscopic heating patterns at the cutting edges, the heating due to inefficiencies in the power head, the progression of the drill through an extended length of variable media, the variation of regolith temperature with depth, and the detailed transient effects as heated cuttings progress upward along the outside of the drill stem.

Material Properties--The thermal effect of the drilling process depends to a great extent on the characteristics of the sampled material: how hard is it to drill, how fast does it transfer heat, and how readily does it heat up. A range of drilling and thermal parameters have been developed from the wealth of data available on characteristics of soils and permafrost on Earth, and the existing data on comets and Mars. The three parameters studied for the sampled material were the energy for drilling or cutting, thermal conductivity, and specific heat. Ranges for specific energies were taken from two papers on drilling from the Cold Regions Reseach and Engineering Laboratory (CRREL): Mellor, et al., 1975 and Mellor, 1977. Other properties were taken mainly from another CRREL monograph: Thermal Properties of Soils by Omar Farouki. Density is intimately related to these properties; soil and rock densities from 1.0 to 3.5 g/cm3 are assumed for Mars. The Martian soil density at the Viking-1 landing site has been measured to be 1.10 $\pm$ 0.15 g/cm^3 (Clark et al., 1977). A density commonly used as a planetary regolith average is 1.5 g/cm^3; basaltic material has a density of 2.8 g/cm^3, and some porous igneous material has been estimated to be as low as 0.12 g/cm^3.

The specific energy required to progress through a certain material depends on the method of cutting, as well as on the characteristics of the material itself. The specific energies used are for drilling methods similar to the proposed method, and are used to estimate the heat energy that passes into the soil per increment of cutting depth. Specific energies for many different materials are shown in Figure 3.5.2-1; the potential range corresponds to changes in temperature and drilling method, material variation, and the variation observed in actual testing. Test data for the Apollo Lunar Drill heating is within the specified range: 66 J/cm^3 for 40% vesicular basalt and 190 J/cm^3 for dense basalt. These values were measured only for the outer drilled material using a solid bit drill, so they cannot be used directly for computation of heating with a coring drill. However, it is important that these tests show the same order-of-magnitude specific energy as other drilling tests and theoretical calculations.

Specific heat and thermal conductivity are absolute properties that depend only on the material characteristics at a specific temperature. Thermal conductivity is not precisely defined for either comets or Martian soil, and terrestrial values must be modified to account for the additional thermal conductivity provided by the presence of air in the soil interstices. Thermal conductivity was assumed to be proportional to density for the lower densities where no data were available. Ranges of thermal conductivities for silts and sands with percentages of ice content from 0 to 100% are shown in Figure 3.5.2-2. The variation of thermal conductivity with temperature was accounted for in that for ice-laden soils it decreased from the values at low temperatures to values at the two selected Martian temperatures because there has been shown to be a major increase in the thermal conductivity of ice with decreasing temperature (about 60% increase from 215 K to 130 K). It was not varied with the slight increase in temperature while thermal modeling the drilling, simply because this would have had no noticable effect. As can be seen in Figure 3.5.2-3, thermal conductivity increases rapidly with an increase in ice content. Thermal conductivity for dry Earth soil encompasses a wide range, due to the type of soil, and increases slowly with an increase in density. With the addition of ice, the thermal conductivity begins to vary quite sharply with the density. This can be explained by the fact that while

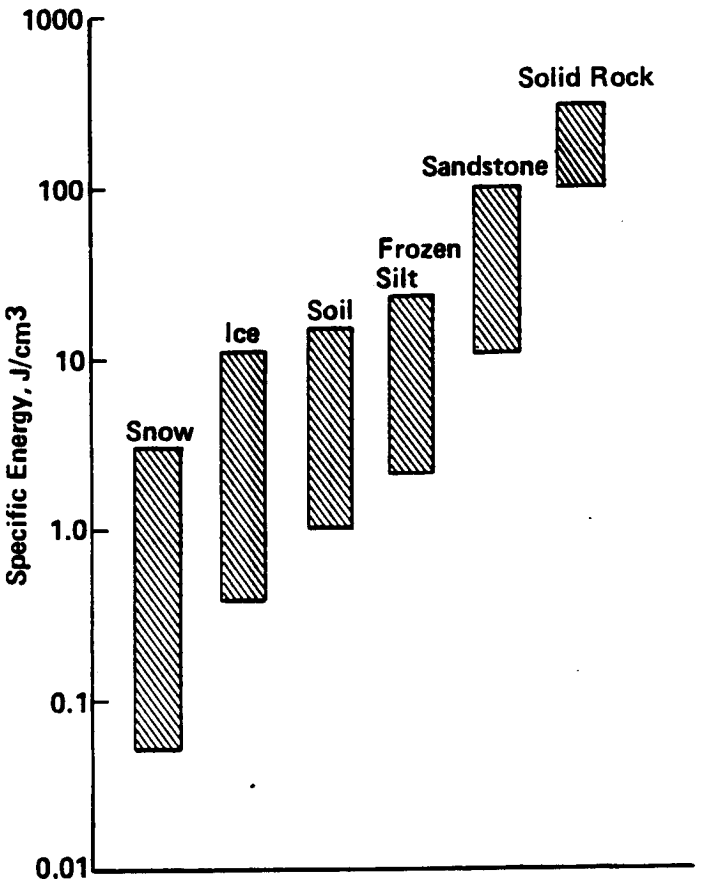

Figure 3.5.2-1 Specific Energy of Cutting for Various Materials

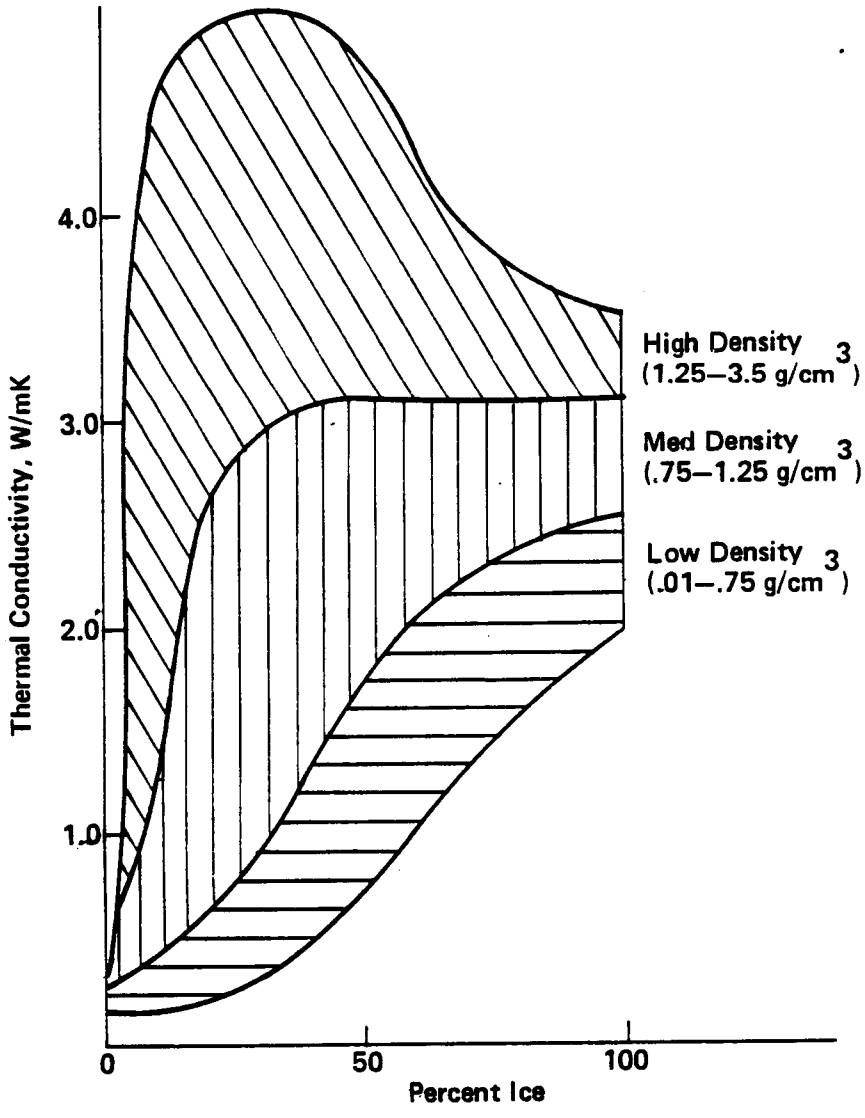

Figure 3.5.2-2 Variation of Soil Thermal Conductivity with Ice Content

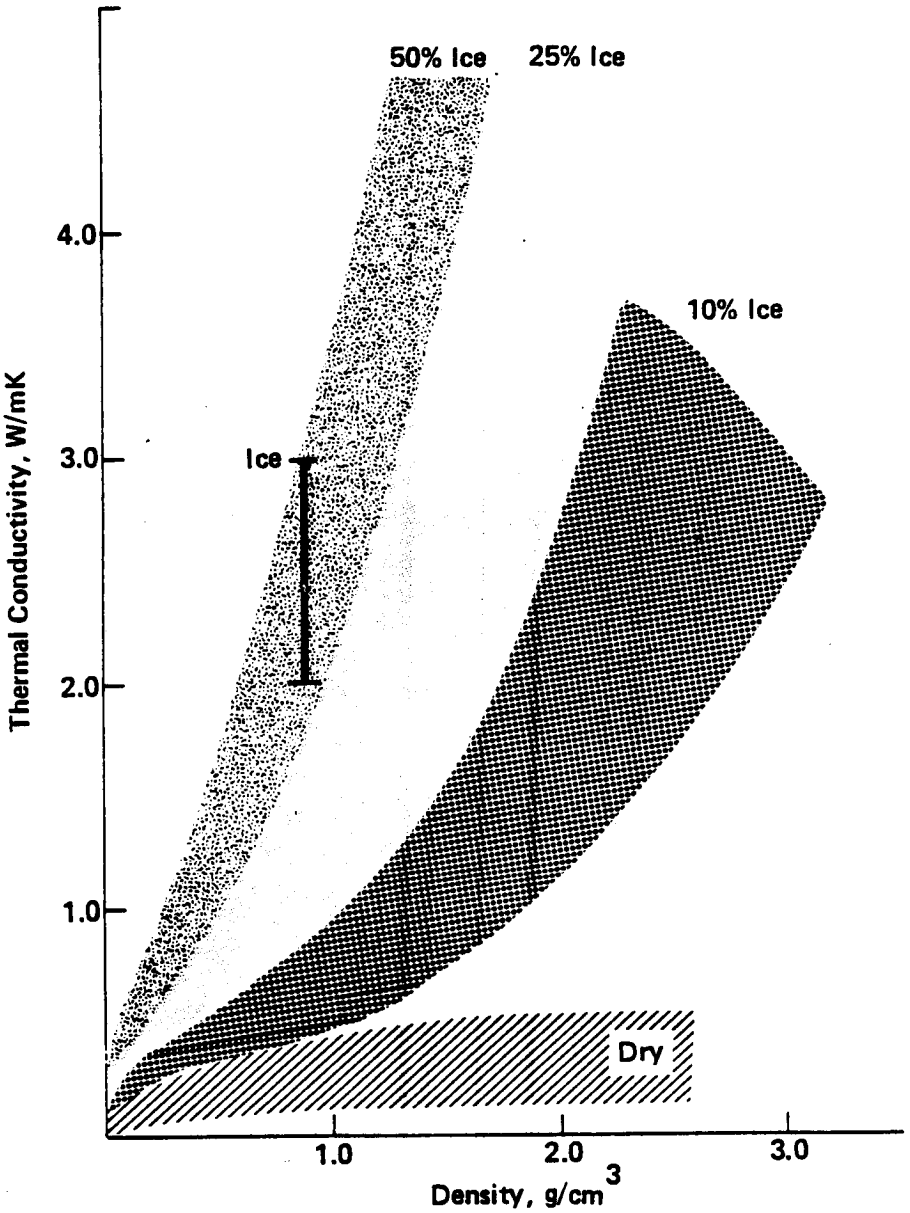

Figure 3.5.2-3 Variation of Soil Thermal Conductivity with Density

dry soil particles have only single-point contacts and so do not conduct markedly more when compressed, ice filling of pores will provide bridges between soil particles and greater conductivity as pore volume decreases. Rocks have a higher thermal conductivity than the soils because the individual particles no longer have a high contact resistance but are in intimate thermal contact in the rock structure. Measurements of the thermal inertia of the Martian surface have shown expanses of material that may have extremely low thermal conductivity. These materials are probably very fine dry particles with a low in situ density.

Specific heat is the parameter that most directly affects the temperature rise of the drilled regolith soil. A low specific heat material will undergo larger temperature fluctuations at the drilled area, and will respond quickly to nearby temperature increases. Specific heat varies with the type of material (i.e., silt, granite, etc.) and is linearly dependent on ice content, as ice has a much higher specific heat than typical soils. The applicable ranges are portrayed in Figures 3.5.2-4 and 3.5.2-5. The range of specific heats for Martian materials was somewhat higher than for comets because of the higher ambient temperature; the range is 0.3 to 2.2 J/g K, depending on the type of material. The specific heat used in nominal model calculations for a dry soil was 0.65 J/g K; the planetary average for Mars is usually taken as 0.84 J/g K. Other calculations were performed for extreme values of 0.3 to 2.2 J/g K.

The values used for each of these parameters are documented in Table 3.5.2-1. Also shown is the thermal inertia, $I=(\rho C_p k)^{1/2}$ for each case, where ρ is density, Cp is specific heat, and k is conductivity. Theoretical and calculated data for planets and comets is usually given as thermal inertia rather than separate values for specific heat, density, and thermal conductivity. The thermal inertia value can be utilized as a check of ranges, but not for unique definition of the specific parameters. The thermal inertia on the surface of Mars has been measured on a 120-km x 120-km scale to be in the range 1.6 to 12 x 10^{-3} cal/cm^{2}s$^{1/2}$ K. The low thermal inertia values are large expanses with fairly uniform surface properties; materials in this area with a lower thermal inertia are unlikely. The higher thermal inertia values are in locations due to areas of high

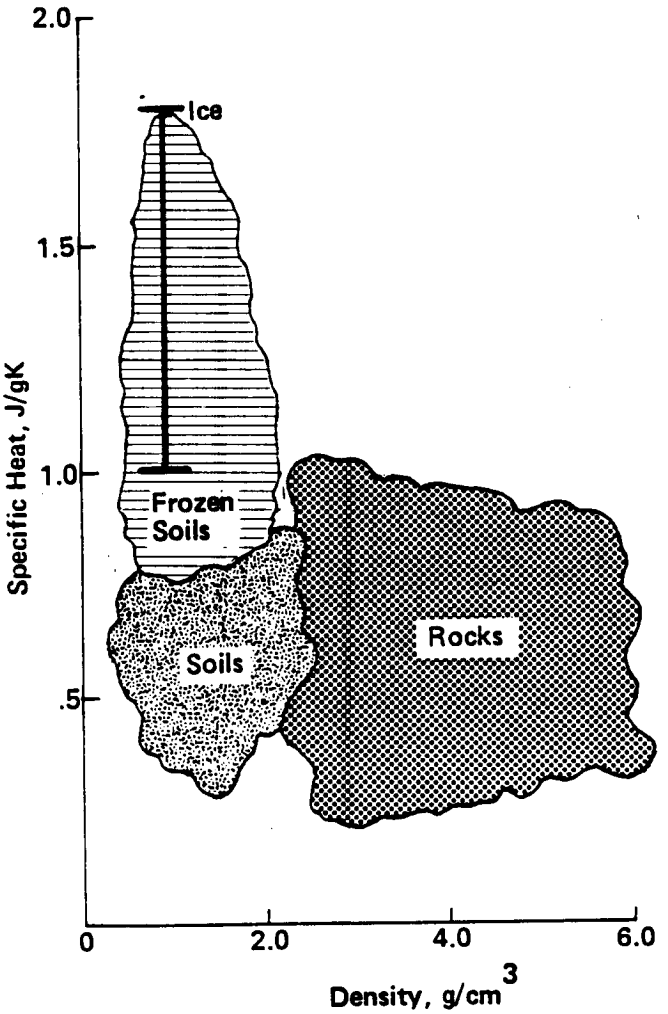

Figure 3.5.2-4 Variation of Specific Heat with Density

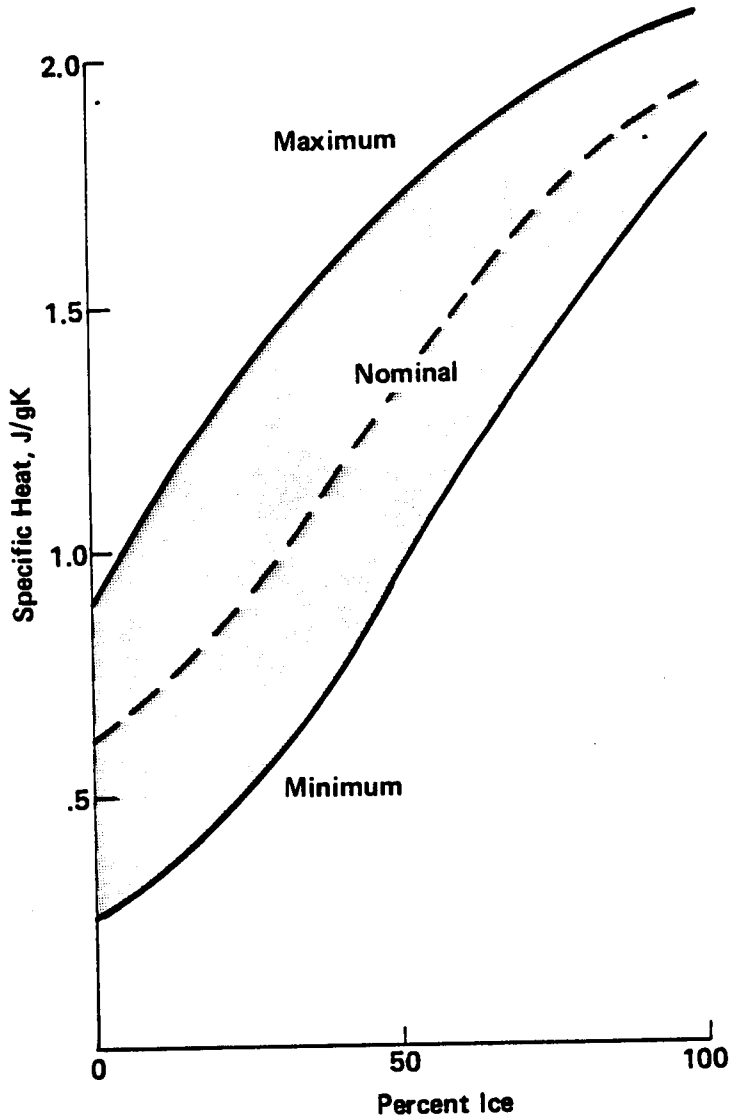

Figure 3.5.2-5 Variation of Specific Heat with Ice Content

Table 3.5.2-1 Mars Material Parameters

Density (g/cm^3)	Ice Content	E_s (J/cm^3)	C_p (J/gK)	k (W/cmK)	I (thermal inertia) (10^{-3} $cal/cm^2s^{1/2}K$)
		0.1	0.25	0.0001	1.3
0.5	dry	0.5	0.45	0.0001	1.6
		2.5	1.0	0.004	10.7
		0.5	0.25	0.00056	2.8
1.0	dry	2.0	0.65	0.002	8.6
		5.0	1.3	0.01	27.3
		0.5	0.65	0.0025	9.6
1.0	25%	2.25	1.0	0.0068	20.1
		6.25	1.8	0.0144	38.5
		0.5	1.2	0.0086	24.3
1.0	50%	2.5	1.7	0.017	40.6
		7.5	2.2	0.03	61.4
		0.5	1.5	0.015	35.8
1.0	100%	3.0	1.8	0.02	45.3
		10.0	1.2	0.025	56.0
		0.75	0.325	0.001	6.1
2.0	dry	2.0	0.78	0.004	18.9
		10.0	1.6	0.01	42.2
		0.75	0.65	0.005	19.3
2.0	25%	2.5	1.2	0.017	48.3
		12.5	1.8	0.029	54.6
		0.75	1.3	0.017	50.2
2.0	50%	3.0	1.7	0.034	57.5
		15.0	2.2	0.06	122.8
		1.0	0.325	0.001	8.1
3.5	dry	3.0	0.78	0.008	35.3
		15.0	1.6	0.015	69.3
		1.0	0.65	0.015	44.1
3.5	25%	3.5	1.2	0.034	90.3
		15.0	1.8	0.058	144.5
		1.0	1.3	0.034	94.0
3.5	50%	5.0	1.7	0.068	152.0
		17.0	2.2	0.119	228.9

Table 3.5.2-1 (concluded)

2.5	sandstone	2.0 10.0 100.0	1.0	0.055	88.6
2.8	dense basalt	100.0 165.0 300.0	0.8	0.036	67.9

inertia material (ice or rock) in a regolith environment. Because the resolution of the measurements was large, it is quite likely that there will be smaller sections that contain a higher inertia material. Thus, the thermal inertia values used in the model range from 1.6 up to 70; 70 is used as an approximate maximum for localized areas rather than 12. The low thermal inertia materials (I=4) are assumed to be made up of very fine, loosely-packed particles. This is very different than the material found in the Viking landing sites, where the thermal inertia was measured to be 9.0 ± 0.5 and 8 ± 1.5 at the two sites. The typical thermal inertia used in this model for a dry soil with a density of unity was 8.6, which fits well with this data. Many Mars models use a thermal inertia of 6 to 8 as a planetary average. The property principally responsible for the variation in thermal inertia is the thermal conductivity. Thus, to define the parameters for low thermal inertia fines, a very low thermal conductivity is used. To characterize the lowest thermal inertia material for the model (I=1.6), a density of 0.5 g/cm^3, specific heat of 0.45 J/g K and thermal conductivity of 0.0001 W/cm K were assumed. Another characteristic thermal inertia used was I=2.8, because peaks in the thermal inertia have been observed on Mars in the ranges 2.5 to 3.5 and 5.5 to 7.5 (JPL, 1980).

Thermal Model--The thermal model of the drilling operation was implemented using a differential thermal analysis program, the Martin Interactive Thermal Anaylsis System (MITAS), an advanced version of the commercial thermal software CINDA. The software is capable of handing 3-dimensional thermal analysis problems, using radiative and linear conductors to solve for steady-state or transient thermal states. The drilling model contained 394 nodes and 750 conductors, and was implemented using Mini-MITAS on an IBM Personal Computer. All conductors used in the model are linear; all radiative transfer within the soil is accounted for by the values used for thermal conductivity of the material. Figure 3.5.2-6 shows the physical representation of the model. The drill stem was sectioned into 20 nodes axially, with the bit partioned into 10 nodes. All the drilled sample material, outer material and drill stem was divided into 0.5-cm sections vertically and 0.2-cm radially. The core material within and below the bit was more finely divided: 0.2-cm sections vertically and 0.05-cm

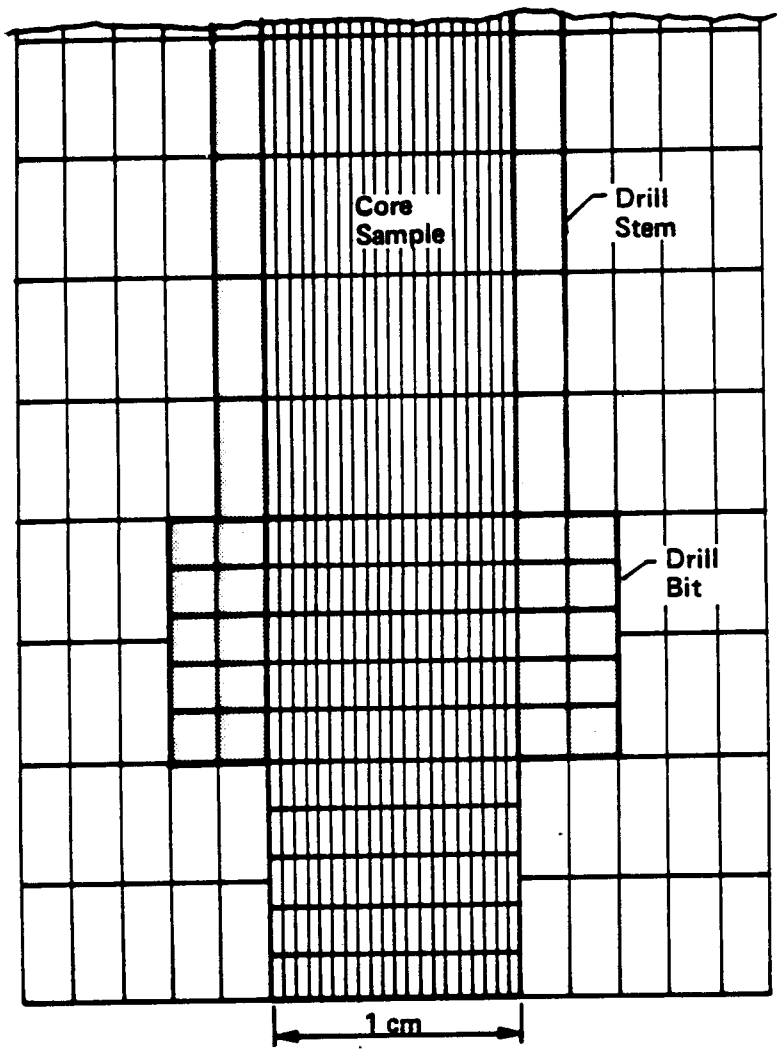

— Each Concentric Ring Represents a Diffusion Node

— Heat Load Partitioning:

30% to Bit
20% Each to Inner and Outer Shells
10% to Shell Below Bit
20% to Cuttings

Figure 3.5.2-6 Drill Thermal Model Nodes

thick concentric rings radially. This portion was more detailed in division to present a realistic picture of the exact behavior of the core material for small time steps with high precision across the analysis area. All outer nodes were connected to the steady-state temperature of the comet or Martian material.

The bit was assumed to be steel or similar material with a kerf of 1.76 cm^2 and a cutting edge thickness of 0.4 cm (0.158 in.). Both the stem and bit materials were varied to determine the effect of differing material thermal characteristics on the resultant temperature rise. Thermal conductivities for boron/epoxy and Kevlar composites, graphite/epoxy, aluminum and beryllium were used as exemplifying poor, average, and good thermal conductors. The stem wall thickness is 0.2 cm (0.080 in.), so that 0.2 cm remains radially for flute extensions along the stem.

The estimated specific energy required to cut the material was used to determine the total amount of heat that is dissipated by the drilling operation. Of this total power load, 30% is assumed to go to the bit, 20% each to the rings of material directly inside and outside the bit, 10% to the ring directly below the bit, and 20% to the cuttings that travel upward and distribute their heat along the stem and outer cylinder of material. A drilling rate of 0.2 cm/s (5 in./min) was used, giving 5 seconds per linear centimeter of material drilled. Some previous studies have shown that the core recovery increases for slower penetration rates until it reaches an optimum where it begins to decrease again. The lowest rate is determined by the friction of the internal walls, because the core will no longer progress into the stem when the inner friction exceeds the penetration force. For one specific drilling study, the optimum rate was found to be about 2 cm per second, with relatively rough inner titanium walls. With the proper treatment on the inner walls, there is no question that the friction can be reduced and slower rates will be profitable. Thus, 0.2 cm/s is a slow rate based upon previous data, but reasonable to use as the mission has no severe time constraints on the drilling operation. Because the power is calculated per unit volume of material, the speed makes relatively little difference in the final thermal equilibrium, although it has the effect of initially heating the outer layer more severely, as shown in Figure 3.5.2-7. During the actual

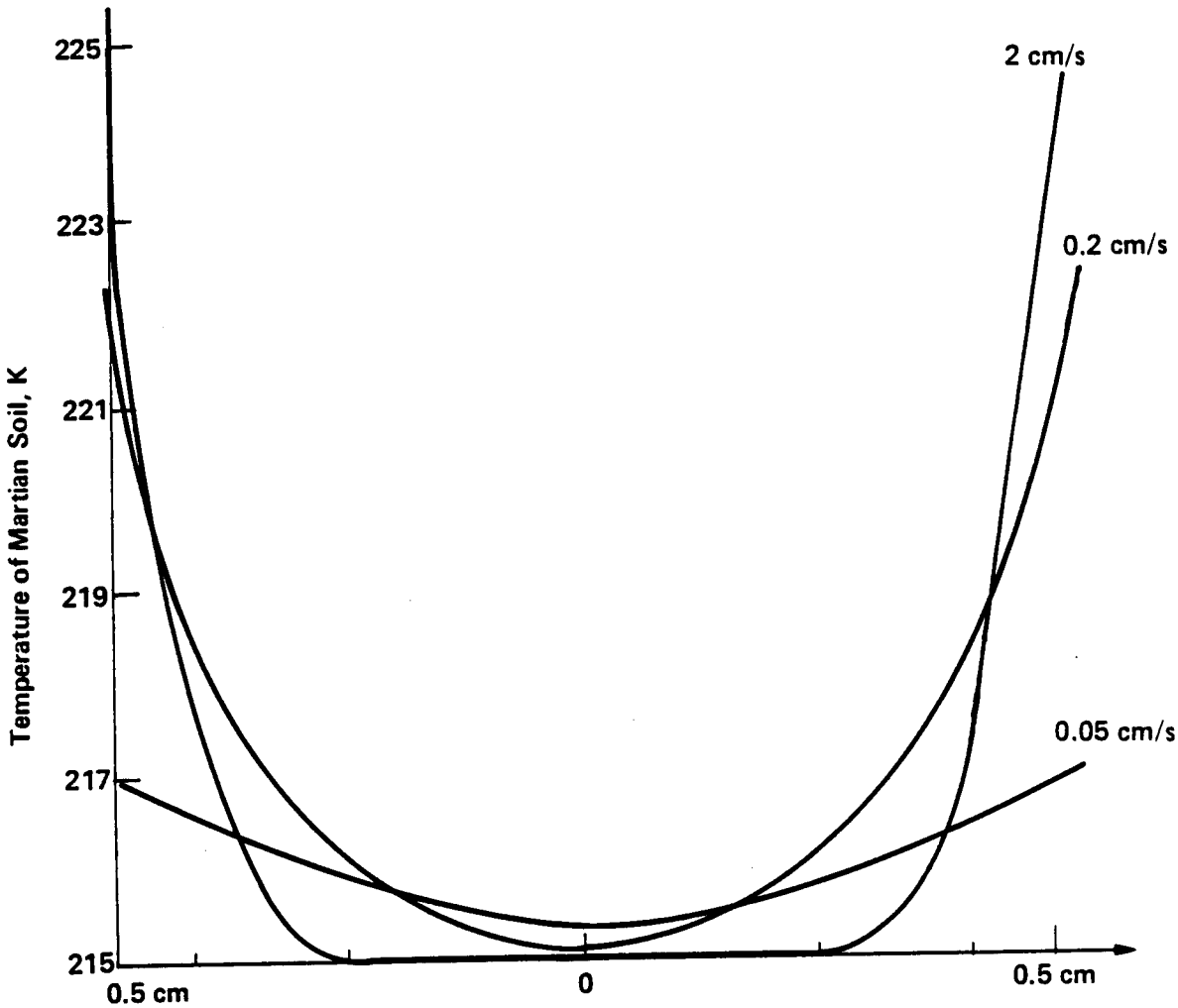

Figure 3.5.2-7 Calculated Thermal Profiles for Coring at Various Penetration Rates

operation, pauses in drilling may be programmed, as practical, to allow dissipation of heat. This could be a problem under certain conditions in icy materials, as pauses might allow freezing of cuttings in the flutes. Pauses could be used effectively in rock, however, when the bit or sample are in danger of overheating.

Thermal Results--Many different combinations of possible parameters were run, but in general the cases that are discussed are the "worst-case" analyses. The two worst-case scenarios used were (1) maximum specific energy (E_s) with average specific heat (C_p) and thermal conductivity, and (2) average E_s with minimum C_p and thermal conductivity. The first case assumes a very hard-to-drill material that would require more heat input, and the second case illustates a material highly affected by heat that will tend not to let the heat dissipate. The maximum specific energy was not paired with minimum specific heat as a worst case, because that model would not be physically realistic.

The least sensitive samples, and the most important, those that contain ices, have higher specific heats than dry soil and thus do not rise to as high temperatures. These samples have higher thermal conductivity, in general, so that the heat distributes more evenly throughout the sample and yields a uniformly lower temperature. The results for Martian core samples show this trend; dry soils and rocks undergo the highest temperature gradients, although the soils are not subjected to more than a 10°C temperature increase at the core surface. The more sensitive permafrosts show a much flatter thermal profile, and do not undergo more than a 5°C increase in the outer 0.1 cm of the core (for 50% ice samples). This does not mean that there is not very localized heating and vaporization of material in contact with the bit, but shows that a very small fraction of the total sample will be affected, and the average temperature of the outer 0.1 cm of the core will not rise more than 5°C. As the fraction of ice decreases, the core surface temperature rise will increase toward 10°C. Figures 3.5.2-8 and 3.5.2-9 show thermal profiles of soils and permafrost cores at the Martian low-latitude temperatures, and Figures 3.5.2-10 and 3.5.2-11 show core sample profiles for the colder polar cap region. Polar sample cores would never experience even 4°C of heating during sample acquisition operations, assuming that the material is at least

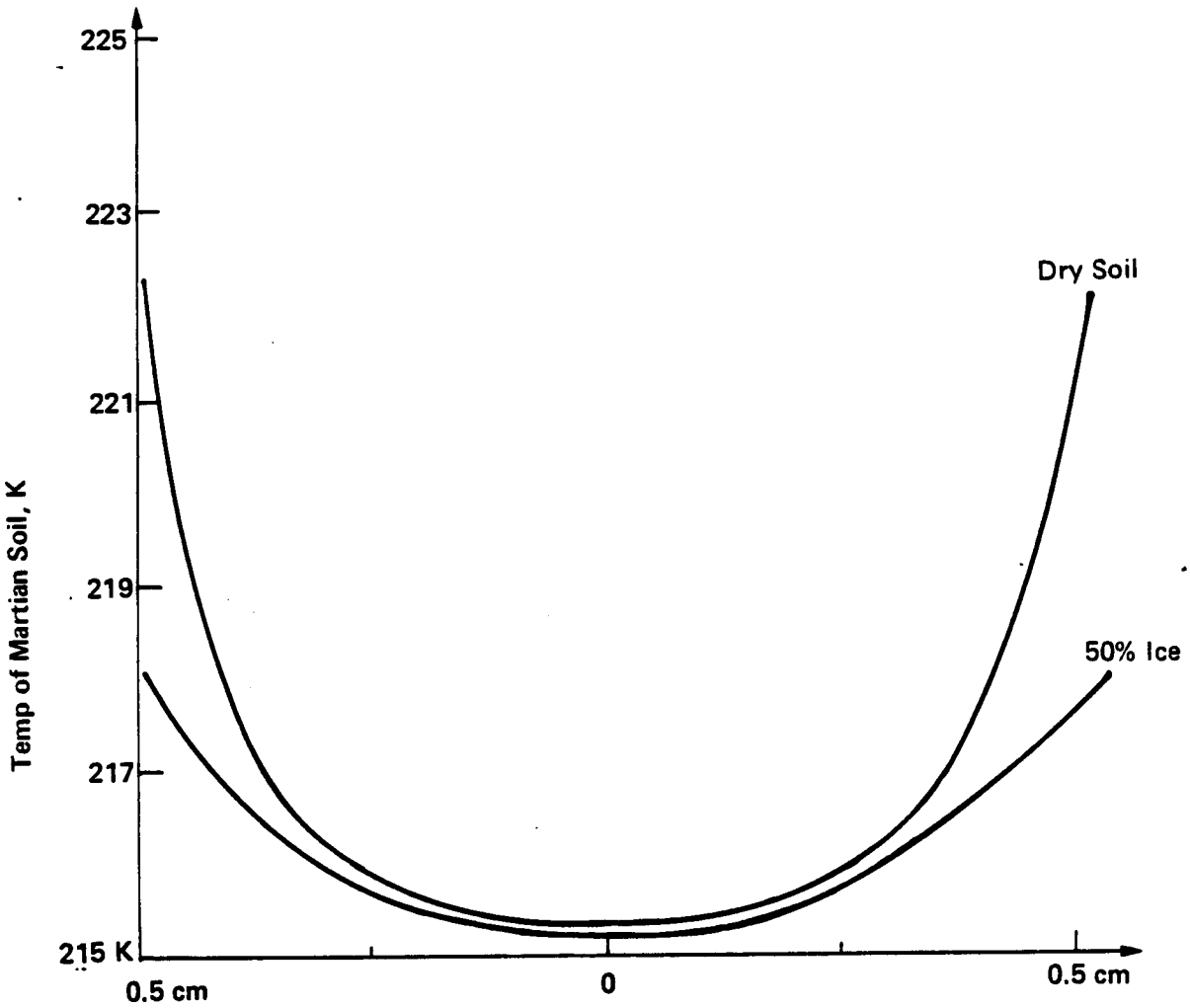

Figure 3.5.2-8 Thermal Profiles for Martian Core Sample (ρ =1.0 g/cm^3)

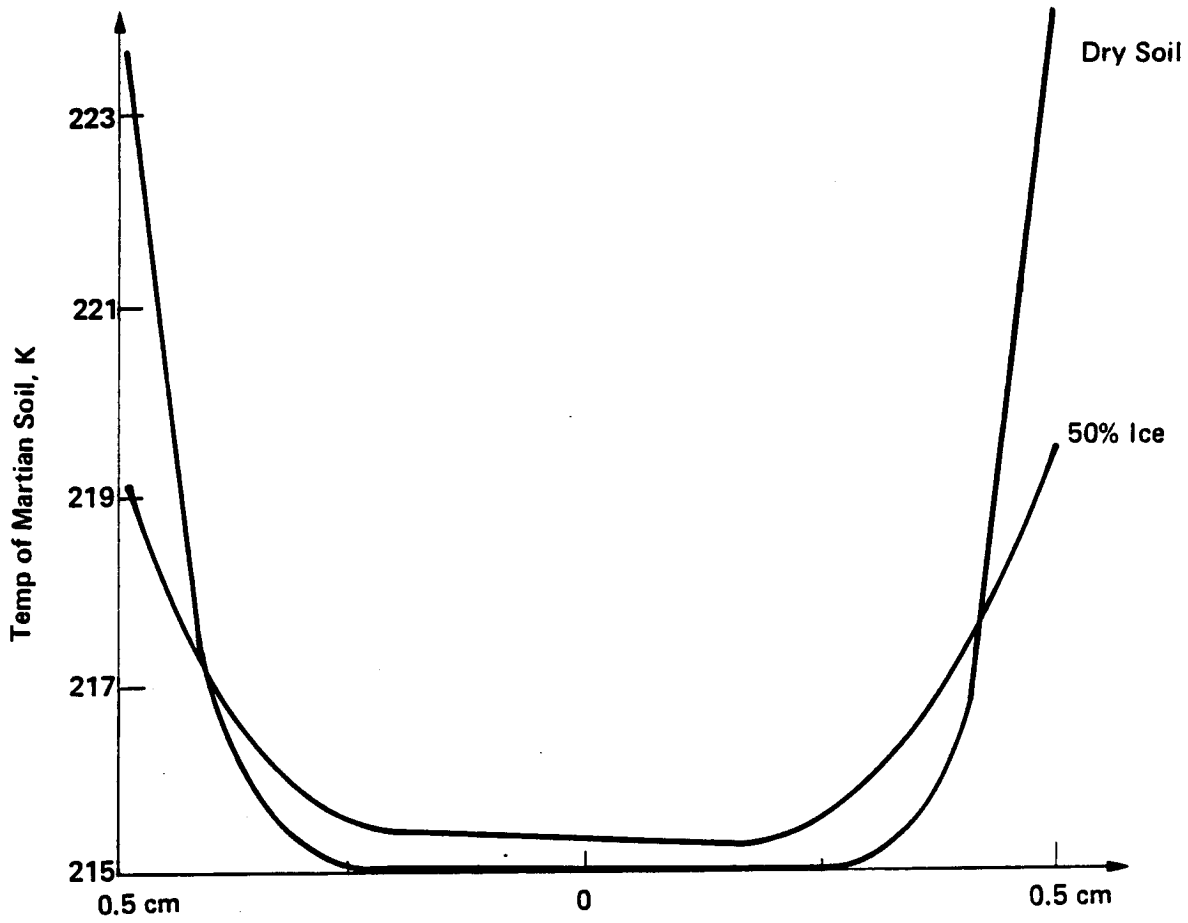

Figure 3.5.2-9 Thermal Profiles for Martian Core Sample (ρ = 2.0 g/cm^3)

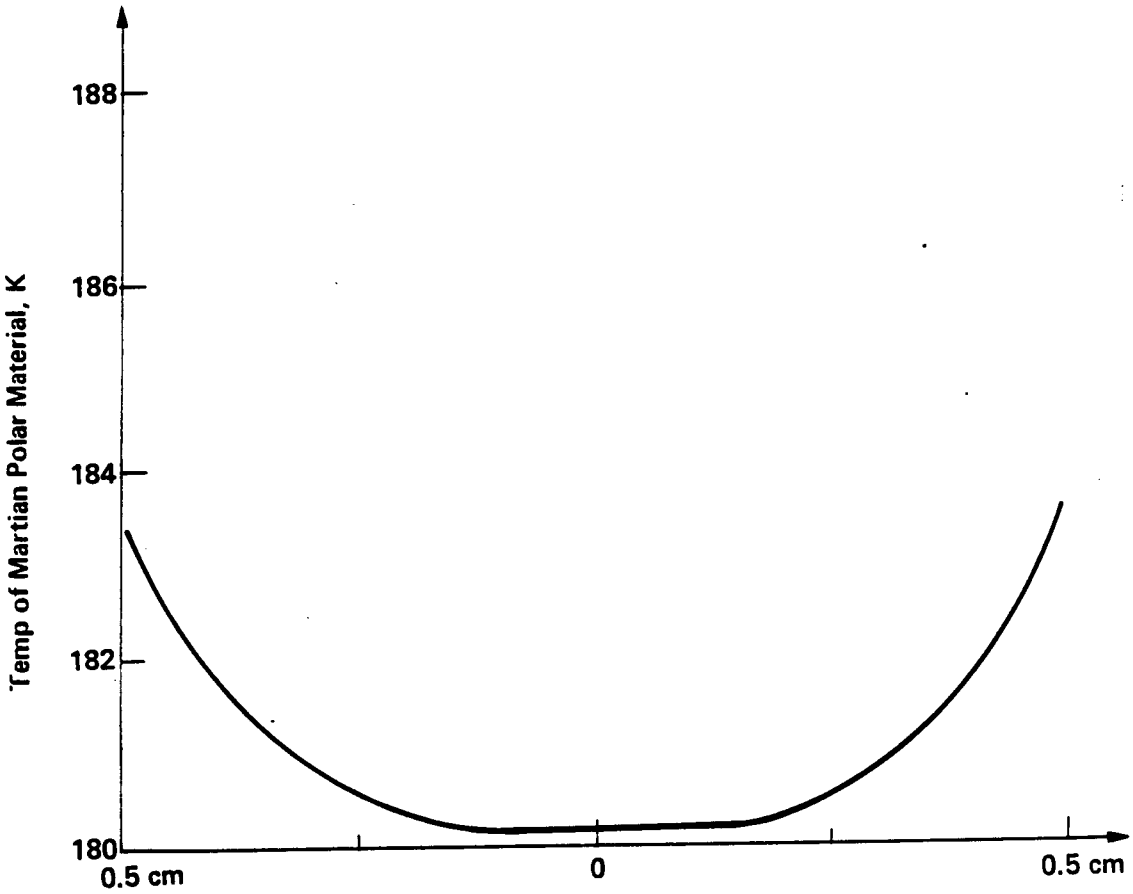

Figure 3.5.2-10 Thermal Profile for Martian Polar Permafrost Core (50% Ice)

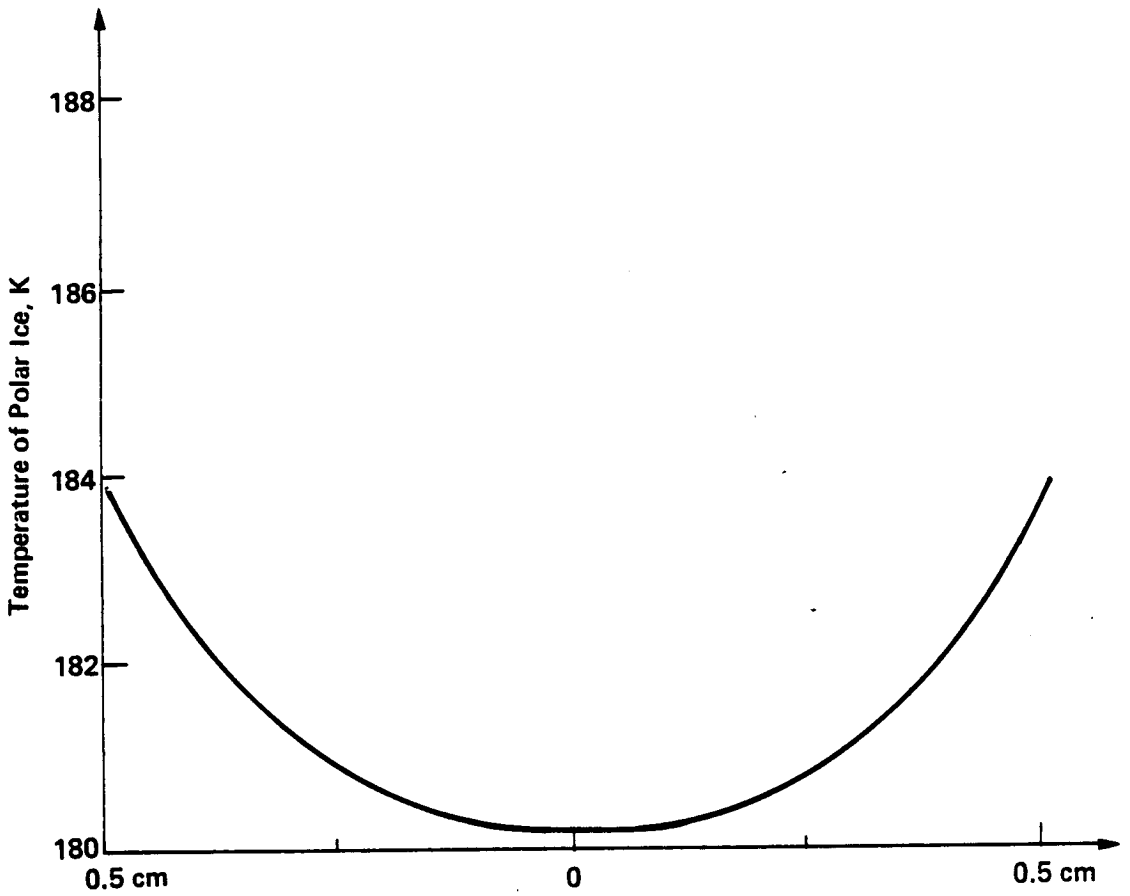

Figure 3.5.2-11 Thermal Profile for Pure Water Ice at Pole

50% water ice. These thermal profiles show the thermal environment at the bit during the drilling operation. Because the soil receives most of the heat load while being drilled, this thermal profile demonstrates approximately the maximum temperature reached by the core surface, with material temperature equalizing across the core further up the shaft as it recovers from drilling. F'gure 3.5.2-12 shows the equilibration of the core temperature with time, as heat flows from the warmer surface and warms the inner portion of the core. Drilling in several types of rocks was analyzed; the worst case of basaltic rock drilling is presented in Figure 3.5.2-13. Here the surface of the core heats by 80 or 90°C, and the inner portion equalizes to a temperature about 20° above the ambient, but it is unlikely that this heating will destroy any information resident in the rock.

A thermal insulator, like Kevlar/epoxy composite, has some disadvantages as candidate material for a drill stem because a larger portion of the heat is retained at the drill bit, rather than dissipating up the drill stem. This heats the bit section more than necessary. Metallic coatings do not provide sufficient thermal path to allieviate this without becoming unreasonably thick. For this reason, most of the portrayed thermal cases are with a graphite/epoxy or aluminum drill stem to provide maximum heat conduction. One problem with a high conductivity drill stem, however, is that scenarios can be envisioned in which it would produce unacceptable results. If the drill passes through a layer of permafrost material and then enters a layer of solid rock or well-consolidated material, as illustrated in Figure 3.5.2-14, the drill bit might heat severely and the heat conducted up the drill stem could alter the permafrost ices. This is one reason for the microprocessor feedback on the drill; the situation could be evaluated and halted before damage to the permafrost zone occurred. In addition, when drilling through a soil profile with a large temperature gradient, a conductive stem will allow colder soil to receive heat from the warmer region, with possible alteration of phases or migration of volatiles. The best solution to this is a metallic bit, possibly with an extension, that will dissipate the heat effectively, and a low thermal conductivity drill stem that can be used to isolate the differing soil regions.

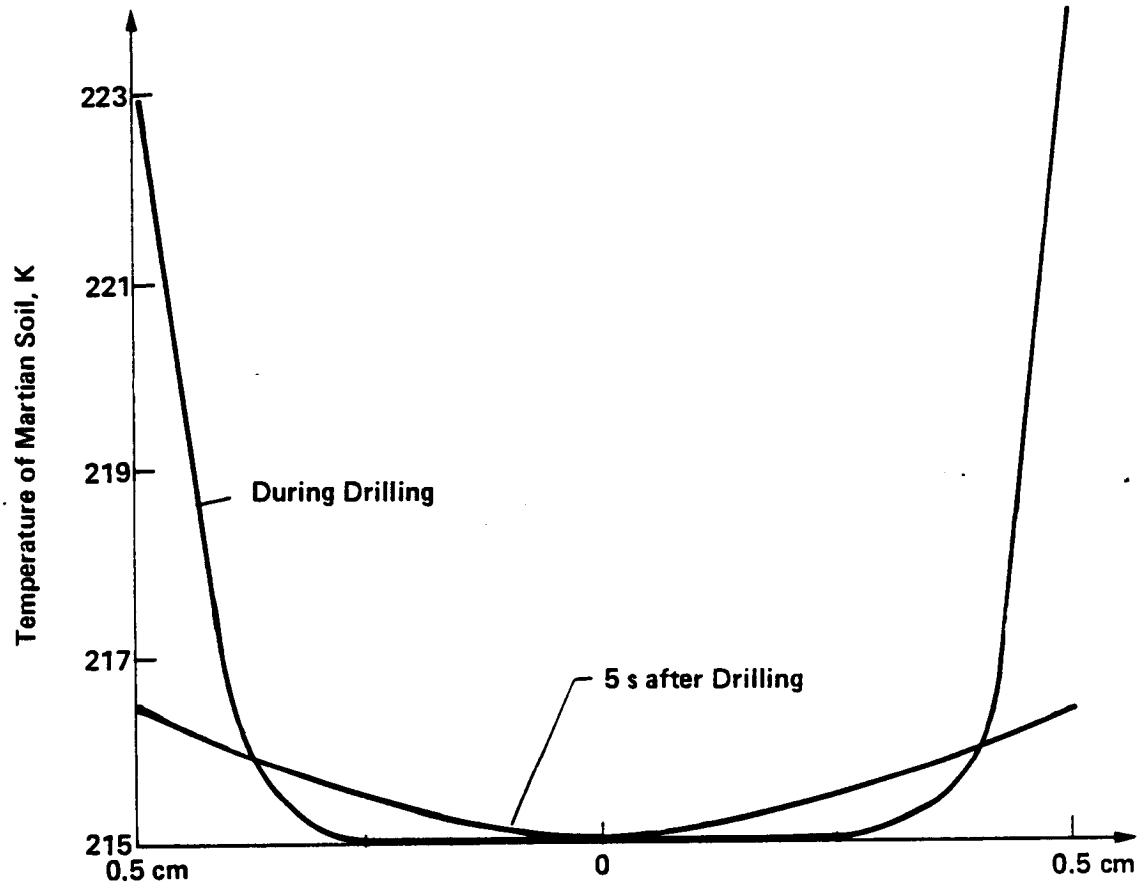

Figure 3.5.2-12 Equilibration of Thermal Profile for Martian Regolith (Dry)

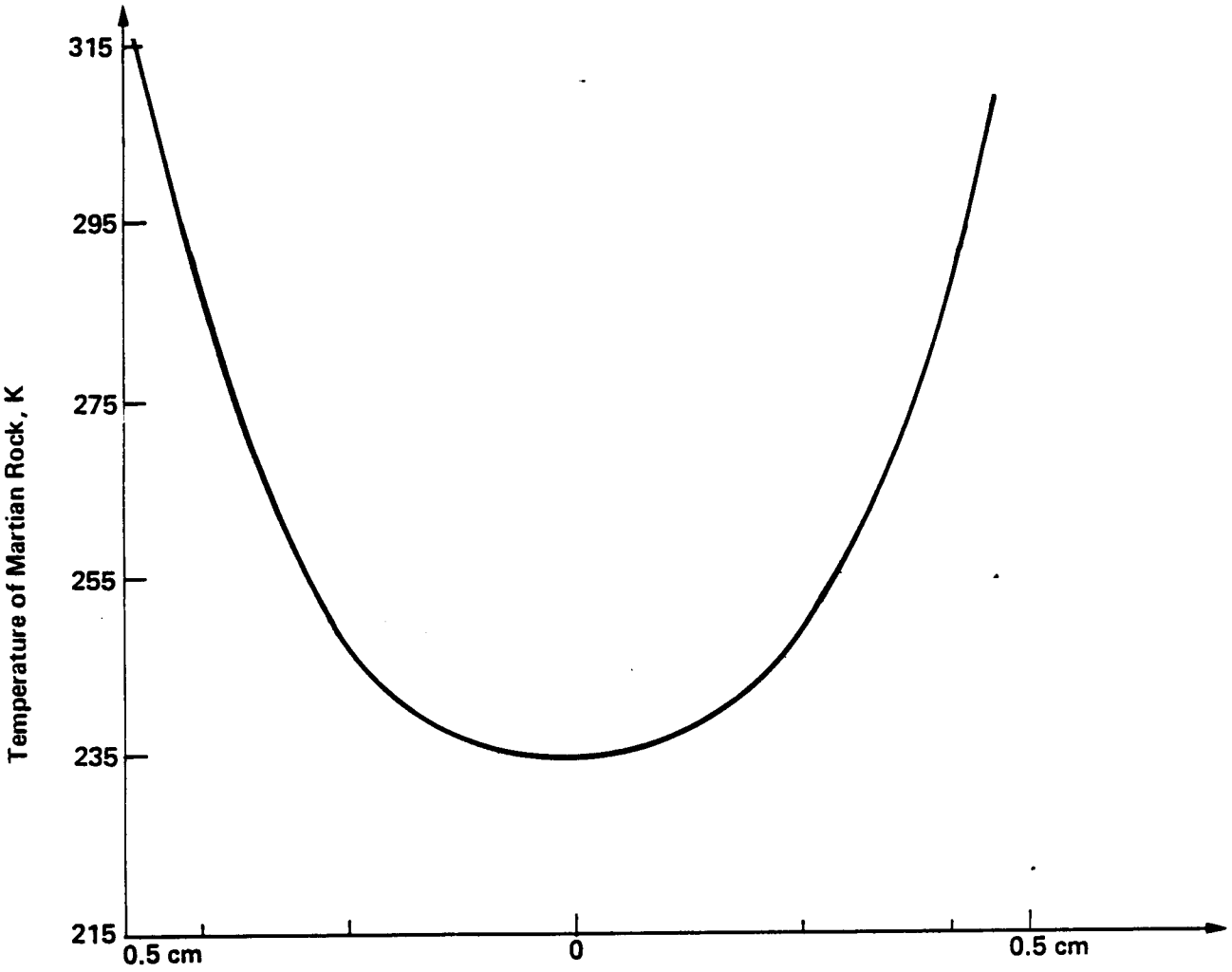

Figure 3.5.2-13 Thermal Profile for Basalt Core (E_s = 300 J/cm ^{3})

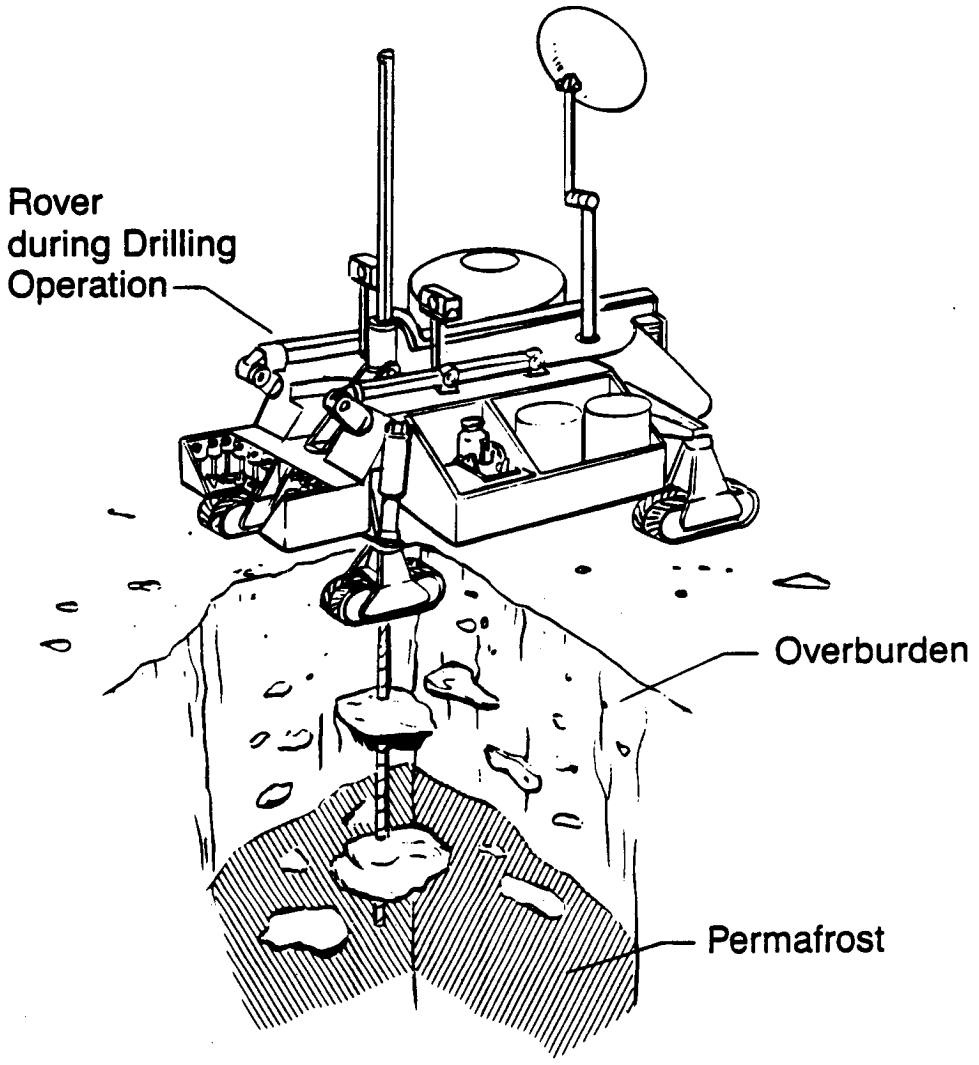

Figure 3.5.2-14 Sampling of Permafrost by Rover

Worst case analyses were done to determine the effect on core temperature if a greater portion (80%) of the heat generated was dissipated in the core or along the stem. The case of drilling through a rock embedded in soil was examined, including the effect of encountering a rock when drilling in very low thermal inertia material. The results of these analyses are shown in Table 3.5.2-2. In general, the core surface temperature will rise by 10° when drilling a dry, ρ =1 soil at the Martian equatorial temperature of 215 K. When the drill begins to penetrate rock, the surface temperature of the core will increase to 27 K above the ambient with a metallic drill stem. If the drill is stopped after 5 seconds of operation in the basalt, the core just above the rock will equilibrate to a temperature only 17 K above the ambient. The core will be disturbed by at least 2° for a length of 6 cm. During rock drilling, the rock core and bit temperature will each rise to about 40°C. Use of a Kevlar stem will increase the bit and rock temperature by about 10°. However, less heat is transmitted up the stem, and the core is disturbed to a distance of only 2.5 cm.

Different cases of heat partitioning were considered to define the effect on the thermal map. With 80% of the incident heat load going to the core, the core temperature change will be 21° during coring, 34° during rock drilling, and will equilibrate to 22° average above the ambient. If 80% of the heat load were to be dissipated in the cuttings, the core surface will be disturbed all along its length (10 cm) by at least 2 degrees. With a Kevlar stem, this distance would only be 2.5 cm.

For lower thermal inertia soils, there is no available data on specific energy, although they are probably very low cohesion, low specific energy materials. A figure of 2 J/cm^3 was used for the specific energy of these materials. For I=2.8, the core will heat by 16° during coring. For the worst case of a material with I=1.6 (lowest observed on the Martian surface), the core surface will heat by 20°, with the conservative assumptions that were made for specific energy. During rock drilling this temperature will increase by only another 1°, which is due mainly to the low thermal conductivity of the material. The low thermal conductivity also means that the inner portion of the core stays cool, so that the equilibration temperature is only 4° above

Table 3.5.2-2 Thermal Result for Martian Regoliths

Conditions	Max Core Temp during drilling	Max Core Temp during rock dr.	Temp after equilibration	Rock Temp during rock	Dist (cm) to 217K temp	Max bit Temp
Martian Soil/Basalt Drilling						
Dry soil	224.5	242.3	232.4	326.9	5.5	300.9
Dry soil, 80% heat to core	236.3	248.8	237.6	407.2	7.0	329.8
Dry soil, 80% heat to cuttings	216.6	250.5	231.4	249.3	9.0	247.8
Dry soil, 80% heat to bit	218.2	262.2	234.3	374.2	5.5	392.0
Dry soil, Kevlar stem	224.6	239.4	232.1	334.6	2.5	311.1
Dry soil, Kevlar, 80% to core	235.9	228.3	229.4	399.6	2.0	323.5
Dry soil, Kevlar, 80% to cuttings	215.9	288.8	243.8	238.3	2.5	236.7
Dry soil, Kevlar, 80% to bit	218.5	235.7	237.4	395.2	2.0	415.8
50% ice soil	217.4	236.0	235.1	303.0	4.0	288.8
50% ice soil, 80% to core	225.3	234.4	236.0	469.4	3.5	282.2
50% ice soil, 80% to cuttings	215.7	235.7	230.9	240.9	4.5	237.8
50% ice, Kevlar stem	217.6	232.1	234.1	309.6	2.0	296.0
Minimum Thermal Inertia Regolith/Basalt Drilling						
I=1.6	234.8	236.0	219.2	326.8	5.5	302.1
I=1.6, 80% to core	293.9	234.6	220.0	480.7	5.5	299.3

Table 3.5.2-2 (concluded)

I=2.8	223.4	241.1	221.2	316.3	4.0	305.4
I=2.8, 80% to core	247.1	240.1	225.7	391.9	5.5	312.5
I=2.8, 80% to cuttings	217.1	235.5	217.1	242.0	6.5	239.7
I=2.8, Kevlar	223.5	241.5	226.0	326.4	2.5	316.8
I=2.8, Kevlar, 80% to core	247.2	228.8	223.9	403.6	2.5	325.8
I=2.8, Kevlar, 80% to cuttings	217.1	289.2	234.2	239.4	3.5	236.4
Martian Dense Soil Drilling						
Dry soil d=2	222.9		216.2		0.0	
Dry soil d=2, 80% to cuttings	216.9		215.5		0.0	
Dry soil d=2, 80% to core	240.3		216.7		0.0	

Note: When not stated otherwise, the following conditions apply:

215K initial temperature
Tribocor bit/Beryllium stem
Regolith density=1.0 g/cm^3
Basalt density=2.65 g/cm^3
Heat distribution: 30% to bit
20% to core
20% to outer material
20% to cuttings
10% below bit
Thermal Inertia I=8.6*10^{-3} cal/cms$^{1/2}$K for dry soil
I=38.6 for 50% ice soil
Specific Energy E=5 J/cm^3 for dry soil, 300 J/cm^3 for basalt

ambient. Even with 80% of the heat load transmitted to the core, the equilibration temperature is only 5° above ambient. However, in this case the model shows the core interface reaching almost 80° above the ambient, but this is confined to less than 0.5 mm of the outer surface. In addition, the specific energy value assumed is a much higher than would be likely to be encountered.

Several drill sizes were analyzed, to determine if a larger diameter core would allow significantly less thermal effect. There is some difference; obviously the larger diameter drills will involve less heating of the central portion. However, because the thermal impacts have not been seen to be deleterious for a 1-cm drill, these larger drills have not been investigated further. Larger drills would require more power, more equipment mass flown on the mission, and probably more returned mass of sample.

3.5.3 Drill Materials

The materials used in the drilling system will have a profound effect on its efficiency and operation. The materials should be selected to allow the system to be lightweight, of high reliability, and minimally contaminating the samples. Because the drill will be used in vacuum or near-vacuum at low temperatures in contact with an unknown variety of materials, there are some unusual requirements on the materials chosen. Coating technologies have been studied for this application for several purposes: a low-friction, low-contamination surface on the inside of the core stem, a non-galling surface for the threaded fittings, and a coated cutting surface that will be both hard and impact-tough at low temperatures.

Stem Materials--For the drill stem materials, low density is a critical factor because there will many stem segments, and portions of these must be in the payload returned to Earth. To withstand the torque requirements of drilling, the stem should have high shear strength and high elastic modulus (stiffness). Because the drill stem design requires minimization of both stem wall thickness and mass of the stem, both strength per unit area and strength per unit of mass (specific strength) are important. For intrinsically high reliability at the required low-temperature regimes, the stem should have good low-temperature fracture toughness, and a low ductile-to-brittle transition temperature. As explained in Section 3.5.2, the drill stem should have

low thermal conductivity to minimize thermal disturbance of the sample. The ease of manufacture of the material into a tube form is a factor; however, as this mission is years into the future, a material for which fabrication techniques are still being developed should not be disqualified.

In considering materials to be used in the drill stem, there are several basic types: unreinforced metals and alloys, ordinary plastics, polymer matrix composites, continuous metal matrix composites, discontinuous metal matrix composites, and combinations of the above. Some basic properties of these are documented in Table 3.5.3-1 and Figure 3.5.3-1. Metals and alloys tend to have moderately high strengths, moderate stiffness, high density, and high thermal conductivity. Plastics have low thermal conductivity and low density but have low strength and tend to be brittle at low temperature. One possibility to achieve the desired combination of qualities is to use a composite material. Polymer matrix composite technology is well developed, and these materials have low densities with potentially good stiffness and strength qualities. The metallic matrix technology is less developed, and especially in the case of the continuous fiber composites, fabrication techniques are still under development. However, these materials exhibit high stiffnesses and strengths, lower density and thermal conductivity than the pure metals, and their properties continue to improve as the technology of wetting a fiber to a metallic matrix becomes better understood and more readily applied. Because this application for the material is at least ten years into the future, it is profitable to examine the qualities that the metal matrix composites have to offer.

Of the metallic alloys, aluminum, titanium, beryllium, and Invar are considered. The coefficient of Thermal Expansion (CTE) of all these metals is high, which will simplify matching the thermal expansion of the stem with a metallic drill bit. Contamination from the metals should not be a concern as they will be coated on all surfaces that contact the sample for long periods of time. Also, most have a built-in protection against contamination in that the specific alloys have very precise percentage of different metals that could be detected in the sample and traced to the alloy. The best specific strength and stiffness qualities are shown by beryllium, but it also has a moderately high thermal conductivity and low fracture strength especially at cold temperatures.

Table 3.5.3-1 Drill Stem Materials

Material	Density (g/cm^3)	E (GPa)	Shear Str. (MPa)	CTE $10^{-6}/^{\circ}C$	E/ρ (GPa/kg/m3)	Fsu/ρ (MPa/kg/m3)	κ
Ti-6-4	4.4	113.0	620	9.5	25.7	140.9	med
Arall1	2.3	67.3	261		29.3	113.5	med
Be	1.9	299.0	206	11.5	157.4	108.4	high
SiC/Ti-6-4	3.8	218.0	345	5.4	57.4	90.8	med
2219 Al	2.8	72.0	240	13.0	25.7	85.7	high
SiC_w/Al	3.0	122.0	170	13.5	40.7	56.7	high
Kevlar/Epoxy	1.4	74.8	68	-4.0	53.4	48.6	low
Graphite/Epoxy	1.6	124.4	68	-0.2	77.8	48.6	med
SiC/Al	2.9	219.0	138	5.7	75.5	47.6	high
SiC_w/Mg	2.1	88.0	150	15.8	41.9	71.4	med
Gr/Al	2.4	204.0	103	2.7	85.0	42.9	high
Gr/Mg	1.9	230.0	48	0.7	121.1	25.3	med

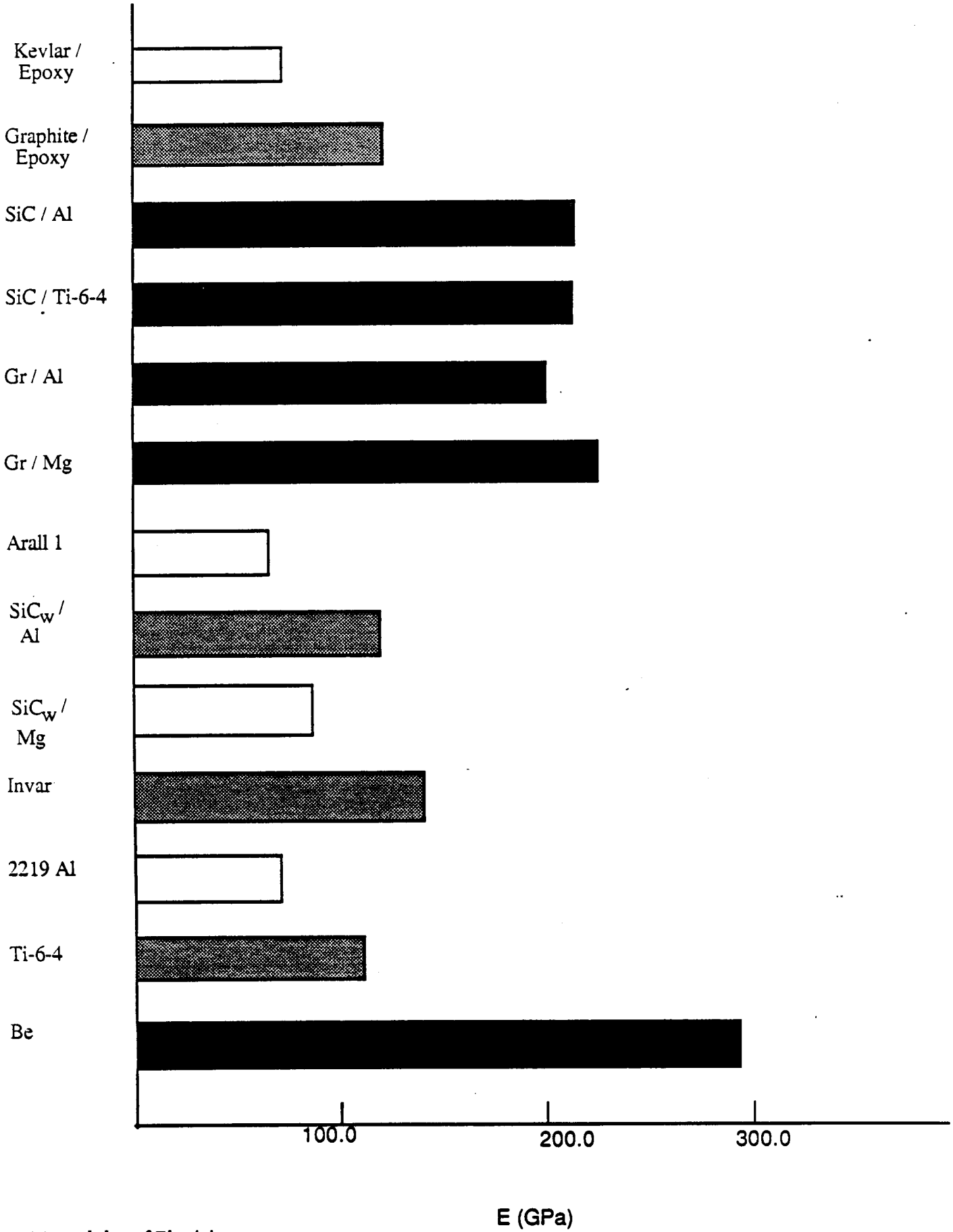

(a) Modulus of Elasticity

Figure 3.5.3-1 Stem Material Properties

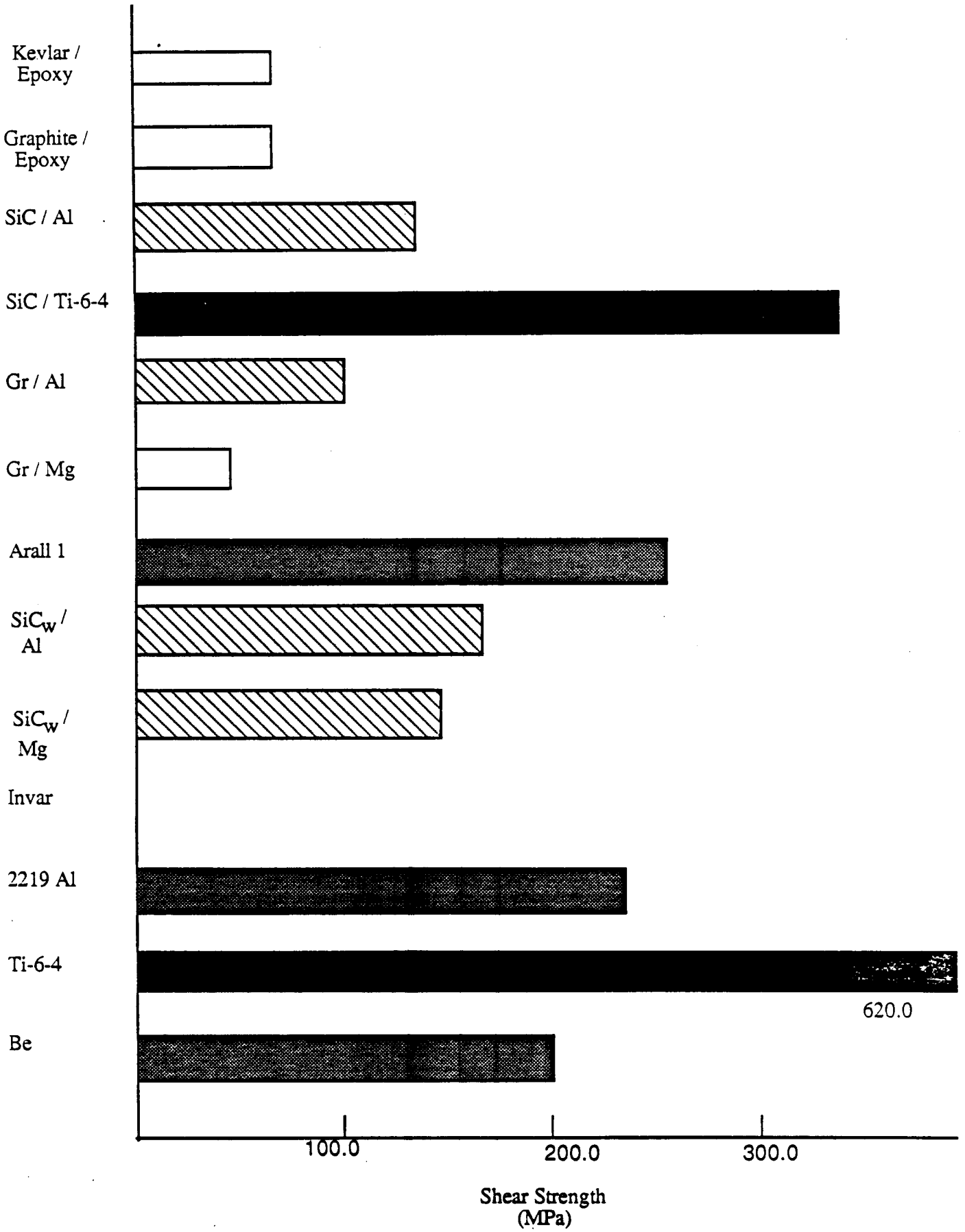

(b) Shear Strength

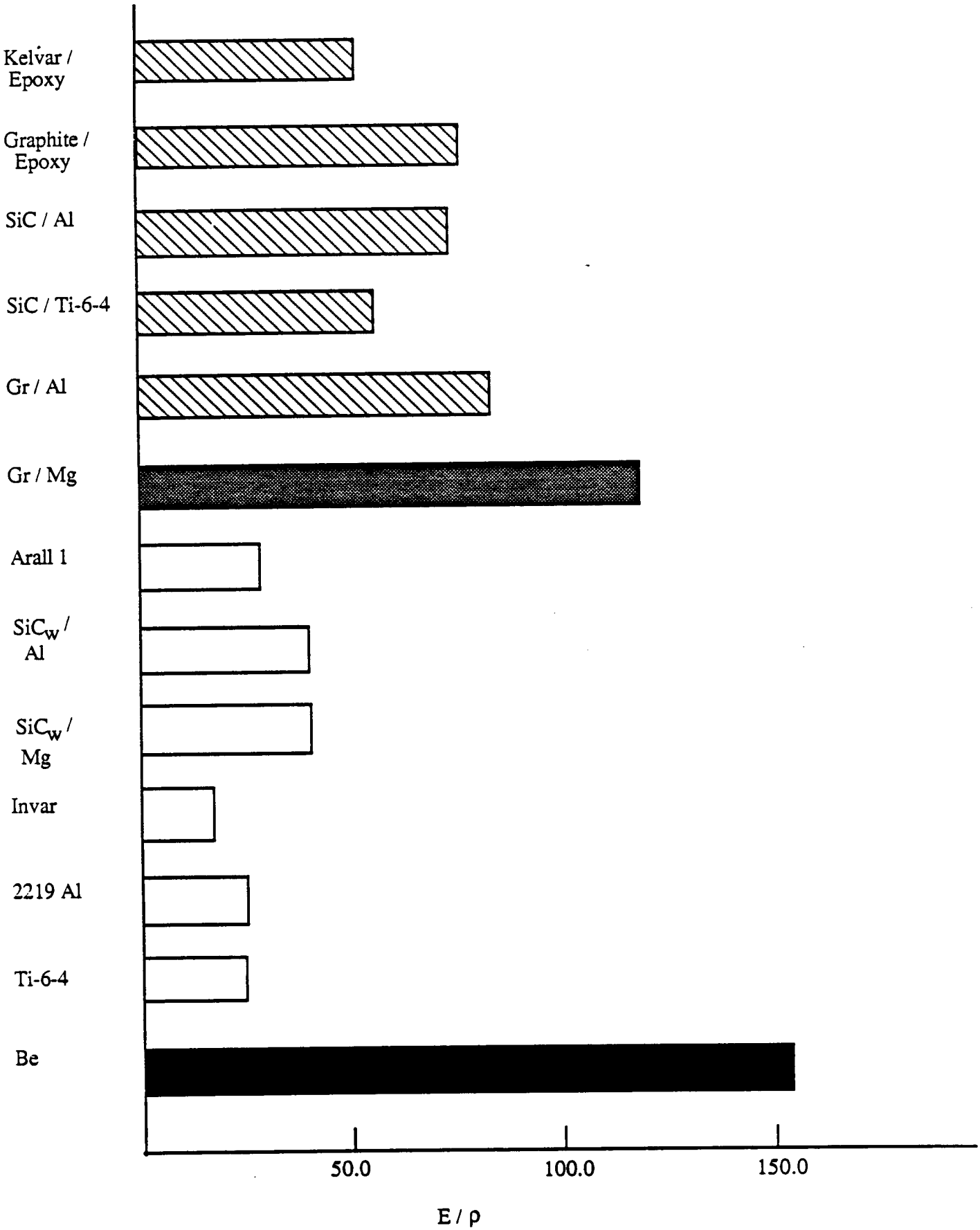

(c) Specific Elastic Modulus

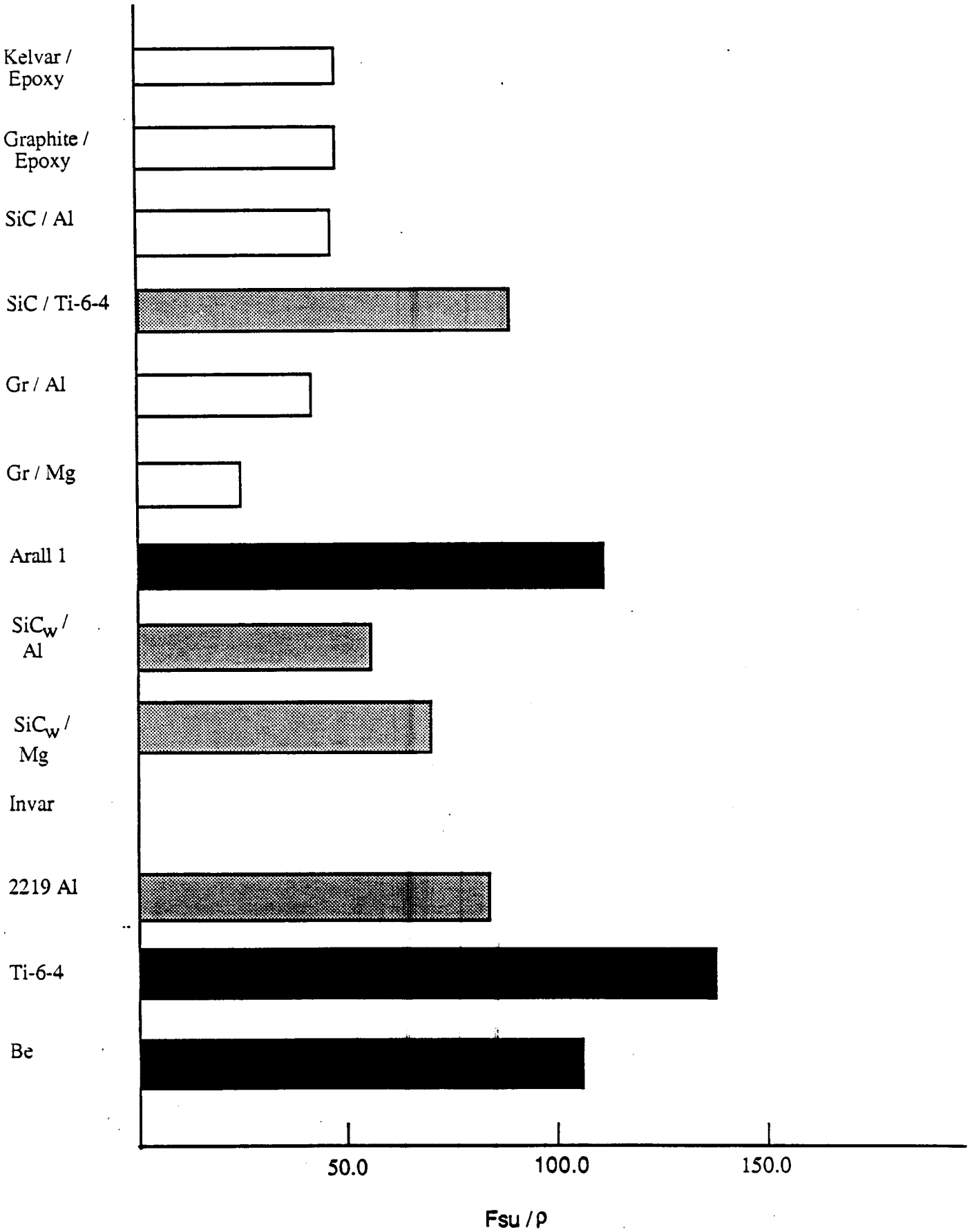

(d) Specific Shear Strength

The titanium alloy with 6% aluminum and 4% vanadium (Ti-6-4) is often used for cryogenic applications requiring strength. The specific shear strength is higher than any of the other materials. Both the stiffness and strength of the alloy increase at temperatures as low as 100 K. Titanium has one of the lowest thermal conductivities of any of the metals, combining a favorable low conductivity similar to the polymer composites with the strength of a metal. This alloy was successfully used for many of the Apollo drill stem sections. The fracture toughness, especially in the properly annealed state, is very high. At low temperatures, however, a low fracture-toughness-to-yield-strength ratio can lead to brittle fracture. The specific stiffness of this metal is relatively low, so the walls of the drill stem would need to be thick and heavy. The relatively high density, the possibility for brittle fracture, and the relatively low stiffness all are drawbacks, but its low temperature strength and prior successful use are benefits that make it worthy of examination. These constraints can be alliviated to some extent by the use of reinforcing fibers, as described below.

Aluminum 2219 is an alloy also used for cryogenic applications, with strength and stiffness not as high as the titanium alloy. These properties increase at low temperature and the thermal conductivity decreases. The fracture toughness is higher than the titanium alloy and increases with decreasing temperature. It is readily weldable and was originally designed for cryogenic applications. The CTE is fairly high, but should be feasible to match with bit materials. The main faults are high thermal conductivity and relatively low stiffness. Again, these are concerns that may be resolvable by the addition of reinforcing fibers.

Invar is a nickel-iron alloy with good stiffness properties, but because of its high density it should not be used for the entire stem. This metal could be useful as an inner layer to one of the polymer matrix composites, to add isotropic shear strength to the composite tube. The reason for using this metal is its extremely low coefficient of thermal expansion, which can be matched by almost any given lay-up of polymer composite. This type of fabrication (Invar liner in a composite tube) has been used for the construction of insulated fuel lines, but its application here would be a developmental project. Despite the matching of room temperature CTEs, there is still a concern with decreased adhesion at low temperatures.

Other potentially useful metals include aluminum-lithium alloys. These contain 2 to 3% lithium, and are being designed for high stiffness, low density, and low fatigue. An aluminum-beryllium alloy is also under development that could combine the high stiffness of beryllium with the high strength and fracture toughness of aluminum. This alloy would be of particular interest because of its potentially superior properties and low density, but little information is available on it at the present time. Beryllium-copper shows good ductility at low temperatures, but does not have the desired low density or low thermal conductivity; drill stems made of this material would weigh 3 or 4 times more than aluminum or beryllium stems. Also it has a low yield strength and would have to be reinforced.

The Ti-5Al-2.5Sn alloy was rejected in favor of the Ti-6Al-4V because it has lower modulus, lower yield strength, and slightly higher thermal conductivity. It also has the same tendency toward brittle fracture at low temperature, although the fracture toughness can be slightly higher. The aluminum alloy 2014 was rejected in favor of 2219 because it has lower fracture toughness and higher thermal conductivity, although it does have slightly higher strength. The high-strength steels (Stabaloy, REX 734) have favorable characteristics for use as a drill stem material, and are often used for Earth-bound rigs, but their specific strength is too low to justify on these mass-critical missions.

Polymer matrix composites have the lowest density of any of the candidate materials. They will be the easiest for a drill or saw on the rover to cut through for subsectioning, although the possibility of contamination from organic or epoxy particles does arise. Unreinforced plastics have low densities, but do not possess the stiffness properties required; many of the high-strength polycarbonates have undesirable properties at low temperature. Any continuous-fiber composite material has the beneficial characteristic that it may be laid up with the fibers in a specified direction to provide the best thermal and/or mechanical properties for that application. Coefficients of thermal expansion of these materials are very low, which might be an asset for coating adhesion at low temperatures, but would have to be examined for compatibility with the CTE of the drill bit fitting. The polymer composites have well developed fabrication technology at present, because they have been available longer than any other composite.

Graphite epoxy has higher stiffness than the other polymer composites, and can be fabricated with differing types of graphite fibers to produce higher strength or higher stiffness. The use of high modulus fibers can produce an exceptionally high specific stiffness material. Graphite epoxy has a thermal conductivity that varies with the directional layup of the fibers. Because in a drill stem most of the fibers will be oriented vertically to produce good stiffness and shear strength, the thermal conductivity will be at the high end of its range, comparable to the titanium alloys discussed above. The graphite epoxy material could be fabricated to have good self-lubrication, which would be useful in a drill stem, but it shows low impact resistance, which may preclude use in a rotary-percussive system.

Kevlar epoxy has moderately high specific stiffness, and possesses the valuable quality of absorbing vibration. This damping property in a drill stem could help avoid the chatter that causes excessive bit chipping and wear. Kevlar has the lowest thermal conductivity of any of the proposed materials; even if it is not used for the basic drill stem material, it could be used for selected drill stem sections that would only be used for sensitive drilling in ice-laden soils. Another potential material is a hybrid between Kevlar epoxy and graphite epoxy, which has been used in some applications, but is not well characterized at the present time. In certain lay-up configurations, this material can combine the low thermal conductivity and vibration absorption qualities of Kevlar with the high stiffness of the graphite fiber.

Two materials that were also considered as reinforcement in an epoxy matrix were boron fibers and alumina fibers. Boron fibers are profitably used in some applications requiring high specific stiffness, but they cannot be bent around less than a 1-in radius without severe fracture potential. Alumina fibers also impart high stiffness to the resin matrix, but this is a developmental process, and the impact resistance is low.

The metal matrix composites are very promising in terms of strength and stiffness. Highest on the list is the Ti-6-4 alloy reinforced with SiC fibers. This composite already demonstrates high specific shear strength and stiffness properties, and techniques for wetting the titanium to the silicon carbide fiber are still being advanced. The metal does not wet perfectly to a pure SiC surface, so alternative

fiber coatings have been studied. The outer suface can be carbon-enriched, which increases the strength of the fiber, but the titanium diffuses into the surface of the fiber and forms a titanium carbide interface that actually decreases the composite properties. An aluminum or high-carbon SiC coating can be used to bond with the titanium while leaving the carbon-rich layer intact. Methods such as these could substantially increase the fiber-matrix bond strength, and potentially improve the composite properties by a factor of two. Another fiber application currently under development is use of beryllium whiskers in a titanium matrix. Because many of the metal matrices are relatively new, properties such as impact strength and low temperature behavior have not yet been fully studied. However, it is expected that as these materials become more common their use can be better evaluated.

Aluminum is another metal that can profit from the addition of a reinforcing fiber. Both silicon carbide and graphite fibers have been used in aluminum with appreciable benefits in terms of improved stiffness. Presently there is some deterioration in the strength of the aluminum with an addition of SiC fibers, but this could be alliviated with improved techniques. The composites presently fabricated show a large range in strength properties, which is due to unpredictable fiber wetting and combination properties. As more research is done, these properties should improve. Several coatings of the SiC fibers are being employed to improve the composite properties. Also, the fibers have been added to the aluminum as whiskers. This eliminates the directional layup option provided by the continuous fiber product, but allows much simpler fabrication by extension of a fluted tube form.

Boron fibers have been used in aluminum, but the problem of potential fracture for small radii bends still arises. The tensile strength and stiffness of aluminum are improved enormously, however. Research has been done on altering fiber surface to allow better fabrication and impact properties; it has been studied as a material for aircraft propellers, which must be able to withstand the impact of a bird at high velocities. One method to improve the fiber-matrix bond is to use a B4C-B fiber. This type of fiber has also been used in developmental cases in a titanium matrix. Another technique is to coat

the boron fiber with SiC, yielding a fiber called Borsic, which has good adhesion properties with many metals. This has been used with an aluminum matrix and titanium foil, and also with aluminum and steel fibers. However, none of these presently have properties that demonstrate them to be better for use than SiC/Al, especially since the fabrication process is fairly complicated.

Magnesium has also been used with both SiC and graphite fibers to improve the stiffness. The measured stiffness of composites however, has rarely been comparable to the predicted theoretical values. Because of its low density and high specific mechanical properties, this material would be ideal for a drill stem and its ductility could allow easier subsectioning.

A recent development in hybrid composite materials is Arall 1. This material is fabricated from aluminum 7075 and Kevlar epoxy. It was developed for structural aerospace applications that are fatigue and fracture critical. Arall is said to be resistant to crack propagation because of the effect that the fibers have in holding small cracks together and preventing their growth. The fracture toughness is very high. The material is laid up with layers of aluminum foil on the outside, and alternating aluminum and Kevlar epoxy layers within. Because the composite is then cured at high temperature, some thermal stress exists when the material is at room temperature resulting from the difference in CTE between the resin and the aluminum. The sheet is stretched after curing to relieve these stresses at normal temperatures. These stresses could be a matter of concern for the desired low temperature ranges, and long-term adhesion could be affected. This, and the developmental nature of the composite that may make tube fabrication difficult, are reasons to reject it as an immediate candidate for a drill stem. However, continued research into this type of hybrid composite may at some point yield a material with properties that will suit a low temperature drill application.

Coatings of the stem should provide a low friction, contamination-free layer that will resist wear or degradation under the operating mechanical and thermal conditions. A process under development is ion implantation of iron in titanium, which forms an amorphous Fe-Ti-C layer. This layer has very low friction properties; such a process could only be used on a titanium, titanium-clad, or iron

alloy drill stem. Teflon is another material that has low-friction and low-contamination properties. This material was proposed for use on the Apollo drill stems, as a combined alumina/Teflon layer. The combination with alumina may eliminate the low temperature creep and fracture properties of Teflon. Lacquer coatings can form a low abrasion surface, but there are many potential problems with both high and low temperature extremes.

There are many commercial coatings available that would suit this purpose, some specialized for certain metals. Magnaplate, Magnadize, Canadize, Tiodize, and Tiolube are a few commercial examples. Most of these involve modification of the surface by nitriding, carburizing, oxidizing, or a combination of these processes. Some achieve low-friction surfaces by a coating or surface infusion of molybenum disulfide. This material (MoS_2) might be used on the outside of the drill stem, but on the inner surface it would provide the potential for sulfide contamination. The inner surface should be very low friction, but not a film lubricant that will influence the sample. A nitrided or Teflonized surface is best for this inner core surface. The threads on all sections will also be coated with a low-friction hard surface to reduce galling, vacuum welding, and friction during the threading operation. The exact type of surfacing can be chosen only when the final decision on drill stem material is made.

Cutter Materials--The material used for the cutters on a rotary percussive drill at low temperatures will have several requirements. To drill efficiently in the rotary mode, the material must have high hardness to avoid wear when drilling a hard material. To operate well in the percussive mode, the material must have high impact strength and fracture toughness. These characteristics will allow the drill to operate without chipping or fracturing the cutters. The material must retain its toughness at low temperature, and have a very low ductile-to-brittle transition temperature. High resistance to thermal shock is another necessary property, because the drill will begin operating in a cold ambient environment, may heat quickly in a material like solid basalt and then cool down quickly when stopped. The CTE of the material must match the bit as far as is possible because if cutters are inserted into the bit they will need to retain their fit at a variety of temperatures. The bit and cutter materials do not have a

stringent low-mass criterion because there will be a limited number of bits, and they will not be returned to Earth with the sample. The ease of fabrication and joining is a concern as the cutters must be fabricated and reliably attached to the bit, and the bit may be threaded for fitting to the stem. Thermal conductivity is a minor consideration, although if the thermal conductivity is extremely low, drilling could cause intense localized heating in the cutters and edge of the core sample.

The cutters are usually a different material than the bit, formed separately and joined to the bit. For Apollo, this attachment was made via brazing, but problems with pullout of the cutters were experienced. Research of other attachment methods would be beneficial. Direct welding is only feasible for metallic teeth, and would probably cause damage to the bit and cutter materials. Epoxy can be used to cement the cutters into the bit, but an epoxy that would be reliable under impact at low temperature may not be available and would provide the potential for organic contamination. Mechanical attachment is the only method that does not involve an intermediate material; clamping, threading, wedging, explosive welding and a shrink fit are all possibilities. Shrink fitting might be unreliable under the extreme temperature variations, while clamping and wedging both involve mechanical complexity that could be detrimental to the bit face design. Screw threaded fittings for the individual cutters introduce the possibility of individual cutter replacement.

Another method is to use a structural bit material that can be coated to form a hard cutting surface. This has the advantage that the underlying structural material can be fairly ductile, and provide some shock-absorbent qualities, while the hard cutting surface is wear resistant. Also there are many techniques that provide a very hard, dense coating that is partially diffused into the base material, and thus will not tend to chip and flake away. The coated surface can be altered, or enriched in one element, to provide better properties than the bulk material.

The standard cutter material used for rotary-percussive drills and used on the Apollo drill is tungsten carbide (WC). This is one of the hardest carbides, approaching the hardness of diamond. Usually it is alloyed with 5 to 15% cobalt to increase the ductility and fracture

toughness. The carbide cutters used on the Apollo drill contained 13% Co and had a hardness of 89.3 Rockwell A. Under rotary drilling action, these cutters exhibited good wear characteristics because of their hardness. However, the repeated impacts in percussive drilling had a tendency to chip and fracture the cutters because of the brittleness of the material itself. Usually the harder carbides have lower fracture toughness, and low temperature fracture toughness will be the critical parameter for some drilling conditions.

One solution suggested for this problem is to use a coating of the hard WC material over a softer metal, such as a steel, that would have higher ductility. Many new techniques in hard-coating have been developed that could benefit this application. Tungsten carbide can be applied to produce a hard, dense coating with superior adhesion properties. Plasma spray of a WC/Ni-Si-Cr-B combination has been found to give high abrasion resistance.

A similar method is to use a hard coating over one of the more fracture resistant grades of tungsten carbide. These are called complex grades of carbide, usually employing a titanium carbide, titanium nitride, or hybrid layer over the tungsten carbide tool surface. These coated tools are superior to tungsten carbide in resistance to abrasive wear and cratering. A thin coating of alumina can also be used over the carbide to provide additional hardness and corrosion resistance.

A new advance is the use of coarser grained WC in cutting tools. These materials were unknown at the time of the Apollo missions, but are now used commonly for mining, and show dramatically lower fracture rates than the fine-grained WC tools. The coarser grained materials have been proven to absorb shock better, and have higher fracture toughness values. In fact, the fracture toughness of these materials is so high that a new scale has been developed to describe it. The new and old toughness scales for several tungsten carbides are shown in Table 3.5.3-2. Kennametal K3560, a coarse-grained WC with 9.5% cobalt, has the highest fracture toughness, and still retains a hardness of 86.4 Rockwell A.

Listed in Table 3.5.3-3 are some potential cutting materials and their properties. Diamond has higher hardness than any other material, however, it has drawbacks in this application. The central problem is

Table 3.5.3-2 Tungsten Carbide Grades

Material	%Co	Hardness Rockwell A	Fracture Toughness mPa-$m^{1/2}$	Fracture Toughness Palmqvist scale	Comments
X-100				>500	Highly expeimental new grade
K3560	9.5	86.4	14.2	497	Coarse-grained, used for mining
K3109	12.0	88.0	14.0	278	Fine-grained, impact resistant
K6T	5.7	88.2	13.5	296	Coarse-grained, used for mining
K68	5.5	92.6	10.2	71	Fine grained, high hardness

Table 3.5.3-3 Cutter Material Properties

Material	Hardness/ Abrasion Resistance	Toughness	Low Temp	Comments
WC-12%Co (K3109)	Superior	Good	Fair	Standard cutter material Impact resistant grade
WC-5.5%Co (K68)	Superior	Fair	Fair	Standard cutter material Some chipping
SIALON ($Si_3Al_3O_3N_5$)	Good	Good	Good	Poor machinability Can coat by CVD at 1200°C
Si_3N_4	Superior	Good	Unkn	Also used with TiC
20% SiC_w in Al_2O_3	Good	Good	Good	
TiB_2	Good	Good	Unkn	Under development
99% Alumina	Good	Fair	Fair	Methods of controlling brittleness under development
Austenitic-Manganese steel	Fair	Fair	Good	Work hardening Embrittlement after re-heating

that a diamond bit normally requires a flush because it cuts by grinding. The grinding produces high heat loads that must be dissipated before heating causes carburization of the diamonds, destroying their cutting ability. Also, if the cuttings are not quickly removed from the hole bottom, they are ground and reground, making the drill operation much less efficient. A drilling flush is very impractical on this mission, and it would be undesirable to choose a tool that might later force this requirement. There is minimal data available concerning use of diamonds for low-temperature percussion drilling.

Alumina has moderately high hardness, but lacks ductility and thus is fracture critical. Several modifications are under development to increase the usefulness of alumina as a cutting tool. Amalox 68 is a high alumina product that is said to be highly wear- and corrosion-resistant, but it achieves these properties through high hardness, and has impact resistance too low for use in a percussive tool. SiC whiskers have been used to increase the fracture toughness to near the WC range. This composite is mixed as a powder, and then hot pressed into the desired form. Surprisingly, although alumina itself has very low tolerance for thermal shock, the SiC addition allows quenching from 900°C without damage. This material shows anisotropic properties, and because of the mismatch in CTE between SiC and Al_2O_3, cracks may form after long-term use at extreme temperatures. This effect should be studied to determine whether it would affect the operation at low temperatures. Also, additions of ZrO_2 have been found to provide additional ductility and provide transformation toughening.

Cubic titanium diboride is in the initial development stages, but so far has shown hardness second only to diamonds, along with a fracture toughness higher than the WC used on the Apollo Lunar Drill. Additions of 2% nickel have been used to increase the fracture toughness values. Cutting tools can be formed by hot pressing or powder metallurgy, or a coating can be electrodeposited on steel or tungsten carbide to form a hard surface.

Silicon nitride (Si_3N_4) has very high hardness but low impact strength and fracture toughness. The brittle nature is a concern, especially for low-temperature cutting. Additions of titanium carbide

have been used to decrease the brittleness. It is used successfully for high-speed machining of metals, but is probably precluded for use in a percussive nature drill. SIALON is a new material that uses alumina and silicon nitride to form a hard material with very good toughness relative to most ceramics. Titanium carbide and yttria additions have been used to increase the ductility of this ceramic.

Structural Bit Materials and Coatings--A method that has been studied, to avoid the use of separate cutters, is a bit with intregal cutters of the same material, coated to give them the wear resistance necessary for a cutting tool. The structural material of the bit can either be a base material unrelated to the coating applied, or it can be a material that reacts to form the hardened surface, so that the cutting surface is continuous with the base material. Candidate bit materials, with properties documented in Table 3.5.3-4, are all also possible for a bit with inserted cutters.

There are several steels that have promising qualities for use as a low temperature drill bit. Frostline and SAE EX55 are two that would require a separate coating of tungsten carbide or titanium carbide, to provide a hard cutting surface. Frostline is a steel that was developed for use as a low-temperature, impact-resistant tool. There is a small addition of niobium in the alloy that leads to increased ductility and low-temperature fracture toughness. SAE EX55 is a rock-bit steel designed for high strength, toughness, and high hardenability. The alloy was developed to provide better carbide retention and is partially carburized for hardness. The impact resistance is very high, and it can be treated to produce a fracture toughness of 70 m-Pa$\sqrt{m}$. Nitronic 50 is a high-strength steel that is nitrided to impart a high surface hardness. This material has not been studied extensively for its low-temperature properties. The nitrided portion of the surface does not normally penetrate deep enough to consider this as a long wearing tool. However, additional nitrogen could be diffused in, ion-implanted, or layered with additional base material during the nitriding process to form a deeper hardened layer. The depth of the modified zone would have to be balanced between becoming so thick as to create the potential for chipping, and being too thin and wearing away after a short period of drilling.

Table 3.5.3-4 Structural Bit Materials

Material	Coating	Impact Strength (J)	Fracture Toughness (mPa-√m)
A286 Steel	Poss. nitrides		125
Inconel 718	Poss. nitrides		96.3
Ti-6Al-4V	TiC or TiN	27	74.6
Frostline	Poss. nitrides	68	~60
EX55	None formed	72	60
Tribocor 532N	TiN and NbN	low	low
Al 2219	None formed		28.8

C-2

Titanium carbide and titanium nitride are both extremely hard, with the former reducing the friction between the tool and the work. The bit material can be a low temperature titanium alloy like Ti-6-4, and the surface can be nitrided or carburized to form a hard cutting suface. Again, ion implantation or diffusion can be used to achieve sufficient depth for the coating. The steels have higher fracture toughness as a base material, but the titanium allows a graded interface with the surface coating that may produce less chipping than a coating over a separate base material. Also, titanium is significantly lower in density and higher in specific strength. Use of titanium for both stem and bit would allow matching of the CTEs; galling can easily be avoided by the common practice of nitriding the titanium surfaces. A similar material for coating is a newly developed alloy called Tribocor 532: a niobium alloy with 30% titanium and 20% tungsten. When nitrided, this material forms an extremely hard surface that is a combination of nitrides of the three metals in the alloy. The hardness of the surface is greater than 2200 on the Vickers scale, and it has high thermal shock resistance. However, the bulk material is brittle because of the 20% tungsten content, and this may render the alloy unusable in a percussive application.

Inconel 718, an iron-nickel-chromium alloy, has a very high fracture toughness of 96.3 m-Pa$\sqrt{m}$ at room temperature. Aluminum 2219 is another material suitable for bit use, although it would need coating or separate cutters. This material would be advantageous if the stem were fabricated from aluminum or an aluminum alloy, as the match in CTEs would minimize stresses experienced at low temperature. The threads would be coated to reduce galling and vacuum welding potential. The fracture toughness is only 28.8 at room temperature, but it increases with decreasing temperature. The CTE of this material is higher than most of the potential coatings by a wide enough margin to cause concern. A286 stainless steel is commonly used for aerospace hardware, and has a fracture toughness of 125 mPa m at room temperature, decreasing slightly at lower temperatures. This material has inherent nitride formers (15% Cr and 2% Ti), which might be used to produce a hardened surface.

3.6 MARS SAMPLE STORAGE

3.6.1 Sample Canister Design

The sample canister design should provide for maintenance of the samples in their original condition with regard to temperature, pressure, and isolation from each other. The thermal environment is maintained by placement of the canister (i.e., shielded from the sun), timing of operations (sampling at night when possible), and the thermal buffer material, discussed below. The pressure is maintained after launch by a hermetic seal, and any particularly sensitive samples are sealed individually when collected. Isolation of the samples is achieved by the manner of packaging and storing each type of sample. Another important criterion is that the sample canister be capable of storing many different types and selections of samples in a mass- and volume-efficient manner.

Several design concepts for a sample canister were considered. Many of the samples taken will be tubular (drill cores, drive tubes, rock mini-cores), and thus a method of holding cylindrical samples is required. The tubes may be stacked together, but a structural framework is required because cylinders do not stack together flush and self-supporting. The structure could be a solid block with cylindrical holes, potentially of thermally insulating material, but this wastes mass and volume and could allow undesirable thermal gradients between samples. A more volume-efficient method is to support the tubes with a lattice-framework that allows minimum space between tubes. With this concept, all rock samples must be placed in identically sized tubes and stacked within the framework. All space between the cylinders is left unused and all rocks must be sized to fit in a 1-cm diameter tube. This not only restricts the selection of rock samples, but wastes space within the tubes when the rocks are not sized to fit together well in a 1-cm cylinder.

The most efficient packing is achieved using hexagonal containers. These can be stacked together with no intervening structure (i.e., with no unused volume), and a cylinder fits into a hexagon with minimum wasted volume. With this type of structure, rocks can be packed directly into the hexagon, utilizing all the avilable volume. To provide flexibility in sizes of rock samples, several types of hexagonal containers can be used. Two, three, four, and seven hexagon

combinations, without intervening walls, provide open areas of various sizes for many sizes of rock samples. A selection of the containers can be made one-third the height of the canister, so that three containers stack to fill the canister.

Pictured in Figure 3.6.1-1 is a sample canister concept that uses these ideas to satisfy all criteria. The thermal environment is maintained after launch by the thermal buffer that surrounds the samples. The buffer is placed on the outside so that it absorbs all thermal transients before they can reach the samples. The buffer container must be leak-tight to avoid loss of buffer material and contamination of the buffer or damage to the canister. Particularly sensitive samples can be placed toward the inside to avoid potential heat spikes from the outside. If deemed necessary because of aerobraking heat or potential ultra-sensitive samples, the design can be extended to include a second ring of more efficient thermal buffer material. All sensitive samples would be placed in the innermost volume, and the structure between the two thermal buffers would be insulative. Samples which are not particularly thermally sensitive, such as rocks, saltated dust, and atmospheric samples would be placed in the outer ring. Thus the entire outer thermal buffer could heat to its melting point, and the outer samples and structure would still offer a significant amount of thermal resistance and inertia so that the inner canister would remain cold.

The lid and the mating sealing surface on the canister each have "temporary seal" rings. These rings are a soft metal seal that is used for temporary sealing during transit to Mars and while on the planetary surface. The "temporary seal" rings are free of contamination at the start of the mission, so they provide a hermetic seal during all Earth operations and transit to Mars. Once the lid has been opened and started to become contaminated, the seal may no longer be perfectly hermetic during operation on Mars, but this is of secondary concern since the Martian atmosphere is not considered a contaminant for most samples. As mentioned earlier, any samples that could be contaminated by contact with the atmosphere will be sealed separately. A selection of methods used to contain different types of samples is shown in Figure 3.6.1-2. The lid is moved by a motor at the hinge that will keep the lid closed or at a 120°-or-less angle during sampling. When

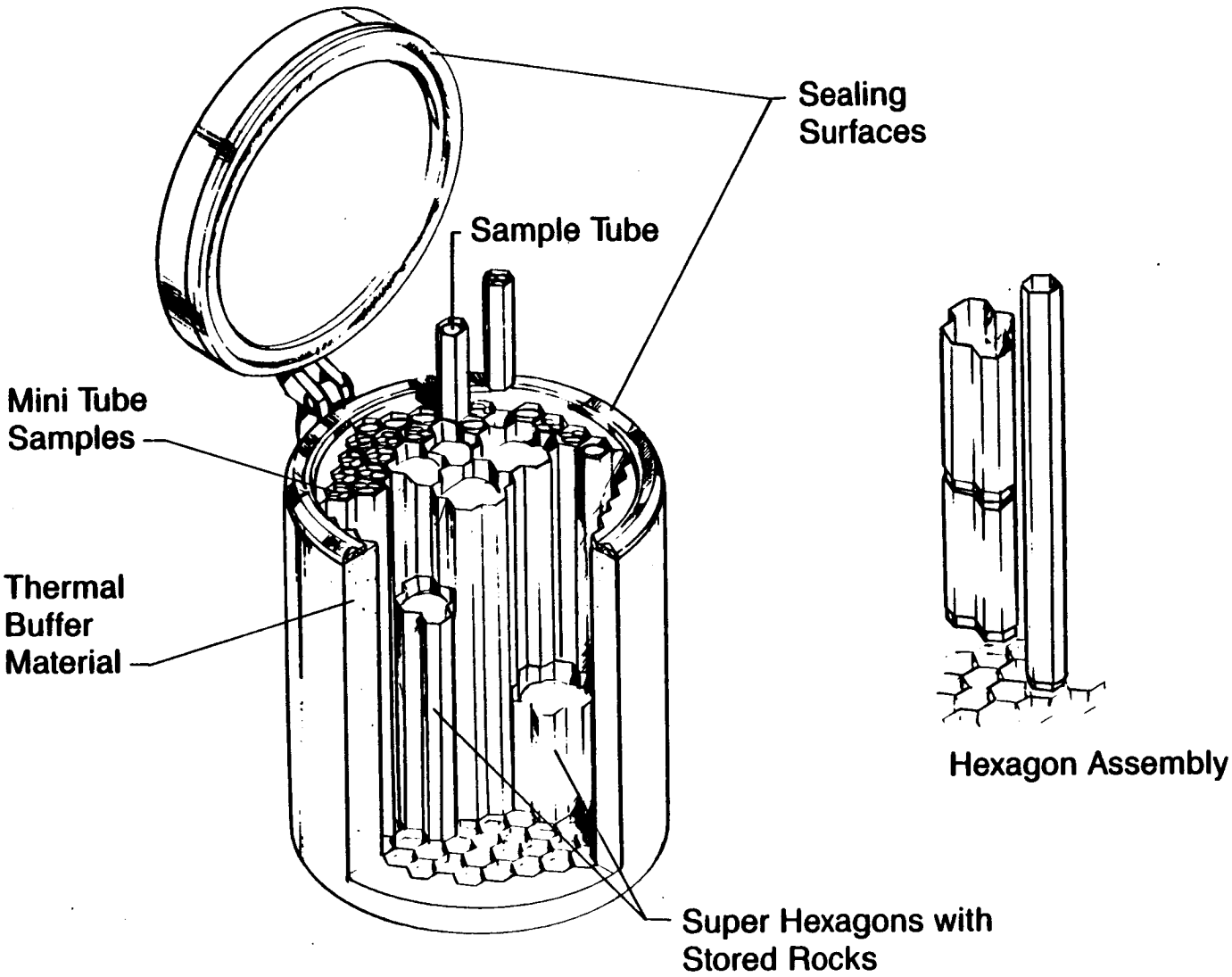

Figure 3.6.1-1 Return Sample Canister

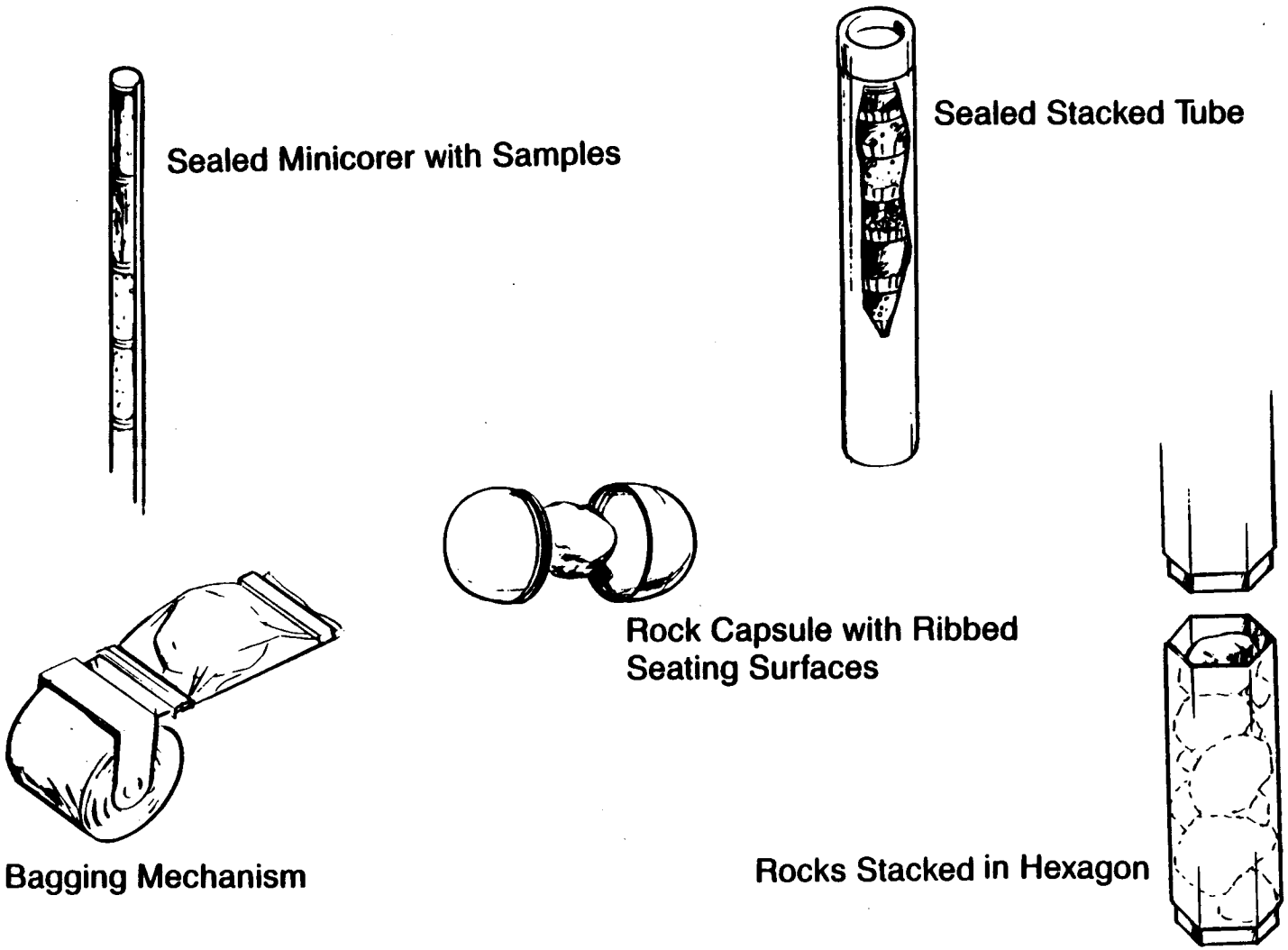

Figure 3.6.1-2 Sampling Sealing Methods

the canister is filled and ready to be sealed for launch, the lid is pulled back to a 180° angle to activate the ejection of the two temporary seal rings. Underneath each is a clean sealing surface that will provide a hermetic seal during the return to Earth and until the samples are ready to be analyzed. The sealing force is provided by clamps arould the perimeter of the canister top that can be electrically activated, manually operated by the rover arm, or capable of both for redundancy. A more complicated design would be to have the sealing force produced as a byproduct of insertion of the canister in the return vehicle, but this involves interdependence of the spacecraft and sample canister designs, and could create problems in removing the sample canister at Earth without breaking the seal.

The hexagonal structure of the sample canister provides not only flexibility in storage but also a highly volume-efficient way of storing the variously shaped samples. The hexagon containers are sized to contain a cylinder the size of a 1-cm drill stem, and each hexagon can hold three of the smaller mini-core stems or soda-straw drive tubes. The larger hexagon arrangements provide a method for storing various sizes of rocks and rock fragments. The canister can be filled in many ways depending on the type of samples selected for return; from a payload consisting solely of drill cores to one of only large rocks. The various lids have the same plug-in pattern used on the base of the can, so single hexagons can be stacked on top of a large hexagon. The position of each sample is documented during placement, so that any sample may be taken out later and properly identified.

Empty hexagons do not stack inside one another efficiently, so it may be necessary to use two sample canisters to hold enough hexagons to allow for the most flexibility in sampling. However, the hexagons do combine well enough so that the sample canister can hold about 130% of the permitted number of filled hexagons. Two sample canisters may be desirable for other reasons, such as use for an initial "safe" sample or simply for redundancy. Once the first sample canister is filled, a large assortment of hexagons will remain for filling the second canister in any manner desired. If it is found to be unacceptable to include two sample canisters, surplus hexagons could be stored on the rover body, ready for selection and use.

Each rock can be placed in a hexagon approximately its own size, so the linear stack of rocks will not be mixed and it will be possible to identify each rock's acquisition sequence and region of origin. A hexagonal container of each size can be left open or easily accessible in the "sample work area" on the rover, and each selected rock placed in the appropriate hexagon. Other methods of identifying the rocks are to encase them in sealed, marked plastic bags or capsules, which has the additional advantage of eliminating any potential cross contamination; mark the surface of each rock with an indelible paint; tag each rock with a marked elastic band; or photographically document each rock as it is collected. The latter would undoubtedly be a standard operating procedure in any case, but may not always be perfectly sufficient for ex post facto identification of samples.

The materials used in this sample canister must be selected not only to be lightweight, but to avoid any unrecognizable or interfering contamination of the samples. The entire thermal range that the canister will undergo must be considered in this selection. This includes not only matching coefficients of thermal expansion to ensure continued sealing and minimal thermal stresses, but also guarding against chemical or physical reaction of materials at the low and high temperature extremes. The outer can containing thermal buffer should be of high specific strength, such as titanium or beryllium, and may require surface passivation to protect against reaction with the thermal buffer and Martian environment. The hexagon structure material requires relatively little strength and a lighter material could be used. Beryllium is a good lightweight structural material, but it is more expensive to fabricate and could be considered unacceptable because of fracture mechanics requirements. Additional candidates are fibrous composite materials that are easily laid up in a hexagonal shape. Graphite epoxy is tough and lightweight, but has possible undesirable qualities, such as outgassing and contamination. It is possible to coat the graphite epoxy to eliminate this problem, but this adds to the complexity and some cost of the fabrication. One promising candidate is aluminum or an aluminum/fiber composite with a hard-anodized surface. An aluminum/fiber composite may be especially attractive. Promising fiber candidates include boron and silicon carbide, and development work is underway on a beryllium/aluminum combination.

Thin leaf seals on individual tubes and the main ring seals on the canister should be metal to provide reliable hermetic seals under potentially dust-contaminated conditions. The standard soft metal used to accomplish this is gold. However, gold is a trace element that may be very important in the analysis of the samples, so it is preferable not to use it and thus avoid any potential gold contamination of the samples. For the protected seal on the sample canister, it may be acceptable to use gold, because the seal should not contact the samples and is only exposed immediately prior to final sealing. For the seals on individual components and for the "contaminated" canister seal, it will definitely be necessary to use another metal. One possibility is indium (used on the seals for the Apollo lunar sample boxes) or copper, which may not be as important scientifically. Alternatively, the metal used for the seal can contain a specific percentage of some unusual element that it not expected in quantity on the planetary surface, such as platinum. This "spiking" of the seal will allow geochemists to determine if a certain metal content is a result of contamination from the seal, or if it is a true component of the soil.

3.6.2 Thermal Buffering During Aerobraking at Earth--The Earth return vehicle, with the sample canister onboard, will probably be designed to undergo aerobraking to enter Earth orbit. This has been determined to be the most mass and, hence, cost-effective method of reentry. However, aerobraking produces a large pulse of heat energy that must be dissipated without allowing unacceptable temperature excursions of the sample canister. All efforts to protect the sample during initial collection and transport will be worthless if the sample is allowed to overheat during Earth entry. Thermal buffer material has been proposed as a method to aid in isolating the samples from this thermal shock. A phase change material within the sample canister would absorb a significant heat load while melting, maintaining the samples at a constant temperature.

A preliminary thermal analysis was performed to determine the thermal effect of an aerobraked orbit insertion. The MITAS thermal differential analysis software was used to calculate temperatures and heat fluxes from the given thermal loads. Models were developed for both Mars and comet return because the spacecraft design and thermal

profiles differ for these two scenarios. The Mars return vehicle was assumed to be 127 kg (279 lbs) with a 0.79 m^2 (7.79 ft^2) aeroshell (Hill, preprint, 1985). The thermal models were simplified, with the spacecraft body, aeroshell, sample canister, and ambient environment as nodes. Radiative and linear conductors were implemented between all nodes, as follows. The sample canister was supported within the spacecraft by 20 cylindrical standoffs of a typical insulator (glass-reinforced plastic, polycarbonate, or Teflon). These were 2 cm in diameter with a 0.28-cm wall 3 cm long. The enclosure was lined with multilayer insulation blenket (MLI). Attachment of the aeroshell to the spacecraft body was approximated by 20 metal contacts, each 8 cm^2 in area and at least 4 cm from the center of the spacecraft. The radiation between the aeroshell and the spacecraft was reduced by use of high-reflectivity coatings or (MLI).

Typical profiles for the thermal impact of aerobraking have been generated; Figure 3.6.2-1 shows the heating profile for this case (Hill, private communication, 1986). For a Mars return mission the entry velocity is 4.3 km/s (38,000 ft/s). The heat pulse profiles were divided into 13 steps of input to the thermal analysis program. The temperature of the sample can'ster was held at the desired temperature (215K for Mars samples) to determine the amount of heat flux into the canister during aerobraking. This allows sizing of the thermal buffer, ablative or phase change material that will thermally protect the sample canister. Material that will absorb heat by the phase change of melting, rather than by vaporizing, was chosen, because this avoids use of a high-pressure container.

The time at which the heated aeroshell is ejected has not been specified, so several times were used as options in sizing the thermal buffer. The appropriate time to jettison the aeroshell is immediately after the heat pulse--about 12 minutes after initial entry. The thermal buffers are sized to absorb 150% of the calculated heat load for each given time because the surface properties of the spacecraft are not yet determined and it could cool slowly after jettison of the areoshell, and there could be other heating before pickup while the spacecraft is in orbit. The calculated masses of materials are meant to serve simply as evaluative criteria for the feasibility of the

method, and not as exact values as too many parameters are undefined. When more is known about the mission and spacecraft configurations, these thermal models can be revised and improved to provide more exact values.

For a Mars return mission the integrated heat pulse into the spacecraft from the convective effects of aerobraking is 5×10^8 J. In 25 minutes, it is estimated that 0.05% of this energy will be absorbed, requiring 2.5 kg of buffer to maintain a constant temperature. In an hour, the spacecraft will experience more of the total heat load, and 4 kg of thermal buffer is found necessary. The typical heat of fusion used for a thermal buffer in the 200 K range is 150 J/g (see below). Methods of decreasing the amount of thermal buffer needed are discussed below in the section dealing with comet return thermal buffering, Section 4.5.

Phase Change Materials--The phase change material must satisfy many criteria to be acceptable for use as a thermal buffer. Because the melting point of the material will determine the temperature at which the samples are stabilized, this is one of the primary criteria. Too high a melting point will allow heat damage to the samples, while too low a melting point will force the buffer to absorb more energy than strictly necessary to protect the samples, resulting in either an oversized thermal buffer or damaged samples because the thermal buffer did not last long enough. Ideally, the melting point of the material should be just exactly the maximum permissible temperature to maintain the samples without damage. The specific heat of fusion of the material should be as high as possible, so that the maximum amount of heat is absorbed for every gram of thermal buffer. The density of the material should also be as high as possible, to minimize volume and thus the mass of the buffer container. Also, the size of the canister will affect design of the return spacecraft and to a lesser extent, the mother spacecraft. The material should have a low vapor pressure at room temperature, and preferably a boiling point well above room temperature to promote ease of handling and also to avoid the use of a pressure vessel for containing the fluid before launch. The phase change material will be in the liquid phase for long periods of time during assembly of the sample canister, before Earth launch, and possibly during periods on Mars. Thus, not only is a low vapor

pressure desirable, but in case of a leak the material should be non-hazardous if practical. This includes low flammability, low toxicity, and minimal reactivity with other materials.

Many compounds were considered, as shown in Table 3.6.2-1. Optimum compounds for certain temperature ranges were selected. For the typical Mars subsurface temperature of 215 K, n-octane is the best candidate, having a high heat of fusion (181 J/g), a low vapor pressure, and a moderate hazard level. Valeric acid (pentanoic acid) is a second choice with a lower heat of fusion, a slightly lower hazard level, and a higher density. Both of these compounds melt within one degree of 215 K. Two compounds that have superior heats of fusion in this temperature range are phosgene and chloropicrin. These were not selected because of excessive hazard, but if either could be used it would decrease the amount of thermal buffer necessary by 10+40%. If the samples could tolerate a slightly higher temperature (238 K), an excellent choice would be cyclopropylamine, having a low vapor pressure, low hazard level, relatively high density, and a very high heat of fusion of 231 J/g.

For the polar regions, assuming a sample temperature of 180 K, a preferred material is n-heptane, with a heat of fusion of 141 J/g and a very low vapor pressure. N-butanol and ethyl acetate are acceptable materials for temperatures just above this (183-190 K). N-hexane has superior qualities for stabilization at 178 K: a heat of fusion of 151 J/g and a low room temperature vapor pressure of 5 psig. If a slightly higher vapor pressure is acceptable, methylamine at a melting point of 179.7 K has a heat of fusion of nearly 200 J/g.

4.0 COMET SAMPLING

4.1 Science Objectives

Although successful, the recent hypervelocity flyby missions to Halley's Comet still leave much to be learned about the detailed nature of the cometary surface. The very irregular shape of the nucleus, the heterogeneous nature of the active regions, the extremely low albedo, and the time variant character of dust and gas releases all testify to a complexity in surface processes that challenge the acquisition system to bring back a representative, yet comprehensive suite of samples.

Table 3.6.2-1 Phase Change Compounds

Compound	M.P. (K)	H_f (J/g)	ρ (g/cc)	Vap. Press (psig)	Flamm	Toxicity	Hazards, Incompatibilities
Propene	88	71.4	0.50	154.	High	Low	Vapor heavier/air, ESD
Ethane	89.9	95.1	0.55	544.	Med	Med	Chlorine, oxidizers, heat
Methane	90.6	60.8	0.55	~1500.			
Ethene	103.7	119.1	0.57	1200.	Med	Med	F_2, fumes on heating
Diborane	104.0	165.7	0.58		High		Explosive
3-Methyl-1-butene	104.6	76.6					
◊ 1-Pentene	107.0	82.9	0.64	10.7	High	Low	Heavier/air, ESD,oxidizers
Nitric oxide	112.0	77.0	1.27	1.9	Low	Med	None
Isopentane	113.3	71.3	0.62	11.6	High	Med	Heavier/air, ESD,comp air
Isobutane	113.6	79.4	0.55	30.7		Low	
Chloroethane	119.0	75.9	0.92				
2-Methylpentane	119.5	72.9	0.65	~5.		Low	
◊ cis-2-Pentene	121.8	101.5	0.66	8.2	High	Low	Acrid fumes on heating
1,4-Pentadiene	124.4	90.2	0.66	12.3	Med	Low	Acrid fumes on heating
Isoprene	127.3	70.3	0.68	9.2	High	Med	Abs O_2, forms peroxide
Methylcyclopentane	130.7	82.5	0.75	~5.			
Dimethyl ether	131.7	107.2		60.	Med	Med	
2-Methylpropene	132.6	105.7	0.59	24.3	High	Low	Oxidizers
◊ trans-2-Pentene	133.0	119.2	0.65	~11.	High	Low	Fumes on heating
◊ cis-2-Butene	134.3	135.1	0.62	~20.	Med	Low	Oxidizers
n-Butane	134.9	80.3		30.	Med		
2-Methyl-1-butene	135.6	113.0	0.65	~11.			
2-Methyl-2-butene	139.4	108.5					
◊ n-Pentane	143.5	116.7	0.63	8.3	Med	Med	Oxidizers,heat
Cyclopropane	145.8	129.4	0.72	92.8	High	Med	Heavier/air, ESD,oxidizers

Table 3.6.2-1 (continued)

Methyl cyclohexane	146.4	68.7		0.45	Med	High	Oxidizers
1-Propanol	147.1	86.4	0.80				
Ethyl Mercaptan	152.0	80.1	0.84	<14.	High	Med	Oxidizers, compressed air
Methyl Mercaptan	152.2	122.8	0.87	~16.	Med	High	Cu, Al under pressure
Methyl disulfide	152.7	97.6					
◊ 1-Heptene	153.5	128.9	0.7	0.9	Expl	Low	Oxidizers,heat
3-Ethylpentane	154.6	95.5					
2-Chloropropane	156.0	94.1	0.86				
Triethylamine	156.1	110.8	0.73	~6.	Med	Low	None found
Ethyl ether	156.9	98.1	0.71				
Ethanol	158.7	109.0	0.79	~7.	Med	Med	Pt, oxidants,CrO_3,etc
Carbon Disulfide	161.5	57.8		7.7	Med	High	Liquid form, Cl_2,F_2, Zinc
2-Methylheptane	164.1	89.9					
◊ 1,3-Butadiene	164.3	147.0	0.63	22.0	High	Med	Cu, oxidizers
◊ Tetrahydrofuran	164.8	118.5	0.89	2.2	High	Med	Forms peroxide in air
Chlorine	170.0	95.5				Med	
Tetramethylsilane	174.0	78.0	0.65		Med	Low	Decomp on heating
Methanol	175.3	99.2	0.79				
◊ n-Hexane	177.8	151.5	0.66	~5.		Low	
Acetone	178.4	98.0	0.79	~8.	High	Low	
◊ Methylamine	179.7	197.5	0.7	28.8	High	Low	Strong base
Dimethylamine	181.0	131.8	0.68	~20.	High	Med	Cu,Sn,Zn
2,5 Dimethylhexane	182.0	112.7					
Nitrous oxide	182.3	148.7	1.23	~200.	Low	Med	
◊ n-Heptane	182.6	141.3	0.68	0.8	High	Med	Oxidizers
◊ n-Butanol	183.4	125.2	0.81	0.2	Med	Med	Oxidizers
Dihydrogen sulfide	183.5	114.4	1.38				Some metals
Isopropanol	183.7	89.4		~6.	Med	Low	
1-phenyl butane	184.5	81.6	0.86	~4.	Med	Low	

Table 3.6.2-1 (continued)

1,trans-2-Dimethyl cyclohexane	185.0	93.0					
2-Butanone (MEK)	186.5	117.0	0.80	~6.			
◊ Ethyl acetate	189.6	119.0	0.9	1.9	High	Med	Nitrates,alkalies,acids, oxidizers
Hydrogen fluoride	190.1	229.2	0.99				Some metals
Arsenic pentafluoride	192.2	69.1					
1-pentanol	194.1	111.5	0.82	0.15	Med	Low	Heat, flame, oxidizers
Sulfur dioxide	200.0	134.9			Low	Low/Med	
Isopropyl toluene	204.1	71.6	0.86	0.01	Med	Med	Oxidizers
Phosgene	209.0	201.6	1.4	22.8	Low	High	K,heat, water,ammonia
Chloropicrin	209.2	201.5	1.7	2.2	Expl	High	Heat, detonates with shock
m-Cymene	209.4	102.1	0.87	~1.			
Chloroform	209.6	73.7	1.48	~7.	Low	Med/High	
◊ Valeric acid	214.2	116.4	0.94	0.02	Low		None found
◊ n-Octane	216.4	180.8	0.71	0.2	Med	Med	Oxidizers
n-Nonane	219.6	120.8					
1,2,4 Trimethylbenzene	229.4	102.9	0.86	~3.	Med	Med	Heat, Oxidizers
γ-Butyrolactone	229.8	111.2	1.13	~0.5	Low	Low	None found
Flourobenzene	231.0	117.7	1.02	~5.	Med	High	Heat, flame, oxidizers
1,1,2-Trichloroethane	236.6	86.5	1.44	~3.			
1,2-Dichloroethane	237.5	88.4		~5.	High	High	Al, K, powder hazardous
◊ Cyclopropylamine	237.8	230.9	0.82	~8.	Med	Low	None found
2-Butyne	240.8	170.7	0.69	~12.	Med	Med	Oxidizers, heat
1,2 Diethylbenzene	241.9	108.7					
n-Decane	243.3	202.4	0.73	0.02	Med	Low	Oxidizers
Cyanogen	246.0	165.9	0.87				
o-Xylene	248.0	128.3	0.88	0.2	Low	Low	
Isodurene	249.0	96.2		~2.			
Carbon tetrachloride	250.2	173.9	1.60	1.9	Low	High	Toxic fumes when heated

Table 3.6.2-1 (concluded)

Benzenethiote	258.1	104.5	1.07	~0.1	Low	Med	Heat, acids
Hydrogen Cyanide	259.8	311.2	0.7	12.0	High	High	Bases, caustics
Nitrogen tetroxide	260.0	252.2					
Ethylene glycol	261.7	181.0	1.11	0.001	Med	Med	Acids
n-Butyric acid	267.5	125.7	0.96	0.01	Low	Low	CrO_3,oxidizers, corrosive
Cyanogen Chloride	268.0	152.5	1.19				

Simply obtaining a set of samples may be a difficult engineering task because of the near-zero gravity attendent with surface operations and the current uncertainties in engineering properties of the nucleus, such as material porosity and strength.

Of primary interest is obtaining a "deep" sample, one below the thermal wave of the alternating cycle of heating and cooling that occurs during each orbit about the sun. Different authors have variously placed this zone as being one to tens of meters thick. Such material will not have been cyclically altered during these "yearly" thermal variations. However, even deeper layers are subject to the increase in average temperature that must result once the comet is removed from the Oort cloud. Thus, the formation temperature of a few tens of Kelvins are significantly exceeded by the 120 to 150 K thermal regime the sample exists at when sampling takes place. A formal consensus is yet to be developed on this point, but seems likely to specify that sampling take place at depths not less than one to a few meters, and that the sample be preserved at its natural temperature.

It does seem to be universally agreed upon, however, that the best method of sampling is by the use of some type of coring drill. It will be important that the drilling operation is of minimal thermal disturbance. Mechanical distortion is also an important factor, but may be permitted if it increases the amount of sample that can be returned--e.g., by longitudinally compacting a core to a reasonable density if it is found that the cometary nucleus is a very low density object, ca. 1 g/cm3.

The size of the sample is also open to specification. A one-centimeter core could provide large amounts of material relative to most analytical requirements. To preserve a large amount of material, a wider diameter core, up to 4 or 8 cm, could be selected. This would provide ample opportunity for many sizable splits if many different participants in the sample analysis were desired or required, especially, as applied to the case of an international sponsorship of the sample return mission.

Obtaining more than one deep sample may be requisite to having a representative suite from the comet. Not only may the cometary nuclei be structurally heterogeneous because of the stochastic nature of the emissions activity, but the mode of formation may have been a mixing

process that involved "cometesimals" of differing origins. It could be extremely desirable, for example, to sample from both active and inactive areas; or, from "equatorial" versus "polar" regions of the nucleus; or, from an invaginated as contrasted to a "normal" surface.

The surface of a comet is thought to contain a crust of nonvolatile material that is composed of particles that do not detach during sublimation of the ices, and fall-back material. This "mantle" layer could be highly variable over the surface of any given comet because of the variations in thermal flux due to surface terrain and rotation of the nucleus. Such layers are expected to vary with time because of competing processes of accumulation and blow-off. Sampling many different areas of the surface could be quite valuable in understanding the dynamics of mantle growth, maturation, and rebirth. Theoretical models of cometary models predict thicknesses from a few millimeters to meters in depth. Sampling techniques and sample return conditions should preserve the stratigraphy of the samples taken. It may also be desirable to obtain samples of the topmost dust particle layer at several loci on the surface.

4.2 Vehicle/Mobility Issues in Comet Sampling

There are two principal approaches for sampling a comet: landed and remote sampling. The most obvious method is to approach, land and secure the lander. A comet differs from a planet in that it has surface gravity on the order of 10^{-3} g, so the spacecraft must be secured to the surface to maintain physical contact. There is no current information available about the penetrability of a cometary surface, so any anchoring method must be designed to penetrate and hold securely in a wide variety of materials. If practical, the method must be reversible; in other words, the anchors should be capable of release or disengagement. The lack of gravity also forces any anchoring method to react its own anchoring thrust so that the spacecraft is not forced away from the comet by the very act of emplacing the anchors. A main purpose of any anchoring method is to react the torques caused by drilling and be sufficiently stable to resist the impact reactions without slipping or loosening. Another unknown factor is the relief of the terrain. If the surface is highly irregular, this will add to the complexity of landing a spacecraft on the surface. Most spacecraft have a number of relatively delicate appendages (solar cell arrays,

antennae, docking structure, return vehicle structure, etc.) that could be damaged in a landing on an irregular surface, or make such a landing impossible. The low temperatures of the cometary surface will provide a severe thermal drain if there is a hard contact between it and the spacecraft body, and any equipment requiring operating temperatures above 130 K must be thermally isolated and heated.

The devolatilized mantle covering the cometary surface could have many deleterious effects on the landing operation and on the landed spacecraft. For example, thick and fluffy mantle material could hide irregularities, making the landing much more hazardous. Selection of a site would also be more difficult if the mantle covered all surface features and heterogeneties. Mantle dust could have several other effects as well. The thermal control surfaces of the spacecraft, for which cleanliness is critical to maintain the optical properties, could be contaminated and their function negated or reversed by coatings of dust. The dust could enter critical moving parts and create difficulties with later operations such as sample sealing. It may be possible to use gas jets to clean the surfaces of the spacecraft, but this might remove not only the dust from the spacecraft but also the dust from the comet surface near the craft. In fact, the mantle dust could be removed from the landing site by the disturbance of landing. The mantle is one of the main interests in comet sampling, and if the spacecraft has a limited sampling area it is important that the mantle remain minimally disturbed in this area. Finally, if the mantle is deeper than expected, the entire spacecraft could sink below the surface during landing. As discussed below, for these and other reasons it may be found more practical to provide a remote or hovering sampling mode that allows contact only by the sampling device(s).

There are many possibilities for the technique used in docking and anchoring to a comet. The spacecraft can be anchored as it docks, using booster rockets to provide the force opposing the entrance resistance. One approach is three legs, as shown in Figure 4.2-1, which provide flexibility and stability as the points contact the surface. The legs end in sharp points to efficiently penetrate a hard, dense material. They also have thorn-like anchor tabs to provide resistance to de-anchoring forces. Above the sharp tabs, the legs flare out into inverted cups or flaps that become progressively larger

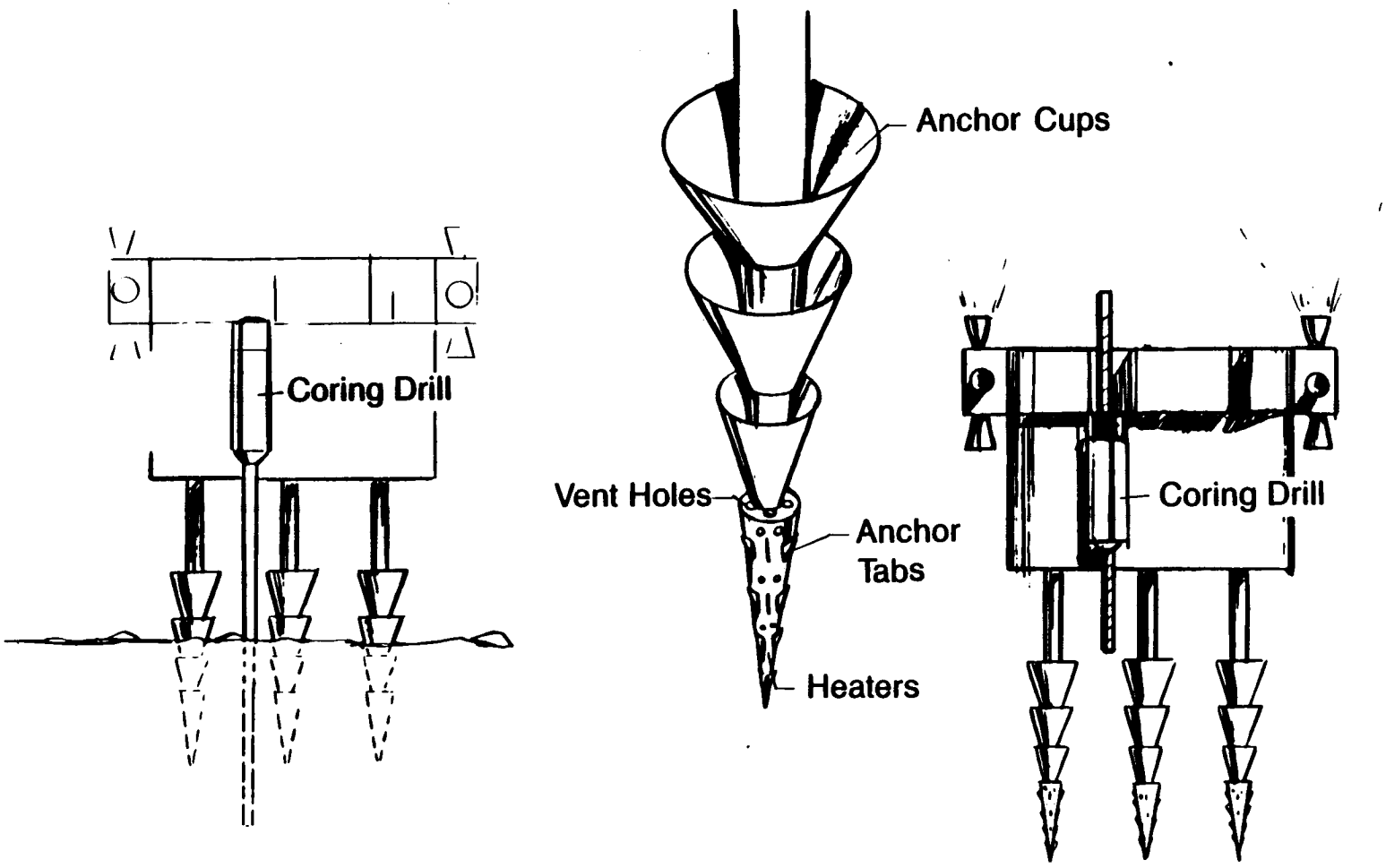

Figure 4.2-1 Anchoring to Comet

the further from the end-spikes. These cones will furnish the anchoring force in soft or fluffy material. The softer the material, the farther the legs will be driven in and the larger the anchoring area available. To ensure the legs can penetrate even the densest ice/dust conglomerate, heaters are also provided on the points of the legs. These can be activated to soften or melt the ice and allow penetration of the legs. Once the legs are implanted, the heaters are turned off and the ice refreezes around them, effectively anchoring the spacecraft. Rapid sublimation and permanent loss of ice could defeat this feature. Problems with this method include potential disturbance of the sampling site, although the drill could either be centered between the legs or extended to the side to avoid the disturbed areas. The system can be designed to anchor in a wide variety of materials, but could still have difficulty if the surface is a very dense low-ice soil conglomerate or an extremely deep fluff. If a change in the sampling area is desired, e.g., once the main sample collection has been accomplished, the legs could potentially be released. This could be attempted by using a combination of booster rockets and reactivation of the leg heaters.

Another concept is to let the anchoring system provide its own reactive forces. The "harpoon and winch" design is pictured in Figure 4.2-2. Again, there are three anchoring points to provide stability and positive contact on all points. The harpoons are fired in by cold gas or propellent-driven ejection, and either the directed gas jet or dead-weight projectile fired upward can provide the reactive forces to the acceleration of the harpoon into the comet. As an option, the projectile fired up could be a small sample canister on a drag line, fired at an angle and later dragged back through the mantle material to collect a sample. The harpoons will penetrate as far as possible into the comet, attached to the spacecraft by a winch line assembly. When the harpoons have successfully been anchored, the winch assembly starts to tighten the lines. The winch lines begin to move the anchors backward, and the frictional force against the cometary material will open out flaps that were compressed along the length of the harpoon during penetration. These provide an anchoring force and the winch lines can be pulled taut, bracing the spacecraft legs firmly against the surface. This method is highly adaptable to a deep mantle

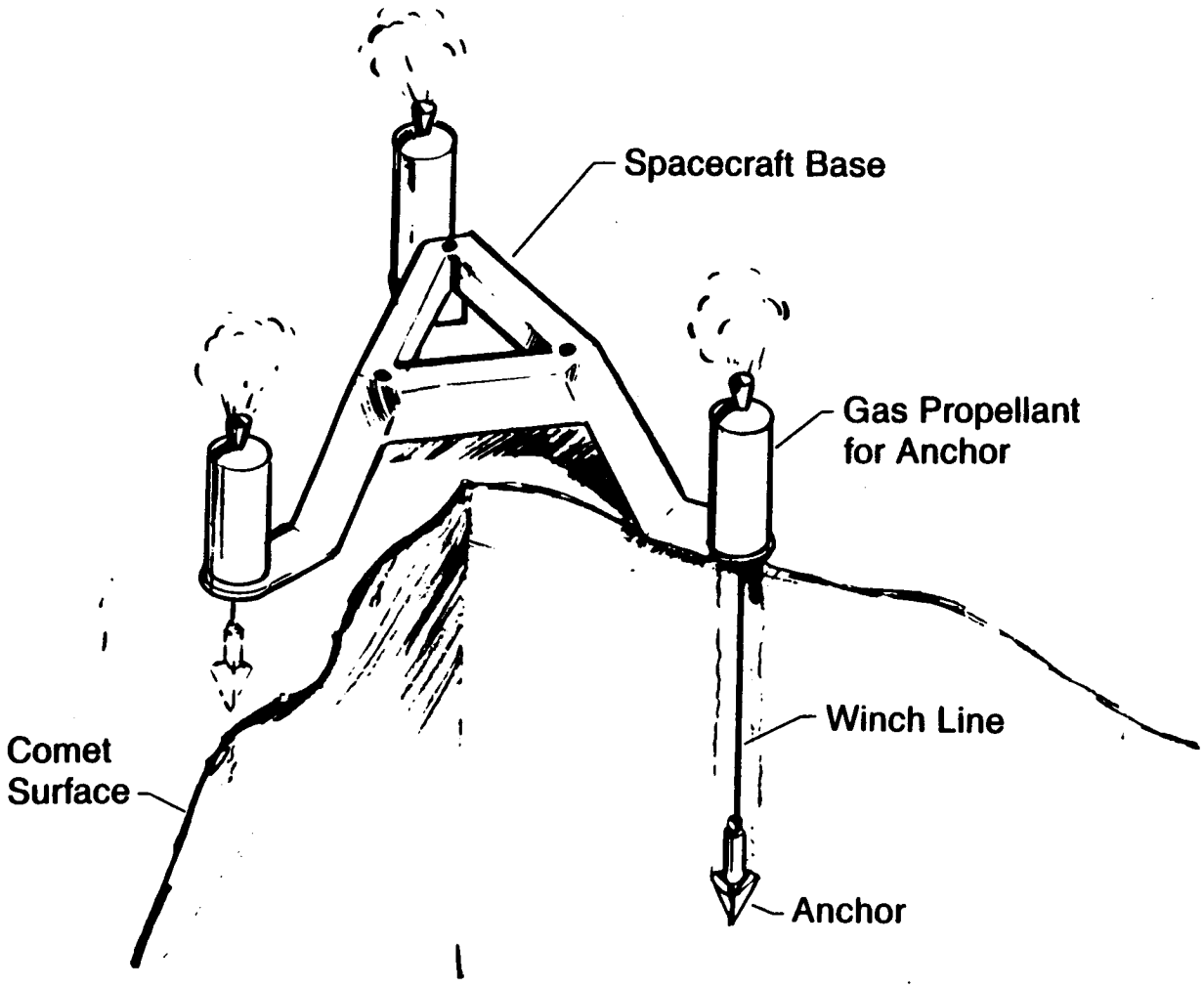

Figure 4.2-2 Fired and Winched Anchoring System

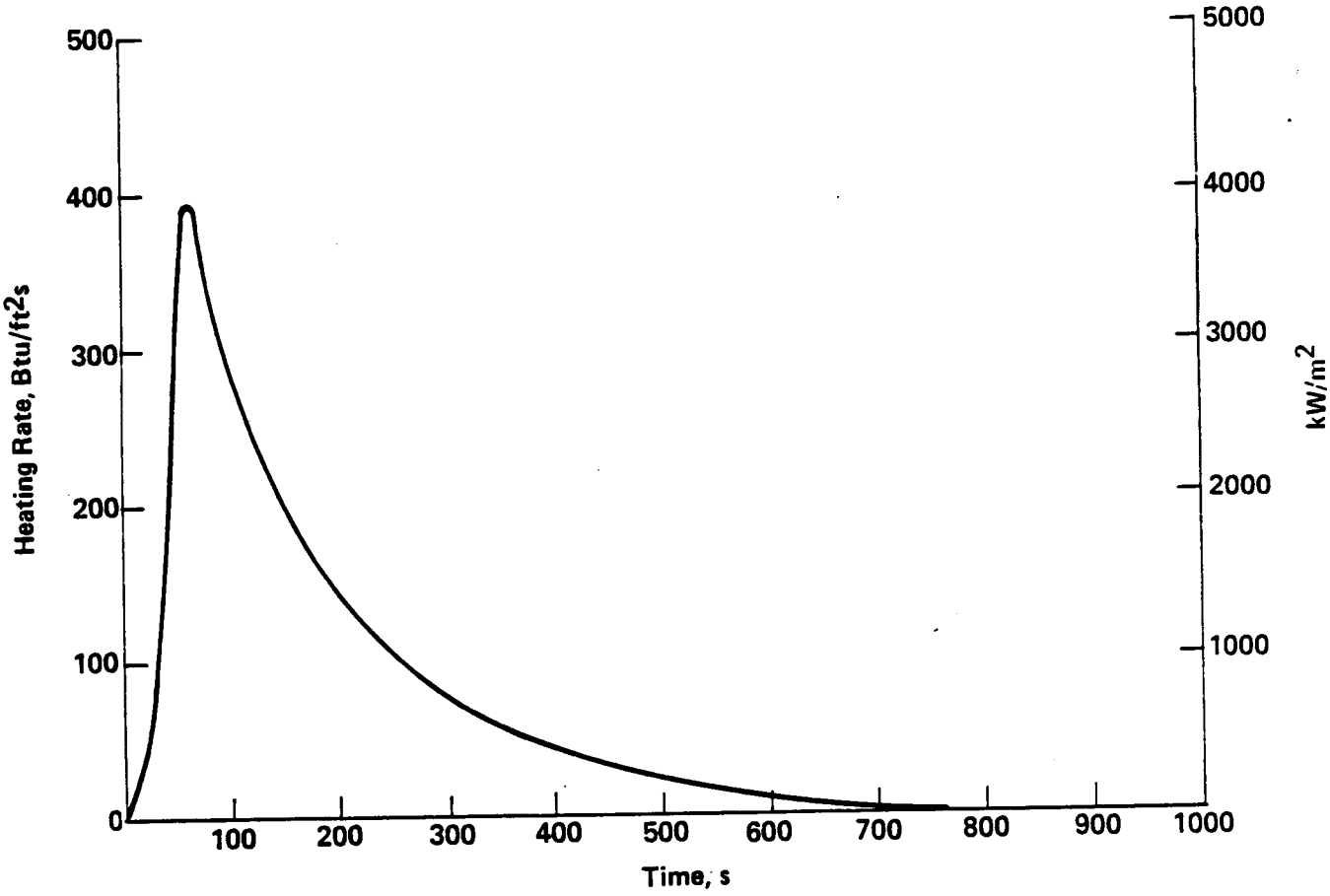

Figure 3.6.2-1 Mars Sample Return Heating Profile (V_i = 11,580 m/s)

configuration, as the anchors will go through a great depth of soft material and reach the nucleus as long as the winch lines are sufficiently long. For this system to be releasable, either the anchor flaps must be electrically activated to go to a third (straight down) position, or the anchors and their winch lines must be discardable. Assuming that the spacecraft was supplied with several sets of harpoons and release systems, this method could be used to sample at several different sites of the comet.

A method using angled cleats comes from the practice of exploratory drilling companies, whereby a hangar-like device is driven by hand into the ground as a tie-down. This device drives two cleats at angles into the surface. The horizontal forces cancel, but the vertical components need to be reacted by the spacecraft inertia and fired thrusters. The pull is then exerted toward the center to provide a clamping action, as shown in Figure 4.2-3. The cleats can be sized so that in hard material the sharp points will penetrate, while in soft material the entire cleat, flared at the aft end, will sink in. The cleats are driven in by a rack-and-pinion drive, and thus can be pulled out and reused at a different location. This method causes minimal disturbance of the surface, but may not be practical for very soft, easily compressible materials, as the cleats would not hold but would continue to move toward each other. A deep mantle layer could render this technique unusable unless the entire anchoring system were mounted on a vertical rack that could be lowered into the mantle.

The second approach to comet sampling, remote rather than docked, involves its own set of unique challenges. The spacecraft must be precisely controlled to remain over the sampling area. This necessitates a continuously active guidance system, which will undoubtedly require autonomous guidance and control (G&C) capabilities to respond quickly to changes in the situation. It is probable that thrust would need to be maintained almost continuously during the sampling operation, both for attitude maintenance and to react the forces against the surface during sampling. This could be a major consideration in sizing the fuel mass, and would place a restriction on the time available for sampling. Any remote method would have to be assured of proper disengagement, so that the entire spacecraft was not permanently locked to the comet involuntarily.

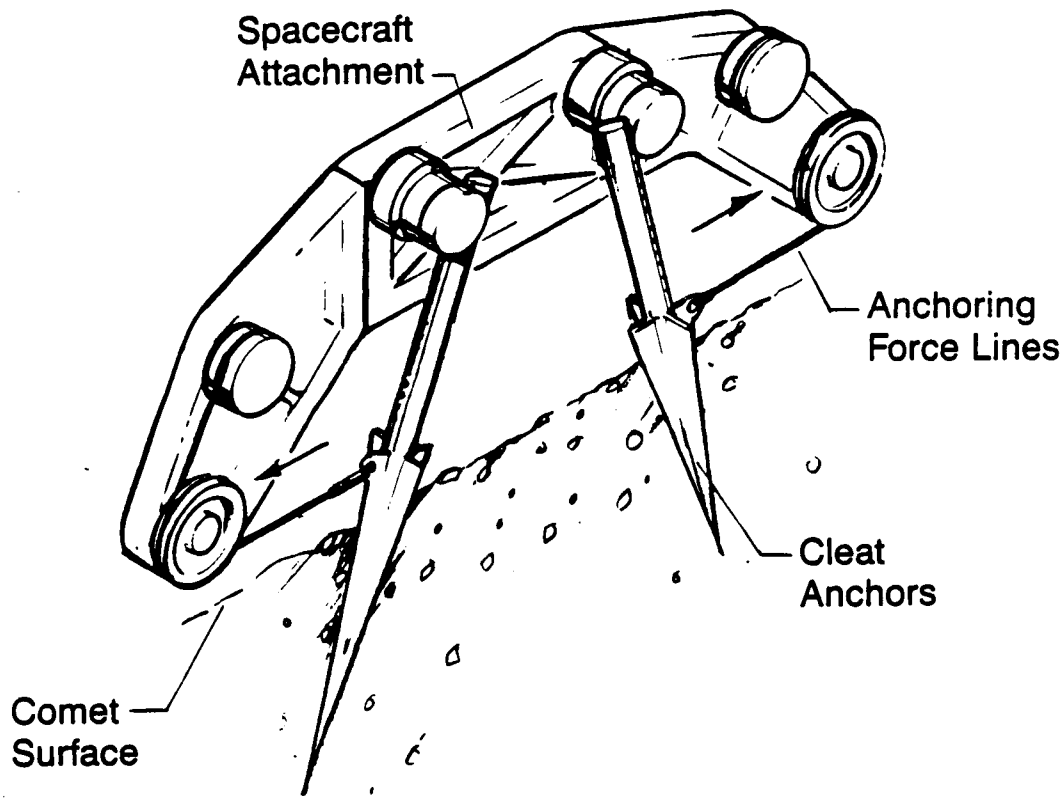

Figure 4.2-3 Anchoring to Comet by Angled Cleats

These remote methods can use either a rigid mechanism or a tether for the connection to the sampling device. The principal sampling device would be a drill or an extended impact tube for acquisition of deep core nucleus samples. The ostensibly simplest approach is to hover the spacecraft over an area to be sampled, and extend a long drive tube to the surface. The forward penetration of the drive tube would be provided by spacecraft thrust. A concern with this method is that it is not adapable to a wide range of materials, and in a dense material the tube might not be capable of withstanding the necessary drive force. This concern can be answered in part by using an extended-shaft drill rather than a drive tube. The torques of drilling would have to be reacted by boosters on the spacecraft. The drill shaft can be a long telescoping rod that locks into its extended position at the comet, Figure 4.2-4. A camera on the spacecraft and/or spacecraft G&C monitors the progression of the drilling operation. After coring, the entire drill stem can either be drawn up through the spacecraft to allow removal of the core, or the telescoping joints of the shaft can be electrically activated to unlock and bring the core back to the spacecraft for removal. The latter approach may be more adaptable to existing spacecraft designs. It is potentially possible to place a device at the end of the drill shaft that would remove each core section, seal, and store it. This device could then be drawn up separately at the conclusion of sampling, and inserted into the sample return canister. This method adds a large mass at the end of the extended shaft, which would place higher loads on the drill shaft during various maneuvers.

A similar method is to extend a platform using a structural boom. The platform would be equipped with feet and a drill assembly. The boom can be of the retractable type, as shown in Figure 4.2-5. Pads on the platform feet could serve to keep it perpendicular to the local surface, or the drill alone could contact the surface. Thrusters on the spacecraft would be necessary to counteract the torques of drilling, unless the surface was sufficiently solid to allow temporary anchoring by "claws" or small anchors on the boom. The sample canister can be placed at the end of the boom without undue stress on the boom structure, and the drill stem sections can be fitted into the canister automatically as they are completed. The boom would then be retracted, or the filled canister pulled along the boom into the spacecraft, at the end of the sampling operation.

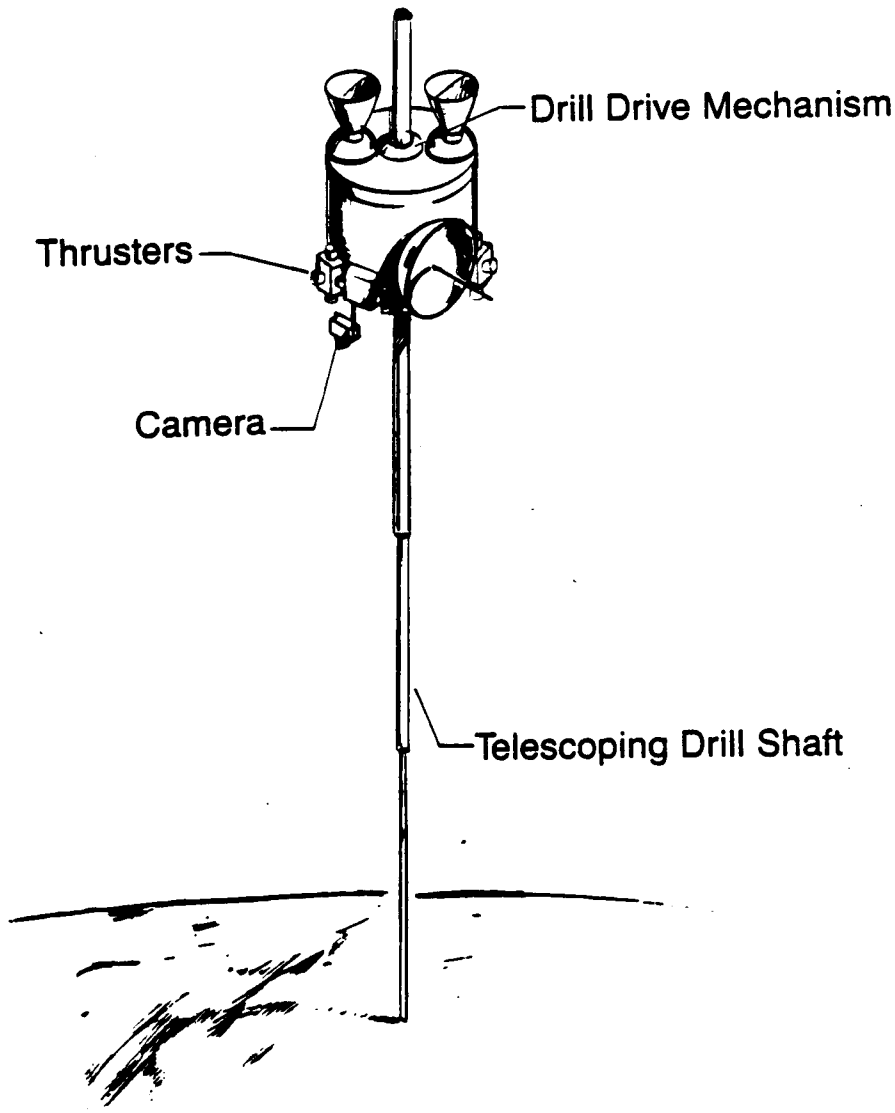

Figure 4.2-4 Remote Sampling of Comet with Extended Drill

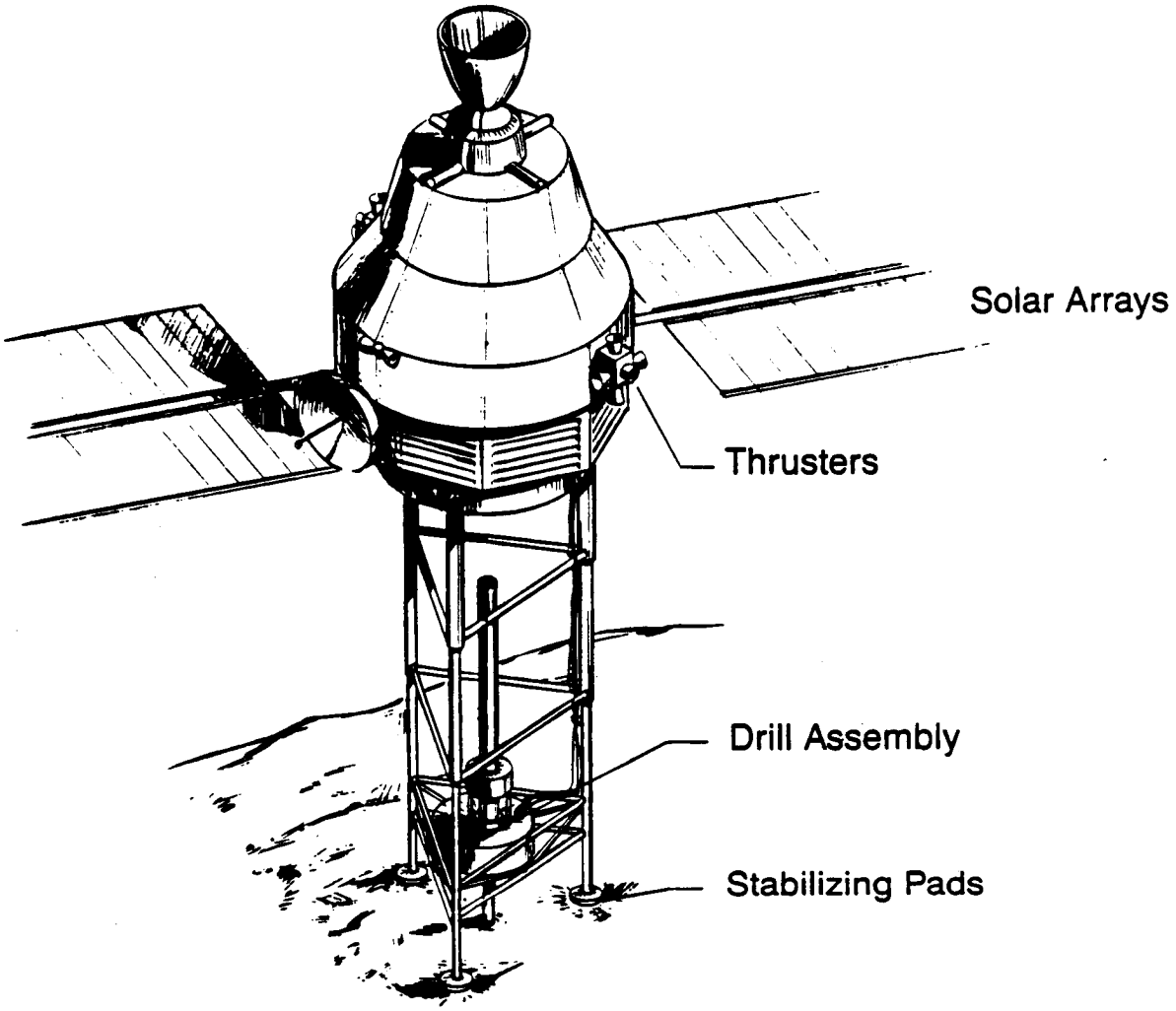

Figure 4.2-5 Remote Sampling of Comet with Drill on Boom

Tethered operations could in general be carried out with the spacecraft further from the comet. An approach that would be capable of obtaining a core sample without drilling or touchdown on the comet is to use an impact drive tube fired at the comet like a harpoon. A rugged drive tube would be used, attached by a cable to a winch assembly on the spacecraft, Figure 4.2-6. The tube would be fired toward the comet using compressed gas, explosives, spring release, or electric solenoids. The cable would have a slip connection, to allow for spin-up of the tube to enhance flight stability. The tube would be reeled back, and either emptied of sample or disengaged and a new tube attached. Disengagement is probably preferable, because spare tubes and a method of tube release are already necessary in case the tube is not returnable from the comet. Core catchers that close off most of the tube, or electrically activated shutters, may be necessary to avoid loss of core material during the extraction and reel-up. One concern with this approach is that a sample tube long enough to collect a meter or more of material may not be practical. Varying depths of sample could be collected by either firing at variable velocities, or stopping the cable at a selected depth. Information on the density and strength profile of the cometary material could be provided by an accelerometer on the impact tube.

The drag line is a tethered method that would collect only surface material. The sample collection canister is a scoop-mouthed box, pulled by the spacecaft via a cable, as in Figure 4.2-7. Jets of gas provide the impulse force to lower the canister to the surface. Dragged at an angle, the canister is held on the surface by the force of the jets, and by the drag force of a scraping blade behind the canister. The lid of the box is hinged on the cable such that when collection is finished and the box is pulled off the surface toward the spacecraft, the lid seals against the open end of the box. Problems with this method include reliably keeping the canister against uneven terrain, and its lack of collection of deep material. Another option for this method is to drag a collective surface, rather than a scoop, that would gather material by adhesion.

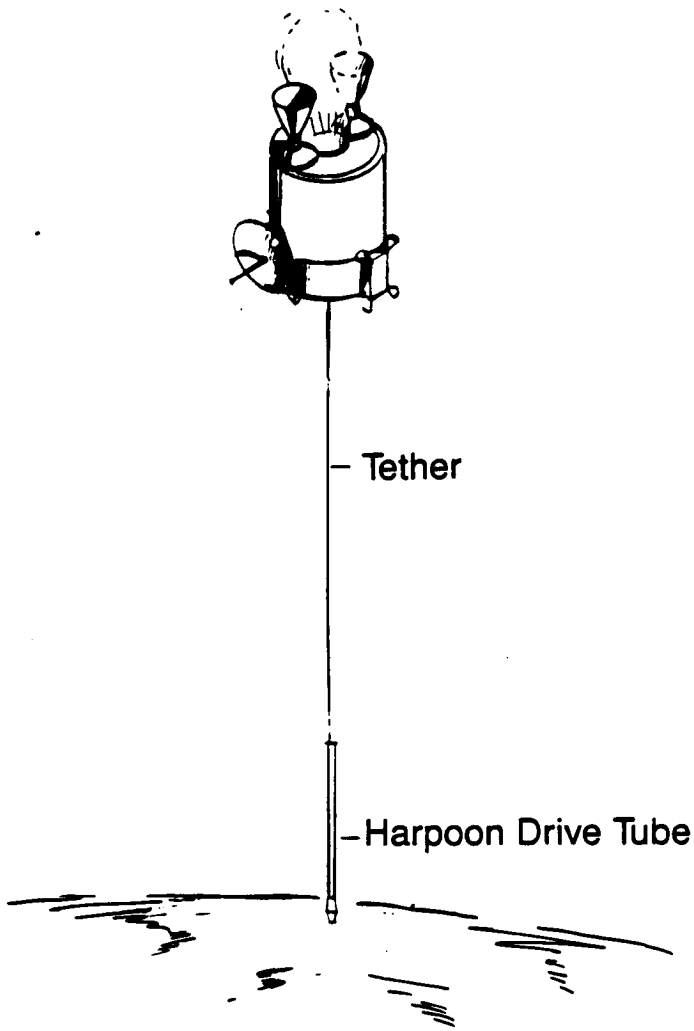

Figure 4.2-6 Remote Sampling of Comet with Tethered Drive Tube

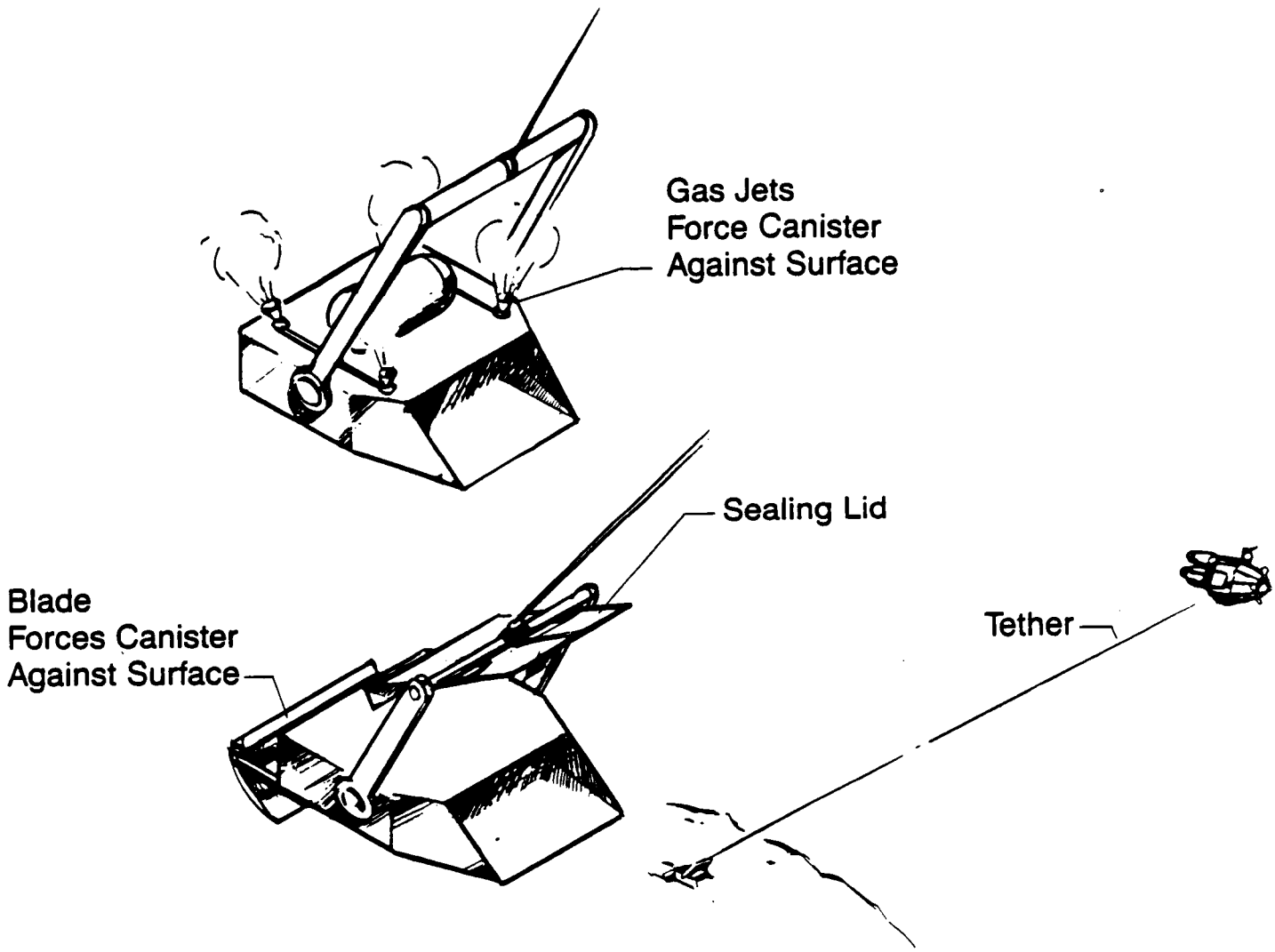

Figure 4.2-7 Remote Sampling of Comet with Collection Canister on Drag Line

4.3 NUCLEUS SAMPLING

There are two basic sample types to be taken from a comet. First is a sample of the mantle material, which could extend to any depth from 1 mm to 1 m. The mantle is likely to be very loose, dry material, with little or no cohesion. Under this is the more pristine nucleus material, and sampling of this to at least a meter of depth is required. The nucleus material may be sampled by the same methods as Martian regolith: a coring drill or drive tube. Here the microprocessor feedback and independently programmable aspects of the drill is also of importance, because little is known about the drilling qualities of the cometary material, and there is likely to be a large assortment of ices that could be irreversibly altered by heating during drilling. Drive tubes could also be used to acquire shallow samples of mantle and nucleus material with little thermal disturbance.

A represenative comet temperature of 130 K was chosen for the thermal model, although the results would not differ greatly for a 160 K comet. A range of densities from 0.01 to 3.5 g/cm^3 is assumed. Comets were assumed to contain only ice/soil conglomerates, and not the cemented sediments or igneous rocks possible on the Martian surface. At the very low densities possible for a comet, no actual data exists for thermal conductivities and specific energies, so numbers for higher densities were scaled down proportionate to the reduction in density. Thermal conductivity values varied from 0.002 W/mK for a dry fluffy comet mantle up to 14 W/mK for a dense soil laden with 50% ice. This fully covers the range cited in the Comet Nucleus Modeling Workshop's final report: 0.002 to 10 W/mK for cometary material. In Campins' final report from the Comet Nucleus Modeling Workshop the range of specific heat is cited (from Squyres et al.,1985) to be 0.3 to 1.0 cal/gK. This is much higher than the general spread of actual soil data reported elsewhere (Farouki, 1981); it also contradicts the nominal thermal inertia used by Weissman and Kieffer in their paper "An Improved Thermal Model for Cometary Nuclei". Weissman's value is $3x10^{-3}$ $cal/cm^2sec^{1/2}K$: Campins' value is 15 [x10-3 $cal/cm2sec^{1/2}K$], a factor of five higher. If one assumes that Campins intended Joules rather than the calories cited for specific heat then the numbers fall into the same range as actual tabulated data

and extrapolations, and also agree with the values determined from Squyres' paper. Campins' thermal inertia becomes 7, differing from Weissman's by only a factor of 2. To conform to the majority of data and papers on the subject, a specific heat range of 0.25 to 1.7 Joules/gK was chosen for cometary material. Table 4.3-1 tabulates the parameters and thermal inertias used for the many cometary models. In general, the maximum specific energy for each case was used with the typical thermal inertia value. The nominal thermal inertia used for a dry comet was 3.3, and for a 25% ice-laden comet the inertia was 13.6. The range of possible thermal inertias has been determined to be 0.06 to 140 with a more likely middle range of 1 to 15 (Campins et al., 1985).

Figures 4.3-1 thru 4.3-3 show the thermal profiles of drill cores for several different cometary nucleus characteristics. In general, the results indicate thermal disturbance as not being a major problem. The most sensitive samples, those that contain ices, have higher specific heats than dry soil and thus do not rise to as high temperatures. These samples also have higher thermal conductivity, in general, so that the heat distributes more evenly throughout the sample and propogates further away from the drill, to yield a uniformly lower temperature. The temperature at the edge of the core never rises more than 6°C for these ice laden samples, and the temperature of the central portion remains within 1 or 2 degrees of the in situ temperature, which is within reasonable goals for minimum thermal disturbance. This does not mean that there is not a very localized heating and vaporization of material in contact with the bit, but shows that only a very small fraction of the total sample will be affected, and the average temperature of the outer 0.1 cm of the core will not rise more than 6°G. For the dry soil cores, the outer edge of the core remains within 12°C of the original temperature, and the inner portion will not heat more than two degrees after the core has equilibrated. These thermal profiles show the thermal environment at the bit during the drilling operation.

Table 4.3-2 shows the results for a group of worst-case calculations including the effects of other possible heat distributions. With 80% of the heat load dissipated at the core edge of a dry sample, the core surface temperature will rise 40°C.

Table 4.3-1 Comet Material Parameters

Density (g/cm^3)	Ice Content	E_s (J/cm^3)	C_p (J/gK)	k (W/cmK)	I (thermal inertia) (10^{-3} $cal/cm^2s^{1/2}K$)
		0.01	0.25	0.00002	0.05
0.01	dry	0.1	0.5	0.005	0.38
		1.0	1.0	0.001	0.76
		0.01	0.25	0.0001	0.38
0.1	dry	0.3	0.5	0.001	1.7
		3.0	1.0	0.0025	3.8
		0.1	0.25	0.0001	0.85
0.5	dry	0.5	0.5	0.0002	1.7
		1.0	1.0	0.002	7.6
		0.1	0.4	0.0005	2.4
0.5	25%	0.75	0.65	0.0025	6.8
		2.0	1.25	0.005	13.4
		0.1	0.5	0.0075	10.3
0.5	50%	1.0	0.85	0.01	15.6
		3.0	1.5	0.0175	27.4
		0.3	1.5	0.01	20.7
0.5	100%	1.5	1.8	0.012	24.8
		5.0	2.0	0.015	29.3
		0.5	0.25	0.0002	1.7
1.0	dry	2.5	0.5	0.0004	3.3
		5.0	1.0	0.005	16.9
		0.5	0.5	0.001	4.8
1.0	25%	1.25	0.8	0.005	13.6
		6.25	1.4	0.01	26.7
		0.5	0.9	0.005	11.9
1.0	50%	1.5	1.3	0.01	22.0
		7.5	1.7	0.02	41.4
		0.5	1.5	0.025	46.3
1.0	100%	2.0	1.8	0.0275	53.2
		10.0	2.2	0.035	63.2

Table 4.3-1 (concluded)

		0.75	0.25	0.001	5.4
2.0	dry	2.0	0.6	0.004	16.5
		10.0	1.2	0.01	37.0
		0.75	0.5	0.006	18.5
2.0	25%	2.5	0.9	0.02	45.3
		12.5	1.4	0.034	52.1
		0.75	1.0	0.02	47.8
2.0	50%	3.0	1.3	0.04	77.1
		15.0	1.7	0.07	116.6
		1.0	0.25	0.001	7.1
3.5	dry	3.0	0.6	0.008	30.9
		15.0	1.2	0.015	60.0
		1.0	0.5	0.018	42.4
3.5	25%	3.5	0.9	0.04	84.8
		15.0	1.4	0.068	138.0
		1.0	1.0	0.04	89.4
3.5	50%	5.0	1.3	0.08	144.2
		17.0	1.7	0.14	218.1

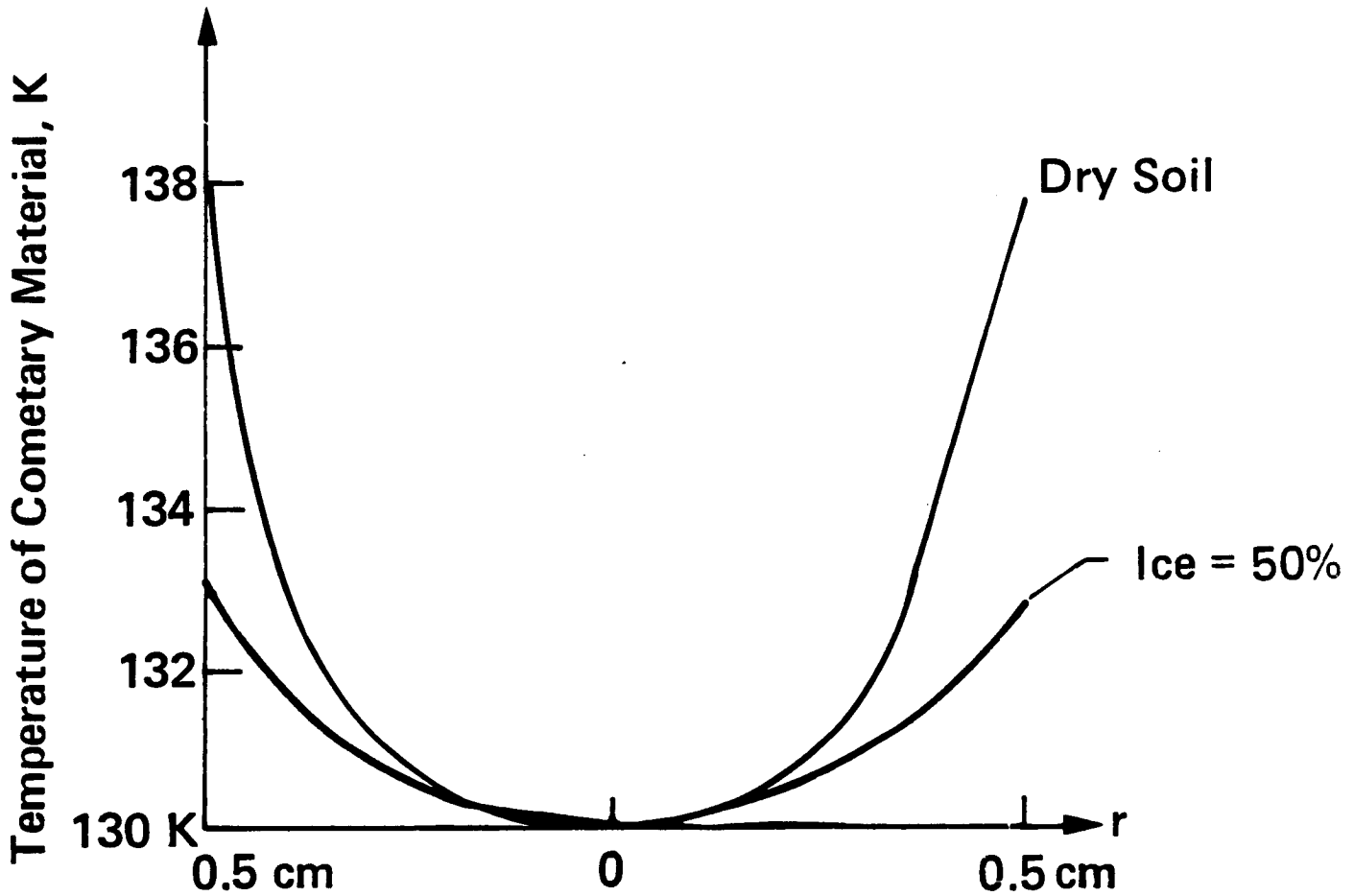

Figure 4.3-1 Thermal Profiles for Comet Core Sample ($\rho = 1.0\ g/cm^3$)

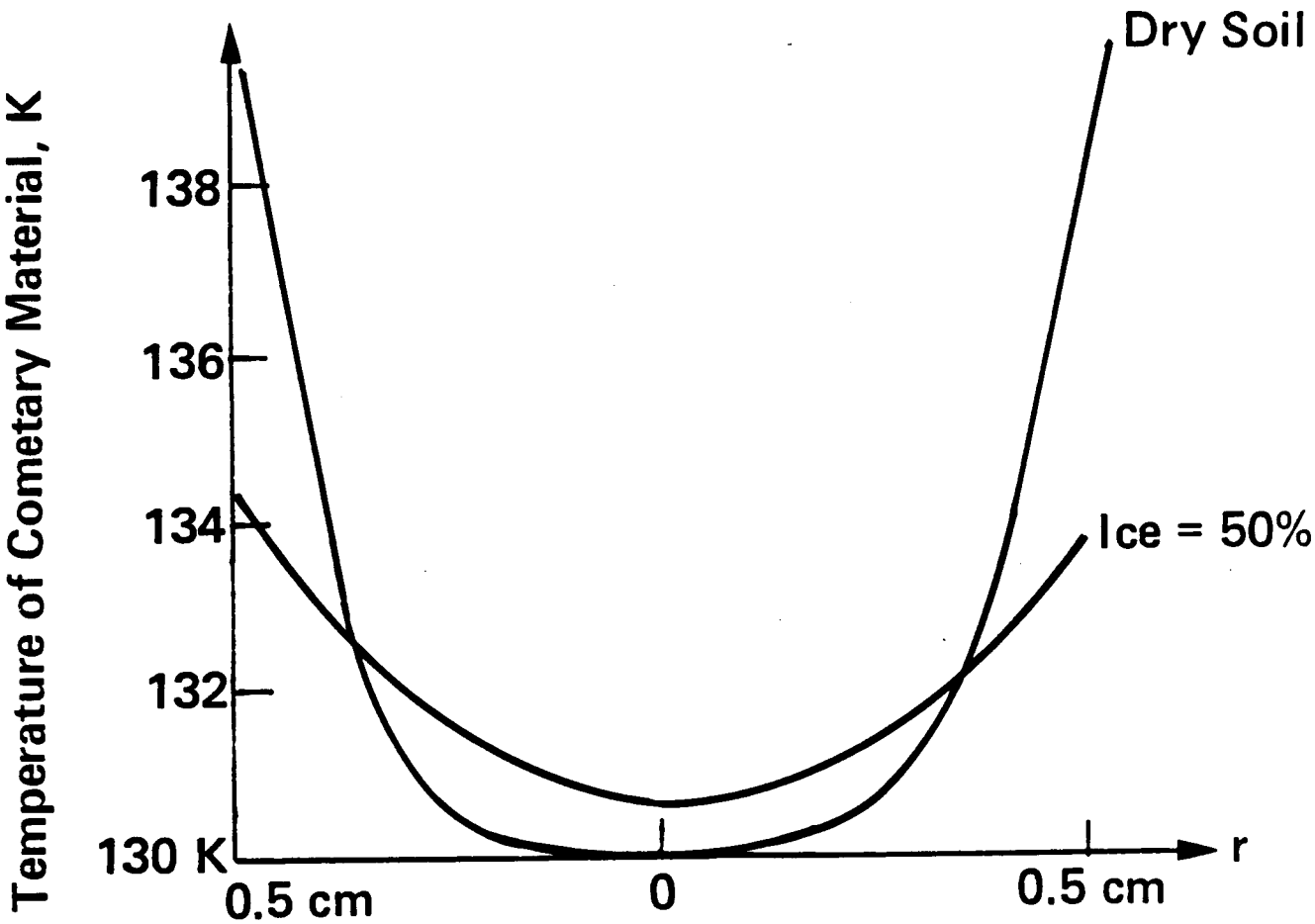

Figure 4.3-2 Thermal Profiles for Comet Core Sample (ρ =2.0 g/cm^3)

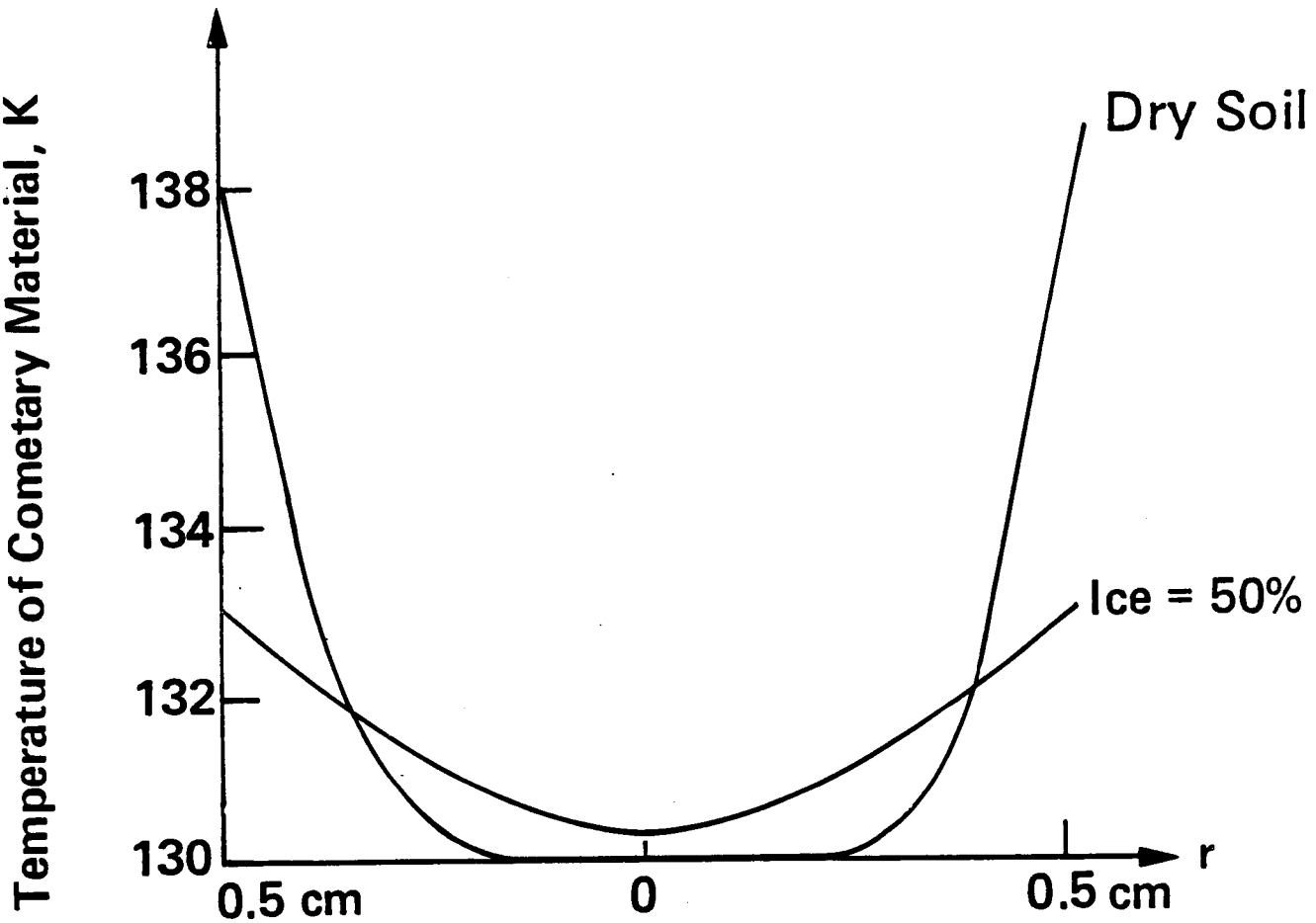

Figure 4.3-3 Thermal Profiles for Comet Core Sample (ρ = 3.5 g/cm^3)

Table 4.3-2 Comet Thermal Calculation Results

Comet Conditions	Max Core Temp during drilling	Temp after equilibration	Dist (cm) to 131K temp
Dry	140.7	131.7	0.0
Dry, 80% to core	169.6	134.0	0.0
Dry, 80% to cuttings	132.6	130.4	2.0
Dry, Kevlar stem	136.5	131.1	0.0
Dry, Kevlar, 80% to core	168.7	133.0	0.0
Dry, Kevlar, 80% to cuttings	131.0	130.4	2.0
25% ice	135.8	131.2	0.0
25% ice, 80% to core	137.7	132.4	0.0
25% ice, 80% to cuttings	130.8	130.5	0.0
25% ice, Kevlar	133.2	131.4	0.0
25% ice, Kevlar, 80% to core	137.9	131.9	0.0
25% ice, Kevlar, 80% to cuttings	130.7	130.4	0.0

Note: When not stated otherwise, the following conditions apply:

130K initial temperature
Tribocor bit/Beryllium stem
Density=1.0 g/cm^3
Heat distribution: 30% to bit
20% to core
20% to outer material
20% to cuttings
10% below bit

However, because of the low thermal conductivity of this material, the core equilibration temperature will be 134 K, only 4 degrees above the ambient. If the sample includes 25% ice, the surface temperature will rise by only 9 degrees if there is 80% dissipation in the core. This will then equilibrate to 132.4 K. A Kevlar/epoxy or other insulating stem will have a slight lowering effect on these temperatures, and also has the advantage of isolating the colder depths of the comet from the relatively warm surface.

Other temperatures such as 160 K were not evaluated, but the results will be very similar. A slight decrease in the amount of thermal disturbance would be observed for higher temperature regimes, because cometary material at a higher temperature will have a higher specific heat. This is a helpful aspect of the problem; in general, when a material is close to its melting point, its specific heat will be higher and thus it will have more resistance to temperature increases. Latent heats of various phase transformations have been neglected in these calculations because of the modest temperature excursions that are found.

4.4 MANTLE SAMPLING

The mantle could constitute more of a challenge to sample, as it may be very thin, and the sampling methods are resticted by working in microgravity with no atmospheric pressure at very low temperatures. Purely mechanical methods include a scoop tool similar to the one already described for Mars, with a lid or funnel arrangement to restrain the sample from floating away. This would be a large-mouth, flat-bladed scoop drawn along the surface by an arm or boom to scoop the mantle material into a canister. This type of scoop could also be thrust out from the spacecraft and returned by a cable in boomerang fashion, so that it collected sample over the entire traverse. Another mechanical candidate is the "belt-trencher" pictured in Figure 4.4-1. This sampler works by scooping the mantle material with blades into a sample canister. Samples culled in different areas are separated by the blades that seal against the sides of the canister. The mechanism is mounted on a rack-and-pinion drive system to allow it to move forward while sampling to take only the surface material.

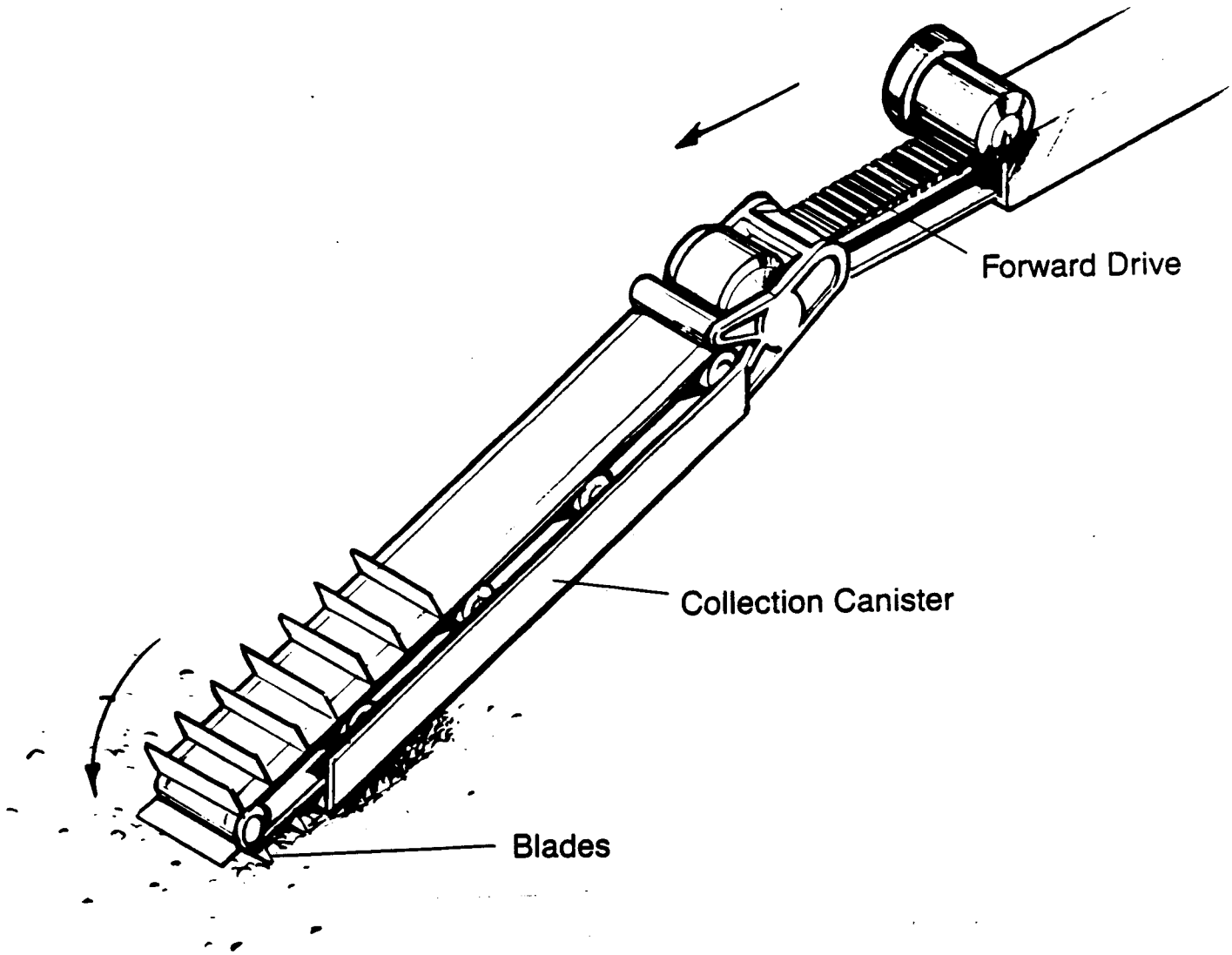

Figure 4.4-1 Comet Mantle Sampling by Belt Trencher

A "tape wheel", portrayed in Figure 4.4-2, is a good candidate for this type of sampling, especially if the mantle is thin and difficult to acquire by other methods. The tape has a surface that will retain any particles contacted: the type of surface normally used to accomplish this would be a sticky or viscid material, but at the low ambient temperatures it is unlikely that this would succeed. Instead, a tape surface of wire mesh or Velcro-like material would be used. The tape is wound off a roll and pressed into the cometary surface by a resilient wheel. The particle-laden tape is then rolled onto a take-up wheel, with a sealing tape wound between layers. Additions that can be made to this are to scrape the larger particles off via a "particle size discriminator" blade, and to add an analysis capablity to determine the composition of the dust as it is collected.

Another option is to use the ambient vacuum environment on the comet surface to benefit the sampling operation. Two methods of accomplishing this are shown in Figures 4.4-3 and 4.4-4. The first is a vacuum bell jar that is pressed down on the comet surface to seal off an undisturbed section of mantle. Gas nozzles are activated to blow dust up off the surface, and a valve on the top of the jar is electronically activated to release the gas. The dust cloud moves with the gas, and is trapped by a filter in-line with the escape valve. There are many of these valve/filter cominations on the jar, and the filters may be of different types to trap different sizes of particles. These filters are removed after use, sealed at the ends and returned intact. The difficulty with this concept is the sealing to a potentially irregular cometary surface. The second method uses the ballistic behavior of the dust when it is struck by moving gas; gas jets are used to blow the surface dust into large funnels, with side jets directing the dust into the funnel mouths if necessary.

The returned sample mass from a comet involves fewer types of material than Mars, but can still encompass a wide number of samples, especially if the drill core is subsampled. The desired types of samples for collection are shown in Table 4.4-1. Table 4.4-2 shows the returned samples for 1-kg and 10-kg payloads; this already encompasses more samples than need be taken in one site, which encourages the exploration of mobile or nonanchored methods of sampling.

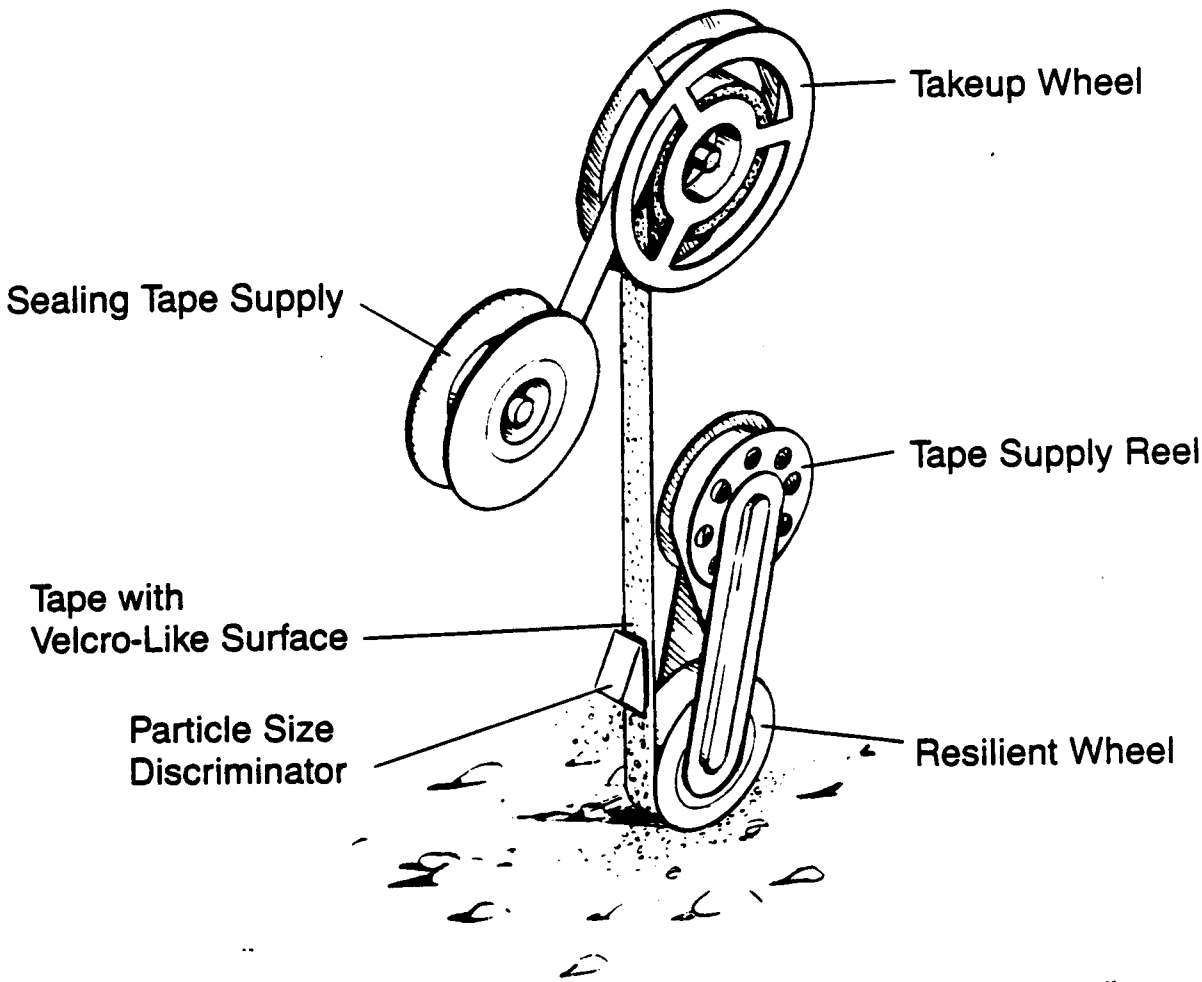

Figure 4.4-2 Comet Mantle Sampling by Contact Tape Wheel

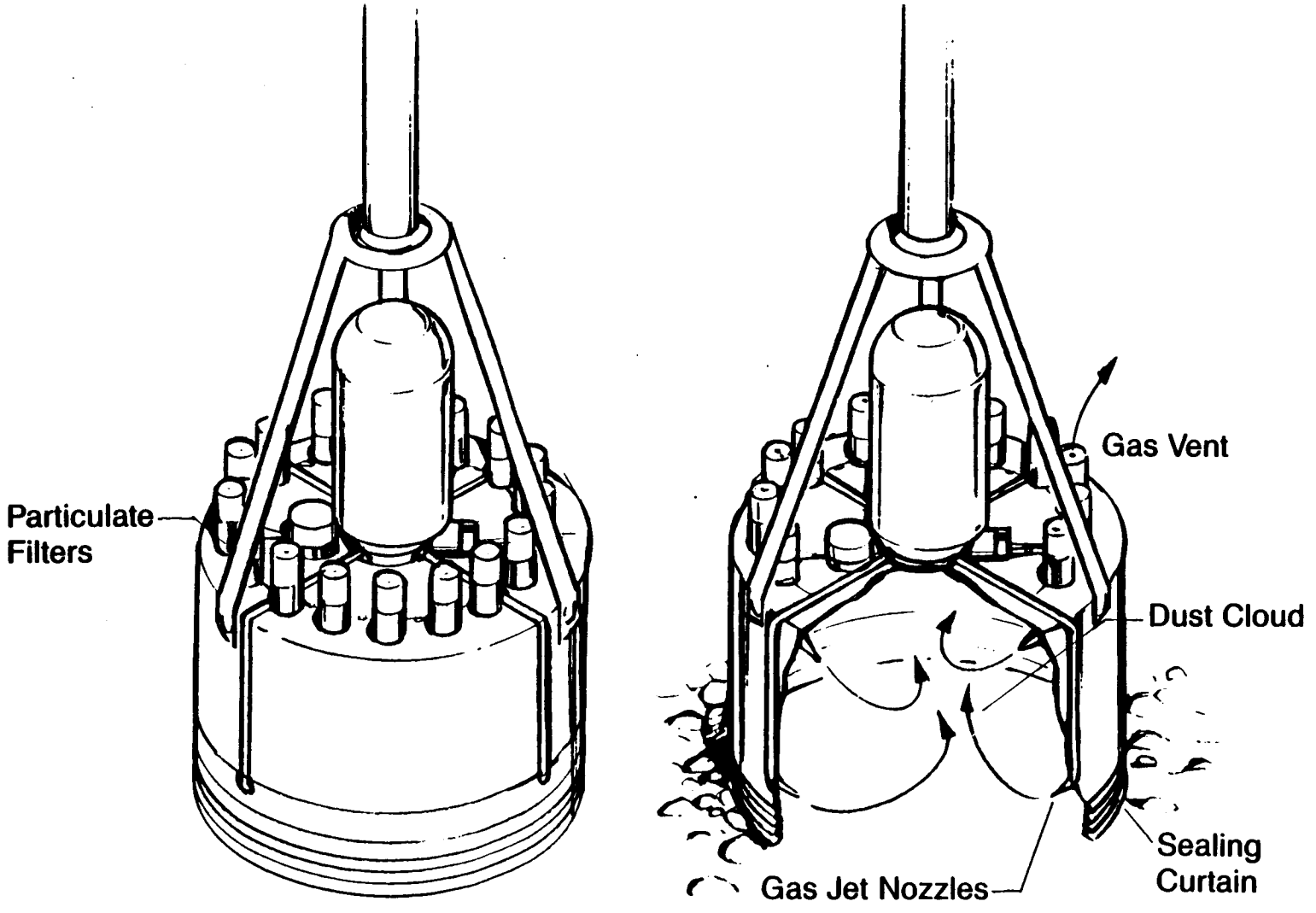

Figure 4.4-3 Mantle Sampling by Gas Jet Bell Jar

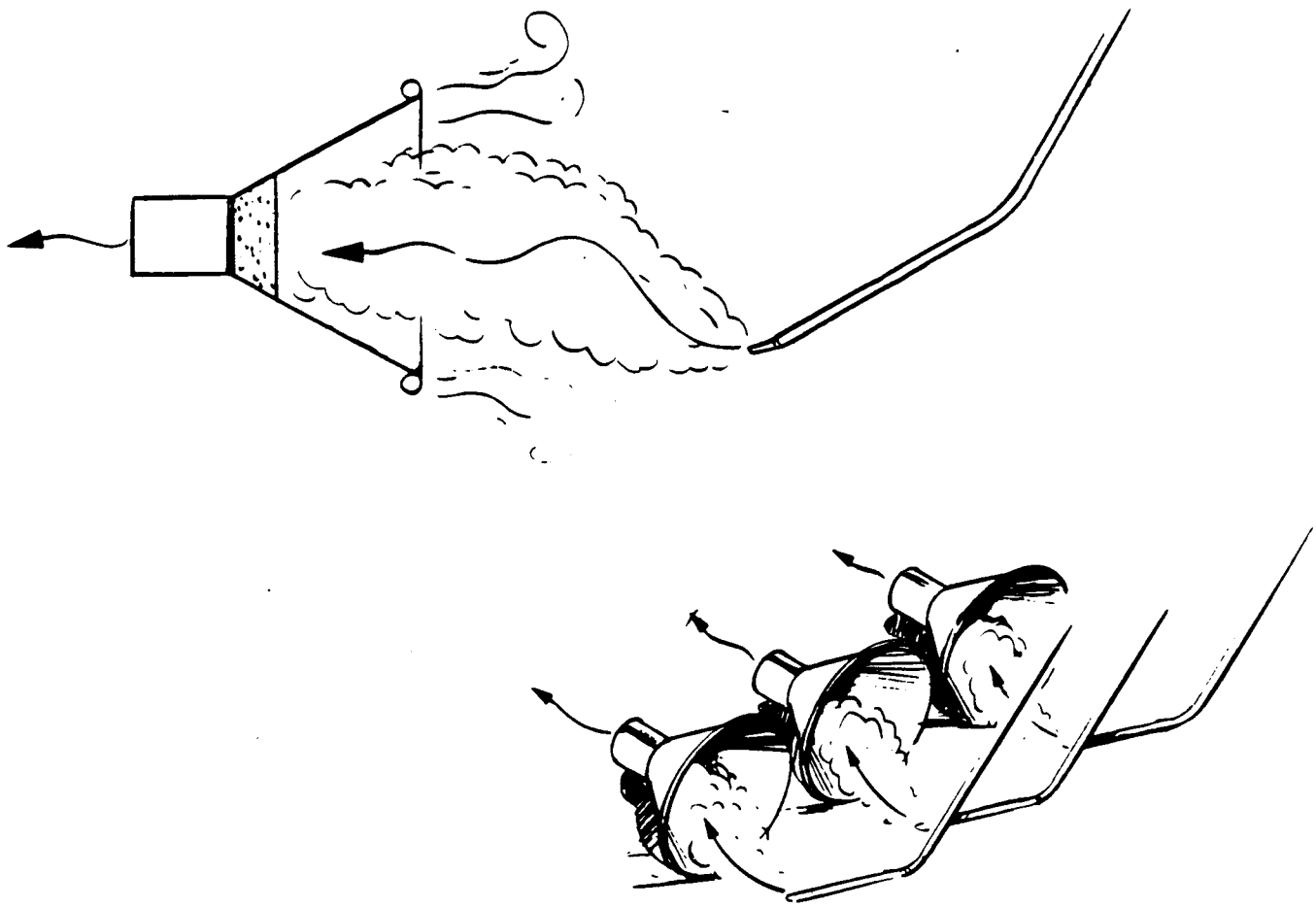

Figure 4.4-4 Mantle Dust Sampling with Gas Jets

Table 4.4-1 Criteria for Scientific Sampling (Comet)

Type	Mass (g)	Volume (cm^3)
A. Cometary Material (density 0.1-2 g/cm^3)		
1. Drive tubes .4 cm I.D., 15 cm long	.2-4	1.9
2. Drill cores	8-157 g/m	78.5 cm^3/m
a. Drill core diameter: 1 cm		
b. Drill depth To reach submantle zone: 1 cm-1 m		
B. Mantle (density .05-1 g/cm^3)		
1. Scoop-type sample	.1-2	2

Table 4.4-2 Comet Return Sample Massess

Comet Conditions	Max Core Temp during drilling	Temp after equilibration	Dist (cm) to 131K temp
Dry	140.7	131.7	0.0
Dry, 80% to core	169.6	134.0	0.0
Dry, 80% to cuttings	132.6	130.4	2.0
Dry, Kevlar stem	136.5	131.1	0.0
Dry, Kevlar, 80% to core	168.7	133.0	0.0
Dry, Kevlar, 80% to cuttings	131.0	130.4	2.0
25% ice	135.8	131.2	0.0
25% ice, 80% to core	137.7	132.4	0.0
25% ice, 80% to cuttings	130.8	130.5	0.0
25% ice, Kevlar	133.2	131.4	0.0
25% ice, Kevlar, 80% to core	137.9	131.9	0.0
25% ice, Kevlar, 80% to cuttings	130.7	130.4	0.0

Note: When not stated otherwise, the following conditions apply:

130K initial temperature

Tribocor bit/Beryllium stem

Density=1.0 g/cm^3

Heat distribution:
- 30% to bit
- 20% to core
- 20% to outer material
- 20% to cuttings
- 10% below bit

4.5 COMET SAMPLE STORAGE

The sample canister design concept is essentially the same as the Mars sample return design concept. It must provide for maintenance of the samples in their original condition with regard to temperature, pressure, and mutual isolation. The thermal environment is maintained by location of the canister (i.e., shielded from the sun), and the thermal buffer material, discussed below. The pressure is preserved by a hermetic seal and thermal control. Any particularly sensitive samples are sealed separately when collected. Isolation of the samples is achieved by the manner of packaging and storing each type of sample.

The same design of canister is used, with a thicker section of thermal buffer for reasons described below. The material choices will be essentially the same, except that there is a lower operating temperature requirement. The flexibility in storage is not as important, although some adaptability is still desired because varying numbers of mantle samples, drill cores, and drive tubes may be selected during mission operations. Two sample canisters are not necessary, and the internal hexagonal structure could be built-in rather than separate units. The only sample types will be drill cores or drive tubes from nucleus sampling, and mantle samples that could be stored in a cylindrical container (i.e., stacked filters or transferred from a scoop into a tube).

Thermal Buffering During Aerobraking at Earth--The thermal model used to evaluate aerobraking on a comet return vehicle was the same as described for the Mars return mission. For the comet return mission, a spacecraft weight of 230 kg (506 lbs) and an outer area of .79 m2 (7.79 ft2) were assumed. The initial entry velocity is 50,000 ft/s for comet return; Figure 4.5-1 shows the aerobraking heat profile for this case (Hill, private communication, 1986). The heat pulse profile was divided into 13 steps of input to the thermal analysis program. The sample canister was held at the desired temperature to determine the amount of heat flux into the sample canister during aerobraking.

The total heat pulse generated while aerobraking a comet return vehicle is 1.39×10^9 J. The heat load that reaches the sample canister assembly (SCA) in 25 minutes is 5.6×10^5 J, or 0.04% of the

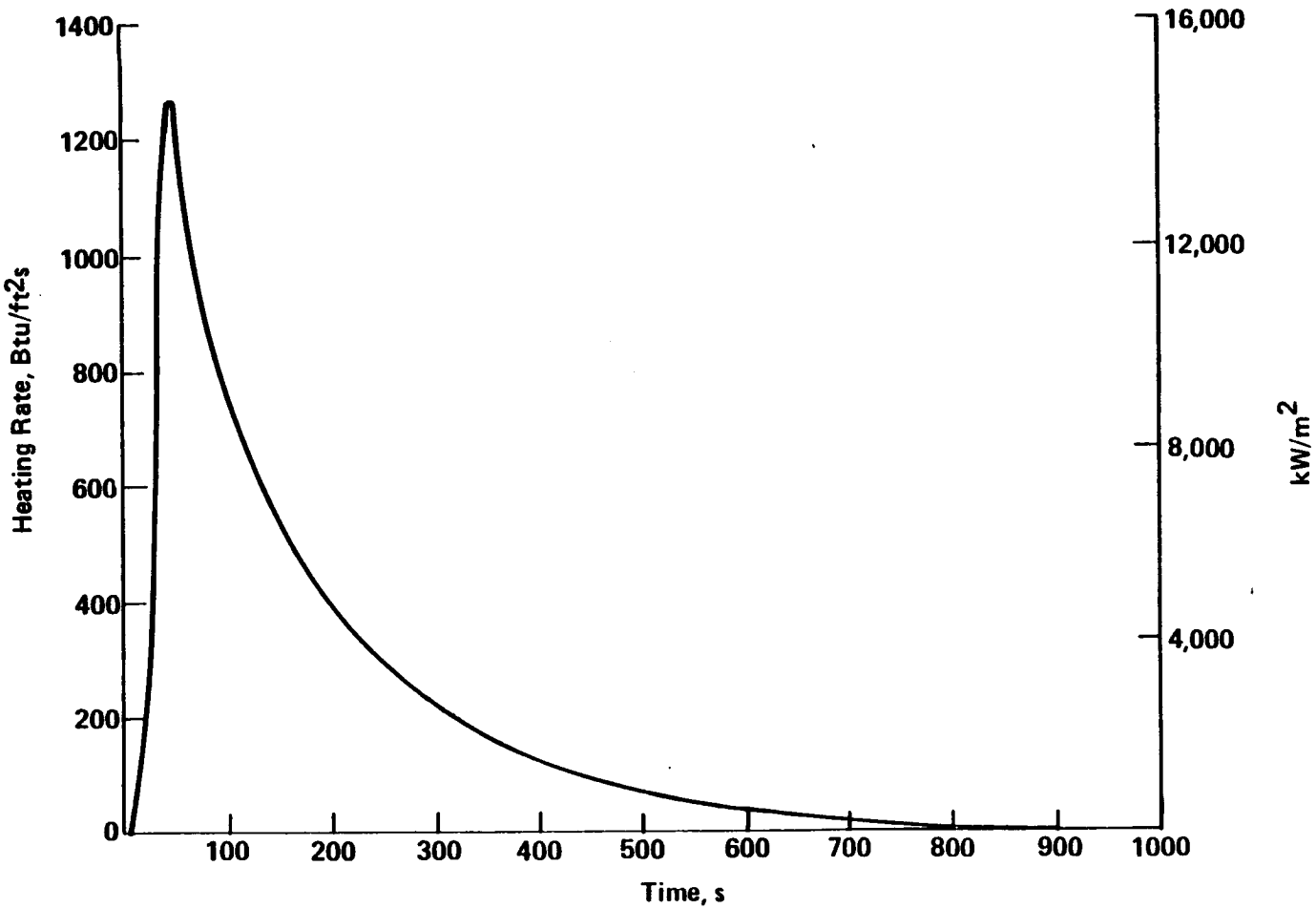

Figure 4.5-1 Comet Sample Return Heating Profile (V_i = 15,240 m/s)

total. Sizing the buffer with a safety factor of 1.5 yields 8.4 kg of phase-change material. This assumes use of a phase-change material with a heat of fusion of 100 J/g (see Section X). One hour after entry, the SCA will have absorbed 8×10^5 J, which requires a thermal buffer mass of 11.9 kg. These masses are relatively large, but not difficult to achieve within a reasonably sized sample canister. A cylindrical sample canister assembly with an outside diameter of 30 cm (12 in.) and height of 25 cm (10 in.) provides space for at least 12 kg of thermal buffering material around a 1-kg sample.

Methods of decreasing the amount of thermal buffer neccessary involve better isolation of either the spacecraft from the aeroshell or the SCA from the spacecraft, or use of a more effective thermal buffer. Most of the higher heat of fusion materials are highly hazardous in terms of toxicity or explosive qualities, so these have not been included in the design. Spacecraft design is not within the scope of this report, so only sample canister isolation is considered. The obvious method is to use support standoffs that provide lower thermal conductivity. However, the linear conduction path through the standoffs is a minor heat leak compared to the radiation heat load from the interior of the spacecraft. Radiation heating can be decreased by additional multilayer insulation blanket (MLI), but reaches an effective minimum with about 80 layers of MLI.

A method to avoid the majority of this radiative-coupling effect is to use a second phase-change thermal buffer. This material can absorb heat (change phase) at a higher temperature than the first thermal buffer, and would be used to keep the enclosure around the SCA at a relatively low radiative temperature. Material that has an extremely high heat of vaporization is water. A cylindrical container for ice could be designed as the surface of the SCA enclosure, and the ice would absorb heat loads from the spacecraft by melting, heating, and vaporizing. Both the radiative and linear heat loads to the canister would come from a lower temperature environment, because the boiling water would keep the walls of the enclosure below 100°C for as long as the water lasts. A 1-in. thick buffer of ice around a canister with 15-in. diameter and 15-in. height would weigh 20 kg and could absorb enough heat to maintain a cool enclosure during all of reentry. The container for the ice would probably weigh 5 or 10 kg. To avoid the necessity for a pressure vessel, the water can be vented to the outside when it starts to boil during Earth orbit entry.

Phase-Change Compounds--The thermal buffer materials are selected with the same criteria as for Mars return, but the thermal ranges are different. The comet samples must be stabilized in the range 100-160 K, so materials from this range were selected. Unfortunately, many of the low melting point materials are highly flammable and/or have high vapor pressures. Also, as the melting points decrease, the heats of fusion of the materials also generally decrease. Refer to Table 3.6.2-1 for an overview of the materials considered from which those listed below were selected. For a relatively warm predicted comet temperature, the material 1,3-butadiene melts at 164 K, and has a high heat of fusion of 147 J/g but also a high vapor pressure. Tetrahydrofuran has a lower heat of fusion but a more acceptable vapor pressure. Progressing to cooler cases, 1-heptene has a melting point of 153.5 K and good properties except for a danger of explosion under extreme heating. At a temperature of 143.5 K, n-pentane is a good candidate with a 116.7 J/g heat of fusion and a low vapor pressure. For the typically predicted 130 K comet temperature, cis-2-butene and trans-2-pentene are both acceptable materials, trans-2-pentene having a lower heat of fusion but also lower vapor pressure. For a somewhat colder temperature, cis-2-pentene is suitable, melting at 121.8 K with a reasonably high heat of fusion (101.5 J/g) and low vapor pressure. For very cold temperature ranges, near 100 K, 1-pentene is the optimum candidate, with a higher heat of fusion than the other low vapor pressure compounds. Isopentane, isobutane, and nitric oxide are all acceptable for this range, although as mentioned they tend to have lower heats of fusion than the higher melting-point compounds. For temperatures below 100 K suitable materials are very difficult to find, because the room temperature vapor pressures are universally very high.

5.0 SUMMARY AND RECOMMENDATIONS

This study has examined several aspects of the techniques that can be applied to acquisition and preservation of samples from Mars and a cometary nucleus. An entire sampling strategy could and should be developed for these two high-priority missions, based on thorough engineering analysis and, where necessary, laboratory experimentation to verify the approaches. This will lead to an approach that can vastly multiply the scientific payoff of such missions compared to that which would result if only minimal effort and little forethought were placed on the problem of sampling. Because of the importance and breadth of this subject, the present study is only the beginning of a systematic development program. In particular, the following tasks should be considered in future work:

1) Drill testing--It is recommended that a laboratory program be undertaken for the evaluation of drill parameters, including materials selection, sizing, and operating modes (independently programmable impact, rotation, feed forces, and rates). These tests must adequately simulate the Mars or comet nucleus environmental conditions and be performed on a range of soils, rocks (for Mars), and ice/soil mixtures.

2) Sample acquisition sequence--A study of timelines, success and failure modes, and adaptive responses for various types of sampling should be undertaken. Sampling sequences could be defined for each type of anticipated sample. Tradeoffs should consider artificial intelligence (AI) for control versus sensor-driven response approaches. Each scenario should be in the context of probable mission operating environments for the two classes of proposed missions.

3) Sample storage and preservation--Indepth engineering studies are recommended to define containers. These must be suitable for sample identification, segregation, contamination protection, and thermal/mechanical preservation during the Earth return launch, cruise, and entry environments. Single and double phase-change

thermal buffers should be considered during these studies. These baselines must be adequate to establish requirements on the vehicle for volume, mass, mass uncertainty, shock isolation, and thermal control during all return phases of the mission. A container designed for "hand-off" from one vehicle to the next should also be considered.

4) Sample loading--Apart from the acquisition techniques, means of loading and sealing the inserts and main container are required. It is recommended that upon completion of Task 3 above, or in conjunction with it, the mechanisms needed for these processes be studied and designed. Reliable, noncontaminating mechanisms must be used. Backup modes, especially to provide full contingency sampling, will also be needed. It is desirable to provide hermetic sealing of individual samples in all cases where the samples may contain volatiles (cometary nucleus, Martian soil and permafrost).

5) Other sampling techniques--In addition to the coring drill (Task 1), it is recommended that selected, promising approaches for other types of sample acquisition and processing be developed further and studied in the laboratory. For the comet, this would include methods of mantle sampling, such as the shallow core sampler, the "soda straw" drive tubes, and the surface monolayer dust collector. For Mars, it could include the mini-drill sub-sampler, the double-drilling approach for core release from large rocks and bedrock, airborne dust samplers, lithic fragment rake sampling, rock size selection, and crushing/chipping tools.

In summary, scientific approaches to sampling, grounded in proven engineering methods, are the key to achieving the maximum science value from the sample return mission. If development of these approaches for collecting and preserving does not preceed mission definition, it is likely that only suboptimum techniques will be available because of the constraints of formal schedule timelines and the normal pressure to select only the most conservative and least sophisticated approaches when development has lagged the mission milestones. With a reasonable investment now, before final mission definition, the sampling approach can become highly developed, ready for implementation, and mature enough to help set the requirements for the mission hardware and its performance.

6.0 BIBLIOGRAPHY

Aerospace Structured Methods Handbook, AFML-TR-68-115, AMMRC, Waterton, MA, dated 1975.

Hatch, A. J., "Alloy Evaluation Program Summary for 1957-1958," TMCA, Tech. Dept., dated 1958.

American Society for Metals, "Metals Handbook Ninth Edition: Volume 3 Properties and Selection: Stainless Steels, Tool Materials and Special-Purpose Metals", ASM Handbook Committee, Metals Park, Ohio, dated 1980.

American Society of Heating, Refrigerating and Air-Conditioning Engineers, Inc., "Ashrae Thermodynamic Properties of Refrigerants", dated 1969.

Beches, P. F., Wei, G. C., "Tuughening Behavior in S. C.-Whisker Reinforced Alumina," Comm of the Am. Ceramic Society, dated December 1984.

Benjamin, D. (Editor), "Properties and Selection: Stainless Steels, Tool Materials, and Special Purpose Metals," Volume 3, Metals Handouts, pp. 721-772, dated 1980.

Bittince, J. C. (Editor), "Guide to Engineered Materials," ASM Publication. CRREL Report 76-16, Mechanics of Cutting and Boring Part II: Kinematics of Axial Rotation Machines, dated June 1976.

Clark, Benton C., et. al, "The Viking X Ray Fluorescence Experiment: Analytical Methods and Early Results," Journal of Geophysical Research, Volume 82, Number 28, dated September 30, 1977.

CRREL Report 76-17, Mechanics of Cutting and Boring Part III: Kinematics of Continuous Belt Machines, dated June 1976.

CRREL Report 77-3, Effect of Temperature on the Strength of Frozen Silt, dated February 1977.

CRREL Report 77-7, Mechanics of Cutting and Boring Part IV: Dynamics and Energetics of parallel Motion Tools, dated April 1977.

CRREL Special Report 226, Mechanics of Cutting and Boring Part I: Kinematics of Transverse Rotation Machines, dated May 1975.

CRREL, SR-126, Drilling Through the Greenland Ice Sheet, dated November 1968.

CRREL, SR-153, Experimental Blasting in Frozen Ground, dated November 1970.

CRREL, SR-81, Coring of Frozen Ground Barrow Alaska, dated Spring 1964.

CRREL, TR-231, Core Drilling Through the Antarctic Ice Sheet, dated December 1969.

CRREL, TR-245, An Investigation of Core Drilling in Perennially Frozen Gravels and Rock, dated December 1973.

Carmichael, Robert S., Ph.D. (Editor), "Handbook of Physical Properties of Rocks", Vol. 1, dated 1982.

Christensen, Philip R. and Kieffer, Hugh H., "Moderate Resolution Thermal Mapping of Mars: The Channel Terrain Around the Chryse Basin", Journal of Geophysical Research, Vol. 84, No. B14, dated December 30, 1979.

Cumming James D., "Diamond Drill Handbook", Toronto, Ontario, June 25, 1958.

Dixon, G., Wright, R. A., Lee, M., "Processes Involved in the Wear of Converted Carbide Tools," G.E. Report, dated May 1983.

Eagle Engineering Report 85-105, NASA Contract NAS9-17176, Final Report for Planetary Sample Rapid Recovery and Handling, dated September 20, 1985.

Ezell, Edward Clinton and Ezell, Linda Neumann, NASA SP-4212, On Mars: Exploration of the Red Planet 1958-1978, dated 1984.

Fansted Materials Data Sheet, Tribocor 532N.

Ferber, M. K., Becher, P. F., Finch, C. B., "Effect of Microstructure on the Properties of TiB_2 Ceramics," Comm of the Am. Ceramic Society, dated January 1983.

Green, Jack (Editor), "Geological Problems in Lunar and Planetary Research", Vol. 25, AAS Science and Technology Series, dated April 1968.

Henderson, Homer and Earl, Jack F., "New Drilling Technique Recovers 100 Percent Continuous Core"., World Oil, p. 111, dated January 1960.

Hvorslev, M. Juul, "Subsurface Exploration and Sampling of Soils for Civil Engineering Purposes", American Society of Civil Engineers, dated 1962.

Industry," NASA Tech. Mem. 83512, dated December 16, 1983.

Jet Propulsion Laboratory Report JPLD-1845, Study Report Mars Sample Return Mission, dated 1984.

Jet Propulsion Laboratory, JPL Publication 80-59, Mars Sample Return: Site Selection and Sample Acquisition Study, dated November 1, 1980.

Jet Propulsion Laboratory, Report JPL-D-1734, "An Improved Thermal Model for Cometary Nuclei", dated July 1984.

Jet Propulsion Laboratory, NASA Technical Memorandum 87564, "Report of the Comet Rendezvous Science Working Group", dated April 1, 1985.

Jet Propulsion Laboratory, Report JPL D-1862, "Thermal Modeling of Halley's Comet", dated September 1984.

Johnson, Nicholas L., "Handbook of Soviet Lunar and Planetary Exploration", Vol. 45, Science and Technology Series, dated 1979.

Kartha, K.K., Ph.D., (Editor), "Cryopreservation of Plant Cells and Organs", dated 1985.

Kieffer, Hugh H., Martin, T.Z., Peterfreund, Alan R., and Jakosky, Bruce M., "Thermal and Albedo Mapping of Mars During the Viking Primary Mission", Journal of Geophysical Research, Vol. 82, No. 28, dated September 30, 1977.

Lange, G. Robert, "Deep Rotary Core Drilling In Ice", Dated February 1973.

Larson, W.C., Svendsen, W.W., Hoffmeister, J.F., and Cozad, R.E., "Retractable Core Bit Drilling System"., Ref. Technical Papers, dated February 1982.

Lavoie, F. J., "Materials Selector 1986," Materials Engr., dated December 1985.
Lewis, C. F. (Editor), "Ceramics Fire the Imagination," Materials Engr., dated July 1986.

Lindsay, John F. and Perry, Richard, "Preliminary Evaluation of the Coring Potential of the Apollo Lunar Surface Drill Titanium Core Stem."

Lockheed Missiles & Space Co., Inc., Report LMSC-D621612, DoD Contract F33615-77-C-5190, Interim Technical Report for Satellite Applications of Metal-Matrix Composites, dated May 1978.

Martin Company Report ER13952, NASA Contract NAS9-3542, Final Report for Lunar Rock Coring Device Design Study, dated October 1965.

Martin Marietta Report DPR-6-1, NAS Contract NAS9-6587, Final Report for Apollo Lunar Surface Drill (ALSD), dated November 1, 1968.

Martin Marietta Report ER 14349P, NASA Contract NAS9-6092, Phase C Final Report/Phase D Technical Proposal for Apollo Lunar Surface Drill (ALSD), dated August 18, 1966.

Martin Marietta Report MCR-79-615, NASA Contract NAS9-15907, Final Report for Study of Sample Drilling Techniques for Mars Sample Return Missions, dated April 1980.

Martin Marietta Report MCR-75-391, NASA Contract NAS7-100, Final Report for Mars Surface Sample Return Tradeoff Studies, dated October 1975.

Martin Marietta Report MCR-73-18, NASA Contract NAS9-9462, Final Report of Apollo 7 Lunar Surface Drill Mission Performance, dated 28 February 1973.

Martin Marietta Report MCR-78-613, NASA Contract NAS9-15613, Final Report for Study of Sample Drilling Techniques for Mars Sample Return Missions, dated March 1979.

Martin Marietta Report MGF-70-429, NASA Contract NAS9-9462, Final Report for Apollo Lunar Surface Drill (ALSD), dated November 20, 1970.

Martinella, R., Chevallard, G., Tostello, C., "Wear Behavior and Structured Characterization of a Nitrogen Implanted Ti-GAR-4V Alloy at Different Temperatures," Reference 2, pp. 711-716.

Marzik, J. V., "CVD Fibers," AVCO Speciality Materials Division presented at Metal and Ceramic Corpsite Processing Conf., dated November 13-15, 1986.

Materials Selector 1986, Materials Engineering, Penton Publications, dated December 1985.

Maurer, Dr. William C., "Novel Drilling Techniques", Pergamon Press, dated 1968.

Mellor, Malcolm and Sellmann, Paul V., "General Considerations for Drill System Design", U.S. Army Cold Regions Research and Engineering Laboratory, dated June 1975.

Metallography of a New Carbon Steel for Low Temperature Service, Metal Progress, pp. 36-41., dated February 1981.

NASA Technical Paper 2066, Interface Control and Mechanical Property Improvements in Silicon Carbide/Titanium Composites, dated 1961.

Oliver, W. C., et. al, "Ion Implanted Ti-GAR-4V," Reference 2, pp. 705-710.

Oliver, W. C., et. al, Hubler, G. K., Holland, O. W., Clayton, C. R., White, C. W. (Editors), "Hardness as a Measure of Wear Resistance, in Ion Implantation and Ion Beam Processing of Materials," MRS Symposia, Volume 27, pp. 603-607, dated 1984.

Pressure Vessel Plates, Alloy Steel Quenched and Tempered 8 and 9 Percent Nickel, ASTM A553-79a.

Pressure Vessel Plates, Five Percent Nickel, Alloy Steel, Specially Heat Treated, ASTM A645-80.

Properties and Proven Uses of Kennametal Hard Carbide Alloys, Kennametal Inc., Latrobe, PA, dated 1977.

Properties and Selection: Stainless Steels, Tool Materials and Special Purpose Metals," Metals Handbook, Ninth Edition, Volume 3, pp. 568-588, ASM, dated 1980.

Rausch, J., Fansteel Corp., "Personal Communication," August 27, 1986.

Salik, J., "A Review of the Use of Wear-Resistant Coatings in the Cutting Tool
Saxena, Surendra K. (Editor), "Updating Subsurface Samplings of Soils and Rocks and Their in-situ Testing", dated January 3-8, 1982.

Scales, S. R., Diesburg, D. C., "A New Rock Bit Steel," Metd Progress, pp. 31-33, dated February 1981.

Scheflan, Leopold, Ph.D., and Jacobs, Morris B., Ph.D., "The Handbook of Solvents", D. Van Nostrand Company, Inc., New York.

Shimada, M., "Structured Nonoxide Ceramics by Hot Pressing," Ceramic Bulletin, Volume 65, No. 8, pp. 1153-1155, dated 1986.

Singer, I. L., Carosella, C. A., Reed, J. R., "Function Behavior of 52100 Stell Modified by Ion Inplanted Ti," Nucl. Instr. and Methods 182/183, pp. 923-932, dated 1981.

Singer, I. L., Jeffries, R. A., "Friction, Wear and Deformation of Soft Steels Inplanted with Ti and Ni, ibid, pp. 667-672.

Smoluchowski, R., "Heat Content and Evolution of Cometary Nuclei", ICARUS 47, 312-319(1981), p. 312, dated April 22, 1981.

Syalon, Lucas Cookson, Sheppard, L. M. (Editor), "Sialon, Another Super Structural Ceramic," Advance Matl's and Processes, dated January 1986.

The Matheson Company, Inc., "Matheson Gas Data Book", Matheson of Canada, Ltd., Whitby, Ontario.

Vardionan, R. G., "Wear Improvement in Ti-GAR-4V by Ion Inplantation," in reference 2, pp. 699-704.

Weast, Robert C., Ph.D., (Editor), "CRC Handbook of Chemistry and Physics", 64th edition, dated 1983.

Weir, J. R., Jr., "Meals and Ceramics Division," Oak Ridge National Laboratory Materials Highlights, dated October 1985.

Appendix A

Comet/Mars Sampling System

Comet/Mars Sampling System
Appendix A
Drill Thermal Analysis

Thermal Analysis Software

Thermal modeling of the operation of the Comet/Mars drill has been performed using the Martin Interactive Thermal Analysis System, Version 2.0 (MITAS - II). This program is an extensively updated version of the commercial thermal analyzer program CINDA - 3G. MITAS is a software system designed to solve lumped parameter network representations of thermal systems. The system has the capability to solve any electrical analog (RC-type) network goverened by diffusion-type equations. The inputs required are thermal capacitances of each node, conductors between nodes, and variables influencing the type and accuracy of solution desired. Conductors between nodes can be either radiative or linear. Both steady-state and transient solutions are possible. Any unit system can be defined by the input values, as long as all units are consistent.

MITAS is formatted for use on an IBM PC in a version known as mini-MITAS, and thermal analysis is accomplished using this software. Models are input as separate data files for node parameters, conductor parameters, constants used to modify the data and control the solution routine, and a logic or command file which implements the desired constants and controls the excecution process. Metric units are used throughout: specific heats in W/K, conductors in W/cm-K, power in watts and time in seconds. Since thermal modeling of a variety of materials is desired, the model is input so as to allow flexibility in both the drilled and drill material. The simplest manner of changing the characteristics of the modeled materials is to incorporate constants in the logic block which describe specific heat or conductivity values. To implement this, the thermal capacitances given in the original data block are only the dimensional volumes of the nodes. The volumes are multiplied by density and specific heat in the logic block, and these thermal capacitances are used in the modeling. Conductances are handled in a similar manner; the conductance in the original data block is the A/l for the conductor, which is multiplied by thermal conductivity in the logic block. Initial node temperatures for the bit and drilled material are also defined in the logic block. This methodology allows all material values to be input via the constants block, and various materials can be modeled without lengthy recomplilation of the entire data block.

Model Definition

The node data block, Table A-1, consists of 394 nodes which define the drill stem and bit, core material within the drill stem, and material

outside of the drill stem. All nodes except nodes at the outer edge of the drilled area are defined as diffusion type: i.e. they have a specific heat which will affect their thermal response. The material outside the drilled area at a distance of 0.6 cm radially from the drill stem and 1.0 cm below the drill stem is assumed to be relatively undisturbed. This assumption is supported by previous thermal modeling, and it was felt to be unnecessary to detail nodes beyond that point. These outer edge nodes are defined as boundary nodes, which remain at a constant (boundary) temperature. Nodes at and near the bit are more detailed since this is the central point of drill-induced heating. Initial temperatures and sources shown in the table are meaningless since these are re-defined in the logic block. Each capacitance given is equal to the volume of the node in cubic centimeters; as stated above, this value is multiplied by density and specific heat in the logic block. All nodes are concentric rings, since the drill is a radially symmetric system. Refer to Figure A-1 for clarification of the numbering scheme described below.

Nodes 100 to141 are used to describe the bit section of the drill. The coring drill bit has a 1 cm ID, 1.8 cm OD, and a 1 cm length. The division into nodes is accomplished by dividing the bit into two concentric rings, each 0.2 cm thick, and splitting each ring into five vertical nodes 0.2 cm high. The resulting ten nodes are descibed in the data block as the bit inner ring and outer ring nodes. Nodes 150 to 320 define the drill stem, with a 1.0 cm ID and 1.4 cm OD. Each node is 0.5 cm in length. The two nodes 330 and 340 are introduced as false nodes to simplify block modification of the stem nodes; they have no effect on the system.

The nodes for the material to be drilled make up the remainder of the node block. The lower core, the section of core from 1.0 cm below the bit to the top of the bit, is detailed by nodes 1000 to 1990. These nodes are described in the model as lower core, first ring to tenth ring. The sectioning is concentric rings of 0.05 cm wall thickness and 0.2 cm height. The nodes are numbered by tens, with the first node at 1 cm below the bit at the minimum diameter of 0.1 cm. The next node defines a ring with a 0.1 cm greater diameter at the same depth, and so forth, until the tenth ring which is at the maximum inner core diameter, 1 cm. Node 1100 begins with the minimum diameter node 0.8 cm below the bit, and numbering progresses by this sequence to node 1990. The upper core extends from the top end of the bit to the top of the drill stem. These nodes are concentric rings of the core: 2000 to 3790, numbered by tens. The ring wall thickness is 0.05 cm, and the height is 0.5 cm. Node 2000 is at minimum diameter, above the drill bit section. Numbering follows increasing diameter, then increasing vertical position, ending with node 3790 at the top of the drill stem with an outer diameter of 1.0 cm. These

nodes are designated upper core, first to tenth ring. The material outside of the drill stem is noded in rings 0.5 cm high, with 0.2 cm wall thickness. The numbering is again done by defining each node, in order of increasing diameter, at a certain height, and then progressing to the next height. In order for similar nodes to correspond by number, the numbering was not sequential. In other words, all node numbers at the minimum outer diameter end in 00, the next diameters end in 10, and so on. Below the drill stem are nodes 5000 to 5130, the two layers of material immediately outside of the bit are nodes 5220 to 5330, and nodes 5410 to 7130 occupy the remaining positions up the drill stem. Boundary nodes are set around the outer perimeter of this entire volume.

The conductor data block consists of 751 linear conductors. The radiative conduction which takes place in a porous soil is taken into account by appropriate linear conductivity values. The values in the conductor data block are in units of cross-sectional area over length, cm^2/cm. Each conductor is numbered according to the node to which it is attached; vertical conductor numbers follow node numbers, and horizontal conductor numbers are 1 greater than node numbers. Further explication of conductor numbers is provided by Table A-2.

The constants data block, Table A-3, consists of control constant data and user constants. Control constants refer to variables used to control the execution of the solution: number of iterations, maximum variation of node temperatures and temperature scale absolute zero point. For transient solutions, output interval and finish times are included. User constants are used in this case to define the parameters of the materials to be modeled. These include densities, specific heats, and conductivities. The heat input of drilling is also determined from these constants using specific energy of cutting, drill bit area, and heat distribution. Actual material values used by the model and example outputs are presented in the body of the final report.

Model Execution

Execution of the model solution is controlled by the logic file, presented in Table A-4, which consists of a set of subroutines. Subroutine 'Execution' is called at the beginning of execution. The initial logic loops define the bit, drill stem, and drilled material specific heats by means of the node volumes and user constants. The following three loops assign thermal conductances between nodes based on the geometric conductors and user constants given. Two separate loops are used to define the initial temperatures of the drilled material and the drill bit. The head of the drill is not defined to be a different temperature than the surrounding material, since this model is concerned mainly with the heating related to cutting.

The temperature of a boundary node at the top of the drill stem could be defined here if analysis of heating due to the drill head is desired. The "forward-backward" differential solution routine is called at the end of 'Execution' and begins solution of the problem.

The subroutine 'Variables 1' is called before each iteration during the solution process. Time-varying heat loads, temperatures and materials are defined in this section. Drill-induced heating is simulated by power applied to the inner core, bit and outer material nodes. Heat is also applied to nodes on the drill stem and the outer material adjacent to the stem to simulate the transmitted heat of drill cuttings. As the drill progresses downward with time, the heat is applied to deeper nodes. This model defines five time steps at which the heat distribution is changed. Unfortunately, this model does not simulate the actual progression of the drill by changing the position of the drill relative to the soil, only by the progressive heat distribution. If this is desirable, appropriate loops can be added to this subroutine. At a time defined in the user constants (TIM6), the drilled material can be changed, to simulate progression into a rock or out of a rock into soil. The specific heat, thermal conductivity and specific energy of the material at and below the bit are changed to simulate the new material. Five new time steps are defined for heat distribution progression. A final time step can be defined at which drilling (i.e., heating) is ceased and thermal analysis of the resulting decay transient is continued.

The subroutine 'Outcalls' is called whenever thermal output is required. For a transient solution, the TSTEPO constant controls how often the output loop is accessed. In this model, outut was produced every 1 or 5 seconds. Steady-state solution output loops are defined by the control constant ITEROT. In this particular logic file, only temperatures are output, but heat flows can also be monitored and output.

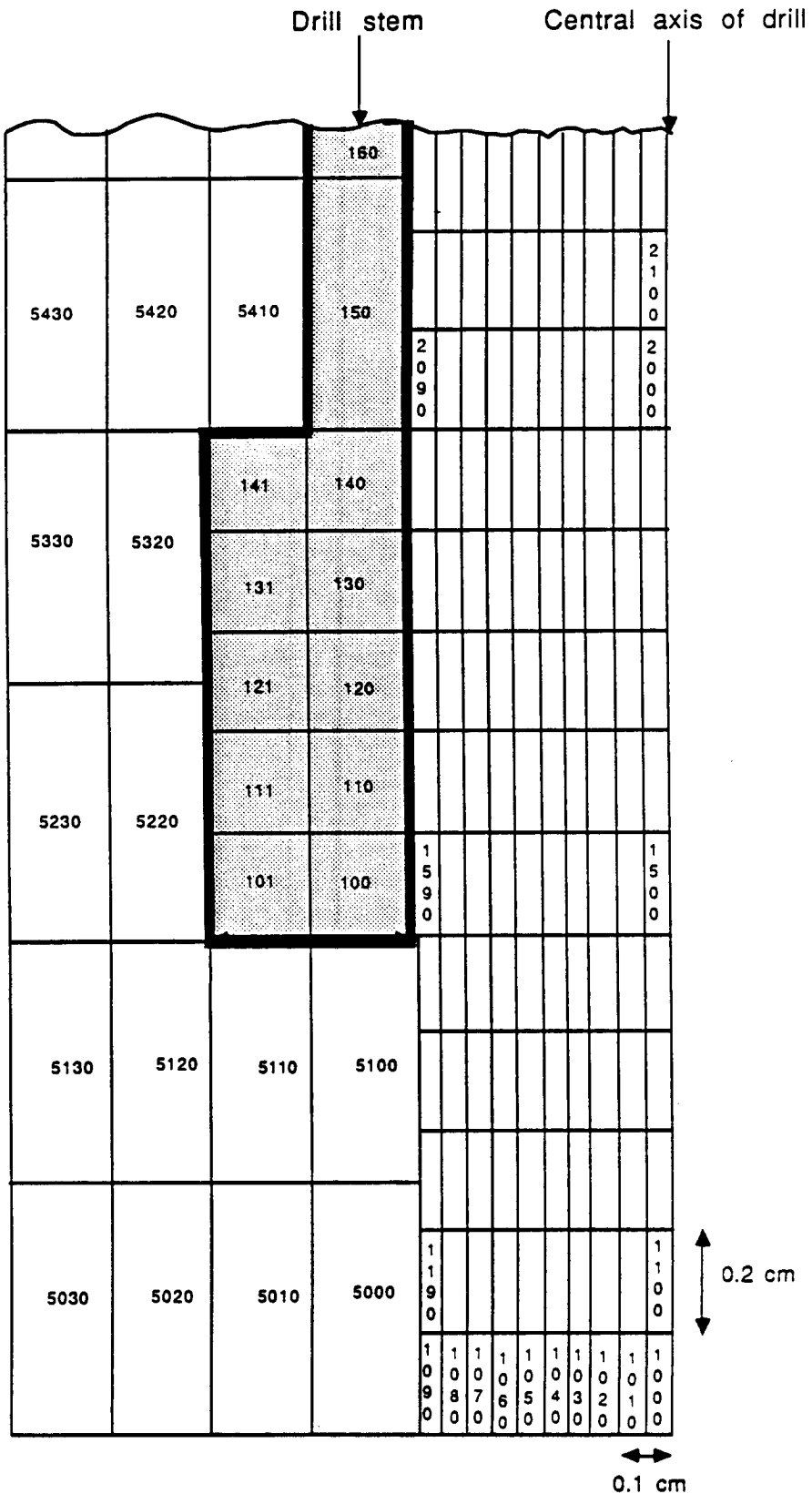

Figure A-1 Cutaway view of node numbering in drill bit area

Table A-1 Node Data Block

NODE DATA--
TOTAL NUMBER OF NODES = 394

SEQ.NO.	NODE	TEMP	CAP	SOURCE	TYPE	COMMENT
1	100	-143.000	1.5E-01	0.0E-01	DIFFUSION	INNER RING BIT
2	101	-143.000	2.0E-01	0.0E-01	DIFFUSION	OUTER RING BIT
3	110	-143.000	1.5E-01	0.0E-01	DIFFUSION	INNER RING BIT
4	111	-143.000	2.0E-01	0.0E-01	DIFFUSION	OUTER RING BIT
5	120	-143.000	1.5E-01	0.0E-01	DIFFUSION	INNER RING BIT
6	121	-143.000	2.0E-01	0.0E-01	DIFFUSION	OUTER RING BIT
7	130	-143.000	1.5E-01	0.0E-01	DIFFUSION	INNER RING BIT
8	131	-143.000	2.0E-01	0.0E-01	DIFFUSION	OUTER RING BIT
9	140	-143.000	1.5E-01	0.0E-01	DIFFUSION	INNER RING BIT
10	141	-143.000	2.0E-01	0.0E-01	DIFFUSION	OUTER RING BIT
11	150	-143.000	3.8E-01	0.0E-01	DIFFUSION	DRILL STEM
12	160	-143.000	3.8E-01	0.0E-01	DIFFUSION	DRILL STEM
13	170	-143.000	3.8E-01	0.0E-01	DIFFUSION	DRILL STEM
14	180	-143.000	3.8E-01	0.0E-01	DIFFUSION	DRILL STEM
15	190	-143.000	3.8E-01	0.0E-01	DIFFUSION	DRILL STEM
16	200	-143.000	3.8E-01	0.0E-01	DIFFUSION	DRILL STEM
17	210	-143.000	3.8E-01	0.0E-01	DIFFUSION	DRILL STEM
18	220	-143.000	3.8E-01	0.0E-01	DIFFUSION	DRILL STEM
19	230	-143.000	3.8E-01	0.0E-01	DIFFUSION	DRILL STEM
20	240	-143.000	3.8E-01	0.0E-01	DIFFUSION	DRILL STEM
21	250	-143.000	3.8E-01	0.0E-01	DIFFUSION	DRILL STEM
22	260	-143.000	3.8E-01	0.0E-01	DIFFUSION	DRILL STEM
23	270	-143.000	3.8E-01	0.0E-01	DIFFUSION	DRILL STEM
24	280	-143.000	3.8E-01	0.0E-01	DIFFUSION	DRILL STEM
25	290	-143.000	3.8E-01	0.0E-01	DIFFUSION	DRILL STEM
26	300	-143.000	3.8E-01	0.0E-01	DIFFUSION	DRILL STEM
27	310	-143.000	3.8E-01	0.0E-01	DIFFUSION	DRILL STEM
28	320	215.000	3.8E-01	0.0E-01	DIFFUSION	DRILL STEM
29	330	-143.000	3.8E-01	0.0E-01	DIFFUSION	FAKE
30	340	-143.000	3.8E-01	0.0E-01	DIFFUSION	FAKE
31	1000	-143.000	1.6E-03	0.0E-01	DIFFUSION	1st RING LOWER CORE
32	1010	-143.000	4.7E-03	0.0E-01	DIFFUSION	2nd RING LOWER CORE
33	1020	-143.000	7.8E-03	0.0E-01	DIFFUSION	3rd RING LOWER CORE
34	1030	-143.000	1.1E-02	0.0E-01	DIFFUSION	4th RING LOWER CORE
35	1040	-143.000	1.4E-02	0.0E-01	DIFFUSION	5th RING LOWER CORE
36	1050	-143.000	1.7E-02	0.0E-01	DIFFUSION	6th RING LOWER CORE
37	1060	-143.000	2.0E-02	0.0E-01	DIFFUSION	7th RING LOWER CORE
38	1070	-143.000	2.3E-02	0.0E-01	DIFFUSION	8th RING LOWER CORE
39	1080	-143.000	2.7E-02	0.0E-01	DIFFUSION	9th RING LOWER CORE
40	1090	-143.000	3.0E-02	0.0E-01	DIFFUSION	10th RING LOWER CORE
41	1100	-143.000	1.6E-03	0.0E-01	DIFFUSION	1st RING LOWER CORE
42	1110	-143.000	4.7E-03	0.0E-01	DIFFUSION	2nd RING LOWER CORE
43	1120	-143.000	7.8E-03	0.0E-01	DIFFUSION	3rd RING LOWER CORE
44	1130	-143.000	1.1E-02	0.0E-01	DIFFUSION	4th RING LOWER CORE
45	1140	-143.000	1.4E-02	0.0E-01	DIFFUSION	5th RING LOWER CORE
46	1150	-143.000	1.7E-02	0.0E-01	DIFFUSION	6th RING LOWER CORE
47	1160	-143.000	2.0E-02	0.0E-01	DIFFUSION	7th RING LOWER CORE
48	1170	-143.000	2.3E-02	0.0E-01	DIFFUSION	8th RING LOWER CORE
49	1180	-143.000	2.7E-02	0.0E-01	DIFFUSION	9th RING LOWER CORE
50	1190	-143.000	3.0E-02	0.0E-01	DIFFUSION	10th RING LOWER CORE
51	1200	-143.000	1.6E-03	0.0E-01	DIFFUSION	1st RING LOWER CORE
52	1210	-143.000	4.7E-03	0.0E-01	DIFFUSION	2nd RING LOWER CORE

MODEL NAME = A:drillf1

NODE DATA--
TOTAL NUMBER OF NODES = 394

SEQ.NO.	NODE	TEMP	CAP	SOURCE	TYPE	COMMENT
53	1220	-143.000	7.8E-03	0.0E-01	DIFFUSION	3rd RING LOWER CORE
54	1230	-143.000	1.1E-02	0.0E-01	DIFFUSION	4th RING LOWER CORE
55	1240	-143.000	1.4E-02	0.0E-01	DIFFUSION	5th RING LOWER CORE
56	1250	-143.000	1.7E-02	0.0E-01	DIFFUSION	6th RING LOWER CORE
57	1260	-143.000	2.0E-02	0.0E-01	DIFFUSION	7th RING LOWER CORE
58	1270	-143.000	2.3E-02	0.0E-01	DIFFUSION	8th RING LOWER CORE
59	1280	-143.000	2.7E-02	0.0E-01	DIFFUSION	9th RING LOWER CORE
60	1290	-143.000	3.0E-02	0.0E-01	DIFFUSION	10th RING LOWER CORE
61	1300	-143.000	1.6E-03	0.0E-01	DIFFUSION	1st RING LOWER CORE
62	1310	-143.000	4.7E-03	0.0E-01	DIFFUSION	2nd RING LOWER CORE
63	1320	-143.000	7.8E-03	0.0E-01	DIFFUSION	3rd RING LOWER CORE
64	1330	-143.000	1.1E-02	0.0E-01	DIFFUSION	4th RING LOWER CORE
65	1340	-143.000	1.4E-02	0.0E-01	DIFFUSION	5th RING LOWER CORE
66	1350	-143.000	1.7E-02	0.0E-01	DIFFUSION	6th RING LOWER CORE
67	1360	-143.000	2.0E-02	0.0E-01	DIFFUSION	7th RING LOWER CORE
68	1370	-143.000	2.3E-02	0.0E-01	DIFFUSION	8th RING LOWER CORE
69	1380	-143.000	2.7E-02	0.0E-01	DIFFUSION	9th RING LOWER CORE
70	1390	-143.000	3.0E-02	0.0E-01	DIFFUSION	10th RING LOWER CORE
71	1400	-143.000	1.6E-03	0.0E-01	DIFFUSION	1st RING LOWER CORE
72	1410	-143.000	4.7E-03	0.0E-01	DIFFUSION	2nd RING LOWER CORE
73	1420	-143.000	7.8E-03	0.0E-01	DIFFUSION	3rd RING LOWER CORE
74	1430	-143.000	1.1E-02	0.0E-01	DIFFUSION	4th RING LOWER CORE
75	1440	-143.000	1.4E-02	0.0E-01	DIFFUSION	5th RING LOWER CORE
76	1450	-143.000	1.7E-02	0.0E-01	DIFFUSION	6th RING LOWER CORE
77	1460	-143.000	2.0E-02	0.0E-01	DIFFUSION	7th RING LOWER CORE
78	1470	-143.000	2.3E-02	0.0E-01	DIFFUSION	8th RING LOWER CORE
79	1480	-143.000	2.7E-02	0.0E-01	DIFFUSION	9th RING LOWER CORE
80	1490	-143.000	3.0E-02	0.0E-01	DIFFUSION	10th RING LOWER CORE
81	1500	-143.000	1.6E-03	0.0E-01	DIFFUSION	1st RING LOWER CORE
82	1510	-143.000	4.7E-03	0.0E-01	DIFFUSION	2nd RING LOWER CORE
83	1520	-143.000	7.8E-03	0.0E-01	DIFFUSION	3rd RING LOWER CORE
84	1530	-143.000	1.1E-02	0.0E-01	DIFFUSION	4th RING LOWER CORE
85	1540	-143.000	1.4E-02	0.0E-01	DIFFUSION	5th RING LOWER CORE
86	1550	-143.000	1.7E-02	0.0E-01	DIFFUSION	6th RING LOWER CORE
87	1560	-143.000	2.0E-02	0.0E-01	DIFFUSION	7th RING LOWER CORE
88	1570	-143.000	2.3E-02	0.0E-01	DIFFUSION	8th RING LOWER CORE
89	1580	-143.000	2.7E-02	0.0E-01	DIFFUSION	9th RING LOWER CORE
90	1590	-143.000	3.0E-02	0.0E-01	DIFFUSION	10th RING LOWER CORE
91	1600	-143.000	1.6E-03	0.0E-01	DIFFUSION	1st RING LOWER CORE
92	1610	-143.000	4.7E-03	0.0E-01	DIFFUSION	2nd RING LOWER CORE
93	1620	-143.000	7.8E-03	0.0E-01	DIFFUSION	3rd RING LOWER CORE
94	1630	-143.000	1.1E-02	0.0E-01	DIFFUSION	4th RING LOWER CORE
95	1640	-143.000	1.4E-02	0.0E-01	DIFFUSION	5th RING LOWER CORE
96	1650	-143.000	1.7E-02	0.0E-01	DIFFUSION	6th RING LOWER CORE
97	1660	-143.000	2.0E-02	0.0E-01	DIFFUSION	7th RING LOWER CORE
98	1670	-143.000	2.3E-02	0.0E-01	DIFFUSION	8th RING LOWER CORE
99	1680	-143.000	2.7E-02	0.0E-01	DIFFUSION	9th RING LOWER CORE
100	1690	-143.000	3.0E-02	0.0E-01	DIFFUSION	10th RING LOWER CORE
101	1700	-143.000	1.6E-03	0.0E-01	DIFFUSION	1st RING LOWER CORE
102	1710	-143.000	4.7E-03	0.0E-01	DIFFUSION	2nd RING LOWER CORE
103	1720	-143.000	7.8E-03	0.0E-01	DIFFUSION	3rd RING LOWER CORE
104	1730	-143.000	1.1E-02	0.0E-01	DIFFUSION	4th RING LOWER CORE

MODEL NAME = A:drillf1

NODE DATA--
TOTAL NUMBER OF NODES = 394

SEQ.NO.	NODE	TEMP	CAP	SOURCE	TYPE	COMMENT
105	1740	-143.000	1.4E-02	0.0E-01	DIFFUSION	5th RING LOWER CORE
106	1750	-143.000	1.7E-02	0.0E-01	DIFFUSION	6th RING LOWER CORE
107	1760	-143.000	2.0E-02	0.0E-01	DIFFUSION	7th RING LOWER CORE
108	1770	-143.000	2.3E-02	0.0E-01	DIFFUSION	8th RING LOWER CORE
109	1780	-143.000	2.7E-02	0.0E-01	DIFFUSION	9th RING LOWER CORE
110	1790	-143.000	3.0E-02	0.0E-01	DIFFUSION	10th RING LOWER CORE
111	1800	-143.000	1.6E-03	0.0E-01	DIFFUSION	1st RING LOWER CORE
112	1810	-143.000	4.7E-03	0.0E-01	DIFFUSION	2nd RING LOWER CORE
113	1820	-143.000	7.8E-03	0.0E-01	DIFFUSION	3rd RING LOWER CORE
114	1830	-143.000	1.1E-02	0.0E-01	DIFFUSION	4th RING LOWER CORE
115	1840	-143.000	1.4E-02	0.0E-01	DIFFUSION	5th RING LOWER CORE
116	1850	-143.000	1.7E-02	0.0E-01	DIFFUSION	6th RING LOWER CORE
117	1860	-143.000	2.0E-02	0.0E-01	DIFFUSION	7th RING LOWER CORE
118	1870	-143.000	2.3E-02	0.0E-01	DIFFUSION	8th RING LOWER CORE
119	1880	-143.000	2.7E-02	0.0E-01	DIFFUSION	9th RING LOWER CORE
120	1890	-143.000	3.0E-02	0.0E-01	DIFFUSION	10th RING LOWER CORE
121	1900	-143.000	1.6E-03	0.0E-01	DIFFUSION	1st RING LOWER CORE
122	1910	-143.000	4.7E-03	0.0E-01	DIFFUSION	2nd RING LOWER CORE
123	1920	-143.000	7.8E-03	0.0E-01	DIFFUSION	3rd RING LOWER CORE
124	1930	-143.000	1.1E-02	0.0E-01	DIFFUSION	4th RING LOWER CORE
125	1940	-143.000	1.4E-02	0.0E-01	DIFFUSION	5th RING LOWER CORE
126	1950	-143.000	1.7E-02	0.0E-01	DIFFUSION	6th RING LOWER CORE
127	1960	-143.000	2.0E-02	0.0E-01	DIFFUSION	7th RING LOWER CORE
128	1970	-143.000	2.3E-02	0.0E-01	DIFFUSION	8th RING LOWER CORE
129	1980	-143.000	2.7E-02	0.0E-01	DIFFUSION	9th RING LOWER CORE
130	1990	-143.000	3.0E-02	0.0E-01	DIFFUSION	10th RING LOWER CORE
131	2000	-143.000	3.9E-03	0.0E-01	DIFFUSION	1st RING UPPER CORE
132	2010	-143.000	1.2E-02	0.0E-01	DIFFUSION	2nd RING UPPER CORE
133	2020	-143.000	2.0E-02	0.0E-01	DIFFUSION	3rd RING UPPER CORE
134	2030	-143.000	2.7E-02	0.0E-01	DIFFUSION	4th RING UPPER CORE
135	2040	-143.000	3.5E-02	0.0E-01	DIFFUSION	5th RING UPPER CORE
136	2050	-143.000	4.3E-02	0.0E-01	DIFFUSION	6th RING UPPER CORE
137	2060	-143.000	5.1E-02	0.0E-01	DIFFUSION	7th RING UPPER CORE
138	2070	-143.000	5.9E-02	0.0E-01	DIFFUSION	8th RING UPPER CORE
139	2080	-143.000	6.7E-02	0.0E-01	DIFFUSION	9th RING UPPER CORE
140	2090	-143.000	7.5E-02	0.0E-01	DIFFUSION	10th RING UPPER CORE
141	2100	-143.000	3.9E-03	0.0E-01	DIFFUSION	1st RING UPPER CORE
142	2110	-143.000	1.2E-02	0.0E-01	DIFFUSION	2nd RING UPPER CORE
143	2120	-143.000	2.0E-02	0.0E-01	DIFFUSION	3rd RING UPPER CORE
144	2130	-143.000	2.7E-02	0.0E-01	DIFFUSION	4th RING UPPER CORE
145	2140	-143.000	3.5E-02	0.0E-01	DIFFUSION	5th RING UPPER CORE
146	2150	-143.000	4.3E-02	0.0E-01	DIFFUSION	6th RING UPPER CORE
147	2160	-143.000	5.1E-02	0.0E-01	DIFFUSION	7th RING UPPER CORE
148	2170	-143.000	5.9E-02	0.0E-01	DIFFUSION	8th RING UPPER CORE
149	2180	-143.000	6.7E-02	0.0E-01	DIFFUSION	9th RING UPPER CORE
150	2190	-143.000	7.5E-02	0.0E-01	DIFFUSION	10th RING UPPER CORE
151	2200	-143.000	3.9E-03	0.0E-01	DIFFUSION	1st RING UPPER CORE
152	2210	-143.000	1.2E-02	0.0E-01	DIFFUSION	2nd RING UPPER CORE
153	2220	-143.000	2.0E-02	0.0E-01	DIFFUSION	3rd RING UPPER CORE
154	2230	-143.000	2.7E-02	0.0E-01	DIFFUSION	4th RING UPPER CORE
155	2240	-143.000	3.5E-02	0.0E-01	DIFFUSION	5th RING UPPER CORE
156	2250	-143.000	4.3E-02	0.0E-01	DIFFUSION	6th RING UPPER CORE

MODEL NAME = A:drillf1

NODE DATA--
TOTAL NUMBER OF NODES = 394

SEQ.NO.	NODE	TEMP	CAP	SOURCE	TYPE	COMMENT
157	2260	-143.000	5.1E-02	0.0E-01	DIFFUSION	7th RING UPPER CORE
158	2270	-143.000	5.9E-02	0.0E-01	DIFFUSION	8th RING UPPER CORE
159	2280	-143.000	6.7E-02	0.0E-01	DIFFUSION	9th RING UPPER CORE
160	2290	-143.000	7.5E-02	0.0E-01	DIFFUSION	10th RING UPPER CORE
161	2300	-143.000	3.9E-03	0.0E-01	DIFFUSION	1st RING UPPER CORE
162	2310	-143.000	1.2E-02	0.0E-01	DIFFUSION	2nd RING UPPER CORE
163	2320	-143.000	2.0E-02	0.0E-01	DIFFUSION	3rd RING UPPER CORE
164	2330	-143.000	2.7E-02	0.0E-01	DIFFUSION	4th RING UPPER CORE
165	2340	-143.000	3.5E-02	0.0E-01	DIFFUSION	5th RING UPPER CORE
166	2350	-143.000	4.3E-02	0.0E-01	DIFFUSION	6th RING UPPER CORE
167	2360	-143.000	5.1E-02	0.0E-01	DIFFUSION	7th RING UPPER CORE
168	2370	-143.000	5.9E-02	0.0E-01	DIFFUSION	8th RING UPPER CORE
169	2380	-143.000	6.7E-02	0.0E-01	DIFFUSION	9th RING UPPER CORE
170	2390	-143.000	7.5E-02	0.0E-01	DIFFUSION	10th RING UPPER CORE
171	2400	-143.000	3.9E-03	0.0E-01	DIFFUSION	1st RING UPPER CORE
172	2410	-143.000	1.2E-02	0.0E-01	DIFFUSION	2nd RING UPPER CORE
173	2420	-143.000	2.0E-02	0.0E-01	DIFFUSION	3rd RING UPPER CORE
174	2430	-143.000	2.7E-02	0.0E-01	DIFFUSION	4th RING UPPER CORE
175	2440	-143.000	3.5E-02	0.0E-01	DIFFUSION	5th RING UPPER CORE
176	2450	-143.000	4.3E-02	0.0E-01	DIFFUSION	6th RING UPPER CORE
177	2460	-143.000	5.1E-02	0.0E-01	DIFFUSION	7th RING UPPER CORE
178	2470	-143.000	5.9E-02	0.0E-01	DIFFUSION	8th RING UPPER CORE
179	2480	-143.000	6.7E-02	0.0E-01	DIFFUSION	9th RING UPPER CORE
180	2490	-143.000	7.5E-02	0.0E-01	DIFFUSION	10th RING UPPER CORE
181	2500	-143.000	3.9E-03	0.0E-01	DIFFUSION	1st RING UPPER CORE
182	2510	-143.000	1.2E-02	0.0E-01	DIFFUSION	2nd RING UPPER CORE
183	2520	-143.000	2.0E-02	0.0E-01	DIFFUSION	3rd RING UPPER CORE
184	2530	-143.000	2.7E-02	0.0E-01	DIFFUSION	4th RING UPPER CORE
185	2540	-143.000	3.5E-02	0.0E-01	DIFFUSION	5th RING UPPER CORE
186	2550	-143.000	4.3E-02	0.0E-01	DIFFUSION	6th RING UPPER CORE
187	2560	-143.000	5.1E-02	0.0E-01	DIFFUSION	7th RING UPPER CORE
188	2570	-143.000	5.9E-02	0.0E-01	DIFFUSION	8th RING UPPER CORE
189	2580	-143.000	6.7E-02	0.0E-01	DIFFUSION	9th RING UPPER CORE
190	2590	-143.000	7.5E-02	0.0E-01	DIFFUSION	10th RING UPPER CORE
191	2600	-143.000	3.9E-03	0.0E-01	DIFFUSION	1st RING UPPER CORE
192	2610	-143.000	1.2E-02	0.0E-01	DIFFUSION	2nd RING UPPER CORE
193	2620	-143.000	2.0E-02	0.0E-01	DIFFUSION	3rd RING UPPER CORE
194	2630	-143.000	2.7E-02	0.0E-01	DIFFUSION	4th RING UPPER CORE
195	2640	-143.000	3.5E-02	0.0E-01	DIFFUSION	5th RING UPPER CORE
196	2650	-143.000	4.3E-02	0.0E-01	DIFFUSION	6th RING UPPER CORE
197	2660	-143.000	5.1E-02	0.0E-01	DIFFUSION	7th RING UPPER CORE
198	2670	-143.000	5.9E-02	0.0E-01	DIFFUSION	8th RING UPPER CORE
199	2680	-143.000	6.7E-02	0.0E-01	DIFFUSION	9th RING UPPER CORE
200	2690	-143.000	7.5E-02	0.0E-01	DIFFUSION	10th RING UPPER CORE
201	2700	-143.000	3.9E-03	0.0E-01	DIFFUSION	1st RING UPPER CORE
202	2710	-143.000	1.2E-02	0.0E-01	DIFFUSION	2nd RING UPPER CORE
203	2720	-143.000	2.0E-02	0.0E-01	DIFFUSION	3rd RING UPPER CORE
204	2730	-143.000	2.7E-02	0.0E-01	DIFFUSION	4th RING UPPER CORE
205	2740	-143.000	3.5E-02	0.0E-01	DIFFUSION	5th RING UPPER CORE
206	2750	-143.000	4.3E-02	0.0E-01	DIFFUSION	6th RING UPPER CORE
207	2760	-143.000	5.1E-02	0.0E-01	DIFFUSION	7th RING UPPER CORE
208	2770	-143.000	5.9E-02	0.0E-01	DIFFUSION	8th RING UPPER CORE

MODEL NAME = A:drillf1

NODE DATA--
TOTAL NUMBER OF NODES = 394

SEQ.NO.	NODE	TEMP	CAP	SOURCE	TYPE	COMMENT
209	2780	-143.000	6.7E-02	0.0E-01	DIFFUSION	9th RING UPPER CORE
210	2790	-143.000	7.5E-02	0.0E-01	DIFFUSION	10th RING UPPER CORE
211	2800	-143.000	3.9E-03	0.0E-01	DIFFUSION	1st RING UPPER CORE
212	2810	-143.000	1.2E-02	0.0E-01	DIFFUSION	2nd RING UPPER CORE
213	2820	-143.000	2.0E-02	0.0E-01	DIFFUSION	3rd RING UPPER CORE
214	2830	-143.000	2.7E-02	0.0E-01	DIFFUSION	4th RING UPPER CORE
215	2840	-143.000	3.5E-02	0.0E-01	DIFFUSION	5th RING UPPER CORE
216	2850	-143.000	4.3E-02	0.0E-01	DIFFUSION	6th RING UPPER CORE
217	2860	-143.000	5.1E-02	0.0E-01	DIFFUSION	7th RING UPPER CORE
218	2870	-143.000	5.9E-02	0.0E-01	DIFFUSION	8th RING UPPER CORE
219	2880	-143.000	6.7E-02	0.0E-01	DIFFUSION	9th RING UPPER CORE
220	2890	-143.000	7.5E-02	0.0E-01	DIFFUSION	10th RING UPPER CORE
221	2900	-143.000	3.9E-03	0.0E-01	DIFFUSION	1st RING UPPER CORE
222	2910	-143.000	1.2E-02	0.0E-01	DIFFUSION	2nd RING UPPER CORE
223	2920	-143.000	2.0E-02	0.0E-01	DIFFUSION	3rd RING UPPER CORE
224	2930	-143.000	2.7E-02	0.0E-01	DIFFUSION	4th RING UPPER CORE
225	2940	-143.000	3.5E-02	0.0E-01	DIFFUSION	5th RING UPPER CORE
226	2950	-143.000	4.3E-02	0.0E-01	DIFFUSION	6th RING UPPER CORE
227	2960	-143.000	5.1E-02	0.0E-01	DIFFUSION	7th RING UPPER CORE
228	2970	-143.000	5.9E-02	0.0E-01	DIFFUSION	8th RING UPPER CORE
229	2980	-143.000	6.7E-02	0.0E-01	DIFFUSION	9th RING UPPER CORE
230	2990	-143.000	7.5E-02	0.0E-01	DIFFUSION	10th RING UPPER CORE
231	3000	-143.000	3.9E-03	0.0E-01	DIFFUSION	1st RING UPPER CORE
232	3010	-143.000	1.2E-02	0.0E-01	DIFFUSION	2nd RING UPPER CORE
233	3020	-143.000	2.0E-02	0.0E-01	DIFFUSION	3rd RING UPPER CORE
234	3030	-143.000	2.7E-02	0.0E-01	DIFFUSION	4th RING UPPER CORE
235	3040	-143.000	3.5E-02	0.0E-01	DIFFUSION	5th RING UPPER CORE
236	3050	-143.000	4.3E-02	0.0E-01	DIFFUSION	6th RING UPPER CORE
237	3060	-143.000	5.1E-02	0.0E-01	DIFFUSION	7th RING UPPER CORE
238	3070	-143.000	5.9E-02	0.0E-01	DIFFUSION	8th RING UPPER CORE
239	3080	-143.000	6.7E-02	0.0E-01	DIFFUSION	9th RING UPPER CORE
240	3090	-143.000	7.5E-02	0.0E-01	DIFFUSION	10th RING UPPER CORE
241	3100	-143.000	3.9E-03	0.0E-01	DIFFUSION	1st RING UPPER CORE
242	3110	-143.000	1.2E-02	0.0E-01	DIFFUSION	2nd RING UPPER CORE
243	3120	-143.000	2.0E-02	0.0E-01	DIFFUSION	3rd RING UPPER CORE
244	3130	-143.000	2.7E-02	0.0E-01	DIFFUSION	4th RING UPPER CORE
245	3140	-143.000	3.5E-02	0.0E-01	DIFFUSION	5th RING UPPER CORE
246	3150	-143.000	4.3E-02	0.0E-01	DIFFUSION	6th RING UPPER CORE
247	3160	-143.000	5.1E-02	0.0E-01	DIFFUSION	7th RING UPPER CORE
248	3170	-143.000	5.9E-02	0.0E-01	DIFFUSION	8th RING UPPER CORE
249	3180	-143.000	6.7E-02	0.0E-01	DIFFUSION	9th RING UPPER CORE
250	3190	-143.000	7.5E-02	0.0E-01	DIFFUSION	10th RING UPPER CORE
251	3200	-143.000	3.9E-03	0.0E-01	DIFFUSION	1st RING UPPER CORE
252	3210	-143.000	1.2E-02	0.0E-01	DIFFUSION	2nd RING UPPER CORE
253	3220	-143.000	2.0E-02	0.0E-01	DIFFUSION	3rd RING UPPER CORE
254	3230	-143.000	2.7E-02	0.0E-01	DIFFUSION	4th RING UPPER CORE
255	3240	-143.000	3.5E-02	0.0E-01	DIFFUSION	5th RING UPPER CORE
256	3250	-143.000	4.3E-02	0.0E-01	DIFFUSION	6th RING UPPER CORE
257	3260	-143.000	5.1E-02	0.0E-01	DIFFUSION	7th RING UPPER CORE
258	3270	-143.000	5.9E-02	0.0E-01	DIFFUSION	8th RING UPPER CORE
259	3280	-143.000	6.7E-02	0.0E-01	DIFFUSION	9th RING UPPER CORE
260	3290	-143.000	7.5E-02	0.0E-01	DIFFUSION	10th RING UPPER CORE

MODEL NAME = A:drillf1

NODE DATA--
TOTAL NUMBER OF NODES = 394

SEQ.NO.	NODE	TEMP	CAP	SOURCE	TYPE	COMMENT
261	3300	-143.000	3.9E-03	0.0E-01	DIFFUSION	1st RING UPPER CORE
262	3310	-143.000	1.2E-02	0.0E-01	DIFFUSION	2nd RING UPPER CORE
263	3320	-143.000	2.0E-02	0.0E-01	DIFFUSION	3rd RING UPPER CORE
264	3330	-143.000	2.7E-02	0.0E-01	DIFFUSION	4th RING UPPER CORE
265	3340	-143.000	3.5E-02	0.0E-01	DIFFUSION	5th RING UPPER CORE
266	3350	-143.000	4.3E-02	0.0E-01	DIFFUSION	6th RING UPPER CORE
267	3360	-143.000	5.1E-02	0.0E-01	DIFFUSION	7th RING UPPER CORE
268	3370	-143.000	5.9E-02	0.0E-01	DIFFUSION	8th RING UPPER CORE
269	3380	-143.000	6.7E-02	0.0E-01	DIFFUSION	9th RING UPPER CORE
270	3390	-143.000	7.5E-02	0.0E-01	DIFFUSION	10th RING UPPER CORE
271	3400	-143.000	3.9E-03	0.0E-01	DIFFUSION	1st RING UPPER CORE
272	3410	-143.000	1.2E-02	0.0E-01	DIFFUSION	2nd RING UPPER CORE
273	3420	-143.000	2.0E-02	0.0E-01	DIFFUSION	3rd RING UPPER CORE
274	3430	-143.000	2.7E-02	0.0E-01	DIFFUSION	4th RING UPPER CORE
275	3440	-143.000	3.5E-02	0.0E-01	DIFFUSION	5th RING UPPER CORE
276	3450	-143.000	4.3E-02	0.0E-01	DIFFUSION	6th RING UPPER CORE
277	3460	-143.000	5.1E-02	0.0E-01	DIFFUSION	7th RING UPPER CORE
278	3470	-143.000	5.9E-02	0.0E-01	DIFFUSION	8th RING UPPER CORE
279	3480	-143.000	6.7E-02	0.0E-01	DIFFUSION	9th RING UPPER CORE
280	3490	-143.000	7.5E-02	0.0E-01	DIFFUSION	10th RING UPPER CORE
281	3500	-143.000	3.9E-03	0.0E-01	DIFFUSION	1st RING UPPER CORE
282	3510	-143.000	1.2E-02	0.0E-01	DIFFUSION	2nd RING UPPER CORE
283	3520	-143.000	2.0E-02	0.0E-01	DIFFUSION	3rd RING UPPER CORE
284	3530	-143.000	2.7E-02	0.0E-01	DIFFUSION	4th RING UPPER CORE
285	3540	-143.000	3.5E-02	0.0E-01	DIFFUSION	5th RING UPPER CORE
286	3550	-143.000	4.3E-02	0.0E-01	DIFFUSION	6th RING UPPER CORE
287	3560	-143.000	5.1E-02	0.0E-01	DIFFUSION	7th RING UPPER CORE
288	3570	-143.000	5.9E-02	0.0E-01	DIFFUSION	8th RING UPPER CORE
289	3580	-143.000	6.7E-02	0.0E-01	DIFFUSION	9th RING UPPER CORE
290	3590	-143.000	7.5E-02	0.0E-01	DIFFUSION	10th RING UPPER CORE
291	3600	-143.000	3.9E-03	0.0E-01	DIFFUSION	1st RING UPPER CORE
292	3610	-143.000	1.2E-02	0.0E-01	DIFFUSION	2nd RING UPPER CORE
293	3620	-143.000	2.0E-02	0.0E-01	DIFFUSION	3rd RING UPPER CORE
294	3630	-143.000	2.7E-02	0.0E-01	DIFFUSION	4th RING UPPER CORE
295	3640	-143.000	3.5E-02	0.0E-01	DIFFUSION	5th RING UPPER CORE
296	3650	-143.000	4.3E-02	0.0E-01	DIFFUSION	6th RING UPPER CORE
297	3660	-143.000	5.1E-02	0.0E-01	DIFFUSION	7th RING UPPER CORE
298	3670	-143.000	5.9E-02	0.0E-01	DIFFUSION	8th RING UPPER CORE
299	3680	-143.000	6.7E-02	0.0E-01	DIFFUSION	9th RING UPPER CORE
300	3690	-143.000	7.5E-02	0.0E-01	DIFFUSION	10th RING UPPER CORE
301	3700	-143.000	3.9E-03	0.0E-01	DIFFUSION	1st RING UPPER CORE
302	3710	-143.000	1.2E-02	0.0E-01	DIFFUSION	2nd RING UPPER CORE
303	3720	-143.000	2.0E-02	0.0E-01	DIFFUSION	3rd RING UPPER CORE
304	3730	-143.000	2.7E-02	0.0E-01	DIFFUSION	4th RING UPPER CORE
305	3740	-143.000	3.5E-02	0.0E-01	DIFFUSION	5th RING UPPER CORE
306	3750	-143.000	4.3E-02	0.0E-01	DIFFUSION	6th RING UPPER CORE
307	3760	-143.000	5.1E-02	0.0E-01	DIFFUSION	7th RING UPPER CORE
308	3770	-143.000	5.9E-02	0.0E-01	DIFFUSION	8th RING UPPER CORE
309	3780	-143.000	6.7E-02	0.0E-01	DIFFUSION	9th RING UPPER CORE
310	3790	-143.000	7.5E-02	0.0E-01	DIFFUSION	10th RING UPPER CORE
311	5000	-143.000	3.8E-01	0.0E-01	DIFFUSION	1st RING OUTER
312	5010	-143.000	5.0E-01	0.0E-01	DIFFUSION	2nd RING OUTER

MODEL NAME = A:drillf1

NODE DATA--
TOTAL NUMBER OF NODES = 394

SEQ.NO.	NODE	TEMP	CAP	SOURCE	TYPE	COMMENT
313	5020	-143.000	6.3E-01	0.0E-01	DIFFUSION	3rd RING OUTER
314	5030	-143.000	7.5E-01	0.0E-01	DIFFUSION	4th RING OUTER
315	5100	-143.000	3.8E-01	0.0E-01	DIFFUSION	1st RING OUTER
316	5110	-143.000	5.0E-01	0.0E-01	DIFFUSION	2nd RING OUTER
317	5120	-143.000	6.3E-01	0.0E-01	DIFFUSION	3rd RING OUTER
318	5130	-143.000	7.5E-01	0.0E-01	DIFFUSION	4th RING OUTER
319	5220	-143.000	6.3E-01	0.0E-01	DIFFUSION	3rd RING OUTER
320	5230	-143.000	7.5E-01	0.0E-01	DIFFUSION	4th RING OUTER
321	5320	-143.000	6.3E-01	0.0E-01	DIFFUSION	3rd RING OUTER
322	5330	-143.000	7.5E-01	0.0E-01	DIFFUSION	4th RING OUTER
323	5410	-143.000	5.0E-01	0.0E-01	DIFFUSION	2nd RING OUTER
324	5420	-143.000	6.3E-01	0.0E-01	DIFFUSION	3rd RING OUTER
325	5430	-143.000	7.5E-01	0.0E-01	DIFFUSION	4th RING OUTER
326	5510	-143.000	5.0E-01	0.0E-01	DIFFUSION	2nd RING OUTER
327	5520	-143.000	6.3E-01	0.0E-01	DIFFUSION	3rd RING OUTER
328	5530	-143.000	7.5E-01	0.0E-01	DIFFUSION	4th RING OUTER
329	5610	-143.000	5.0E-01	0.0E-01	DIFFUSION	2nd RING OUTER
330	5620	-143.000	6.3E-01	0.0E-01	DIFFUSION	3rd RING OUTER
331	5630	-143.000	7.5E-01	0.0E-01	DIFFUSION	4th RING OUTER
332	5710	-143.000	5.0E-01	0.0E-01	DIFFUSION	2nd RING OUTER
333	5720	-143.000	6.3E-01	0.0E-01	DIFFUSION	3rd RING OUTER
334	5730	-143.000	7.5E-01	0.0E-01	DIFFUSION	4th RING OUTER
335	5810	-143.000	5.0E-01	0.0E-01	DIFFUSION	2nd RING OUTER
336	5820	-143.000	6.3E-01	0.0E-01	DIFFUSION	3rd RING OUTER
337	5830	-143.000	7.5E-01	0.0E-01	DIFFUSION	4th RING OUTER
338	5910	-143.000	5.0E-01	0.0E-01	DIFFUSION	2nd RING OUTER
339	5920	-143.000	6.3E-01	0.0E-01	DIFFUSION	3rd RING OUTER
340	5930	-143.000	7.5E-01	0.0E-01	DIFFUSION	4th RING OUTER
341	6010	-143.000	5.0E-01	0.0E-01	DIFFUSION	2nd RING OUTER
342	6020	-143.000	6.3E-01	0.0E-01	DIFFUSION	3rd RING OUTER
343	6030	-143.000	7.5E-01	0.0E-01	DIFFUSION	4th RING OUTER
344	6110	-143.000	5.0E-01	0.0E-01	DIFFUSION	2nd RING OUTER
345	6120	-143.000	6.3E-01	0.0E-01	DIFFUSION	3rd RING OUTER
346	6130	-143.000	7.5E-01	0.0E-01	DIFFUSION	4th RING OUTER
347	6210	-143.000	5.0E-01	0.0E-01	DIFFUSION	2nd RING OUTER
348	6220	-143.000	6.3E-01	0.0E-01	DIFFUSION	3rd RING OUTER
349	6230	-143.000	7.5E-01	0.0E-01	DIFFUSION	4th RING OUTER
350	6310	-143.000	5.0E-01	0.0E-01	DIFFUSION	2nd RING OUTER
351	6320	-143.000	6.3E-01	0.0E-01	DIFFUSION	3rd RING OUTER
352	6330	-143.000	7.5E-01	0.0E-01	DIFFUSION	4th RING OUTER
353	6410	-143.000	5.0E-01	0.0E-01	DIFFUSION	2nd RING OUTER
354	6420	-143.000	6.3E-01	0.0E-01	DIFFUSION	3rd RING OUTER
355	6430	-143.000	7.5E-01	0.0E-01	DIFFUSION	4th RING OUTER
356	6510	-143.000	5.0E-01	0.0E-01	DIFFUSION	2nd RING OUTER
357	6520	-143.000	6.3E-01	0.0E-01	DIFFUSION	3rd RING OUTER
358	6530	-143.000	7.5E-01	0.0E-01	DIFFUSION	4th RING OUTER
359	6610	-143.000	5.0E-01	0.0E-01	DIFFUSION	2nd RING OUTER
360	6620	-143.000	6.3E-01	0.0E-01	DIFFUSION	3rd RING OUTER
361	6630	-143.000	7.5E-01	0.0E-01	DIFFUSION	4th RING OUTER
362	6710	-143.000	5.0E-01	0.0E-01	DIFFUSION	2nd RING OUTER
363	6720	-143.000	6.3E-01	0.0E-01	DIFFUSION	3rd RING OUTER
364	6730	-143.000	7.5E-01	0.0E-01	DIFFUSION	4th RING OUTER

MODEL NAME = A:drillf1

NODE DATA--
TOTAL NUMBER OF NODES = 394

SEQ.NO.	NODE	TEMP	CAP	SOURCE	TYPE	COMMENT
365	6810	-143.000	5.0E-01	0.0E-01	DIFFUSION	2nd RING OUTER
366	6820	-143.000	6.3E-01	0.0E-01	DIFFUSION	3rd RING OUTER
367	6830	-143.000	7.5E-01	0.0E-01	DIFFUSION	4th RING OUTER
368	6910	-143.000	5.0E-01	0.0E-01	DIFFUSION	2nd RING OUTER
369	6920	-143.000	6.3E-01	0.0E-01	DIFFUSION	3rd RING OUTER
370	6930	-143.000	7.5E-01	0.0E-01	DIFFUSION	4th RING OUTER
371	7010	-143.000	5.0E-01	0.0E-01	DIFFUSION	2nd RING OUTER
372	7020	-143.000	6.3E-01	0.0E-01	DIFFUSION	3rd RING OUTER
373	7030	-143.000	7.5E-01	0.0E-01	DIFFUSION	4th RING OUTER
374	7110	-143.000	5.0E-01	0.0E-01	DIFFUSION	2nd RING OUTER
375	7120	-143.000	6.3E-01	0.0E-01	DIFFUSION	3rd RING OUTER
376	7130	-143.000	7.5E-01	0.0E-01	DIFFUSION	4th RING OUTER
377	900	-143.000	0.0E-01	0.0E-01	BOUNDARY	BOUNDARY UNDER CORE
378	910	-143.000	0.0E-01	0.0E-01	BOUNDARY	BOUNDARY UNDER CORE
379	920	-143.000	0.0E-01	0.0E-01	BOUNDARY	BOUNDARY UNDER CORE
380	930	-143.000	0.0E-01	0.0E-01	BOUNDARY	BOUNDARY UNDER CORE
381	940	-143.000	0.0E-01	0.0E-01	BOUNDARY	BOUNDARY UNDER CORE
382	950	-143.000	0.0E-01	0.0E-01	BOUNDARY	BOUNDARY UNDER CORE
383	960	-143.000	0.0E-01	0.0E-01	BOUNDARY	BOUNDARY UNDER CORE
384	970	-143.000	0.0E-01	0.0E-01	BOUNDARY	BOUNDARY UNDER CORE
385	980	-143.000	0.0E-01	0.0E-01	BOUNDARY	BOUNDARY UNDER CORE
386	990	-143.000	0.0E-01	0.0E-01	BOUNDARY	BOUNDARY UNDER CORE
387	4900	-143.000	0.0E-01	0.0E-01	BOUNDARY	BOUNDARY UNDER OUTER
388	4910	-143.000	0.0E-01	0.0E-01	BOUNDARY	BOUNDARY UNDER OUTER
389	4920	-143.000	0.0E-01	0.0E-01	BOUNDARY	BOUNDARY UNDER OUTER
390	4930	-143.000	0.0E-01	0.0E-01	BOUNDARY	BOUNDARY UNDER OUTER
391	7210	-143.000	0.0E-01	0.0E-01	BOUNDARY	BOUNDARY ABOVE OUTER
392	7220	-143.000	0.0E-01	0.0E-01	BOUNDARY	BOUNDARY ABOVE OUTER
393	7230	-143.000	0.0E-01	0.0E-01	BOUNDARY	BOUNDARY ABOVE OUTER
394	9000	-143.000	0.0E-01	0.0E-01	BOUNDARY	SIDE BOUNDARY

Table A-2 Conductor Data Block

CONDUCTOR DATA--
TOTAL NUMBER OF CONDUCTORS = 751

SEQ.NO.	COND.NO.	NODE I	NODE J	VALUE	TYPE
1	102	100	101	4.3960	LINEAR
2	110	100	110	3.7700	LINEAR
3	111	101	111	5.0200	LINEAR
4	112	110	111	4.3960	LINEAR
5	120	110	120	3.7700	LINEAR
6	121	111	121	5.0200	LINEAR
7	122	120	121	4.3960	LINEAR
8	130	120	130	3.7700	LINEAR
9	131	121	131	5.0200	LINEAR
10	132	130	131	4.3960	LINEAR
11	140	130	140	3.7700	LINEAR
12	141	131	141	5.0200	LINEAR
13	142	140	141	4.3960	LINEAR
14	150	140	150	2.1500	LINEAR
15	160	150	160	1.5100	LINEAR
16	170	160	170	1.5100	LINEAR
17	180	170	180	1.5100	LINEAR
18	190	180	190	1.5100	LINEAR
19	200	190	200	1.5100	LINEAR
20	210	200	210	1.5100	LINEAR
21	220	210	220	1.5100	LINEAR
22	230	220	230	1.5100	LINEAR
23	240	230	240	1.5100	LINEAR
24	250	240	250	1.5100	LINEAR
25	260	250	260	1.5100	LINEAR
26	270	260	270	1.5100	LINEAR
27	280	270	280	1.5100	LINEAR
28	290	280	290	1.5100	LINEAR
29	300	290	300	1.5100	LINEAR
30	310	300	310	1.5100	LINEAR
31	320	310	320	1.5100	LINEAR
32	340	330	340	1.5000	LINEAR
33	1000	900	1000	0.39000E-01	LINEAR
34	1010	910	1010	0.11800	LINEAR
35	1011	1000	1010	1.2560	LINEAR
36	1020	920	1020	0.19600	LINEAR
37	1021	1010	1020	2.5100	LINEAR
38	1030	930	1030	0.27400	LINEAR
39	1031	1020	1030	3.7700	LINEAR
40	1040	940	1040	0.35300	LINEAR
41	1041	1030	1040	5.0200	LINEAR
42	1050	950	1050	0.43200	LINEAR
43	1051	1040	1050	6.2800	LINEAR
44	1060	960	1060	0.51000	LINEAR
45	1061	1050	1060	7.5400	LINEAR
46	1070	970	1070	0.58900	LINEAR
47	1071	1060	1070	8.7900	LINEAR
48	1080	980	1080	0.66700	LINEAR
49	1081	1070	1080	10.050	LINEAR
50	1090	990	1090	0.74600	LINEAR
51	1091	1080	1090	11.300	LINEAR
52	1100	1000	1100	0.39000E-01	LINEAR

MODEL NAME = A:drillf1

CONDUCTOR DATA--
TOTAL NUMBER OF CONDUCTORS = 751

SEQ.NO.	COND.NO.	NODE I	NODE J	VALUE	TYPE
53	1110	1010	1110	0.11800	LINEAR
54	1111	1100	1110	1.2560	LINEAR
55	1120	1020	1120	0.19600	LINEAR
56	1121	1110	1120	2.5100	LINEAR
57	1130	1030	1130	0.27400	LINEAR
58	1131	1120	1130	3.7700	LINEAR
59	1140	1040	1140	0.35300	LINEAR
60	1141	1130	1140	5.0200	LINEAR
61	1150	1050	1150	0.43200	LINEAR
62	1151	1140	1150	6.2800	LINEAR
63	1160	1060	1160	0.51000	LINEAR
64	1161	1150	1160	7.5400	LINEAR
65	1170	1070	1170	0.58900	LINEAR
66	1171	1160	1170	8.7900	LINEAR
67	1180	1080	1180	0.66700	LINEAR
68	1181	1170	1180	10.050	LINEAR
69	1190	1090	1190	0.74600	LINEAR
70	1191	1180	1190	11.300	LINEAR
71	1200	1100	1200	0.39000E-01	LINEAR
72	1210	1110	1210	0.11800	LINEAR
73	1211	1200	1210	1.2560	LINEAR
74	1220	1120	1220	0.19600	LINEAR
75	1221	1210	1220	2.5100	LINEAR
76	1230	1130	1230	0.27400	LINEAR
77	1231	1220	1230	3.7700	LINEAR
78	1240	1140	1240	0.35300	LINEAR
79	1241	1230	1240	5.0200	LINEAR
80	1250	1150	1250	0.43200	LINEAR
81	1251	1240	1250	6.2800	LINEAR
82	1260	1160	1260	0.51000	LINEAR
83	1261	1250	1260	7.5400	LINEAR
84	1270	1170	1270	0.58900	LINEAR
85	1271	1260	1270	8.7900	LINEAR
86	1280	1180	1280	0.66700	LINEAR
87	1281	1270	1280	10.050	LINEAR
88	1290	1190	1290	0.74600	LINEAR
89	1291	1280	1290	11.300	LINEAR
90	1300	1200	1300	0.39000E-01	LINEAR
91	1310	1210	1310	0.11800	LINEAR
92	1311	1300	1310	1.2560	LINEAR
93	1320	1220	1320	0.19600	LINEAR
94	1321	1310	1320	2.5100	LINEAR
95	1330	1230	1330	0.27400	LINEAR
96	1331	1320	1330	3.7700	LINEAR
97	1340	1240	1340	0.35300	LINEAR
98	1341	1330	1340	5.0200	LINEAR
99	1350	1250	1350	0.43200	LINEAR
100	1351	1340	1350	6.2800	LINEAR
101	1360	1260	1360	0.51000	LINEAR
102	1361	1350	1360	7.5400	LINEAR
103	1370	1270	1370	0.58900	LINEAR
104	1371	1360	1370	8.7900	LINEAR

MODEL NAME = A:drillf1

CONDUCTOR DATA--
TOTAL NUMBER OF CONDUCTORS = 751

SEQ.NO.	COND.NO.	NODE I	NODE J	VALUE	TYPE
105	1380	1280	1380	0.66700	LINEAR
106	1381	1370	1380	10.050	LINEAR
107	1390	1290	1390	0.74600	LINEAR
108	1391	1380	1390	11.300	LINEAR
109	1400	1300	1400	0.39000E-01	LINEAR
110	1410	1310	1410	0.11800	LINEAR
111	1411	1400	1410	1.2560	LINEAR
112	1420	1320	1420	0.19600	LINEAR
113	1421	1410	1420	2.5100	LINEAR
114	1430	1330	1430	0.27400	LINEAR
115	1431	1420	1430	3.7700	LINEAR
116	1440	1340	1440	0.35300	LINEAR
117	1441	1430	1440	5.0200	LINEAR
118	1450	1350	1450	0.43200	LINEAR
119	1451	1440	1450	6.2800	LINEAR
120	1460	1360	1460	0.51000	LINEAR
121	1461	1450	1460	7.5400	LINEAR
122	1470	1370	1470	0.58900	LINEAR
123	1471	1460	1470	8.7900	LINEAR
124	1480	1380	1480	0.66700	LINEAR
125	1481	1470	1480	10.050	LINEAR
126	1490	1390	1490	0.74600	LINEAR
127	1491	1480	1490	11.300	LINEAR
128	1500	1400	1500	0.39000E-01	LINEAR
129	1510	1410	1510	0.11800	LINEAR
130	1511	1500	1510	1.2560	LINEAR
131	1520	1420	1520	0.19600	LINEAR
132	1521	1510	1520	2.5100	LINEAR
133	1530	1430	1530	0.27400	LINEAR
134	1531	1520	1530	3.7700	LINEAR
135	1540	1440	1540	0.35300	LINEAR
136	1541	1530	1540	5.0200	LINEAR
137	1550	1450	1550	0.43200	LINEAR
138	1551	1540	1550	6.2800	LINEAR
139	1560	1460	1560	0.51000	LINEAR
140	1561	1550	1560	7.5400	LINEAR
141	1570	1470	1570	0.58900	LINEAR
142	1571	1560	1570	8.7900	LINEAR
143	1580	1480	1580	0.66700	LINEAR
144	1581	1570	1580	10.050	LINEAR
145	1590	1490	1590	0.74600	LINEAR
146	1591	1580	1590	11.300	LINEAR
147	1592	1590	100	20.930	LINEAR
148	1600	1500	1600	0.39000E-01	LINEAR
149	1610	1510	1610	0.11800	LINEAR
150	1611	1600	1610	1.2560	LINEAR
151	1620	1520	1620	0.19600	LINEAR
152	1621	1610	1620	2.5100	LINEAR
153	1630	1530	1630	0.27400	LINEAR
154	1631	1620	1630	3.7700	LINEAR
155	1640	1540	1640	0.35300	LINEAR
156	1641	1630	1640	5.0200	LINEAR

MODEL NAME = A:drillf1

CONDUCTOR DATA--
TOTAL NUMBER OF CONDUCTORS = 751

SEQ.NO.	COND.NO.	NODE I	NODE J	VALUE	TYPE
157	1650	1550	1650	0.43200	LINEAR
158	1651	1640	1650	6.2800	LINEAR
159	1660	1560	1660	0.51000	LINEAR
160	1661	1650	1660	7.5400	LINEAR
161	1670	1570	1670	0.58900	LINEAR
162	1671	1660	1670	8.7900	LINEAR
163	1680	1580	1680	0.66700	LINEAR
164	1681	1670	1680	10.050	LINEAR
165	1690	1590	1690	0.74600	LINEAR
166	1691	1680	1690	11.300	LINEAR
167	1692	1690	110	20.930	LINEAR
168	1700	1600	1700	0.39000E-01	LINEAR
169	1710	1610	1710	0.11800	LINEAR
170	1711	1700	1710	1.2560	LINEAR
171	1720	1620	1720	0.19600	LINEAR
172	1721	1710	1720	2.5100	LINEAR
173	1730	1630	1730	0.27400	LINEAR
174	1731	1720	1730	3.7700	LINEAR
175	1740	1640	1740	0.35300	LINEAR
176	1741	1730	1740	5.0200	LINEAR
177	1750	1650	1750	0.43200	LINEAR
178	1751	1740	1750	6.2800	LINEAR
179	1760	1660	1760	0.51000	LINEAR
180	1761	1750	1760	7.5400	LINEAR
181	1770	1670	1770	0.58900	LINEAR
182	1771	1760	1770	8.7900	LINEAR
183	1780	1680	1780	0.66700	LINEAR
184	1781	1770	1780	10.050	LINEAR
185	1790	1690	1790	0.74600	LINEAR
186	1791	1780	1790	11.300	LINEAR
187	1792	1790	120	20.930	LINEAR
188	1800	1700	1800	0.39000E-01	LINEAR
189	1810	1710	1810	0.11800	LINEAR
190	1811	1800	1810	1.2560	LINEAR
191	1820	1720	1820	0.19600	LINEAR
192	1821	1810	1820	2.5100	LINEAR
193	1830	1730	1830	0.27400	LINEAR
194	1831	1820	1830	3.7700	LINEAR
195	1840	1740	1840	0.35300	LINEAR
196	1841	1830	1840	5.0200	LINEAR
197	1850	1750	1850	0.43200	LINEAR
198	1851	1840	1850	6.2800	LINEAR
199	1860	1760	1860	0.51000	LINEAR
200	1861	1850	1860	7.5400	LINEAR
201	1870	1770	1870	0.58900	LINEAR
202	1871	1860	1870	8.7900	LINEAR
203	1880	1780	1880	0.66700	LINEAR
204	1881	1870	1880	10.050	LINEAR
205	1890	1790	1890	0.74600	LINEAR
206	1891	1880	1890	11.300	LINEAR
207	1892	1890	130	20.930	LINEAR
208	1900	1800	1900	0.39000E-01	LINEAR

MODEL NAME = A:drillf1

CONDUCTOR DATA--
TOTAL NUMBER OF CONDUCTORS = 751

SEQ.NO.	COND.NO.	NODE I	NODE J	VALUE	TYPE
209	1910	1810	1910	0.11800	LINEAR
210	1911	1900	1910	1.2560	LINEAR
211	1920	1820	1920	0.19600	LINEAR
212	1921	1910	1920	2.5100	LINEAR
213	1930	1830	1930	0.27400	LINEAR
214	1931	1920	1930	3.7700	LINEAR
215	1940	1840	1940	0.35300	LINEAR
216	1941	1930	1940	5.0200	LINEAR
217	1950	1850	1950	0.43200	LINEAR
218	1951	1940	1950	6.2800	LINEAR
219	1960	1860	1960	0.51000	LINEAR
220	1961	1950	1960	7.5400	LINEAR
221	1970	1870	1970	0.58900	LINEAR
222	1971	1960	1970	8.7900	LINEAR
223	1980	1880	1980	0.66700	LINEAR
224	1981	1970	1980	10.050	LINEAR
225	1990	1890	1990	0.74600	LINEAR
226	1991	1980	1990	11.300	LINEAR
227	1992	1990	140	20.930	LINEAR
228	2000	1900	2000	0.22000E-01	LINEAR
229	2010	1910	2010	0.67000E-01	LINEAR
230	2011	2000	2010	3.1400	LINEAR
231	2020	1920	2020	0.11200	LINEAR
232	2021	2010	2020	6.2800	LINEAR
233	2030	1930	2030	0.15700	LINEAR
234	2031	2020	2030	9.4200	LINEAR
235	2040	1940	2040	0.20200	LINEAR
236	2041	2030	2040	12.560	LINEAR
237	2050	1950	2050	0.26700	LINEAR
238	2051	2040	2050	15.700	LINEAR
239	2060	1960	2060	0.29200	LINEAR
240	2061	2050	2060	18.840	LINEAR
241	2070	1970	2070	0.33600	LINEAR
242	2071	2060	2070	21.980	LINEAR
243	2080	1980	2080	0.38100	LINEAR
244	2081	2070	2080	25.120	LINEAR
245	2090	1990	2090	0.42600	LINEAR
246	2091	2080	2090	28.260	LINEAR
247	2092	2090	150	52.330	LINEAR
248	2100	2000	2100	0.15700E-01	LINEAR
249	2110	2010	2110	0.47100E-01	LINEAR
250	2111	2100	2110	3.1400	LINEAR
251	2120	2020	2120	0.78500E-01	LINEAR
252	2121	2110	2120	6.2800	LINEAR
253	2130	2030	2130	0.10990	LINEAR
254	2131	2120	2130	9.4200	LINEAR
255	2140	2040	2140	0.14100	LINEAR
256	2141	2130	2140	12.560	LINEAR
257	2150	2050	2150	0.17300	LINEAR
258	2151	2140	2150	15.700	LINEAR
259	2160	2060	2160	0.20400	LINEAR
260	2161	2150	2160	18.840	LINEAR

MODEL NAME = A:drillf1

CONDUCTOR DATA--
TOTAL NUMBER OF CONDUCTORS = 751

SEQ.NO.	COND.NO.	NODE I	NODE J	VALUE	TYPE
261	2170	2070	2170	0.23600	LINEAR
262	2171	2160	2170	21.980	LINEAR
263	2180	2080	2180	0.26700	LINEAR
264	2181	2170	2180	25.120	LINEAR
265	2190	2090	2190	0.29800	LINEAR
266	2191	2180	2190	28.260	LINEAR
267	2192	2190	160	52.330	LINEAR
268	2200	2100	2200	0.15700E-01	LINEAR
269	2210	2110	2210	0.47100E-01	LINEAR
270	2211	2200	2210	3.1400	LINEAR
271	2220	2120	2220	0.78500E-01	LINEAR
272	2221	2210	2220	6.2800	LINEAR
273	2230	2130	2230	0.10990	LINEAR
274	2231	2220	2230	9.4200	LINEAR
275	2240	2140	2240	0.14100	LINEAR
276	2241	2230	2240	12.560	LINEAR
277	2250	2150	2250	0.17300	LINEAR
278	2251	2240	2250	15.700	LINEAR
279	2260	2160	2260	0.20400	LINEAR
280	2261	2250	2260	18.840	LINEAR
281	2270	2170	2270	0.23600	LINEAR
282	2271	2260	2270	21.980	LINEAR
283	2280	2180	2280	0.26700	LINEAR
284	2281	2270	2280	25.120	LINEAR
285	2290	2190	2290	0.29800	LINEAR
286	2291	2280	2290	28.260	LINEAR
287	2292	2290	170	52.330	LINEAR
288	2300	2200	2300	0.15700E-01	LINEAR
289	2310	2210	2310	0.47100E-01	LINEAR
290	2311	2300	2310	3.1400	LINEAR
291	2320	2220	2320	0.78500E-01	LINEAR
292	2321	2310	2320	6.2800	LINEAR
293	2330	2230	2330	0.10990	LINEAR
294	2331	2320	2330	9.4200	LINEAR
295	2340	2240	2340	0.14100	LINEAR
296	2341	2330	2340	12.560	LINEAR
297	2350	2250	2350	0.17300	LINEAR
298	2351	2340	2350	15.700	LINEAR
299	2360	2260	2360	0.20400	LINEAR
300	2361	2350	2360	18.840	LINEAR
301	2370	2270	2370	0.23600	LINEAR
302	2371	2360	2370	21.980	LINEAR
303	2380	2280	2380	0.26700	LINEAR
304	2381	2370	2380	25.120	LINEAR
305	2390	2290	2390	0.29800	LINEAR
306	2391	2380	2390	28.260	LINEAR
307	2392	2390	180	52.330	LINEAR
308	2400	2300	2400	0.15700E-01	LINEAR
309	2410	2310	2410	0.47100E-01	LINEAR
310	2411	2400	2410	3.1400	LINEAR
311	2420	2320	2420	0.78500E-01	LINEAR
312	2421	2410	2420	6.2800	LINEAR

MODEL NAME = A:drillf1

CONDUCTOR DATA--
TOTAL NUMBER OF CONDUCTORS = 751

SEQ.NO.	COND.NO.	NODE I	NODE J	VALUE	TYPE
313	2430	2330	2430	0.10990	LINEAR
314	2431	2420	2430	9.4200	LINEAR
315	2440	2340	2440	0.14100	LINEAR
316	2441	2430	2440	12.560	LINEAR
317	2450	2350	2450	0.17300	LINEAR
318	2451	2440	2450	15.700	LINEAR
319	2460	2360	2460	0.20400	LINEAR
320	2461	2450	2460	18.840	LINEAR
321	2470	2370	2470	0.23600	LINEAR
322	2471	2460	2470	21.980	LINEAR
323	2480	2380	2480	0.26700	LINEAR
324	2481	2470	2480	25.120	LINEAR
325	2490	2390	2490	0.29800	LINEAR
326	2491	2480	2490	28.260	LINEAR
327	2492	2490	190	52.330	LINEAR
328	2500	2400	2500	0.15700E-01	LINEAR
329	2510	2410	2510	0.47100E-01	LINEAR
330	2511	2500	2510	3.1400	LINEAR
331	2520	2420	2520	0.78500E-01	LINEAR
332	2521	2510	2520	6.2800	LINEAR
333	2530	2430	2530	0.10990	LINEAR
334	2531	2520	2530	9.4200	LINEAR
335	2540	2440	2540	0.14100	LINEAR
336	2541	2530	2540	12.560	LINEAR
337	2550	2450	2550	0.17300	LINEAR
338	2551	2540	2550	15.700	LINEAR
339	2560	2460	2560	0.20400	LINEAR
340	2561	2550	2560	18.840	LINEAR
341	2570	2470	2570	0.23600	LINEAR
342	2571	2560	2570	21.980	LINEAR
343	2580	2480	2580	0.26700	LINEAR
344	2581	2570	2580	25.120	LINEAR
345	2590	2490	2590	0.29800	LINEAR
346	2591	2580	2590	28.260	LINEAR
347	2592	2590	200	52.330	LINEAR
348	2600	2500	2600	0.15700E-01	LINEAR
349	2610	2510	2610	0.47100E-01	LINEAR
350	2611	2600	2610	3.1400	LINEAR
351	2620	2520	2620	0.78500E-01	LINEAR
352	2621	2610	2620	6.2800	LINEAR
353	2630	2530	2630	0.10990	LINEAR
354	2631	2620	2630	9.4200	LINEAR
355	2640	2540	2640	0.14100	LINEAR
356	2641	2630	2640	12.560	LINEAR
357	2650	2550	2650	0.17300	LINEAR
358	2651	2640	2650	15.700	LINEAR
359	2660	2560	2660	0.20400	LINEAR
360	2661	2650	2660	18.840	LINEAR
361	2670	2570	2670	0.23600	LINEAR
362	2671	2660	2670	21.980	LINEAR
363	2680	2580	2680	0.26700	LINEAR
364	2681	2670	2680	25.120	LINEAR

MODEL NAME = A:drillf1

CONDUCTOR DATA--
TOTAL NUMBER OF CONDUCTORS = 751

SEQ.NO.	COND.NO.	NODE I	NODE J	VALUE	TYPE
365	2690	2590	2690	0.29800	LINEAR
366	2691	2680	2690	28.260	LINEAR
367	2692	2690	210	52.330	LINEAR
368	2700	2600	2700	0.15700E-01	LINEAR
369	2710	2610	2710	0.47100E-01	LINEAR
370	2711	2700	2710	3.1400	LINEAR
371	2720	2620	2720	0.78500E-01	LINEAR
372	2721	2710	2720	6.2800	LINEAR
373	2730	2630	2730	0.10990	LINEAR
374	2731	2720	2730	9.4200	LINEAR
375	2740	2640	2740	0.14100	LINEAR
376	2741	2730	2740	12.560	LINEAR
377	2750	2650	2750	0.17300	LINEAR
378	2751	2740	2750	15.700	LINEAR
379	2760	2660	2760	0.20400	LINEAR
380	2761	2750	2760	18.840	LINEAR
381	2770	2670	2770	0.23600	LINEAR
382	2771	2760	2770	21.980	LINEAR
383	2780	2680	2780	0.26700	LINEAR
384	2781	2770	2780	25.120	LINEAR
385	2790	2690	2790	0.29800	LINEAR
386	2791	2780	2790	28.260	LINEAR
387	2792	2790	220	52.330	LINEAR
388	2800	2700	2800	0.15700E-01	LINEAR
389	2810	2710	2810	0.47100E-01	LINEAR
390	2811	2800	2810	3.1400	LINEAR
391	2820	2720	2820	0.78500E-01	LINEAR
392	2821	2810	2820	6.2800	LINEAR
393	2830	2730	2830	0.10990	LINEAR
394	2831	2820	2830	9.4200	LINEAR
395	2840	2740	2840	0.14100	LINEAR
396	2841	2830	2840	12.560	LINEAR
397	2850	2750	2850	0.17300	LINEAR
398	2851	2840	2850	15.700	LINEAR
399	2860	2760	2860	0.20400	LINEAR
400	2861	2850	2860	18.840	LINEAR
401	2870	2770	2870	0.23600	LINEAR
402	2871	2860	2870	21.980	LINEAR
403	2880	2780	2880	0.26700	LINEAR
404	2881	2870	2880	25.120	LINEAR
405	2890	2790	2890	0.29800	LINEAR
406	2891	2880	2890	28.260	LINEAR
407	2892	2890	230	52.330	LINEAR
408	2900	2800	2900	0.15700E-01	LINEAR
409	2910	2810	2910	0.47100E-01	LINEAR
410	2911	2900	2910	3.1400	LINEAR
411	2920	2820	2920	0.78500E-01	LINEAR
412	2921	2910	2920	6.2800	LINEAR
413	2930	2830	2930	0.10990	LINEAR
414	2931	2920	2930	9.4200	LINEAR
415	2940	2840	2940	0.14100	LINEAR
416	2941	2930	2940	12.560	LINEAR

MODEL NAME = A:drillf1

CONDUCTOR DATA--
TOTAL NUMBER OF CONDUCTORS = 751

SEQ.NO.	COND.NO.	NODE I	NODE J	VALUE	TYPE
417	2950	2850	2950	0.17300	LINEAR
418	2951	2940	2950	15.700	LINEAR
419	2960	2860	2960	0.20400	LINEAR
420	2961	2950	2960	18.840	LINEAR
421	2970	2870	2970	0.23600	LINEAR
422	2971	2960	2970	21.980	LINEAR
423	2980	2880	2980	0.26700	LINEAR
424	2981	2970	2980	25.120	LINEAR
425	2990	2890	2990	0.29800	LINEAR
426	2991	2980	2990	28.260	LINEAR
427	2992	2990	240	52.330	LINEAR
428	3000	2900	3000	0.15700E-01	LINEAR
429	3010	2910	3010	0.47100E-01	LINEAR
430	3011	3000	3010	3.1400	LINEAR
431	3020	2920	3020	0.78500E-01	LINEAR
432	3021	3010	3020	6.2800	LINEAR
433	3030	2930	3030	0.10990	LINEAR
434	3031	3020	3030	9.4200	LINEAR
435	3040	2940	3040	0.14100	LINEAR
436	3041	3030	3040	12.560	LINEAR
437	3050	2950	3050	0.17300	LINEAR
438	3051	3040	3050	15.700	LINEAR
439	3060	2960	3060	0.20400	LINEAR
440	3061	3050	3060	18.840	LINEAR
441	3070	2970	3070	0.23600	LINEAR
442	3071	3060	3070	21.980	LINEAR
443	3080	2980	3080	0.26700	LINEAR
444	3081	3070	3080	25.120	LINEAR
445	3090	2990	3090	0.29800	LINEAR
446	3091	3080	3090	28.260	LINEAR
447	3092	3090	250	52.330	LINEAR
448	3100	3000	3100	0.15700E-01	LINEAR
449	3110	3010	3110	0.47100E-01	LINEAR
450	3111	3100	3110	3.1400	LINEAR
451	3120	3020	3120	0.78500E-01	LINEAR
452	3121	3110	3120	6.2800	LINEAR
453	3130	3030	3130	0.10990	LINEAR
454	3131	3120	3130	9.4200	LINEAR
455	3140	3040	3140	0.14100	LINEAR
456	3141	3130	3140	12.560	LINEAR
457	3150	3050	3150	0.17300	LINEAR
458	3151	3140	3150	15.700	LINEAR
459	3160	3060	3160	0.20400	LINEAR
460	3161	3150	3160	18.840	LINEAR
461	3170	3070	3170	0.23600	LINEAR
462	3171	3160	3170	21.980	LINEAR
463	3180	3080	3180	0.26700	LINEAR
464	3181	3170	3180	25.120	LINEAR
465	3190	3090	3190	0.29800	LINEAR
466	3191	3180	3190	28.260	LINEAR
467	3192	3190	260	52.330	LINEAR
468	3200	3100	3200	0.15700E-01	LINEAR

MODEL NAME = A:drillf1

CONDUCTOR DATA--
TOTAL NUMBER OF CONDUCTORS = 751

SEQ.NO.	COND.NO.	NODE I	NODE J	VALUE	TYPE
469	3210	3110	3210	0.47100E-01	LINEAR
470	3211	3200	3210	3.1400	LINEAR
471	3220	3120	3220	0.78500E-01	LINEAR
472	3221	3210	3220	6.2800	LINEAR
473	3230	3130	3230	0.10990	LINEAR
474	3231	3220	3230	9.4200	LINEAR
475	3240	3140	3240	0.14100	LINEAR
476	3241	3230	3240	12.560	LINEAR
477	3250	3150	3250	0.17300	LINEAR
478	3251	3240	3250	15.700	LINEAR
479	3260	3160	3260	0.20400	LINEAR
480	3261	3250	3260	18.840	LINEAR
481	3270	3170	3270	0.23600	LINEAR
482	3271	3260	3270	21.980	LINEAR
483	3280	3180	3280	0.26700	LINEAR
484	3281	3270	3280	25.120	LINEAR
485	3290	3190	3290	0.29800	LINEAR
486	3291	3280	3290	28.260	LINEAR
487	3292	3290	270	52.330	LINEAR
488	3300	3200	3300	0.15700E-01	LINEAR
489	3310	3210	3310	0.47100E-01	LINEAR
490	3311	3300	3310	3.1400	LINEAR
491	3320	3220	3320	0.78500E-01	LINEAR
492	3321	3310	3320	6.2800	LINEAR
493	3330	3230	3330	0.10990	LINEAR
494	3331	3320	3330	9.4200	LINEAR
495	3340	3240	3340	0.14100	LINEAR
496	3341	3330	3340	12.560	LINEAR
497	3350	3250	3350	0.17300	LINEAR
498	3351	3340	3350	15.700	LINEAR
499	3360	3260	3360	0.20400	LINEAR
500	3361	3350	3360	18.840	LINEAR
501	3370	3270	3370	0.23600	LINEAR
502	3371	3360	3370	21.980	LINEAR
503	3380	3280	3380	0.26700	LINEAR
504	3381	3370	3380	25.120	LINEAR
505	3390	3290	3390	0.29800	LINEAR
506	3391	3380	3390	28.260	LINEAR
507	3392	3390	280	52.330	LINEAR
508	3400	3300	3400	0.15700E-01	LINEAR
509	3410	3310	3410	0.47100E-01	LINEAR
510	3411	3400	3410	3.1400	LINEAR
511	3420	3320	3420	0.78500E-01	LINEAR
512	3421	3410	3420	6.2800	LINEAR
513	3430	3330	3430	0.10990	LINEAR
514	3431	3420	3430	9.4200	LINEAR
515	3440	3340	3440	0.14100	LINEAR
516	3441	3430	3440	12.560	LINEAR
517	3450	3350	3450	0.17300	LINEAR
518	3451	3440	3450	15.700	LINEAR
519	3460	3360	3460	0.20400	LINEAR
520	3461	3450	3460	18.840	LINEAR

MODEL NAME = A:drillf1

CONDUCTOR DATA--
TOTAL NUMBER OF CONDUCTORS = 751

SEQ.NO.	COND.NO.	NODE I	NODE J	VALUE	TYPE
521	3470	3370	3470	0.23600	LINEAR
522	3471	3460	3470	21.980	LINEAR
523	3480	3380	3480	0.26700	LINEAR
524	3481	3470	3480	25.120	LINEAR
525	3490	3390	3490	0.29800	LINEAR
526	3491	3480	3490	28.260	LINEAR
527	3492	3490	290	52.330	LINEAR
528	3500	3400	3500	0.15700E-01	LINEAR
529	3510	3410	3510	0.47100E-01	LINEAR
530	3511	3500	3510	3.1400	LINEAR
531	3520	3420	3520	0.78500E-01	LINEAR
532	3521	3510	3520	6.2800	LINEAR
533	3530	3430	3530	0.10990	LINEAR
534	3531	3520	3530	9.4200	LINEAR
535	3540	3440	3540	0.14100	LINEAR
536	3541	3530	3540	12.560	LINEAR
537	3550	3450	3550	0.17300	LINEAR
538	3551	3540	3550	15.700	LINEAR
539	3560	3460	3560	0.20400	LINEAR
540	3561	3550	3560	18.840	LINEAR
541	3570	3470	3570	0.23600	LINEAR
542	3571	3560	3570	21.980	LINEAR
543	3580	3480	3580	0.26700	LINEAR
544	3581	3570	3580	25.120	LINEAR
545	3590	3490	3590	0.29800	LINEAR
546	3591	3580	3590	28.260	LINEAR
547	3592	3590	300	52.330	LINEAR
548	3600	3500	3600	0.15700E-01	LINEAR
549	3610	3510	3610	0.47100E-01	LINEAR
550	3611	3600	3610	3.1400	LINEAR
551	3620	3520	3620	0.78500E-01	LINEAR
552	3621	3610	3620	6.2800	LINEAR
553	3630	3530	3630	0.10990	LINEAR
554	3631	3620	3630	9.4200	LINEAR
555	3640	3540	3640	0.14100	LINEAR
556	3641	3630	3640	12.560	LINEAR
557	3650	3550	3650	0.17300	LINEAR
558	3651	3640	3650	15.700	LINEAR
559	3660	3560	3660	0.20400	LINEAR
560	3661	3650	3660	18.840	LINEAR
561	3670	3570	3670	0.23600	LINEAR
562	3671	3660	3670	21.980	LINEAR
563	3680	3580	3680	0.26700	LINEAR
564	3681	3670	3680	25.120	LINEAR
565	3690	3590	3690	0.29800	LINEAR
566	3691	3680	3690	28.260	LINEAR
567	3692	3690	310	52.330	LINEAR
568	3700	3600	3700	0.15700E-01	LINEAR
569	3710	3610	3710	0.47100E-01	LINEAR
570	3711	3700	3710	3.1400	LINEAR
571	3720	3620	3720	0.78500E-01	LINEAR
572	3721	3710	3720	6.2800	LINEAR

MODEL NAME = A:drillf1

CONDUCTOR DATA--
TOTAL NUMBER OF CONDUCTORS = 751

SEQ.NO.	COND.NO.	NODE I	NODE J	VALUE	TYPE
573	3730	3630	3730	0.10990	LINEAR
574	3731	3720	3730	9.4200	LINEAR
575	3740	3640	3740	0.14100	LINEAR
576	3741	3730	3740	12.560	LINEAR
577	3750	3650	3750	0.17300	LINEAR
578	3751	3740	3750	15.700	LINEAR
579	3760	3660	3760	0.20400	LINEAR
580	3761	3750	3760	18.840	LINEAR
581	3770	3670	3770	0.23600	LINEAR
582	3771	3760	3770	21.980	LINEAR
583	3780	3680	3780	0.26700	LINEAR
584	3781	3770	3780	25.120	LINEAR
585	3790	3690	3790	0.29800	LINEAR
586	3791	3780	3790	28.260	LINEAR
587	3792	3790	320	52.330	LINEAR
588	5000	4900	5000	1.5070	LINEAR
589	5001	1090	5000	5.0200	LINEAR
590	5002	1190	5000	5.0200	LINEAR
591	5003	1290	5000	2.5100	LINEAR
592	5004	1290	5100	2.5100	LINEAR
593	5010	4910	5010	2.0100	LINEAR
594	5011	5000	5010	10.990	LINEAR
595	5020	4920	5020	2.5120	LINEAR
596	5021	5010	5020	14.130	LINEAR
597	5030	4930	5030	3.0140	LINEAR
598	5031	5020	5030	17.270	LINEAR
599	5041	5030	9000	20.410	LINEAR
600	5100	5000	5100	1.5070	LINEAR
601	5101	1390	5100	5.0200	LINEAR
602	5102	1490	5100	5.0200	LINEAR
603	5110	5010	5110	2.0100	LINEAR
604	5111	5100	5110	10.990	LINEAR
605	5120	5020	5120	2.5120	LINEAR
606	5121	5110	5120	14.130	LINEAR
607	5130	5030	5130	3.0140	LINEAR
608	5131	5120	5130	17.270	LINEAR
609	5141	5130	9000	20.410	LINEAR
610	5200	5100	100	3.0140	LINEAR
611	5210	5110	101	4.0200	LINEAR
612	5220	5120	5220	2.5120	LINEAR
613	5221	101	5220	11.300	LINEAR
614	5222	111	5220	11.300	LINEAR
615	5223	121	5220	5.6500	LINEAR
616	5224	121	5320	5.6500	LINEAR
617	5230	5130	5230	3.0140	LINEAR
618	5231	5220	5230	17.270	LINEAR
619	5241	5230	9000	20.410	LINEAR
620	5310	5410	141	4.0200	LINEAR
621	5320	5220	5320	2.5120	LINEAR
622	5321	131	5320	11.300	LINEAR
623	5322	141	5320	11.300	LINEAR
624	5330	5230	5330	3.0140	LINEAR

MODEL NAME = A:drillf1

CONDUCTOR DATA--
TOTAL NUMBER OF CONDUCTORS = 751

SEQ.NO.	COND.NO.	NODE I	NODE J	VALUE	TYPE
625	5331	5320	5330	17.270	LINEAR
626	5341	5330	9000	20.410	LINEAR
627	5411	150	5410	21.980	LINEAR
628	5420	5320	5420	2.5120	LINEAR
629	5421	5410	5420	14.130	LINEAR
630	5430	5330	5430	3.0140	LINEAR
631	5431	5420	5430	17.270	LINEAR
632	5441	5430	9000	20.410	LINEAR
633	5510	5410	5510	2.0100	LINEAR
634	5511	160	5510	21.980	LINEAR
635	5520	5420	5520	2.5120	LINEAR
636	5521	5510	5520	14.130	LINEAR
637	5530	5430	5530	3.0140	LINEAR
638	5531	5520	5530	17.270	LINEAR
639	5541	5530	9000	20.410	LINEAR
640	5610	5510	5610	2.0100	LINEAR
641	5611	170	5610	21.980	LINEAR
642	5620	5520	5620	2.5120	LINEAR
643	5621	5610	5620	14.130	LINEAR
644	5630	5530	5630	3.0140	LINEAR
645	5631	5620	5630	17.270	LINEAR
646	5641	5630	9000	20.410	LINEAR
647	5710	5610	5710	2.0100	LINEAR
648	5711	180	5710	21.980	LINEAR
649	5720	5620	5720	2.5120	LINEAR
650	5721	5710	5720	14.130	LINEAR
651	5730	5630	5730	3.0140	LINEAR
652	5731	5720	5730	17.270	LINEAR
653	5741	5730	9000	20.410	LINEAR
654	5810	5710	5810	2.0100	LINEAR
655	5811	190	5810	21.980	LINEAR
656	5820	5720	5820	2.5120	LINEAR
657	5821	5810	5820	14.130	LINEAR
658	5830	5730	5830	3.0140	LINEAR
659	5831	5820	5830	17.270	LINEAR
660	5841	5830	9000	20.410	LINEAR
661	5910	5810	5910	2.0100	LINEAR
662	5911	200	5910	21.980	LINEAR
663	5920	5820	5920	2.5120	LINEAR
664	5921	5910	5920	14.130	LINEAR
665	5930	5830	5930	3.0140	LINEAR
666	5931	5920	5930	17.270	LINEAR
667	5941	5930	9000	20.410	LINEAR
668	6010	5910	6010	2.0100	LINEAR
669	6011	210	6010	21.980	LINEAR
670	6020	5920	6020	2.5120	LINEAR
671	6021	6010	6020	14.130	LINEAR
672	6030	5930	6030	3.0140	LINEAR
673	6031	6020	6030	17.270	LINEAR
674	6041	6030	9000	20.410	LINEAR
675	6110	6010	6110	2.0100	LINEAR
676	6111	220	6110	21.980	LINEAR

MODEL NAME = A:drillf1

CONDUCTOR DATA--
TOTAL NUMBER OF CONDUCTORS = 751

SEQ.NO.	COND.NO.	NODE I	NODE J	VALUE	TYPE
677	6120	6020	6120	2.5120	LINEAR
678	6121	6110	6120	14.130	LINEAR
679	6130	6030	6130	3.0140	LINEAR
680	6131	6120	6130	17.270	LINEAR
681	6141	6130	9000	20.410	LINEAR
682	6210	6110	6210	2.0100	LINEAR
683	6211	230	6210	21.980	LINEAR
684	6220	6120	6220	2.5120	LINEAR
685	6221	6210	6220	14.130	LINEAR
686	6230	6130	6230	3.0140	LINEAR
687	6231	6220	6230	17.270	LINEAR
688	6241	6230	9000	20.410	LINEAR
689	6310	6210	6310	2.0100	LINEAR
690	6311	240	6310	21.980	LINEAR
691	6320	6220	6320	2.5120	LINEAR
692	6321	6310	6320	14.130	LINEAR
693	6330	6230	6330	3.0140	LINEAR
694	6331	6320	6330	17.270	LINEAR
695	6341	6330	9000	20.410	LINEAR
696	6410	6310	6410	2.0100	LINEAR
697	6411	250	6410	21.980	LINEAR
698	6420	6320	6420	2.5120	LINEAR
699	6421	6410	6420	14.130	LINEAR
700	6430	6330	6430	3.0140	LINEAR
701	6431	6420	6430	17.270	LINEAR
702	6441	6430	9000	20.410	LINEAR
703	6510	6410	6510	2.0100	LINEAR
704	6511	260	6510	21.980	LINEAR
705	6520	6420	6520	2.5120	LINEAR
706	6521	6510	6520	14.130	LINEAR
707	6530	6430	6530	3.0140	LINEAR
708	6531	6520	6530	17.270	LINEAR
709	6541	6530	9000	20.410	LINEAR
710	6610	6510	6610	2.0100	LINEAR
711	6611	270	6610	21.980	LINEAR
712	6620	6520	6620	2.5120	LINEAR
713	6621	6610	6620	14.130	LINEAR
714	6630	6530	6630	3.0140	LINEAR
715	6631	6620	6630	17.270	LINEAR
716	6641	6630	9000	20.410	LINEAR
717	6710	6610	6710	2.0100	LINEAR
718	6711	280	6710	21.980	LINEAR
719	6720	6620	6720	2.5120	LINEAR
720	6721	6710	6720	14.130	LINEAR
721	6730	6630	6730	3.0140	LINEAR
722	6731	6720	6730	17.270	LINEAR
723	6741	6730	9000	20.410	LINEAR
724	6810	6710	6810	2.0100	LINEAR
725	6811	290	6810	21.980	LINEAR
726	6820	6720	6820	2.5120	LINEAR
727	6821	6810	6820	14.130	LINEAR
728	6830	6730	6830	3.0140	LINEAR

MODEL NAME = A:drillf1

CONDUCTOR DATA--
TOTAL NUMBER OF CONDUCTORS = 751

SEQ.NO.	COND.NO.	NODE I	NODE J	VALUE	TYPE
729	6831	6820	6830	17.270	LINEAR
730	6841	6830	9000	20.410	LINEAR
731	6910	6810	6910	2.0100	LINEAR
732	6911	300	6910	21.980	LINEAR
733	6920	6820	6920	2.5120	LINEAR
734	6921	6910	6920	14.130	LINEAR
735	6930	6830	6930	3.0140	LINEAR
736	6931	6920	6930	17.270	LINEAR
737	6941	6930	9000	20.410	LINEAR
738	7010	6910	7010	2.0100	LINEAR
739	7011	310	7010	21.980	LINEAR
740	7020	6920	7020	2.5120	LINEAR
741	7021	7010	7020	14.130	LINEAR
742	7030	6930	7030	3.0140	LINEAR
743	7031	7020	7030	17.270	LINEAR
744	7041	7030	9000	20.410	LINEAR
745	7110	7010	7110	2.0100	LINEAR
746	7111	320	9000	1500.0	LINEAR
747	7120	7020	7120	2.5120	LINEAR
748	7121	7110	7120	14.130	LINEAR
749	7130	7030	7130	3.0140	LINEAR
750	7131	7120	7130	17.270	LINEAR
751	7141	7130	9000	20.410	LINEAR

Table A-3 Constants Data Block

CONTROL CONSTANT DATA--

SEQ.NO.	NAME	DEFAULT	CURRENT	DESCRIPTION
1	ITERMX	50	100	Maximum Iterations Allowed
2	DRLXCA	1.000E-01	5.000E-01	Max Diffusion Temp Change Allowed
3	ARLXCA	1.000E-01	5.000E-01	Max Arithmetic Temp Change Allowed
4	EBALSA	1.000E+01	3.000E+02	Max System Energy Balance Allowed
5	EBALNA	5.000E+00	3.000E+02	Max Nodal Energy Balance Allowed
6	ABSZRO	0.000E-01	0.000E-01	Absolute Zero
7	SBCNST	1.000E+00	5.670E-08	Stefan Boltzman Constant
8	EXTLIM	5.000E+01	5.000E+01	Max Extrapolation Temp Change
9	ITERXT	3	3	Extrap Iteration Interval
10	TIMEO	0.000E-01	0.000E-01	Problem Start Time
11	TIMEND	1.000E+01	1.500E+01	Problem Stop Time
12	TSTEPI	1.000E-01	2.000E-01	Computation Time Interval
13	TSTEPO	1.000E+00	5.000E+00	Output Time Interval
14	ITEROT	0	0	Intermediate Printout Interval

USER CONSTANT DATA--
TOTAL NUMBER OF USER CONSTANTS = 33

SEQ.NO.	NAME	TYPE	VALUE	COMMENT
1	AREA	REAL	1.760E+00	KERF AREA CM2
2	BITCP	REAL	3.000E-01	CP OF BIT
3	BITK	REAL	4.000E-01	K OF BIT
4	CMTCP	REAL	2.500E-01	MULT FACTOR FOR MIN/MAX CP
5	CMTK	REAL	5.600E-04	MULT FACTOR FOR MIN/MAX K
6	DRILCP	REAL	6.900E-01	SPECIFIC HEAT OF DRILL
7	DRILLK	REAL	1.300E-02	THERMAL K OF DRILL STEM
8	HBEL	REAL	1.000E-01	FRACT. OF HEAT TO BELOW
9	HBIT	REAL	3.000E-01	FRACT. OF HEAT TO BIT
10	HCUT	REAL	2.000E-01	FRACT. OF HEAT TO CUTTINGS
11	HEAT	REAL	2.000E+00	INPUT J/CC
12	HIN	REAL	2.000E-01	FRACTION OF HEAT TO INNER
13	HOUT	REAL	2.000E-01	FRACT. OF HEAT TO OUTER
14	RATE	REAL	2.000E-01	PEN. RATE IN CM/S
15	RCP	REAL	8.000E-01	ROCK SPECIFIC HEAT
16	RHEAT	REAL	3.000E+02	ROCK SPECIFIC E IN J/cc
17	RHO	REAL	1.000E+00	COMET/MARS DENSITY
18	RHOB	REAL	7.500E+00	DENSITY OF BIT
19	RHOD	REAL	1.400E+00	DENSITY OF DRILL STEM
20	RHOR	REAL	2.800E+00	ROCK DENSITY
21	RK	REAL	3.600E-02	ROCK K IN W/cmK
22	TBIT	REAL	2.150E+02	TEMP OF BIT NODES
23	TEST	REAL	0.000E-01	0 TO GO TO ROCK AT TIM6, 1 NOT
24	TIM1	REAL	0.000E-01	None
25	TIM2	REAL	1.000E+00	None
26	TIM3	REAL	2.000E+00	None
27	TIM4	REAL	3.000E+00	None
28	TIM5	REAL	4.000E+00	None
29	TIM6	REAL	5.000E+00	None
30	TIM7	REAL	1.000E+01	TIME FOR END OF HEATING
31	TMPMTL	REAL	2.150E+02	TEMP OF INSITU MATERIAL
32	TSINK	REAL	2.150E+02	TEMP OF DRILL STEM TOP
33	NCUT	INTEGER	10	NUMBER OF CUTTINGS NODES

Table A-4 Execution Logic File

```
C*************************
      SUBROUTINE EXECTN
C*************************
      character*80 comm
C
C ---- EXECUTION ROUTINE - CALL ALL SOLUTION ROUTINES HERE
FSTART
C
C     SET ALL THERMAL CAPACITANCES WITHIN THESE LOOPS
C     BY USING VOLUME OF NODE * DENSITY * SPECIFIC HEAT
C
      DO 10 I=1,NNT
      IF (NODSEQ(I).GT.400) C(I)=C(I)*RHO*CMTCP
10    CONTINUE
C
      DO 20 I=1,NNT
      IF (NODSEQ(I).LT.150) C(I)=C(I)*RHOB*BITCP
20    CONTINUE
C
      DO 30 I=1,NNT
      IF (NODSEQ(I).LE.400.AND.NODSEQ(I).GE.150) C(I)=C(I)*RHOD*DRILCP
30    CONTINUE
C
C     SET ALL CONDUCTANCES WITHIN THESE LOOPS
C
      DO 40 I=1,NGT
      IF (CNDSEQ(I).GT.400) G(I)=G(I)*CMTK
40    CONTINUE
C
      DO 50 I=1,NGT
      IF (CNDSEQ(I).LT.150) G(I)=G(I)*BITK
50    CONTINUE
C
      DO 60 I=1,NGT
      IF (CNDSEQ(I).LE.400.AND.CNDSEQ(I).GE.150) G(I)=G(I)*DRILLK
60    CONTINUE
C
C     SET DRILLED MATERIAL TEMPERATURE
C
      DO 70 I=1,NNT
      T(I)=TMPMTL
70    CONTINUE
C
C     SET DRILL BIT TEMPERATURE
C
      DO 80 I=1,30
      T(I)=TBIT
80    CONTINUE
C
C     INPUT COMMENT FOR LABELING RUN
      write (*,*)' input comment now'
      read (*,'(a)') comm
      write (nout,'(/,a,/)') comm
C
C     CALL TRANSIENT ROUTINE
      CALL FWDBCK
C
      RETURN
      END
FSTOP
```

```
C*************************
      SUBROUTINE VARBL1
C*************************
C ---- THIS ROUTINE IS EXECUTED BEFORE EACH SOLUTION ITERATION
C
C     SET HEATING RATES AT DRILL BIT AND MATERIAL NODES
C
C     INNER CORE NODES
      Q1590=0.0
      Q1690=0.0
      Q1790=0.0
      Q1890=0.0
      Q1990=0.0
      IF (TIMEN.GE.TIM1.AND.TIMEN.LE.TIM2) Q1990=AREA*HEAT*RATE*HIN
      IF (TIMEN.GT.TIM2.AND.TIMEN.LE.TIM3) Q1890=AREA*HEAT*RATE*HIN
      IF (TIMEN.GT.TIM3.AND.TIMEN.LE.TIM4) Q1790=AREA*HEAT*RATE*HIN
      IF (TIMEN.GT.TIM4.AND.TIMEN.LE.TIM5) Q1690=AREA*HEAT*RATE*HIN
      IF (TIMEN.GT.TIM5.AND.TIMEN.LE.TIM6) Q1590=AREA*HEAT*RATE*HIN
C
C     BELOW BIT
      Q5100=AREA*HEAT*RATE*HBEL
      Q5110=AREA*HEAT*RATE*HBEL
C
C     OUTER MATERIAL NODES
      Q5320=0.0
      Q5220=0.0
      IF (TIMEN.GT.TIM1.AND.TIMEN.LT.TIM3) Q5320=AREA*HEAT*RATE*HOUT
      IF (TIMEN.GE.TIM3) Q5220=AREA*HEAT*RATE*HOUT
C
C     BIT NODES
      Q100=0.0
      Q110=0.0
      Q120=0.0
      Q130=0.0
      Q140=0.0
      IF (TIMEN.GE.TIM1.AND.TIMEN.LE.TIM2) Q140=AREA*HEAT*RATE*HBIT
      IF (TIMEN.GT.TIM2.AND.TIMEN.LE.TIM3) Q130=AREA*HEAT*RATE*HBIT
      IF (TIMEN.GT.TIM3.AND.TIMEN.LE.TIM4) Q120=AREA*HEAT*RATE*HBIT
      IF (TIMEN.GT.TIM4.AND.TIMEN.LE.TIM5) Q110=AREA*HEAT*RATE*HBIT
      IF (TIMEN.GT.TIM5.AND.TIMEN.LE.TIM6) Q100=AREA*HEAT*RATE*HBIT
      Q101=0.0
      Q111=0.0
      Q121=0.0
      Q131=0.0
      Q141=0.0
      IF (TIMEN.GE.TIM1.AND.TIMEN.LE.TIM2) Q141=AREA*HEAT*RATE*HBIT
      IF (TIMEN.GT.TIM2.AND.TIMEN.LE.TIM3) Q131=AREA*HEAT*RATE*HBIT
      IF (TIMEN.GT.TIM3.AND.TIMEN.LE.TIM4) Q121=AREA*HEAT*RATE*HBIT
      IF (TIMEN.GT.TIM4.AND.TIMEN.LE.TIM5) Q111=AREA*HEAT*RATE*HBIT
      IF (TIMEN.GT.TIM5.AND.TIMEN.LE.TIM6) Q101=AREA*HEAT*RATE*HBIT
C
FSTART
C     CUTTINGS
      DO 120 I=11,14
      Q(I)=AREA*HEAT*RATE*HCUT/NCUT
120   CONTINUE
C
      DO 130 I=319,323,2
      Q(I)=AREA*HEAT*RATE*HCUT/NCUT
130   CONTINUE
```

```
C
      DO 140 I=326,332,3
      Q(I)=AREA*HEAT*RATE*HCUT/NCUT
140   CONTINUE
C
      T(28)=TSINK
C
C     CHANGE TYPE OF MATERIAL DRILLED AT TIM6 IF REQUIRED
C
      IF (TIMEN.GT.TIM6.AND.TEST.EQ.0.0) THEN
         DO 150 I=31,130
         C(I)=C(I)*RHOR*RCP/RHO/CMTCP
         HEAT=RHEAT
150      CONTINUE
C
         DO 160 I=33,227
         G(I)=G(I)*RK/CMTK
160      CONTINUE
C
         TEST=1.0
         TIM1=TIM1+TIM6
         TIM2=TIM2+TIM6
         TIM3=TIM3+TIM6
         TIM4=TIM4+TIM6
         TIM5=TIM5+TIM6
         TIM6=TIM6+TIM6
      ENDIF
C
C     CEASE DRILLING AND MONITOR TEMPERATURE DECAY IF REQUIRED
C
      IF (TIMEN.GT.TIM7) THEN
         DO 170 I=1,NNT
         Q(I)=0.0
170      CONTINUE
      ENDIF
C
      RETURN
      END
C*************************
      SUBROUTINE VARBL2
C*************************
C
C ---- THIS ROUTINE IS EXECUTED AFTER CONVERGENCE (AT EACH TIME STEP IF
C     TRANSIENT)
C
      RETURN
      END
FSTOP
C*************************
      SUBROUTINE OUTCAL
C*************************
C
C ---- THIS ROUTINE IS EXECUTED AT INTERVALS SPECIFIED BY THE ITEROT AND
C     TSTEPO CONTROL CONSTANTS, ALSO AT THE INITIATION OF A SOLUTION
C     ROUTINE AND AT THE END OF STEADY STATE CONVERGENCE
FSTART
C
C     WRITE TEMPERATURE OUTPUTS
C
      IF (TIMEN.GT.0.2) THEN
```

```
          DO 110 I=1,320,10
             WRITE (NOUT,100) (T(J),J=I,I+9)
110       CONTINUE
C
100       FORMAT (10(3X,F7.2))
C
          WRITE (NOUT,'(/,/)')
C
       ENDIF
        RETURN
        END
FSTOP
```

Appendix B

Drilling Test Facility

APPENDIX B. DRILLING TEST FACILITY.

Design Issues--Testing the drilling system is a vital part of the design effort not only to verify performance predictions, but to evaluate the practicality of new, as well as standard, methods of drilling under the unusual ambient conditions. The testing facility must provide a sample bed of a selected material for drilling, control of the bed at a specified temperature, ambient temperature, and pressure to simulate Martian or cometary environments, and a drilling mechanism with little or no heat leak to the laboratory. To simulate cometary nucleus temperatures, the sample bed temperature should encompass a range of 100 to 180 K; to simulate the Martian surface requires a range of 180 to 270 K. The ambient temperature should be capable of this same range. The sample bed material will normally be a water-ice/soil conglomerate, but to determine the effects of different detailed compositions, the sample bed must be easily replaced or altered. The Martian ambient pressure is about 5 torr of CO_2, and the cometary ambient pressures will be very low--mandating a simulation well below 10^{-4} torr.

Design--One immediate problem is maintaining the low ambient pressure while the drilled material is emitting potentially large amounts of sublimated vapor. This necessitates a pumping system that can accommodate copious quantities of water vapor, other gases, and particulates while maintaining a low ambient pressure. An optically dense inlet filter can be used with the pumping system to capture particles, although this will slow the pumping speed, and the high levels of particulates still eliminate consideration of a turbo-molecular pump. This leaves the pumping choices of a mechanical roughing pump, a cryosorption pump, a cryogenic pump, and a diffusion pump. A cryogenic system will in general have a higher pumping speed, with less peculiarities like directional mounting and problems with oil backstreaming that are common to diffusion pumps. The amount of vapors pumped may be enough to require frequent regeneration of the pumping system, which is a standard automated feature of many cryopumps. A diffusion pump might be overloaded by the huge water vapor load that is sure to be coming from the sample bed.

The best choice is a heavy-duty roughing system that can be used to evacuate the system down to about 10^{-3} torr. The addition of a Roots blower to the roughing system will ensure its ability to handle the generated vapors. A moderately-sized cryopump (such as a Cryo-Torr 8) would only be valved in when lower pressures were desired, thus maintaining its cleanliness. A battery of cryosorption pumps could be used in place of the cryopump, but would entail more labor and support time for regeneration. To hold the system stably at the higher pressures desired, a vacuum regulator valve would be installed inline with the pumping system. Such a valve can maintain any pressure between 1 and 740 torr.

There are various methods of mounting the entire chamber and sample bed. The sample bed can stand vertically within the cylindrical chamber, and for access to the can either the top can be on a hoist or the base can move down and swing out. The chamber can lay horizontally, with the sample can horizontal inside, which negates the effect of gravity on the drilling operation and makes both ends of the chamber easily accessible, but means that the sample material must be well-consolidated or contained prior to freezing so that it does not slide out of the can.

To keep the sample bed and the ambient temperature low, there must be fluid lines not only in the sample can but in a shroud surrounding the sample bed. The sample bed is recommended to be at least 10 cm in diameter by 30 cm high, and the structure must include fluid lines as an integral part to ensure adequate and uniform heat transfer. This entails a metal cylinder with welded-in or integral piping, supported on insulating standoffs. The shroud should be as small as possible and close to this sample bed to minimize thermal losses, but large enough to allow clear viewing of the sample bed and avoid interference with the drilling operation. A shroud 25 cm in diameter by 40 cm high would be acceptable, although this could be modified to fit standard equipment sizes if necessary. The cooling fluid lines for both the shroud and the sample bed must pass through the chamber walls in insulative feedthroughs. The optimum arrangement is for the shroud lines and sample bed lines to be independent, so the ambient temperature can be varied independently of the sample material temperature. There

are several possiblities for the cooling fluid. The standard fluid is liquid nitrogen (LN2), which is at 77 K. This could be used to stabilize the sample bed at its coldest temperature, but for warmer temperatures another method is neecessary. The warmer temperatures can be achieved by starting and stopping the flow of liquid nitrogen, but this makes it very difficult to reliably stabilize at a given temperature. The fluid lines can also be used for gaseous nitrogen that can be warmed or cooled to produce most of the desired temperatures. The optimum system, however, and the one most suited for computer control, is a refrigerant system. A fluid-like Refrigerant 11, 22, or 502 can provide more than the required range of temperatures, can be easily warmed and cooled under automated control without disasterous change in vapor pressure or changes in state, and runs without replacement of fluid.

To obtain the maximum amount of information from the testing, the sample bed must be instrumented to give temperatures inside the drilled region of material, and the drill stem could incorporate thermocouples to aid in determination of the core temperature. The sensors in the sample bed must be accurately positioned, capable of simple repositioning when the sample bed is changed, and include very close to the drill path to give the necessary information. To accomplish this, an internal support structure inside the sample bed is necessary. This structure should be fabricated of a low-thermal conductance material such as fiberglass that does not affect the natural thermal fluxes within the sample material. It could be a honeycomb structure with thermocouples at all pertinent points. There could even be a thin instrumented post that would pass inside the core as the drill descends, allowing exact determination of the core temperature during drilling. This would require highly accurate positioning. The assembly is also adaptable, so that it may be reconfigured if a larger diameter or differently shaped drill is tested.

The drilling system feedthrough is another challenge unique to this system. The feedthrough must be capable of transmitting the rotary, percussive, and forward motions of the drill stem, and in turn allow the power system to sense the resistance to drilling at the bit. There must be a moderately insulative break in the drill stem to isolate the sample bed from any external, laboratory, and power head thermal loads.

The ranges of motion of the feedthrough must be rotation up to 300 rpm, axial force of up to 100 lbs, axial impact of up to 40 in-lb at 2000 ipm, at least 12 in. of linear motion and ability to transmit up to 20 ft-lbs of torque. These parameters are necessary to allow experimentation with the drilling operation and drilling of many material types. The 12 in. of linear motion is necessary to allow deep drilling in the sample bed, unless the alternative method of raising the sample bed, rather than lowering the drill, is chosen. There is no standard feedthrough available that meets these specifications, although there is no inherent reason that one could not be developed. However, as there is no applicable feedthrough available commercially, it must be assumed that the development of such an item would be costly as well as involving the risk that it could not be accomplished. Another method is to use a feedthrough that would transmit only the rotary and percussive motion. Such a feedthrough is readily available. The sample bed would be on a movable plate, so that it could be raised rather than lowering the drill (Fig. B-1). This arrangement forces the electrical and fluid connections to be flexible lines with at least a foot of possible travel. This approach adds complexity to the system and decreases its adaptability, but avoids the concern of new feedthrough development.

A third option is to use a standard rotary feedthrough for transmitting drill motion, and insert it into the vacuum chamber through differentially pumped slip rings. This would probably allow some leakage during operation of the drill, but with a high throughput pumping system, the low pressure could be maintained during a limited drilling period. This method avoids development of a feedthrough, but it is difficult to evaluate the leak rate for this type of drilling feedthrough without testing.

The capability to perform more than one coring run per test sequence would greatly increase the efficiency of testing with this system. If only one coring operation is possible, vacuum must be broken and the sample bed renovated after each test. An option that allows multiple testing is to place the sample bed on a rotary table capable of 180° rotation in either direction. This requires some flexibility in the cooling and electrical lines, and additional feedthroughs for the rotary mechanism. With this addition, the sample

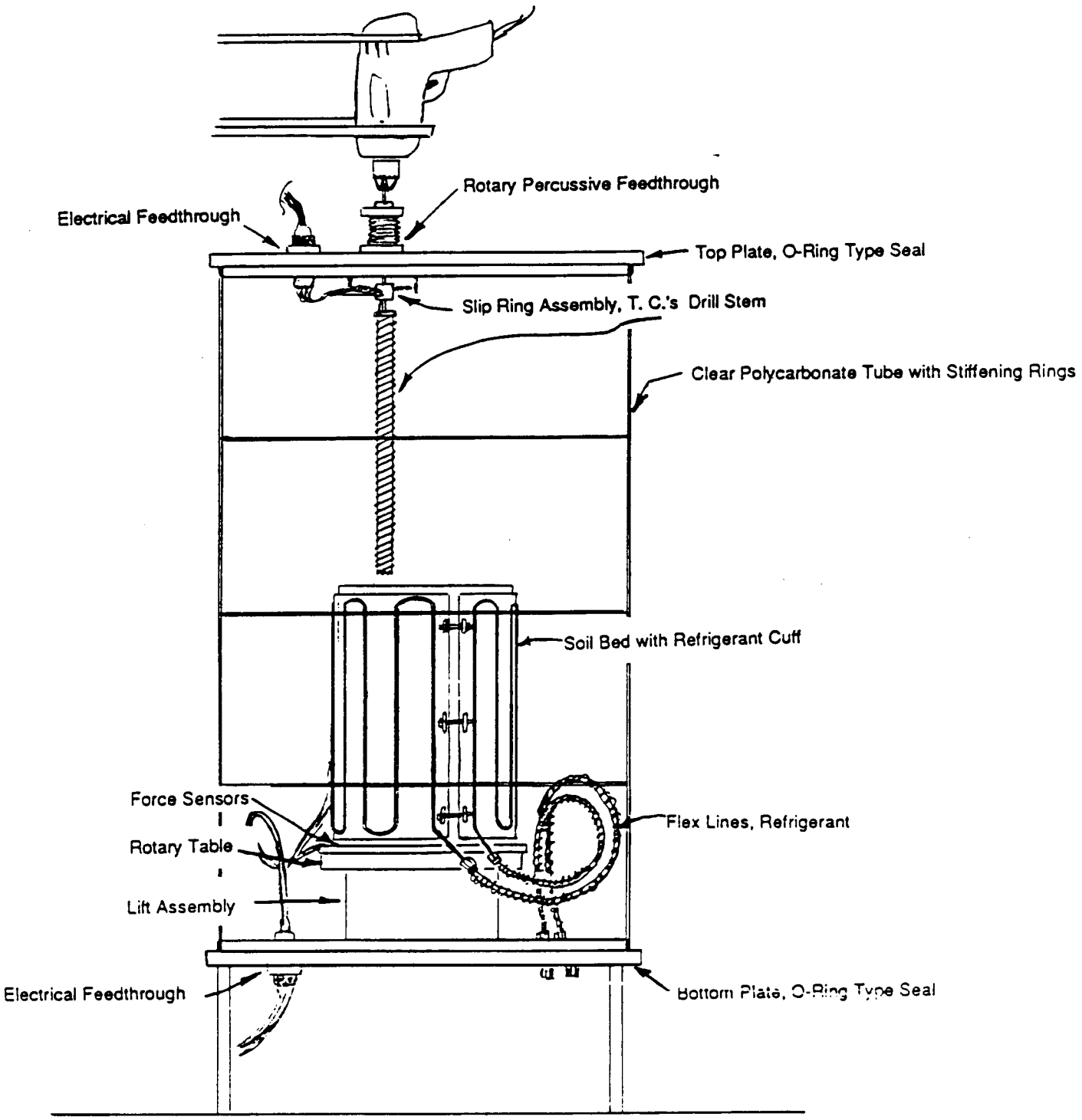

Figure B-1 Drill Testing Facility

C-3

bed can be drilled 10 or 12 times around the periphery in a single test sequence. This allows the variation of many parameters without the intervening time for opening, change, and pumpdown of the system.

The optimum assembly would have all parameters computer-controlled, so that any variable can be changed instantaneously and precisely. This includes control of: the pumping system, which should be able to vary the pressure from 10 Torr down to 10^{-4} Torr and regenerate automatically; the sample bed and ambient temperatures as well as their readouts; and all variable drilling parameters. This entails multiplexing the pumping system, valves, refrigerant system, temperature sensors and drill control through a central computer.